UNIVERSITY OF SOUTHAMPTON

FACULTY OF MEDICINE

Cancer Sciences Unit

C-terminal binding proteins link glycolytic metabolism with the adaptive response to tumour hypoxia and pH regulation

by

Mira Kreuzer

Thesis for the degree of Doctor of Philosophy (PhD)

March 2018

Supervision: Dr Jeremy P. Blaydes and Dr Ali Tavassoli

UNIVERSITY OF SOUTHAMPTON

ABSTRACT

FACULTY OF MEDICINE

Academic Unit of Cancer Sciences

Doctor of Philosophy

C-TERMINAL BINDING PROTEINS LINK GLYCOLYTIC METABOLISM WITH THE ADAPTIVE RESPONSE TO TUMOUR HYPOXIA AND PH REGULATION

By Mira Kreuzer

Aberrant blood flow and avascular growth create areas of sub-physiological oxygen pressure within tumours (hypoxia), thereby negatively affecting therapy outcome. To maintain ATP production in hypoxia, cancer cells upregulate glycolysis. Both processes combined lead to the accumulation of acidic metabolites. Adaptive responses are mediated by the transcription factor Hypoxia-inducible factor-1 (HIF-1) which upregulates the expression of genes involved in glycolysis and pH regulation, including the transmembrane-spanning enzyme carbonic anhydrase 9 (CA9). CA9 mediates cancer cell survival by generating protons and bicarbonate from CO_2 and water, thus maintaining an alkaline intracellular pH while further engraving extracellular acidosis. C-terminal binding proteins (CtBPs) couple glycolysis with gene transcription via their NADH-dependent activation, thus functioning as co-regulators of transcription. It is unknown, whether CtBPs link glycolysis with the adaptive response to hypoxia to promote tumour cell survival. In hypoxic MCF7 breast cancer cells, or in MCF7 incubated in 1 mM DMOG, the role of glycolysis was investigated by inhibition with 2-deoxyglucose (2-DG) and in fructose-grown MCF7. The role of CtBPs was determined by transfection with CtBP-targeting siRNA, the inhibitor MTOB, and in MCF7 either expressing mutant CtBP monomers or overexpressing wildtype CtBP2. Reverse-transcription PCR and Western blotting demonstrated, that the HIF-induced CA9 mRNA and protein expression, but not of other HIF-target genes, is potentially regulated via a functional interaction between CtBPs and HIF. Colony forming assays showed that the transient silencing of p53 and CtBP or of p53 and CA9 impairs the survival of MCF7 breast cancer cells in hypoxia-induced acidosis. In epithelial-like breast cancer cells, this study establishes a novel link between glycolysis and pH regulation via the activation of CtBPs. Additionally, this work further strengthens CtBPs as a therapeutic target and contributes to the growing body of evidence that CtBPs are not mere co-repressors, but are versatile co-regulators of gene transcription instead.

Table of Contents

List of Tables

List of Figures

List of Equations

DECLARATION OF AUTHORSHIP

I, Mira Kreuzer, declare that this thesis and the work presented in it are my own and have been generated by me as the result of my own original research.

Title of thesis: C-terminal binding proteins link glycolytic metabolism with hypoxia-induced pH regulation in a model of oestrogen-receptor-positive breast cancer

I confirm that:

1. This work was done wholly or mainly while in candidature for a research degree at this University;
2. Where any part of this thesis has previously been submitted for a degree or any other qualification at this University or any other institution, this has been clearly stated;
3. Where I have consulted the published work of others, this is always clearly attributed;
4. Where I have quoted from the work of others, the source is always given. With the exception of such quotations, this thesis is entirely my own work;
5. I have acknowledged all main sources of help;
6. Where the thesis is based on work done by myself jointly with others, I have made clear exactly what was done by others and what I have contributed myself;
7. None of this work has been published before

Signed: .....

Date: .....

Acknowledgements

First, I acknowledge the financial support of the Institute for Life Sciences, University of Southampton, which made this project possible. I would also like to express my gratitude to my supervisor Dr Jeremy P. Blaydes for giving me the chance to realise a project in the exciting field of cancer cell metabolism, and to guide me through my PhD towards successful completion. I am indebted to Matt Darley who thoroughly trained me in cell culture, PCR, and Western blotting, and whose technical expertise was most helpful. I also thank Dr Charles Birts for providing me with the standard curve for the Bradford assay for protein quantification and for supporting me with his expertise in transient transfections of mammalian cells. I also thank Dr Arindam Banerjee for demonstrating the colony forming assay and crystal violet staining and for providing me with the protocol.

I am most thankful for my family who always supported me on my meandering journey towards a PhD in life sciences and who never questioned my decision to pursue this dream in a foreign and expensive country. Thanks are also due to my partner and my English family for their unconditional support and understanding, and for giving me a second home.

Abbreviations

2-Deoxyglucose	2-DG
Initiation factor 4E-binding protein	4E-BP1
Adrenomedullin	ADM
Anion exchangers	AEs
Aldolase A	ALD-A
Aldehyde dehydrogenase 1	ALDH 1
Angiopoietin-like 4	ANGPTL4
Activating protein 1	AP1
Alternative reading frame	ARF
Adenosine triphosphate	ATP
Bromodomain and extra-terminal (protein)	BET
Basic helix-loop-helix	bHLH
Basic Kruppel-like factor	BKLF
Breast cancer 1/2	BRCA1/2
Bromodeoxyuridine/fluorodeoxyuridine	BrdU
Bovine serum albumin	BSA
Carbonic anhydrase 9	CA9
Clear cell renal cell carcinoma	ccRCC
CREB-binding protein	CBP
Chemokine CC-chemokine ligand 28	CCL28
Chromatin immunoprecipitation	ChIP
Chemotherapy	ChT
Cancer stem cell-like cells	CSCs
C-terminal binding proteins	CtBPs

C-terminal transactivation domain	C-TAD
Dulbecco's Modified Eagle Medium	DMEM
Dimethyloxalylglycine	DMOG
Enhancer box	E-box
Extracellular acidification rate	ECAR
Egl-9 homolog 3	EGLN3
Epithelial-mesenchymal transition	EMT
Erythropoietin	EPO
Oestrogen Receptor	ER
Extracellular Signal-regulated kinase	ERK
Endocrine therapy	ET
Flavin adenine dinucleotide	$FADH_2$
Family with Sequence Similarity 162 Member A	FAM162A
Fetal calf serum	FCS
Fluorodeoxyglucose	F-FDG
Factor inhibiting HIF-1	FIH-1
Fructose-6-phosphate	F6P
Fructose-1,6-bisphosphate	F16BP
Granulocyte colony stimulating factor	G-CSF
Growth factor	GF
Glucose	GLUC
Glucose transporter (1)	GLUT (1)
Glutathione	GSH
Glucose-6-phosphate	G6P
Hours	h
Histone	H

Histone acetyl transferase	HAT
Bicarbonate	HCO_3^-
Histone deacetylases	HDACs
Human mouse double minute 2 homolog	HDM2
Human Epithelial Growth Factor Receptor 2	HER2
Hypoxia-inducible factor	HIF
Histone lysine demethylase	HKDMs
Histone lysine methyltransferases	HKMTs
Homeodomain-interacting protein kinase 2	HIPK2
Hexokinases	HKs
Histone methyl transferase	HMTs
Heterochromatin protein 1	HP1
Hypoxia responsive element	HRE
Horseradish peroxidase	HRP
Insulin induced gene 2	INSIG2
Initiation SWI	ISWI
Kruppel-like factor 8	KLF8
L1 cell adhesion molecule	L1CAM
Lactate dehydrogenase A	LDH-A
Lysyl oxidase	LOX
Lysine-specific histone demethylase 1	LSD1
Mitogen-activated protein kinase	MAPK
Myeloid cell leukaemia sequence 1	MCL-1
Monocarboxylate transporters	MCTs
Multidrug resistance 1	MDR1
Myeloid-derived suppressor cells	MDSCs

MAPK/ERK kinase	MEK
Membrane-type 4 matrix metalloproteinase	MMP-4
Mammalian target of rapamycin	mTOR
Na+/H+ exchangers	NHEs
Minutes	min
2-keto-4-methylthio-2-oxo butyrate	MTOB
Nicotinamide adenine dinucleotide	NADH
Na+-dependent Na+/HCO3- co-transporters	NBCs
National Centre for Biotechnology Information	NCBI
Na^+/H^+ exchanger	NHEs
Nitric oxide synthase	nNOS
Octamer-binding transcription factor 4	OCT4
Oestrogen receptor-positive	ER^+
Ornithine decarboxylase	ODC
Oxygen-dependent degradation domain	ODD
Oxidative phosphorylation	OXPHOS
Poly ADP ribose polymerase	PARP
PER-ARNT-SIM	PAS
Phosphate-buffered saline	PBS
PBS-tween	PBS-T
Polycomb group protein	PcG
Progesterone receptor-positive	PR^+
Pyruvate dehydrogenase	PDH
Pyruvate dehydrogenase kinase 1	PDK1
Phosphoenolpyruvate	PEP
Positron emission tomography	PET

Phosphofructokinase 1	PFK1
6-phospho-2-kinase/fructose-2-6-bisphosphatase	PFKFB
Proteoglycan region	PG
Phosphoglycerate kinase 1	PGK1
Programmed death-1	PG-1
Prolyl hydroxyl dehydrogenases	PHDs
pH, extracellular	pH_e
pH, intracellular	pH_i
Propidium iodide	PI
Phosphoinositide3 kinase	PI3K
Pyruvate kinase muscle 1/2	PKM 1/2
Pentose Phosphate Pathway	PPP
Progesterone-receptor-positive	PR^+
Polycomb response elements	PREs
Phosphatase and tensin homolog	PTEN
Permeability transition pore	PTP
Von Hippel-Lindau protein	pVHL
Proline-X-Aspartic acid-Leucine-Serine	PXDLS
Reactive oxygen species	ROS
Rounds per minute	rpm
Receptor tyrosine kinases	RTKs
Regulated in development and DNA damage responses 1	REPP1
Ribosomal protein 6S kinase-1	S6K1
S-adenosylmethionine	SAM
SREBP cleavage-activating proteins	SCAP
Sodium Dodecyl Sulphate Polyacrylamide Gel Electrophoresis	SDS-PAGE

Standard error of mean	SEM
Signalling kinases	SKs
Solute carrier superfamily	SLC family
Sex-determining region Y box 2	SOX2
Specifity protein 1	SP1
Sterol regulatory-binding proteins	SREBPs
Signal transducer and activation of transcription 3	STAT3
Switch/Sucrose Non Fermentable	SWI/SNF
Tricabonic acid cycle	TCA (cycle)
Transcription factor 4	TCF-4
T cell lymphoma invasion and metastasis protein 1	Tiam1
TP53-induced glycolysis and apoptosis regulator	TIGAR
Transmembrane protein 45A	TMEM45A
Triple negative breast cancer	TNBC
Tumour necrosis factor-related apoptosis-inducing ligand	TRAIL
Regulatory T cells	Tregs
Voltage-dependent anion channel	VDAC
Vascular endothelial growth factor	VEGF
Zink finger E-box binding homeobox 1	ZEB1

Chapter 1: Introduction

1.1 A brief introduction into breast cancer

In the year 2012, 1.67 million women were diagnosed with breast cancer. Therefore, breast cancer was the most frequent cancer in women, the most frequent cancer-related death in women in less developed countries, and the second cause of cancer death following lung cancer in the developed world (Ferlay et al., 2013). Therefore, breast cancer remains a major burden of illness and requires further research efforts.

1.1.1 The molecular landscape of breast cancer

Breast cancer is not a single disease entity but rather consists of distinctive molecular subtypes with implications for tumour biology, progression of the disease, prognosis, and therapeutic strategy (reviewed by (Dai et al. 2015). Gene expression studies resulted in the identification of three major subtypes of breast cancers (The Cancer Genome Atlas Network 2012). This classification is based on the expression of oestrogen receptors (ER) and progesterone receptors (PR), the overexpression of human epidermal growth factor receptor 2 (HER2), and the lack of expression of hormone receptors and HER2. Proliferation status is determined by Ki67 expression (Dai et al. 2015; The Cancer Genome Atlas Network 2012). These subtypes differ in their expression of oncogenes and mutations spectrum, such as in the expression of *TP53* (Tab. 1.1). Breast cancers of the luminal A subtype frequently express the wildtype form of *TP53*, whereas luminal B tumours often express oncogenic *TP53*. The mutation rate for *TP53* is even higher in HER2-overexpressing tumours and basal-like breast cancers (The Cancer Genome Atlas Network 2012). This may explain the poor response to chemotherapy in wildtype p53-expressing luminal tumours (Bertheau et al. 2013; Jackson et al. 2012). The role of p53 in HR^+ breast cancers is discussed in greater detail in chapter 6.3.2.

Tab. 1.1: Summary of the characteristics of major breast cancer subtypes.
The information summarised in this table is based on (Dai et al. 2015; Senkus et al. 2015; The Cancer Genome Atlas Network 2012).

Subtype	Receptor profile	Molecular characteristics	Differentiation	Therapy	Prognosis
Luminal A	ER^+PR^+ $HER2^-Ki67^-$	PTEN loss Wildtype p53	Resembles differentiated epithelium	Endocrine therapy (ET)	Good, compared to other subtypes
Luminal B	ER^+PR^+ $HER2^-Ki67^+$ or ER^+PR^+ $HER2^+Ki67^+$	$p53^{-/-}$ or wildtype p53	Resembles differentiated epithelium	ET, chemotherapy (ChT) anti-HER2	Similar to $HER2^+$ positive subtype
$HER2^+$	ER^-PR^- $HER2^+$	$PIK3CA^{mut}$ $p53^{-/-}$	Intermediate/low	ChT, anti-HER2	Poor, due to high grade tumours
Basal-like	$ER^-PR^-HER2^-$, basal $markers^+$	$p53^{-/-}$ *Breast Cancer 1 (BRCA1)* loss PI3K/Akt HIF Myc	low	ChT	Poor, due to aggressive growth and lack of selective therapy

1.1.1.1 Implications for therapy

The distinctive tumour biology of each molecular subtype reflects in the requirement of different treatment strategies (Senkus et al. 2015). Luminal tumours respond to endocrine therapy but show a decreased pathologic complete response (pCR) to neoadjuvant chemotherapy, when compared to $HER2^+$ and basal-like tumours (Dai et al. 2015; Rouzier et al. 2005). There is evidence that endocrine therapy alone is sufficient in patients with localised ER^+ breast cancer, which strongly reduces toxicity of the treatment (Spring et al. 2016). Tumours of the luminal B subtype proliferate faster and patients exhibit a high relapse rate within the first five years post-diagnosis. Therefore, luminal B tumours resemble $HER2^+$ and basal-like tumours in their biology and are additionally treated with chemotherapy (Ades et al. 2014). $HER2^+$ tumours have a poor prognosis due to their aggressive growth (Slamon et al. 1987). However, these tumours respond to chemotherapy, and the development of the HER2-targeting monoclonal antibody trastuzumab majorly improved prognosis for these patients (Smith et al. 2007). Triple negative breast cancers (TNBCs) of basal origin respond to chemotherapy but have the worst prognosis due to the lack of targeted therapies (triple negative paradox) (Carey et al. 2007). Therefore, further research efforts, in order to identify new treatment options and to overcome therapy resistance, are especially important in this subtype of breast cancer.

1.1.2 Basal-like and triple negative breast cancers

Triple negative breast cancers form no homogenous biological subtype and are merely defined by the absence of hormone receptors and HER2 overexpression (Bauer et al. 2007; Denkert et al. 2017). The majority of TNBCs belongs to the basal subgroup of breast cancers (Cheang et al. 2008). Gene expression studies identified various subgroups, but depending on the method that was applied, these subgroups substantially deviate between studies (Burstein et al. 2014; Foulkes et al. 2010; Lehmann et al. 2011). However, recurring themes are differences in infiltrating immune cells, proliferation rate, the expression of androgen receptors, and defects in homologous recombination (reviewed by (Denkert et al. 2017)). Based on the determination of these subgroups, clinical trials are currently performed because patients may benefit from checkpoint inhibitors (Nanda et al. 2016), androgen receptor-targeting therapy (Bonnefoi et al. 2016) or PARP inhibitors (Robson et al. 2017). However, neither of these therapies are available as standard treatments and therefore, TNBC remains challenging to treat.

1.1.3 Hypoxia and the Warburg effect in breast cancer

O_2 only defuses 100-200 µm from the blood capillary (Gatenby et al. 2007). Therefore, tumours quickly outgrow their O_2 supply provided by the blood vessel. In this light, it is not surprising that one third of breast cancers exhibit O_2 levels below 0.3%, compared to the physiological level of 9%. 40% of all breast cancers and 50% of advanced breast cancers exhibit hypoxic cores with negative impact on prognosis and survival (reviewed by (Ward et al. 2013)). On the molecular level, adaptive responses to hypoxia are mediated by the transcription factor hypoxia-inducible factor 1 (HIF-1) (Wang & Semenza 1995). HIF-1 target genes promote the reprogramming of cellular metabolism towards a glycolytic phenotype (Chen et al. 2001; Semenza et al. 1994), invasion and metastasis, pH regulation (McIntyre *et al.*, 2016; Parks and Pouyssegur, 2015; Wykoff et al. 2000), angiogenesis (Forsythe et al. 1996; Garayoa et al. 2000), and de-differentiation (see 1.4 for a detailed introduction). Additionally, hypoxia promotes resistance to radiotherapy due to the lack of sufficient O_2 concentrations which are required to produce lethal concentrations of reactive oxygen species (ROS). Hypoxia also promotes resistance to chemotherapy which targets highly proliferating cells because of the reduced rate of cell proliferation caused by hypoxia (Ward et al. 2013). Therefore, there is a strong therapeutic need for developing hypoxia-targeting therapies in order to overcome resistance, and to improve disease outcome.

The upregulation of glycolysis in cancer cells in a hypoxia-dependent or -independent manner was first described by Otto Warburg. He also noticed an increase in glycolysis with increasing degree

of malignancy (Warburg 1924; Warburg et al. 1927). *In memoriam* to his pioneering work, this observation was coined the "Warburg effect". It is now appreciated that cancer cells rely on glycolytic metabolism to enable rapid biomass production as many intermediates of glycolysis are precursors of macromolecules and are fed into other anabolic pathways (reviewed by (Thompson 2011)). Additionally, glycolysis generates nicotinamide adenine dinucleotide phosphate (NADH). NADH is an important cofactor and reducing power for metabolic enzymes, which also acts as antioxidant. This is of high importance for tumour cells in order to counteract the high amount of reactive oxygen species (ROS) derived from mitochondrial metabolism in hypoxia (Chandel et al. 2000) or from radiation-induced re-oxygenation (Moeller et al. 2004).

It is more and more appreciated that glycolysis plays an important role in growth and survival in poorly oxygenized and vascularized regions within a tumour. Additionally, glycolysis is an important factor for driving tumour development towards an invasive phenotype by providing a survival advantage under hypoxic and acidic conditions (Gatenby et al. 2007; Ibrahim-Hashim et al. 2017). Consequently, tumor cell glycolysis and hypoxia are major driving forces of tumorigenesis (Gatenby et al. 2007).

As evaluated above, tumour hypoxia and upregulated glycolysis are of high clinical relevance. Increased HIF-1α expression correlates with reduced disease-free survival and increased likelihood of chemotherapy failure in ER^+ breast cancers (Generali et al. 2006). HIF-1α expression also correlates with tumour aggressiveness in $HER2^+$ breast cancer patients (Giatromanolaki et al. 2004), and with early relapse in a cohort of unselected patients (Dales et al. 2005). These findings are confirmed by (Tan et al. 2009), who determined that the hypoxia marker carbonic anhydrase 9 (CA9; see section 1.6) is highly expressed in $HER2^+$ and basal cancers, and correlates with high grade, ER-negativity, reduced overall survival, and resistance to chemotherapy.

Invasive breast cancers, especially $HER2^+$ and basal-like subtypes, show strongly upregulated glycolysis. Clinically, this reflects in increased fluorodeoxyglucose (FDG) uptake of TNBCs compared to HR^+ cancers (Basu et al. 2008; Groheux et al. 2012), and in the increased expression of the glycolytic markers glucose transporter 1 (GLUT1) (Kang et al. 2002) and monocarboxylate transporter 1 (MCT1) (Pinheiro et al. 2010) in HR^- and basal-like subtypes. The upregulated expression of glycolytic markers also correlates with increased metastasis, reduced disease-free survival, and reduced overall survival. In this light, tumour hypoxia and glycolysis are promising therapeutic targets, especially in triple negative breast cancers and basal-like subtypes where no selective therapies are currently available. Importantly, genetic signatures and mutation frequencies are highly heterogeneous in these tumours, whereas HIF-target genes, such as CA9 and GLUT1, are overexpressed throughout different subtypes (The Cancer Genome Atlas Network

2012). Therefore, the targeting of tumour hypoxia and glycolysis is a promising therapeutic approach in basal-like and TNBC, showing encouraging results in preclinical studies (Ward et al. 2013).

1.2 Glucose metabolism is strictly regulated in mammalian cells

The oxidation of glucose is a vital source of energy for eukaryotic cells and glucose is precursor for glycoproteins, triglycerides and glycogen. However, mammalian metabolism is strictly regulated in order to prevent autonomous cell growth and division.

1.2.1 Glucose metabolism in cellular homeostasis

In the quiescent state, cells only exhibit basal rates of glycolysis and rely on oxidative phosphorylation (OXPHOS) as their main energy source (reviewed by (Vander Heiden et al. 2009)). Consequently, pyruvate is a substrate for pyruvate dehydrogenase (PDH) which mediates the conversion of pyruvate into acetyl-coA that is fed into the tricabonic acid cycle (TCA) (reviewed by (Cairns et al. 2011)). NADH and Flavin Adenine Dinucleotide ($FADH_2$) are fed into oxidative phosphorylation within the mitochondrial membrane. Oxidative phosphorylation comprises a chemiosmotic cycle which is driven by the transport of electrons within the inner membrane of mitochondria in order to produce adenosine triphosphate (ATP) and CO_2 (Buchakjian & Kornbluth 2010). Proliferating signals such as high concentrations of glucose or insulin activate receptor tyrosine kinases (RTKs) or G- protein-coupled receptors. Both promote glucose uptake by increasing the expression of GLUT1 at the cell surface via signalling through phosphoinositide3 kinase (PI3K) and Akt (Rathmell et al. 2003). Alternatively, Akt mediates the upregulation of *GLUT1* mRNA through mammalian target of rapamycin (mTOR) signalling (Taha et al. 1999).

Oncogenic signalling is fundamentally involved in the reprogramming of cancer cell metabolism and is discussed in greater detail in the sections below. The increase in glucose uptake initiated by proliferation signals leads to an increased flux of glucose through glycolysis (Thompson 2011). In proliferating non-cancerous cells pyruvate has two fates. First, it can be reversibly converted into lactate by lactate dehydrogenase (LDH) in the cytosol and extruded by MCTs (Dimmer et al. 2000). Alternatively, pyruvate is converted into acetyl-CoA by pyruvate dehydrogenase and enters mitochondrial metabolism. Acetyl-CoA is fed into the TCA cycle where it serves as precursor for fatty acid synthesis and the generation of ATP via oxidative phosphorylation (reviewed by (Cairns et al. 2011)).

1.2.2 Regulatory mechanisms of glycolysis

Glycolysis is strictly regulated by various mechanisms. The first rate-limiting step is the GLUT-mediated uptake of glucose (Ren et al. 1993). The next rate-limiting step is the phosphorylation of glucose into glucose-6-phosphate (G6P) by hexokinases (HKs). There are four isoforms in mammals with various tissue distributions (reviewed by (Robey & Hay 2006). HK1 and HK2 are the most prominent isoforms whereas HK2 plays an important role in maintaining the glycolytic flux in cancer (Bustamante et al. 1981; Liu et al. 2017). HK4 (glucokinase) is expressed in the liver and the pancreas (German 1993). Another rate-limiting enzyme is phosphofructokinase 1 (PFK1) which controls the reversible conversion of fructose-6-phosphate (F6P) into fructose-1,6-bisphosphate (F16BP) and therefore the flux of glucose-derived carbon through glycolysis (Zancan et al. 2010).

Downstream of PFK1, pyruvate kinase (PK) converts phosphoenolpyruvate into pyruvate (Zammit et al. 1978). The isoform PK muscle (PKM) is the most common isoform and exists in the alternative splice variants PKM1 and PKM2. The isoform PKM1 is expressed in adult tissues, whereas PKM2 is found in embryonic tissues and cancers (Christofk et al. 2008). The PKM isoform decides the fate of pyruvate and therefore is an important rate-limiting glycolytic enzyme. PKM1 promotes the feeding of pyruvate into the TCA cycle, whereas PKM2 inhibits pyruvate dehydrogenase and therefore maintains glycolysis (Christofk et al. 2008). The role of PKM2 in cancer is discussed in greater detail below. Additionally, pyruvate dehydrogenase kinase 1 (PDK1) prevents pyruvate from entering the TCA cycle by inhibiting PDH (McFate et al. 2008; Kim et al. 2006).

Lactate concentrations also regulate glycolytic flux. LDH reversibly converts pyruvate into lactate which is removed by MCTs, thereby maintaining glycolytic phenotype and promoting tumour growth (Doherty et al. 2014; Fantin et al. 2006). Most importantly, glycolysis is also regulated at the transcriptional level. This will be illustrated in the context of malignant reprogramming of glycolysis in the sections 1.3 and 1.4.

1.3 Cancer cell metabolism is modified to promote tumour growth and survival

Cancer cells drastically differ in their metabolism as they overcome controls that normally block proliferation under stressful metabolic conditions. Additionally, cancer cells have increased biosynthetic demands due to increased cell proliferation and division. Furthermore, cancer cells are exposed to increased concentrations of ROS which requires the enhanced synthesis of reducing equivalents. Cancer cells also rely on rapid ATP generation to maintain their energy status (reviewed by (Thompson 2011)).

In reference to the hallmarks of cancer defined by (Hanahan & Weinberg 2011), (Pavlova & Thompson 2016) identified three hallmarks of tumour cell metabolism. First, cancer cell metabolism is characterised by oncogene-directed nutrient uptake which leads to deregulated uptake of glucose and amino acids such as glutamine and to opportunistic modes of nutrient acquisition. Second, the reprogramming of intracellular metabolism is characterised by the utilisation of metabolites for biosynthesis and NADPH production as well as by an increased demand for nitrogen. The third hallmark comprises a metabolite-directed change in cell behaviour and function, which is accompanied by alteration of metabolite-driven gene regulation and interaction with the microenvironment.

The uncoupling of cytosolic glycolysis from the mitochondrial TCA cycle and OXPHOS is a prominent feature of metabolic reprogramming (Christofk 2008; Gaglio et al. 2011; Meierhofer et al. 2004). Cancer cells upregulate other metabolic pathways including the pentose phosphate pathway (PPP) for the generation of nucleotide precursors (Boros et al. 2000; Ying et al. 2012) and reducing equivalents (Ros et al. 2012), and glutaminolysis (Wise et al. 2008). During glutaminolysis, glutamine is converted into glutamate by deamination and further converted into α-ketoglutarate which is fed into the TCA cycle in order to generate ATP, and to provide precursors for the synthesis of amino acids, nucleotides, lipids and reducing equivalents (Schulze & Harris 2012). This pathway is upregulated in many cancer cells (Gaglio et al. 2011; Jin et al. 2015; Reitzer et al. 1979). However, this thesis focuses on glycolysis as the driving forces of tumorigenesis by modulating the transcription of genes relevant for tumour progression; directly via metabolites or indirectly via the activation of transcriptional co-regulators.

1.3.1 Cancer cells exhibit deregulated glucose uptake

(Warburg 1924) first described that tumours produce more lactate and exhibit increased glycolysis in anoxia, compared to blood or frog muscle. However, when tumour tissue was transferred into normoxic conditions glycolysis was only slightly reduced. Additionally, he discovered that malignant tumours produce three to four times more lactate than benign tumours. Therefore, the rate of glycolysis corresponds with the degree of malignancy. Further, he discovered that cancers are highly addicted to glucose as tumour-derived tissues consume 70 mg glucose/ 100 cc blood, compared to 2-16 mg in non-cancerous tissue, from which 66% is utilized for glycolysis (Warburg et al. 1927). In memoriam to Otto Warburg, the observation that cancer cells exhibit upregulated glycolysis in normoxia is coined the Warburg effect. The Warburg effect is of clinical relevance as it is applied in tumour diagnosis, staging and monitoring where glucose uptake is visualised by positron emission tomography (PET)-based imaging of the radioactive fluorine-labelled glucose analogue F-fluorodeoxyglucose (F-FDG) (Endo et al. 2006). Corresponding to Warburg's findings, the increased uptake of glucose correlates with poor prognosis (Groheux et al. 2012).

1.3.2 Uncoupled glycolysis in cancer cells promotes malignant progression

Cancer cells actively uncouple glycolysis from mitochondrial metabolism to support the synthesis of macromolecules and reducing equivalents as well as to reduce ROS generation (Cairns et al. 2011). Oncogenic signalling contributes to this process. The oncogenic activation of PI3K is mediated by inactivating mutations of its inhibitor phosphatase and tensin homolog (PTEN) (Li et al. 1997), via activating mutations in its catalytic domain (PI3KCA) (Samuels et al. 2004) or mutations in its upstream receptors (Moscatello et al. 1998). Both, constitutive signalling via PI3KCA and via its downstream effector Akt is sufficient to drive cancer cells towards a glycolytic phenotype, and to induce a strong dependence on glucose for cell growth and survival (Elstrom et al. 2004; Foster et al. 2012). Metabolic reprogramming mediated by Akt also plays a crucial role in preventing apoptosis and in supporting growth factor-independent growth as constitutively active Akt1 promotes the translocation of GLUT1 to the cell membrane and sustains its expression. This results in Akt-dependent increase in glucose uptake and subsequently enhanced HK1 activity, which prevents conformational changes in Bax upon growth factor withdrawal, and consequently protects cells from apoptosis (Rathmell et al. 2003).

Alternatively, Ras-mediated transformation reprograms metabolism by increasing glycolytic flux and by inhibiting the TCA cycle (Gaglio et al. 2011). However, the central role of oncogenic signalling in metabolic reprogramming lies in the hypoxia- and pVHL-independent activation of

HIF which regulates the expression of key metabolic proteins such as GLUT1 (Chen et al. 2001), HK2 (Kim et al. 2007; Mathupala et al. 2001), PDK1 (Dupuy et al. 2015; Kim et al. 2006), *Lactate dehydrogenase A* (LDH-A) (Ebert 1995; Semenza et al. 1994) and MCT4 (Ullah et al. 2006), and thus promoting HIF-mediated metabolic reprogramming and tumour progression (Fig. 1.1). Hypoxia-independent stabilisation of HIF is illustrated in greater detail in the section 1.4.2.

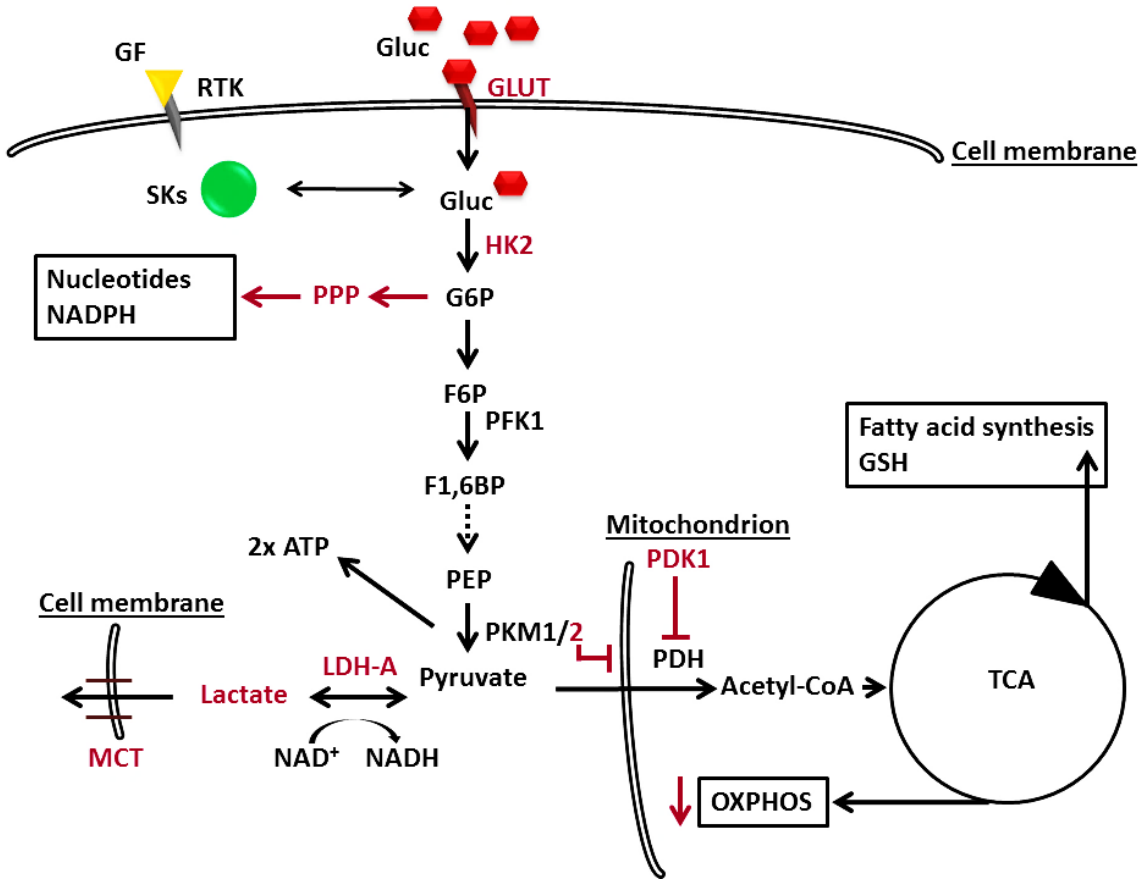

Fig. 1.1: The reprogramming of glucose metabolism by oncogenic signalling and HIF-1. Oncogenic activation of receptor tyrosine kinases and signalling kinases augments the uptake of glucose and glycolysis in a manner dependent or independent from HIF-1. Mechanisms dependent and independent from O_2 stabilise HIF-1 which in turn mediates glucose flux through glycolysis via the activation of rate-limiting proteins (purple). The upregulation of GLUTs increases glucose uptake, whereas enhanced HK2 expression upregulates glycolytic flux by increasing the turnover of glucose into glucose-6-phophate which can be alternatively fed into the PPP to generate nucleotide precursors and reducing equivalents. Glycolytic flux is maintained by suppressing OXPHOS and by directing pyruvate towards the conversion into lactate. Cancer cells express PKM2 instead of PKM1 which inhibits pyruvate translocation to the mitochondrion. Additionally, PDK1 inhibits PDH which prevents the conversion of pyruvate into Acetyl-CoA. Glycolytic flux is further maintained by upregulated LDH-A which preferentially converts pyruvate into lactate and by MCTS transporting lactate out of the cell. Key: GF, growth factor; RTK, receptor tyrosine kinase; SKs, signalling kinases, Gluc, glucose; GLUTs, glucose transporters; HK2, hexokinase 2; G6P, glucose-6-phosphate; F6P, fructose-6-phosphate; PFK1, phosphofructokinase 1; F1,6,BP, fructose-1,6,-bispohosphate; PEP, phosphoenolpyruvate; PKM1/2, pyruvate kinase muscle 1/2; PDK1, pyruvate kinase 1; PDH, pyruvate dehydrogenase; GSH, glutathione; LDH-A, lactate dehydrogenase A; MCT, monocarboxylate transporter. This image is based on (Schulze & Harris 2012).

An additional transcriptional control mechanism is the regulation of glycolytic flux by the transcription factor p53. p53 activates the expression of TP53-induced glycolysis and apoptosis regulator (TIGAR) which reduces levels of F26BP and thus inhibits glycolysis and protects cells from ROS-induced apoptosis (Bensaad et al. 2006). Additionally, p53 inhibits the expression of GLUT1 and GLUT4, thereby inhibiting glycolysis by reducing glucose uptake (Schwartzenberg-bar-yoseph et al. 2004). However, p53 wildtype function is commonly lost in cancers (Bergh et al. 1995; Rodrigues et al. 1990; Vollan et al. 2015). Therefore, loss of p53 function promotes metabolic reprogramming by losing inhibitory control mechanisms of glycolysis.

The transcription factor c-Myc also promotes metabolic reprogramming. c-Myc promotes glycolysis by activating the transcription of *GLUT1* and *PFK1* (Osthus et al. 2000). In cooperation with HIF, c-Myc activates the transcription of *HK2* and *PDK1*, thereby promoting sustained glycolysis (Kim et al. 2007). Additionally, c-Myc controls the expression of *MCT1* which is required to maintain glycolytic flux and glutathione synthesis in order to prevent ROS-induced cell death (Doherty et al. 2014). *LDHA* is also a c-Myc target gene. In pancreatic cancer, c-Myc-LDH-A-mediated signalling promotes glucose consumption and lactate production, resulting in tumour growth and metastasis (He et al. 2015). Additionally, c-Myc expression also promotes glutaminolysis and drives cells towards glutamine addiction. This results in increased glutamine uptake which is not fed into protein synthesis, but into lactate production (Wise et al. 2008).

1.4 Hypoxia-inducible factors in oxygen sensing and tumour progression

Physiologists and clinicians define hypoxia as a state of reduced O_2 availability or O_2 pressure below a tissue specific threshold leading to the abolishment or restriction of organ, tissue or cell function; often visible as necrosis. Anoxia on the other hand is defined as the complete absence of O_2 within a tissue. However, cancerous tissues have lost their physiological functions and therefore this loss-of-function criterion cannot be applied to tumours even though necrosis is commonly found in hypoxic areas. Therefore, the definition of hypoxia in tumours is complex (reviewed by (Höckel & Vaupel 2001)). In this work, hypoxia is defined as the O_2 tension that is required to induce HIF activation and the expression of its target genes as adaptive response to low concentrations of O_2.

1.4.1 Cells adapt to low oxygen levels by activating Hypoxia-inducible factors

Tumour cells grow distant from the blood vessel and are separated from their O_2 supply via their basement membranes. This causes a drastic drop in O_2 concentration, as close as five cell diameters away from the blood vessel. Further, O_2 has a limited diffusion capacity of 100 µm (Gatenby et al. 2007). Mal-formed blood vessels with irregular perfusion or the absence of angiogenesis further contribute to tumour hypoxia. These processes create a heterogeneous environment in which hypoxic areas can be found across the tumour. Within these areas hypoxia can be chronic, acute, or intermittent (Höckel & Vaupel 2001).

Cellular adaptions to hypoxia are mediated by the heterodimeric transcription HIF (Fig. 1.2). HIF-1 is formed by two subunits which both bind DNA. The subunit HIF-1α comprises 120 kDa and the slightly smaller subunit HIF-1β spans 91-94 kDa (Wang & Semenza 1995). Both subunits contain basic helix-loop-helix (bHLH) and (PER-ARNT-SIM) PAS domains (Wang et al. 1995). The bHLH domains mediate DNA binding, whereas the PAS domains mediate dimerization. The stability of HIF-α is mediated via the oxygen-dependent degradation domain (ODD). It controls HIF activity by degradation via the ubiquitin-proteasome pathway (Huang et al. 1998; Yu et al. 2001). The ODD was identified as a 200 amino acid long sequence in the central region of HIF-1α, and deletion of this region alone stabilises HIF-1α protein in normoxia. Similarly, expression of the ODD alone gives rise to oxygen-instable proteins when fused to proteins (Huang et al. 1998). The ODD mediates HIF-1α stabilisation via the hydroxylation of proline residue 564 within the ODD, which is required for the binding of von Hippel-Lindau protein and HIF-1α degradation in normoxia (Yu et al. 2001). The C-terminal transactivation domain (C-TAD) enables the binding of the co-activator complex and histone acetyl transferase p300/CREB-binding protein (CBP) (D. Lando et al. 2002). HIF-1α is the most studied isoform and mediates acute responses to (tumour) hypoxia,

whereas the expression of HIF-2α seems to be restricted to cells within high energy-consuming tissues such as glial cells, cardiomyocytes, hepatocytes or kidney fibroblasts (Wiesener et al. 2003). Target gene selectivity between HIF-1 and HIF-2 is not determined by their DNA-binding domain but via the difference in their C-terminal transactivation domains, which differs in each isoform (Lau et al. 2007). The function of HIF-3α however, is less clear. It lacks the transactivation domain and was thought to act as a dominant negative by preventing the dimerization of HIF-1 α and β (Makino et al. 2001). Interestingly, newer research has shown that HIF-3 also activates target gene expression via the recognition of HREs in an oxygen-responsive manner. HIF-1 and HIF-3 target genes overlap but HIF-3 also selectively regulates target genes such as *Regulated in development and DNA damage responses 1* (*REDD1)* (Zhang et al. 2014). Therefore, HIF-1 and HIF-3 exert overlapping but selective functions in the regulation of HIF-target genes, which questions the role of HIF-3 as sole inhibitor of HIF-1/2 function.

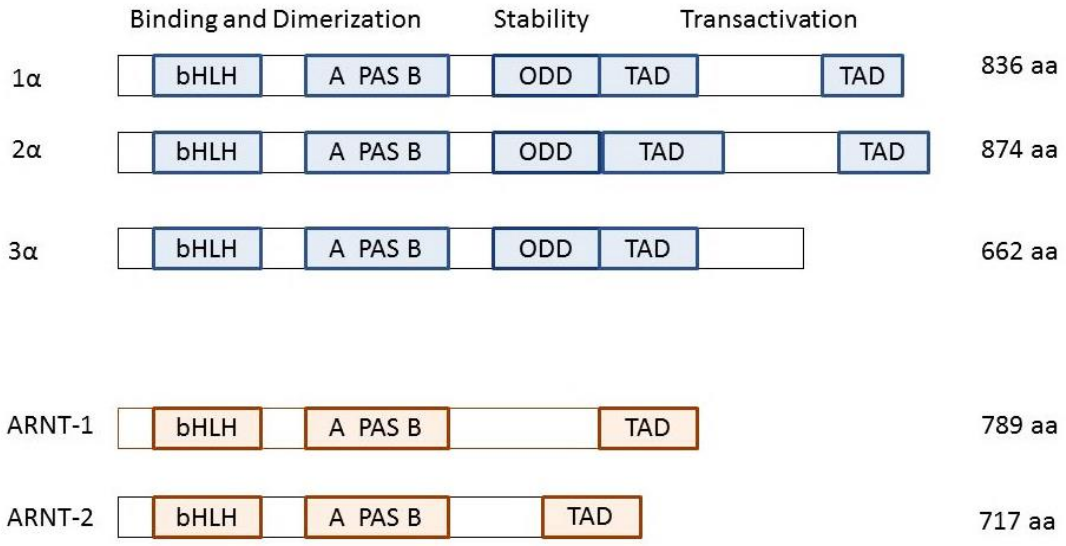

Fig. 1.2: The functional domains of HIF family members. The basic helix loop helix and PAS domain are involved in dimerization and binding to DNA. The α-subunit uniquely contains an oxygen-dependent degradation domain (ODD) which is involved in protein stability. Furthermore, HIF-1α and HIF2α possess two transactivation domains (TAD), whereas all other isoforms only possess one. Numbers represent the position of amino acids. This image was modified after (Rankin & Giaccia 2008).

(Semenza & Wang 1992) described for the first time that hypoxia upregulates *erythropoietin* (*EPO*) expression in human hepatocarcinoma cells by up to 50-fold via the activation of a nuclear factor. The subunits of HIF are produced by *de novo* protein synthesis (Wang & Semenza 1993a) and are regulated via posttranslational modifications of HIF-α in normoxia (Wang et al. 1995; Wang & Semenza 1995).

In the presence of oxygen, prolyl hydroxylases hydroxylate the proline residues P564 and P402 in HIF-1α and P530 and P405 in HIF-2α (Ivan et al. 2001; Yu et al. 2001). PHDs are also important regulators of HIF-1 activity in hypoxia as the isoforms PHD2 and PHD3 are HIF-1 target genes (Henze et al. 2010; Marxsen et al. 2004; Pescador et al. 2005). PHD2 and PHD3, induced by chronic hypoxia, control HIF-1α levels which protects cells from hypoxia-induced cell death (Henze et al. 2010). Moreover, the HIF-induced expression of PHD2 and PHD3 enables the rapid degradation of the HIF-1α subunit after reoxygenation as the hydroxylation in hypoxia decreases the half-life of HIF-1α and therefore avoids pathological activation of HIF in normoxia (Henze et al. 2010; Marxsen et al. 2004). Proline hydroxylation at the ODD enables the binding of pVHL which is part of an E3 ligase complex formed by elongin C, elongin B, Cul2 and RB1/Ruc1 (Jaakkola et al. 2001). The pVHL binds the HIF-α subunit with its β-domain and elongin C with its α-domain, therefore acting as an adaptor between HIF-α and the E3 ubiquitin ligase complex. Following the binding of HIF-α with pVHL, HIF-α is ubiquitinated and degraded via proteosomal degradation (Ohh et al. 2000). Additionally, the asparagyl hydroxylase factor inhibiting HIF-1 (FIH-1) hydroxylates asparagine residue N803 (1α) or N851 (2α) located within the C-terminal transactivation domain. This prevents the recruitment of the p300/CBP complex (Lando 2002a; Lando et al. 2002b).

PHD activity is strictly dependent on iron and oxygen (Ivan et al. 2001). Consequently, when O_2 levels drop below physiological thresholds or cells are depleted of iron, the HIF-α subunit is stabilised due to inactivated PHDs. This enables the translocation of HIF-1α to the nucleus where it binds to constitutively expressed HIF-β. Consequently, the heterodimer binds to the consensus sequence 5' TACGTGCT3' within the hypoxia responsive elements (HREs) of HIF target gene promoters (Bos *et al*. 2001).

However, the dimerization of HIF-1α and HIF-1β is not sufficient to induce strong activation of HIF-1 target gene transcription (Arany et al. 1996; Ebert & Bunn 1998). Therefore, HIF binds with the co-activator complex p300/CBP (Fig. 1.3). The p300/CBP co-activator complex not only functions as adaptor but also functions as histone acetyl transferase (HAT) by acetylating all four core histones in nucleosomes (Ogryzko et al. 1996). This HAT activity exerted by p300/CBP was demonstrated to be crucial for the transcriptional regulation of many, but not all, HIF target genes

(Kasper et al. 2005). As mentioned above, HIF was discovered as activator of *EPO* transcription in hypoxic hepatocarcinoma cells. However, soon after its discovery, transcription of the glycolytic enzymes *aldolase A* (*ALD-A*), *phosphoglycerate kinase 1* (*PGK1*), *PKM*, *LDH-A*, *PFK*, and the pro-angiogenic factor *VEGF* were identified to be activated by HIF-1 in non EPO-producing mammalian cells via a similar mechanism (Wang &Semenza 1993b; Semenza et al. 1994; Forsythe et al. 1996).

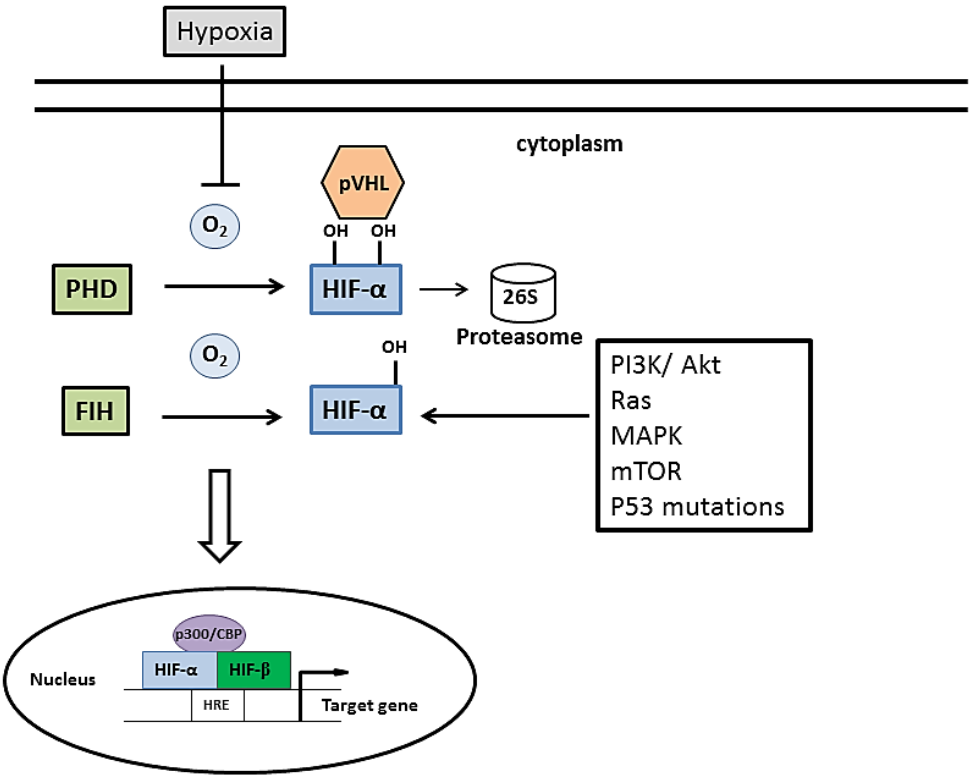

Fig. 1.3: The HIF-α subunit is stabilized by hypoxia-dependent and –independent mechanisms. This enables translocation to the nucleus where it binds its HIF-β subunit and the co-activator complex p300/ CBP. The transcription of target genes is initiated via the binding of HIF to hypoxia responsive elements (HRE) of HIF target genes. This image is based on (Rankin & Giaccia 2008).

1.4.2 Oxygen-independent mechanisms of HIF-stabilisation

Additionally to its activation by O_2, HIF is also activated by oxygen-independent mechanisms. This includes the activation by dysfunctional pVHL. Somatic mutations in pVHL abolish the binding to HIF-α, which causes the constitutive activation of HIF commonly found in renal clear cell carcinoma (Krieg et al. 2000). In this context, (Wiesener et al. 2001) demonstrated that the constitutive and dose-dependent activation of the HIF-1 target genes *VEGF* and *GLUT1* is induced by impaired pVHL as it is only found in renal cancer cells exhibiting mutations in pVHL. Additionally, hereditary mutations of pVHL in the von Hippel-Lindau disease contribute to the formation of highly vascularised tumours that overexpress *CA9* and *GLUT1* due to constitutive activation of HIF in normoxia (Mandriota et al. 2002).

Alternatively, the metabolites lactate and pyruvate stabilize HIF-1α in normoxia via the competitive inhibition of PHDs. Lactate is converted back into pyruvate by LDH-A which consequently stabilizes the HIf-1α protein, resulting in the activation of the HIF-target genes *VEGF*, *EPO*, *GLUT3* and *ALDA* (Lu et al. 2002). This is mediated by the competitive binding of pyruvate to the active site of PHDs as the pyruvate-induced stabilisation of HIF-1α and subsequent activation of a HRE-containing promoter construct is reversed by ascorbate *in vitro* (Lu et al. 2005). The pyruvate-mediated stabilisation of HIF-1 is mediated by pyruvate dehydrogenase kinases phosphorylating the PDH subunit PDH e1α (PDHα). This results in reduced pyruvate dehydrogenase complex (PDC) activity and to subsequent HIF-1α stabilisation by glucose or glycolytic metabolites (McFate et al. 2008). (McFate et al. 2008) demonstrated that PDK1-mediated HIF stabilisation contributes to a more invasive phenotype in head and neck cancer cells *in vitro.* The silencing of *PDK1* by siRNA reduces colony forming in soft agar, VEGF secretion, the invasion of Matrigel™-coated Boyden chambers, and enhances cell death in hypoxia. These findings are replicated *in vivo* as *PDK1* silencing causes a strong reduction of xenograft growth and vascularisation, as well as of phosphorylation of PDHα. Consequently, glycolysis-derived metabolites feed into a positive feedback loop fuelling malignant progression by stabilising HIF-1α in normoxia (McFate et al. 2008). Lactate was also found to directly stabilise HIF-1α by inhibiting PHD2 in a competitive manner. However, this was restricted to primary cancer cells and cell lines mainly relying on oxidative phosphorylation rather than glycolysis (de Saedeleer et al. 2012).

ROS also stabilize HIF-1α. Oxidative stress derived from oncogenic H-ras^{V12} signalling in normoxia promotes PHD2 homo-dimerization via the formation of disulphide bonds and thus inactivating PHD activity. This stabilizes HIF-1α and enables translocation to the nucleus, activation of HIF-target genes, resulting in aerobic glycolysis and lactate production. This is reversible by *PHD2* silencing or by treatment with antioxidants (Lee et al. 2016). Another major source for oxidative

stress is mitochondrial-derived ROS in hypoxia. Hypoxia induces superoxide generation at mitochondrial complex III which is catalysed into H_2O_2 by superoxide dismutase in the cytoplasm and results in the stabilisation HIF-1α (Chandel et al. 2000). A central tumour-relevant source for ROS is not derived from the tumour itself but is a consequence of radiation-induced reoxygenation. ROS generated upon reoxygenation stabilizes HIF-1α and leads to increased accumulation in the nucleus and enhanced VEGF secretion which protects vasculature from radiation-induced damage (Moeller et al. 2004). Consequently, the stabilisation and activation of HIF-1α by ROS-generation is an important factor in HIF-mediated therapy resistance.

HIF is also activated by oncogenic signalling which mainly contributes to malignant transformation within tissues. In this context, epidermal growth factor-induced PI3K/Akt/FRAP signalling activates HIF-1 in normoxia and induces VEGF secretion in prostate cancer cells (Zhong et al. 2000). (Laughner et al. 2001) demonstrated that HER2 overexpression in murine 3T3 cells or induction of HER2 signalling by heregalin in MCF7 breast cancer cells also stabilizes HIF-1α via the same pathway and thereby promotes angiogenesis. Alternatively, loss of function of the Akt inhibitor PTEN also induces HIF-1α activation via growth factor-activated PI3K-Akt signalling which is augmented by hypoxia (Zundel et al. 2000). Importantly, HIF-1α stabilisation via the PI3K-RAS signalling pathway contributes to the maintenance of glycolytic flux. (Chen et al. 2001) demonstrated that PI3K via activated H-Ras stabilizes HIF-1α in normoxia and induces transcription of *GLUT1* mRNA which is enhanced in hypoxia. Additionally, (Blancher et al. 2001) determined that a specific PI3K inhibitor inhibits HIF-1α mRNA and protein synthesis, and consequently *VEGF* expression in a Ras-dependent manner. The PI3K-Ras-mediated stabilisation was shown to be independent from pVHL as it also occurs in VHL-negative renal carcinoma cells.

Sustained signalling through oncogenic Ras was demonstrated not only to be important for the promotion of HIF-mediated angiogenesis but also for sustained glycolysis as inhibited Ras impairs signalling through PI3K and Akt. As a consequence, the expression of HIF-1α and of the glycolytic enzymes LDH-A, 6-phospho-2-kinase/fructose-2-6bisphosphatase 4 (PFKFB4) and Aldolase C, of the glucose transporter GLUT1 and of VEGF is reduced. Additionally, the inhibition of Ras reduces the glycolytic rate and causes severe energy stress and ATP depletion in glioblastoma multiformes cells. This highlights the role of Ras in sustaining glycolysis (Blum et al. 2005). Extracellular proliferative signalling is transduced via the Ras/Raf/MAPK/ERK kinase (MEK) pathway and results in activation of target genes via extracellular signal-regulated kinases (ERK) ERK1 and ERK2 (p44 and p42) (Brunet et al. 1999; Lenormand et al. 1998; Lange-Carter & Johnson 1994). The inhibition of MEK1 reduces HIF-1 activity in normoxia and hypoxia, the transactivation of HIF-1α, and the interaction with p300/CBP with HIF-1α at the C-terminal transactivation domain in hypoxia. Consequently, Mitogen-activated protein kinase (MAPK)-signalling promotes the interaction

between CBP/p300 and HIF-1α, and therefore fine-tunes the response to hypoxia (Sang et al. 2003). Additionally, ERK1 and ERK2 were demonstrated to phosphorylate HIF-1α independent from hypoxia increasing basal levels of HIF-1α transcription in quiescent Chinese hamster fibroblasts and to induce transcription of *VEGF* (Richard et al. 1999). This phosphorylation is mediated by ERK2 (p42) at Serine residue 641 and 643, thereby promoting the nuclear accumulation and activity of HIF-1α (Mylonis et al. 2006).

Alternatively, HIF is activated as signalling target downstream of mTOR. On the transcriptional level, mTORC1 enhances the transcription of Hif1α mRNA in hypoxia by phosphorylating signal transducer and activation of transcription 3 (STAT3) on serine residue 727 (Ser727). On the translational level, mTORC1 promotes the accumulation of HIF-1α protein by increasing translation of HIF-1α mRNA by ribosomal protein 6S kinase-1 (S6K1) which promotes translation by phosphorylating initiation factors. Additionally, HIF-1α translation is promoted by binding of the initiation factor 4E-binding protein (4E-BP1). Consequently, S6K1, 4E-BP1 and STAT3 act in concert to promote the mTOR-dependent activation of *VEGF* and therefore promote angiogenesis (Dodd et al. 2015).

1.4.3 HIF-1-mediated glycolysis is a driving force of tumorigenesis

HIF-1 mediated responses play an important role in cancer as 50-60% of solid tumours contain areas of hypoxia or anoxia (Vaupel et al. 1991). Furthermore, HIF 1α and 2α are overexpressed in the perinecrotic areas of many cancers where expression levels correlate with advanced stages and poorly differentiated lesions with high proliferation (Talks *et al*. 2000; Bos *et al.* 2001). Under physiological conditions, HIF-1-mediated responses protect organs from ischemia (Feinman *et al*. 2010). In cancer however, the overexpression of HIF-1α and its target genes is associated with reduced overall survival and poor prognosis due to increased resistance to radiotherapy (Harada et al. 2012), increased invasiveness (Zhang et al. 2012) and angiogenesis (Cao et al. 2009), the maintenance of stem cell-like features (Mathieu et al. 2011), immune evasion (Facciabene et al. 2011) as well as altered metabolism (Papandreou et al. 2006) and pH regulation (McIntyre et al. 2016).

Tumour cells are highly glycolytic compared to non-cancerous and embryonic tissue. This was first described by Otto Warburg (Warburg 1956). As mentioned before, HIF-1 is an important modulator of tumour cell metabolism as HIF-1 target genes encode for genes contributing to the maintenance of glycolytic flux (Baenke et al. 2015; Fantin et al. 2006), the *de novo* synthesis of lipids and nucleic acids (Chesney et al. 1999; Minchenko et al. 2002; Obach et al. 2004), as well as the suppression of mitochondrial respiration and the generation of ROS (Kim et al. 2006) (Fig. 1.4).

The glucose transporter *GLUT1* is a HIF-1 target gene (Ebert et al. 1995). It plays a central role in glucose uptake by cancer cells as the suppression of hypoxia-induced GLUT-1 expression impairs glucose uptake and lactate secretion. Further, growth and migration of hepatocellular carcinoma cells is impaired in *GLUT1*-deficient cells which demonstrates the role of GLUT1 in tumour cell proliferation and migration (Amann et al. 2009). GLUT1 is also overexpressed in a variety of human cancers, including breast cancer (Brown & Wahl 1993), cervical carcinoma (Mendez et al. 2002), and hepatocellular carcinoma (Amann et al. 2009). GLUT1 overexpression correlates with higher proliferation as determined by Ki-67 expression, more advanced tumour stages, and poor differentiation (Amann et al. 2009).

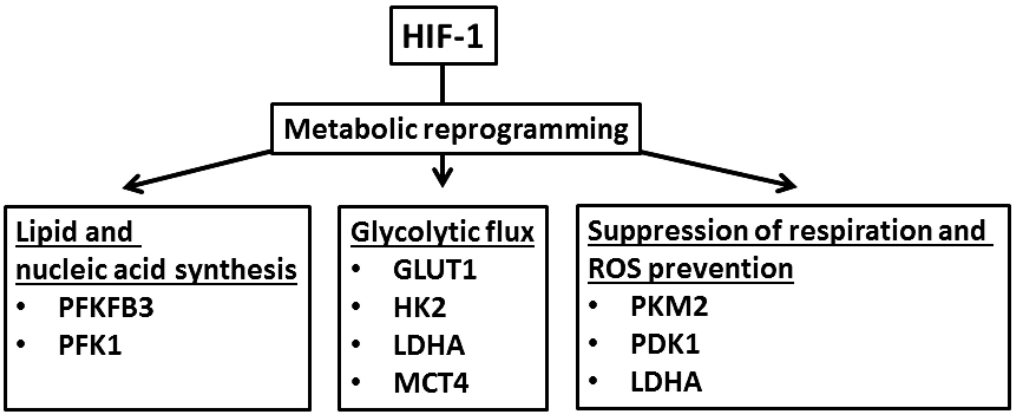

Fig. 1.4: Hypoxia-induced HIF-1 target genes maintain the glycolytic phenotype in cancer cells. HIF-1 target genes also reprogram cellular metabolism to promote lipid and nucleic acid synthesis, suppress the generation of ROS and respiration, thereby driving tumour progression.

The HIF-1 target gene *LDHA* catalyses the reversible conversion of pyruvate into lactate and the recycling of NAD^+. This prevents the generation of ROS and ATP depletion in glycolysis-dependent cancer cells, thereby enabling tumour initiation, progression and proliferation *in vivo* (Le et al. 2010). Additionally, HIF-1-activated LDH-A prevents ROS-induced apoptosis by suppressing mitochondrial oxidative phosphorylation which contributes to cisplatin resistance in ovarian cancer cells *in vitro* (Ai et al. 2016). LDH-A expression also sustains proliferation in hypoxia as the inhibition of LDH-A expression by shRNA impairs proliferation in hypoxia, depletes ATP levels, and reverses glycolysis to mitochondrial respiration. *In vivo*, breast cancer cells lacking LDH-A expression show delayed tumour onset and reduced growth rate compared to control cells, when transplanted into mammary fat pads of mice. Therefore, LDH-A expression is required for tumour progression (Fantin et al. 2006).

MCTs extrude lactate from the cell and are therefore important for the maintenance of the glycolytic flux, and in pH regulation. The isoform MCT4 is induced by HIF-1, whereas MCT1 is not

(Ullah et al. 2006). Most glycolytic cancers overexpress MCT4 where it is an independent prognostic factor for metastatic-free survival. MCT4 expression also correlates with breast cancer aggressiveness as MCT4 expression is the highest in triple negative breast cancers, followed by HER2 overexpressing cancers (50%) and hormone receptor positive cancers which displayed the lowest expression of MCT4 (30%) (Doyen et al. 2014). An unbiased functional RNA screen in breast cancer cells performed by (Baenke et al. 2015) identified MCT4 expression as a requirement for tumour cell survival *in vitro* as well as *in vivo*. MCT4 expression supports redox balance, pH regulation and metabolite transport whereas MCT4-depleted cells are unable to form spheroids or to initiate xenograft growth *in vivo*. Further, MCT4-depleted cells exhibit increased oxidative metabolism and upregulated glutaminolysis.

HIF-1 target genes also contribute to maintaining glycolytic flux by actively suppressing the TCA cycle and mitochondrial respiration. In this context, hypoxia-induced PDK1 reduces the entry of pyruvate into the TCA cycle by inhibiting pyruvate dehydrogenase. This leads to increased conversion of pyruvate into lactate and reduced mitochondrial oxygen consumption (Papandreou et al. 2006). PDK1 also reduces the delivery of NADH and $FADH_2$ to the electron transport chain in the outer mitochondrial membrane which provides protection from ROS-induced apoptosis. (Kim *et al.*, 2006) demonstrated that the overexpression of PDK1 protects murine HIF-1α $^{-/-}$ fibroblasts from ROS-induced apoptosis.

Pyruvate kinase mediates the conversion of phosphoenolpyruvate to pyruvate. Adult tissues express the splice form PKM1, whereas PKM2 is exclusively found in embryonic and cancerous tissues. Consequently, breast and colon cancer tissue expresses PKM2, whereas matched epithelial controls are expressing the M1 splice form. PKM2 expression is associated with increased glucose uptake, lactate production, and reduced respiration which is reversed upon forced expression of PKM1. Further, xenografts expressing PKM2 but not PKM1 are able to induce lung cancer xenograft growth *in vivo* (Christofk et al. 2008). (Luo et al. 2011) identified PKM2 as HIF-target gene but also described PKM2 as co-activator of HIF-1, thus creating a positive feedback loop. Additionally, PKM2 potentially increases the binding of HIF-1α to HREs in the target genes *GLUT1*, *LDHA* and *PDK1*, the binding of p300, and histone acetylation in EpB3 and HeLa cells.

One important function of glycolysis in cancer cells is providing precursors for nucleic acids and lipids to cater the needs of rapidly proliferating and dividing cancer cells (reviewed by (Cairns et al. 2011)). HIF-1 also supports the *de novo* synthesis of nucleic acids as HIF-1 activates the glycolytic regulatory enzyme 6-phospho-2-kinase/fructose-2-6-bisphosphatase (PFKFB) (Minchenko et al. 2002; Obach et al. 2004). The isoform PFKFB3 regulates fructose-2,6-

bispohosphate levels which activate the downstream enzyme PFK1. PFK1 ensures the flow of carbon through the pentose phosphate pathway and therefore mediates the *de novo* synthesis of nucleic acids (Chesney et al. 1999).

The importance of glycolysis for the generation of precursors of macromolecules is highlighted by findings of (Smith et al. 2016). They demonstrated that glycolytic pathways are maintained in even severe hypoxia as tumour spheroids grown in 0.1% oxygen display upregulated glycolysis, HIF-1α and c-Myc expression, as well as increased GLUT and MCT transporter and PFK1 activity. Protein expression and activity of HK2, LDH-A, G6PDH and PKM on the other hand is impaired.

However, tumour cells remain metabolically flexible and adaptive responses might also depend on the tissue of origin or the metastatic site as breast cancer cell metastases of the liver but not of the bone and the lungs convert pyruvate into lactate and reduce mitochondrial metabolism by the overexpression of PDK1. This is strongly dependent of HIF-1 as impaired HIF-1 expression reduces the liver metastatic burden *in vivo* by 80%. Further, PDK1 is overexpressed in liver metastases of breast cancer patients, together with LDH-A, ALD-A, ALD-C, HK1, and GLUT-1 (Dupuy et al. 2015). This highlights the role for glycolysis in tumour progression but also that tumour cells are metabolically flexible, which enables the colonisation of different tissues. Consequently, glycolysis upregulated by HIF-1 supports all aspects important for cancer progression. This includes the maintenance of glycolytic flux which ensures sufficient precursors of macromolecules, and the suppression of mitochondrial respiration to avoid the lethal accumulation of ROS. Consequently, HIF-1 promotes tumour initiation, and growth and progression within hypoxic areas, leading to reduced overall survival of cancer patients.

1.4.4 HIF-1 promotes the classic hallmarks of cancer

Angiogenesis ensures the supply of tissues with oxygen and nutrients by neovascularisation which is induced when the balance between pro-and anti-angiogenic factors is tipped towards pro-angiogenic factors (“angiogenic switch”) (Carmeliet & Jain 2000). However, the tumour vasculature is highly disorganised. Often, blood vessels are dilated, uneven in diameter, suffer from excessive branching and irregular blood flow, and are leaky and heterogeneous (Carmeliet & Jain 2000; Hashizume et al. 2000; Morikawa et al. 2002; Tian et al. 2002;). HIF-1 induces the expression of many pro-angiogenic factors to support oxygen delivery to tumour tissues and to promote metastasis. The extensively studied VEGF-A is a potent pro-angiogenic factor and expressed in a large number of tumours. *VEGF-A* was identified as HIF-1 target gene by (Forsythe et al. 1996). VEGF is involved in major stages of tumour angiogenesis, including vessel sprouting and assembly, lumen formation, and vessel dilation and permeability (Yuan et al. 1996).

Consequently, VEGF-A is of crucial importance for tumour growth and metastases, impairing prognosis and survival of cancer patients (Cao et al. 2009; Han et al. 2001; Linderholm et al. 2009).

HIF-1 does not only mediate survival of the primary tumour but also plays a central role in the support of different steps in the metastatic cascade. The transcription factor TWIST is activated by hypoxia-induced HIF-1 and mediates epithelial-mesenchymal transition (EMT) and invasion *in vitro* and *in vivo* by supressing E-cadherin expression in head and neck cancer cell lines. In patients with head and neck squamous cell carcinoma, TWIST is co-expressed with HIF-1α and Snail, and correlates with number of metastases and poor overall survival (Yang et al. 2008). Additionally, the transcriptional repressor Snail (Imai et al. 2003) and the transcription factor Zink finger E-box binding homeobox 1 (ZEB1) (Zhang et al. 2015) also promote EMT and invasion in a HIF-dependent manner by supressing *E-cadherin* expression.

In MDA-MB-231 cells, the secretion of HIF-1-induced angiopoietin-like 4 (ANGPTL4) inhibits epithelial cell interaction and promotes invasion by supporting extravasation. This was accompanied by the hypoxia-induced and HIF-dependent expression of L1 cell adhesion molecule (L1CAM) which increases the adherence of MDA-MB-231 to epithelial cells. The treatment with the HIF-1 inhibitor digoxin reduces growth of primary tumours, the expression of *GLUT1* and *HK1* mRNA, and the size and number of lung metastases (Zhang et al. 2012). (Wong et al. 2012) demonstrated that in a model of mammary fat pat-derived triple negative breast cancer HIF-1 activates isoforms of the collagen remodelling enzymes LOX which provide a path for migrating cancer cells and bone marrow-derived cells to the lung. HIF-1 also supports metastasis by activating the target gene membrane-type 4 matrix metalloproteinase (MMP-4) which mediates the degradation of the extracellular matrix (Huang et al. 2009). The HIF-1 target gene adrenomedullin (*ADM)* promotes osteolytic metastases of MDA-MB-231 breast cancer cells to the bone and reduces survival *in vivo* (Siclari et al. 2014). Consequently, HIF-1 supports all steps of the metastatic cascade which highlights its role in tumour progression and its importance as therapeutic target.

Hypoxic areas within tumours are acidic due to the generation of lactic acid and H^+ by anaerobic glycolysis (Warburg 1924) and CO_2 generated by the pentose phosphate pathway (Helmlinger et al. 2002). The lack of functioning blood vessels as well as long diffusion distances lead to the accumulation of these acidic metabolites (Gatenby et al. 2007). Extracellular pH is further actively decreased by carbonic anhydrases. Consequently, tumour cells are forced to adapt to low extracellular pH to survive and HIF-mediated responses to hypoxia-induced acidosis play a crucial role in tumour cell survival and active reduction of pH_e which is evaluated in greater detail in the section 1.6.

The expansion of stem cell-like cancer cell populations contributes to relapse and metastasis in numerous human cancers (Charafe-Jauffret et al. 2010; Hermann et al. 2007; Merlos-Suárez et al. 2011). In human cancer cell lines and primary cancer cells, hypoxia-activated HIF-1 induces a gene signature comparable to genes upregulated in human embryonic stem cells. Immunohistochemistry staining of primary prostate cancer tissue confirms the co-localisation of HIF-1α and the stem cell-associated transcription factors NANOG and octamer-binding transcription factor 4 (OCT4) *in situ* (Mathieu et al. 2011). HIF also induces CD133 expression via the activation of OCT4 and Sex-determining region Y box 2 (SOX2) in an *in vitro* human lung cancer model (Lida et al. 2012). Interestingly, cycling hypoxia is sufficient to expand stem cell-like $CD44^+CD24^-ESA^+$ breast cancer cell populations within the cell lines MDA-MB-231 and BCM2. These cells are highly tumorigenic *in vivo* and exhibit an mesenchymal phenotype (Louie et al. 2010).

Hypoxia caused by anti-angiogenic agents expands aldehyde dehydrogenase 1 (ALDH 1) expression *in vitro* and *in vivo* which is mediated by the HIF-1α-mediated phosphorylation of β-catenin (Conley et al. 2012). Moreover, paclitaxel and gemcitabine-induced ROS production was shown to increase cancer stem cell-like $ALDH1^+$ populations in metastatic and non-metastatic breast cancer cells. Chemotherapy resistance in these populations is promoted by the HIF-1α and HIF-2α-dependent expression of MDR1. Therefore, the co-administration of chemotherapeutic agents and HIF-inhibitors leads to tumour eradication *in vitro* as well as *in vivo.* This demonstrates the importance of HIF-mediated tumour maintenance by supporting the expansion of cancer stem cell-like cells (CSCs) (Samanta et al. 2014).

Tumour hypoxia and HIF actively promote the recruitment of immune cells to induce tumour tolerance by the host immune system, and to support invasion and angiogenesis (Du et al. 2008). HIF-1α mediates tumour tolerance by inducing the rapid differentiation of myeloid-derived suppressor cells (MDSCs) into tumour-associated macrophages. Tumour-associated MDSCs exhibit increased nitric oxide production and arginase activity, resulting in increased suppression of T cell effector functions (Corzo et al. 2010). This HIF-1α-mediated suppression of T cell activity by MDSCs and tumour-associated macrophages is mediated by the secretion of IL-6 and IL-10, following the activation of programmed death-1 (PG-1) (Noman et al. 2014).

Hypoxia also protects cancer cells from anti-tumour immunity by activating STAT3 and HIF-1α which impairs the cytotoxic T cell-induced lysis of lung cancer cells (Noman et al. 2009). Tumour hypoxia-induced HIF further prevents host anti-tumour immunity by promoting the recruitment of $CD4^+CD25^+Foxp3^+$ regulatory T cells (T_{regs}) via the secretion of the chemokine CC-chemokine ligand 28 (CCL28). The attracted T_{regs} effectively suppress T cell effector function and induce angiogenesis

as well as tumour tolerance by the host immune system (Facciabene et al. 2011). Lactic acid derived from aerobic or anaerobic tumour cell metabolism stabilizes HIF-1α and thereby induces M2 polarization and VEGF expression in tumour associated macrophages (Colegio et al. 2014). The studies described above highlight the role of hypoxia and HIF-promoted attraction of immunosuppressive and -modulatory cells to dampen anti-tumour immunity, and to support tumour growth, invasion and metastases, relating to poor prognosis for cancer patients.

Defects in cell cycle checkpoints and DNA repair mechanisms contribute to genetic instability and promote tumorigenesis (Hanahan & Weinberg 2011). There is emerging evidence that hypoxia supports genetic instability via the repression of DNA repair pathways via HIF-dependent and –independent mechanisms.

(Kondo et al. 2001) determined that hypoxia enriches cultures of colon cancer cells for cells deficient in the mismatch repair gene *MLH-1*. This sub-population becomes hypersensitive to microsatellite instability and acquires resistance to the treatment with cisplatin. Reoxygenation following hypoxia also promotes genetic instability by inducing transition to S phase, and by drastic overamplification of DNA which is accompanied by an increase in cell volume. (Pires et al. 2010) demonstrated the importance of intermittent hypoxia for the inhibition of DNA damage repair pathways as chronic hypoxia induces irreversible replication arrest defined by blocked initiation and elongation, and G_2 arrest mediated by a deficiency in dNTPs. On the other hand, cells exposed to short cycles of hypoxia followed by reoxygenation are able to re-induce replication which leads to p53-dependent apoptosis. However, most cancer cells exhibit p53 mutations and consequently proceed with DNA replication, even in the presence of ROS-induced DNA damage.

Hypoxia also decreases the expression of mismatch repair proteins by reducing c-Myc binding to the *MLH1* and *MSH2* promoter, relative to the binding of the repressive co-regulators Max, Mad1 and Mnt, in an HIF-independent manner (Bindra & Glazer 2007). The repression of *BRCA1* causes a reduction of homologous recombination but non-homologues end joining is still maintained, thereby promoting genetic instability (Bindra et al. 2005). *BRCA1* expression is also suppressed in hypoxia by the NADH-dependent activation of C-terminal binding proteins (Deng et al. 2010). These studies described above highlight the importance of hypoxia to the contribution of genetic instability. The role of HIF however remains less clear and requires further research.

1.5 C-terminal binding proteins link glycolysis with gene transcription

Differential gene expression is crucial for the development and function of complex tissues and of multicellular organisms. However, aberrant gene regulation contributes to oncogenesis and promotes tumour progression (reviewed by (Rankin & Giaccia 2008; Thiery et al. 2009)). In this light, the following section highlights important mechanisms of gene regulation and introduces the transcriptional co-regulators C-terminal binding proteins (CtBPs) as promising therapeutic targets.

1.5.1 The multiple layers of eukaryotic gene regulation

1.5.1.1 Regulation of chromatin structure by histone-modifying enzymes

The core unit of chromatin is the nucleosome, which consists of 147 bp negatively charged DNA wrapped around an octamer of the four positively charged core histones (H) H3, H4, H2A, and H2B. This structure enables strong condensation (Kornberg & Thomas 1974; Oudet et al. 1975). Therefore, access to promoters by the transcription machinery is an important modulator of gene expression.

The modification of histones at the globular domain or the N-terminus by either phosphorylation, ubiquitination, SUMOylation, methylation, or acetylation regulates chromatin structure, and therefore, transcription (Bannister & Kouzarides 2011). Acetylation and methylation of lysine residues are discussed in greater detail below due to their relevance to CtBP function.

Histone modifications are performed by specialised enzymes (Tab. 1.2). Acetylation is catalysed by acetyl-CoA-dependent histone acetyl transferases (HATs), and is associated with gene expression and euchromatin (Marmorstein & Trievel 2009). The HAT CBP/p300 is commonly found in complexes which activate gene transcription, *e.g.* together with HIF-1 at the promoter of HIF-target genes (Arany et al. 1996; Ebert & Bunn 1998). CBP/p300 has been described to acetylate all four core histones (Ogryzko et al. 1996). The acetylation of core histones by HATs is reversed by histone deacetylation and is mediated by histone deacetylases (HDACs). There are four classes of HDACs, but only HDACs class III (sirtuins) are NAD^+-dependent. All HDAC classes exert low substrate specifity and promote chromatin condensation and gene repression (Marmorstein & Trievel 2009).

Histone methylation is complex and promotes active as well as closed states of chromatin. Another layer of complexity is added by the different impact of di- and tri-methylation. Di-methylation of lysine residue 4 at histone 3 (H3K4) by the methyltransferase Set1 promotes an

inactive state, whereas tri-methylation, mediated by the same enzyme, is associated with active euchromatin (Santos-Rosa et al. 2002). The catalytic domain of histone lysine methyltransferases (HKMTs) contains a SET domain, which mediates the transfer of methyl groups from S-adenosylmethionine (SAM) to the ε-amino group within the lysine side chain (Jenuwein et al. 1998; Rea et al. 2000). In contrast to HATS and HDACs, HKMTs modify specific residues (Tab. 1.2). Histone lysine demethylases (HKDMs) on the other hand, specifically remove mono-, di-, or tri-methyl groups. This either promotes gene silencing or gene activation, depending on the context (Bannister & Kouzarides 2011). Lysine-specific demethylase 1 (LSD1) requires FAD as cofactor and specifically removes mono- or di-methyl groups from H3K4 (H3K4me1/2) (Shi et al. 2004). The hydroxylase activity of Jumonji domain-containing HKDMs is dependent on iron and α-ketoglutarate. This makes them interesting candidates for oxygen-regulated chromatin modifications (Shmakova et al. 2014). H3 methylation can promote repressive and active states of chromatin, whereas H4 methylation is mostly associated with gene silencing, such as the di- or trimethylation of H4K20 (H4K20me2/3) (Handy et al. 2011).

Tab. 1.2: Examples of histone-modifying enzymes and their impact on transcription and chromatin structure.
This table is based on (Bannister & Kouzarides 2011; Handy et al. 2011).

Family	Family member	Modification	Target	Impact on transcription and chromatin structure
Histone acetyltransferases	CBP/p300	Acetylation	Lysine residues in N-termini of core histones	Gene activation, euchromatin
Histone deacetylases	HDAC1	Deacetylation	Low substrate specifity	Gene silencing, heterochromatin
Histone lysine methyltransferases	Set7/9	Methylation	H3K4me1	Gene activation, euchromatin
	Ga9	Methylation	H3K9me2	Mostly repressive, heterochromatin
Histone lysine demethylases				
Lysine-specific	LSD1	Demethylation	H3K4me1/2	Gene activation, euchromatin
Jumonji domain proteins	JMJD2A	Demethylation	H3K9me2/3	Gene activation, euchromatin

Histone modifications modulate chromatin structure and gene expression by acting as a marker for accessory proteins. Lysine acetylation is recognised by bromodomain and extra-terminal (BET) proteins, which recruit transcription factors. In this context, BRD4 binds H3K27 within the *CA9* promoter, thus enabling the binding of HIF-1 and *CA9* transcription in hypoxia (da Motta et al. 2017). Methylation promotes the binding of the chromatin modifier heterochromatin protein 1

(HP1), leading to chromatin condensation and gene silencing (Bannister et al. 2001). Consequently, the orchestrated activity of chromatin modifiers, transcription factors, and transcriptional cofactors is crucial for the regulation of gene expression (Luo et al. 2012; Ray et al. 2014; Shi et al. 2003). Examples of how histone-modifying enzymes, transcription factors and cofactors, such as CtBPs, co-operate in order to regulate gene expression are given in section 1.5.2.2.

Additionally, chromatin structure is modified by ATP-dependent chromatin modifying complexes, such as enzymes belonging to the class of Switch/Sucrose Non Fermentable (SWI/SNF) or initiation SWI (ISWI). Both groups utilize ATP hydrolysis to alter histone composition or spacing, promoting either gene activation or silencing (Vignali et al. 2000). ATP-dependent chromatin modifications also play a role in transcriptional responses to hypoxia. SWI/SNF components recruit NF-κB and RNA polymerase II to the *HIF-1α* promoter, thereby promoting *HIF-1α* transcription (Kenneth et al. 2009). ISWI on the other hand, inhibits HIF-target gene expression, by enhancing RNA polymerase loading at the *FIH* promoter. This includes the expression of *CA9* (Melvin et al. 2011).

1.5.1.2 Regulation of transcription initiation

Basal transcription of protein-encoding genes comprises the recognition and binding of general transcription factors and RNA polymerase II to promoters, and is found at almost all promoters, even at genes without detectable transcript expression (Guenther et al. 2007). Therefore, promoter occupation of the pre-initiation complex is unspecific and requires further regulation.

Transcription initiation is regulated by *cis*-acting DNA sequences, which are either promoter-proximal distant silencer or enhancer sequences, and are bound by specialised transcription factors (Long et al. 2016). Examples for promoter-proximal regulatory sequences are hypoxia-responsive elements in HIF-target genes (section 1.4.1) or Enhancer boxes (E-boxes). The bHLH transcription factor Snail binds E-boxes within the *CDH-1* promoter, leading to the repression of E-cadherin expression in epithelial cancer cell lines (Batlle et al. 2000). On the other hand, c-Myc and Max activate expression of genes involved in DNA repair (Bindra & Glazer 2007).

Distant regulatory sequences are defined as 100-1000 bp non-coding DNA sequences which act independently from promoter location, distance, and orientation. Distant enhancers contain clusters of transcription factor recognition motifs, and are bound by clusters of transcription factors and cofactors (Long et al. 2016). These complexes enhance transcription by interacting with the basal transcription machinery by forming DNA loops (Su et al. 1991). Enhancer elements are regulated by alterations in their sequences, such as via expansion of transposable elements or

via duplication. In contrast to transcription factor interaction, enhancer sequences are highly dynamic and are also frequently altered in cancer (Bradner et al. 2017).

Additionally, gene expression is regulated by *trans*-acting, specialised transcription factors and cofactors (Spitz & Furlong 2012). Transcription factors generate specifity for target genes, whereas cofactors modulate the rate of gene transcription by recruiting chromatin modifying and remodelling enzymes, and via crosstalk with the basal transcription machinery (Long et al. 2016). Transcription factors and cofactors modulate gene expression by either co-operative binding (Kyo et al. 2000), competition (Yu-Rice et al. 2016) or antagonism (Postigo et al. 2003).

Specific gene regulation is controlled intrinsically, such as the autoregulatory loop of p53 expression. p53 induces the expression of MDM2, which mediates the ubiquitination and degradation of p53, thus maintaining balanced p53 expression (Haupt et al. 1997; Kubbutat et al. 1997). Alternatively, specific gene regulation is controlled by the microenvironment, such as the oxygen-dependent activation of HIF-1 (Wang & Semenza 1993b). However, transcription is highly dysregulated in cancer (Bradner et al. 2017). This dysregulation includes the activation of transcription factors normally active in early development, e.g. OCT4, leading to the activation of genes associated with the embryonic phenotype and pluripotency (Mathieu et al. 2011). Additionally, mutations of transcription factors such as p53 or c-Myc are commonly found in highly proliferative cancers (The Cancer Genome Atlas Network 2012). Oncogenic signalling leads to aberrant function of co-factors and induction of gene expression (Richard et al. 1999). Alternatively, an altered microenvironment is integrated by co-factors and transcription factors, such as an increased NADH:NAD^+ ratio in tumour cells with upregulated glycolysis, which promotes the CtBP-dependent suppression of epithelial and pro-apoptotic genes (Grooteclaes et al. 2003) (see 1.5.2.3). The oncogenic activation of HIF-1 is mediated by both, oncogenic signalling and pathologic oxygen concentrations within tumorous tissue (Laughner et al. 2001; Wykoff et al. 2000)(see section 1.4).

1.5.1.3 Post-transcriptional mechanisms of gene regulation

MicroRNAs (miRNAs) exert important functions in the post-transcriptional regulation of protein-coding genes. The primary transcript of miRNA genes, the pri-miRNA, comprises a stem-loop structure and is 1 kb in length. Pri-miRNA is matured by two cleaving processes. The first one occurs in the nucleus and is performed by the microprocessor complex, consisting of the nuclear RNase III Drosha and its cofactor DGCR8. Drosha removes the stem-loop structure, thus creating the hairpin-shaped and 65 bp long pre-miRNA. Following the export into the cytoplasm, the pre-miRNA is further cleaved by DICER, creating a small RNA duplex of 22 bp. In complex with AGO protein, the mature miRNA forms the RNA-induced silencing complex (RISC). The RISC supresses

translation by binding to conserved or un-conserved sequences in the 3' untranslated region (UTR) of the mature mRNA (reviewed by (Ha & Kim 2014)). Tumour hypoxia has been identified as major modulator of miRNA expression profiles (Kulshreshtha et al. 2007). The miRNA miR-210 has been identified as HIF-1 target and contributes to the downregulation of mitochondrial metabolism by inhibiting the expression of the electron transport chain component *iron-sulphur cluster scaffold protein* (*ISCU*) (Favaro et al. 2010). Additionally, miR-210 was also shown to impair DNA damage response in hypoxia by supressing *RAD52* expression (Crosby et al. 2009).

Gene expression is also regulated on the level of translation initiation. The modulation of the activity and affinity of eukaryotic initiation factors (eIFs) to the 7-methyl-guanosine cap structure at the 5' end of the mRNA impacts the binding of the pre-initiation complex, and thus the rate of translation (reviewed by (Pelletier et al. 2015)). This mode of regulation is responsive to cellular signalling pathways, such as mTOR and MAPK signalling (Dodd et al. 2015; Korneeva et al. 2016). In this light, (Dodd et al. 2015) have shown that the mTORC1-mediated increase in eIF4E activity occurs via the inhibition of 4E-BP1 and results in the enhanced translation of HIF-1α mRNA, and consequently in increased *VEGF* expression levels.

Regulating gene expression on the posttranslational level involves the enzymatic removal or addition of functional groups to amino acid side chains. In this light it has been demonstrated that HIF-1α protein is both stabilised and destabilised by phosphorylation (Bullen et al. 2016; Herzog et al. 2016; Warfel et al. 2013). Additionally, it has been shown that deacetylation by histone deacetylase 4 (HDAC4) promotes HIF-1α protein stability, whereas acetylation contributes towards its degradation (Geng et al. 2011). Demethylation of HIF-1α by lysine-specific demethylase 1 supports (LSD1) protein stability in hypoxia, while methylation by SET7/9 methyltransferase in normoxia promotes HIF-1α degradation (Kim et al. 2016). Finally, the most important determinants of HIF-1α protein stability are the oxygen-dependent hydroxylation within the ODD by PHDs, and its subsequent ubiquitination by pVHL, leading to its rapid degradation in normoxia (see section 1.4.1).

1.5.2 C-terminal-binding proteins

Co-regulators of transcription fine-tune gene expression and link gene expression with the extracellular environment. Transcriptional co-regulators are activated by components of the cellular signalling network or by the redox state within a cell as it is the case for CtBPs (Grivas & Papavassiliou 2013). The activation results in modulation of gene expression by cross-talking with histone-modifying enzymes which results in altered chromatin structure (Shi *et al* 2003). Therefore, transcriptional co-regulators such as CtBPs act as sensors as they integrate environmental signals and translate them into a genetic response by interacting with chromatin-modifying enzymes.

1.5.2.1 The structure of C-terminal-binding proteins

The co-regulator CtBP is named after the ability to bind to the C-terminus of the adenoviral protein E1A via the consensus sequence Proline-X-Aspartic acid-Leucine-Serine (PXDLS) (Verger et al. 2006). There are two CtBP encoding genes in humans. *CtBP1* is located on chromosome 4p6 and is expressed in higher numbers than CtBP2. *CtBP2* is located on chromosome 10q26.13. Both homologues are found in adult as well as in embryonic tissues (Bergman et al. 2006). The protein is 440 amino acids long and consists of three domains (Fig. 1.5). The substrate binding site contains a PXDLS binding cleft as wells as a human MDM2 (HDM2)-binding site. The central nucleotide-binding domain is highly homological between CtBP1 and 2. It shows NAD^+-dependent dehydrogenase activity and is involved in NAD/H binding with a greater affinity for NADH.

The binding of NADH induces a conformational change which enables dimerization and consequent activation. This NADH-dependent activation defines CtBPs as metabolic sensors and is of central importance for its function as mechanistic and functional link between metabolism and gene regulation. The dimers exhibit two PXDLS-binding motives. PXDLS motives are found in numerous transcriptions factors and effectors of gene expression such as histone modifying enzymes, underlining its importance as co-regulator of transcription. The C-terminal region of both CtBP1 and CtBP2 is believed to exert regulatory functions as it can be phosphorylated by Homeodomain-interacting protein kinase 2 (HIPK2) at residue S422 (Quinlan et al. 2006).

CtBP homo- and heterodimers are located in the nucleus as well as in the cytoplasm (Verger et al. 2006). It is suggested that the binding of NADH followed by dimerization favours nuclear localization, whereas the binding of Acyl-CoA results in a monomeric and cytoplasmic form. Furthermore, the SUMOylation at lysine 428 and the interaction with SUMO E3 ligases promotes the nuclear localization of CtBP1, whereas the interaction with neuronal nitric oxide synthase

(nNOS) at the PDZ domain at the C-terminus leads to a cytoplasmic localization (reviewed in (Bergman & Blaydes 2006)).

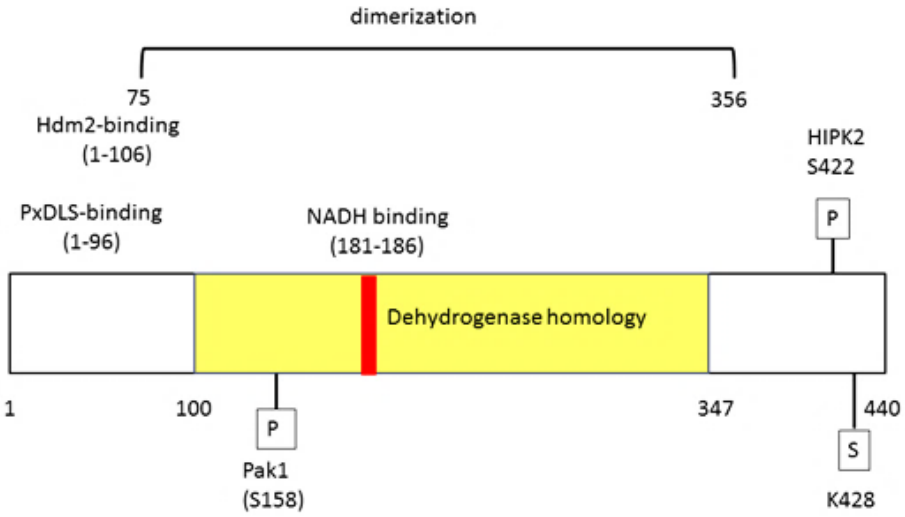

Fig. 1.5: The domain structures of CtBP1 representative for both human isoforms. CtBP2 has a similar domain structure but is shorter in length. Displayed are functional domains as well as locations of post-translational modifications. Numbers represent the position of amino acids within the protein. This figure was modified after (Bergman & Blaydes 2006).

1.5.2.2 CtBPs fine-tune transcriptional regulation by interacting with regulators of gene transcription

In the nucleus of epithelial cells, CtBPs act as important transcriptional co-regulator via numerous mechanisms. Historically, CtBPs were first discovered as co-repressors which suppress the transcription of target genes via mechanisms summarized in Fig. 1.6. One mechanism involves the recruitment of a repressor and of histone-modifying enzymes such as histone methyltransferases, histone demethylases and histone deacetylases (HDACs) (Shi *et al* 2003). In this context, CtBP1 is recruited to the *BRCA2* promoter by the transcriptional repressor SLUG where it binds both SLUG and HDAC-1 via the recognition of PXDLS motives. The recruitment of HDAC-1 by CtBP1 consequently leads to the deacetylation of histones at the *BRCA2* promoter, resulting in inactive chromatin and the suppression of *BRCA2* transcription (Tripathi et al. 2005).

Further, CtBPs are able to form repressive complexes with the polycomb protein complex 2 which was demonstrated to repress transcription *in vitro* (Sewalt et al. 1999). In transgenic *Drosophila melanogaster*, the mammalian Polycomb group protein (PcG) YY1 binds to Polycomb response elements (PREs) in target gene DNA and to CtBPs via the recognition of PXDLS motives. CtBP-

binding consequently results in the recruitment of a PcG complex and the methylation of H3 at K27. This enables Pc binding and results in the transcriptional repression of target genes (Srinivasan & Atchison 2004).

Moreover, CtBPs repress the p300-mediated activation of transcription by binding p300 via the recognition of a PXDLS motif within the bromodomain required for histone binding. This inhibits histone acetylation within promoters and consequently activation of transcription in a NADH-dependent manner. Therefore, CtBPs exert a central function in energy-dependent gene regulation (Kim et al. 2005). CtBPs also interacts with transcriptional repressors to supress transcription, independent from histone modifying enzymes. This includes the interactions via PXDLS motives with the zinc finger proteins Ikaros (Koipally & Georgopoulos 2000), δEF1 (Furusawa et al. 1999) and ZEB1 (Postigo & Dean 1999).

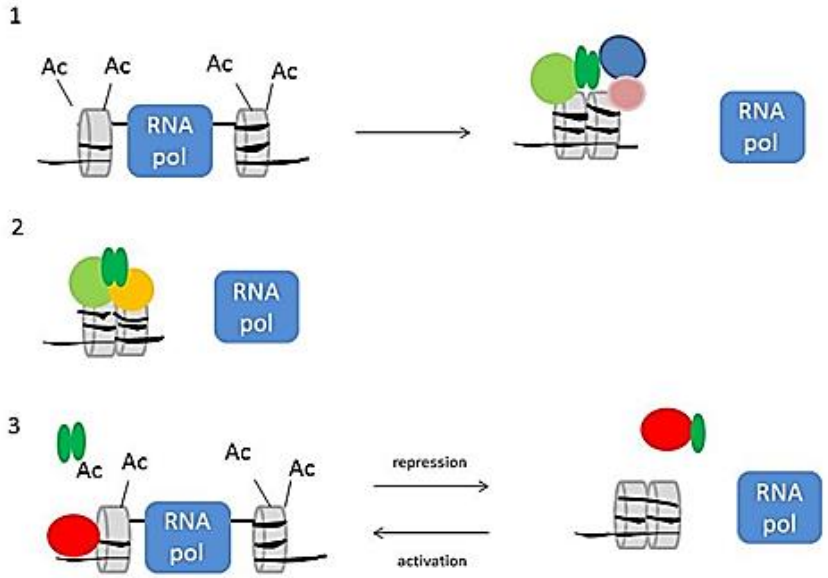

Fig. 1.6: Three mechanisms by which CtBPs repress gene transcription. 1: CtBP forms a co-repressor complex with histone deacetylases (HDAC) and histone methyltransferases (HMT) which results in chromatin condensation. This blocks access for the RNA polymerase. **2**: RNA polymerase binding is prevented by the recruitment of polycomb proteins. **3**: CtBP interacts with histone acetyltransferase (HAT) co-activators e.g. p300 and therefore prevent co-activator binding to chromatin. Key: light green: repressor, dark green: dimerized CtBP, salmon: HDAC, blue: HMT, yellow: polycomb protein, red: HAT-co-activator e.g. p300. Modified after (Bergman & Blaydes 2006).

It becomes more and more evident that CtBPs also act as co-activators of transcription, highlighting their role as plastic modulators of gene regulation. In this context, the regulation of transcription of secretin, β-glucokinase, insulin I and insulin II in endocrine cells of the intestine and pancreas is mediated by the binding of the transcription factor NeuroD1 and the demethylase Lysine-specific histone demethylase 1 (LSD1). NeuroD1 and RRBEB1 bind DNA which recruits CtBP via binding to PXDLS motives. Consequently, CtBPs bind LSD1 via the same mechanism leading to the LSD1-mediated removal of methyl groups from H3K9me2. This facilitates histone acetylation by p300/CBP bound to NeuroD1 and promotes transcriptional activation (Ray et al. 2014). Furthermore, CtBP2 co-activates the transcription of T cell lymphoma invasion and metastasis protein 1 (Tiam1) in conjunction with Krueppel-like factor 8 (KFL8) to promote cancer cell migration *in vitro* (Paliwal et al. 2012). CtBP2 also positively regulates transcription factor 4 (TCF-4) signalling, thereby promoting self-renewal and growth of colon cancer stem cells (Patel et al. 2014). Furthermore, CtBPs directly bind to the *MDR1* promoter which leads to *MDR1* activation and the promotion of multi drug resistance in cancer cells (Jin et al. 2007).

1.5.2.3 The physiological functions of CtBPs and their role in tumour progression

CtBPs exert vital functions in mammal development as *Ctbp1*^{null} mice are smaller and die earlier than their heterozygous and wildtype littermates. Additionally, *Ctbp2*^{null} mice are not viable due to devoid blood vessel formation in the yolk sack and the labyrinth layer of the placenta, which is accompanied by aberrant heart formation and delayed development of the forebrain, midbrain and the spinal cord (Hildebrand & Soriano 2002). However, little is known about the role of CtBPs in human development.

CtBPs also control the spindle assembly checkpoint in mitosis and therefore contribute to homeostatic cell division (Birts et al. 2011). CtBP-depleted cells show mitotic defects, including defects in chromosome alignment and defects in the activation of the spindle assembly checkpoint. Additionally, the progression into anaphase is interrupted due to reduced levels of aurora B expression. This leads to the accumulation of chromatin in the prophase and prometaphase. Moreover, CtBPs are directly involved in mitosis as CtBP1 is differentially phosphorylated throughout the cell cycle, exerting its peak during mitosis. Additionally, CtBPs localize to centrosomes in mitosis and form a complex with ɣ-tubulin and PIK. CtBPs are also involved in the maintenance of the Golgi membrane as abolishing CtBP function prevents Golgi partition prior to mitosis (Birts et al. 2011).

The nuclear activity of CtBPs is highly relevant to tumour progression. Importantly, CtBPs link upregulated glycolysis via hypoxia-dependent and –independent mechanisms with the regulation of gene expression relevant to tumour progression. The reversal of the epithelial phenotype is a central event during EMT, thus promoting the invasion of adjacent and distant tissues. CtBPs are commonly overexpressed in invasive cancers such as invasive ductal breast cancer (Zhang et al. 2006) or hepatocellular carcinoma (Zhang et al. 2013) where CtBP overexpression correlates with reduced E-cadherin expression. (Zhang et al. 2006) demonstrated the role of hypoxia-induced upregulation of NADH in the joint suppression of *E-cadherin* transcription by ZEB1 and CtBP1. Repression is mediated via the deacetylation of H3 and results in increased invasion of breast cancer cells *in vitro*. In liver cancer, CtBP-promoted silencing of *E-cadherin* expression also results in increased invasion *in vitro* by protecting cells from apoptosis (Zhang et al. 2013). The NADH-dependent up-regulation of CtBP expression additionally promotes invasion of cancer cells by increasing the resistance towards anoikis in addition to the silencing of *E-cadherin* transcription (Grooteclaes et al. 2003).

Furthermore, CtBP expression increases resistance of cancer cells against apoptosis by repressing pro-apoptotic genes such as *Pten* and *Bax* (Grooteclaes et al. 2003). The basic Kruppel-like factor (BKLF) recruits CtBP2 to the promoter of the pro-apoptotic gene *Bik* through its PXDLS motif. This suppression of *Bik* is antagonized by the tumour suppressor alternative reading frame (ARF). By binding to CtBP2, ARF inhibits its effector function and repression of the *Bik* promoter is relieved. This results in the transcriptional activation of *Bik*, and in apoptosis. However, ARF is frequently inactivated in human cancers (Kovi et al. 2010).

Importantly, CtBPs provide a link between cancer metabolism and genomic instability as high levels of NADH lead to the CtBP-dependent repression of DNA repair genes such as *BRCA1*. The repression of *BRCA1* transcription by CtBP2 in ovarian cancer cells is accompanied by decreased acetylation of H3K9 and H3K14 as well as increased methylation of H3. Interestingly, inhibition of CtBP2 by MTOB increases the sensitivity of ovarian cancer cells towards the Poly ADP ribose polymerase (PARP) inhibitor Olaparib (May *et al.* 2013). In head and neck cancer, CtBP1 represses *BRCA1* transcription by binding the transcription factor E2F4 in an NADH-dependent manner. This co-repression of *BRCA1* by CtBP1 and E2F4 is reversed by antioxidant treatment (Deng et al. 2010). Complementing these *in vitro* findings, (Deng et al. 2010) detected nuclear CtBP1 staining as early as the hyperplastic state where it correlates with reduced BRCA1 expression. These findings highlight the role of CtBPs in hypoxia and NADH-mediated promotion of genetic instability which is commonly found within tumours.

Additionally, CtBPs promote resistance against cell cycle inhibition and therefore support the overcoming of senescence, a crucial step in tumour formation. In this context, CtBP1 expression negatively correlates with the expression of the cyclin-dependent protein kinase inhibitor $p16^{INK4a}$ in melanoma patients (Deng et al. 2013). Furthermore, CtBPs contribute to the overcoming of senescence in hypoxic tumour cells by supressing $p16^{INK4a}$ expression. This corresponds with repressive trimethylation of histone 3 at lysine 27 (H3K27me3) at the *p16* promoter (Mroz et al. 2008).

(Di et al. 2013) demonstrated that the central role for CtBPs in cancer progression relies in linking glycolytic metabolism with the modulation of central genetic networks. In breast cancer, CtBP activity promotes EMT, the acquiring of a stem cell-like phenotype and genomic instability. This is reversible upon CtBP depletion, inhibition by a small molecule inhibitor, or calorie restriction. Furthermore, the downregulation of CtBP target genes is associated with more aggressive breast cancer subtypes and predicts poor clinical outcome and reduced median survival (Di et al. 2013).

The literature cited above highlights the relevance of CtBPs in tumour progression. The role of CtBPs in the contribution to EMT, resistance to apoptosis and senescence, as well as promoting genetic instability is well defined. However, the potential role for CtBPs in the survival of hypoxia-induced acidosis is unknown. As outlined above, hypoxia-induced acidosis, actively induced and caused by anaerobic metabolism, contributes to aggressive (breast) cancer subtypes. Therefore, this thesis aims to determine whether upregulated glycolysis, caused by hypoxia, activates HIF-mediated adaptive gene responses to support the survival of breast cancer cells of hypoxia-induced acidosis through activation of CtBPs.

1.6 Intratumoural pH regulation promotes tumour progression

Intratumoural pH is highly heterogeneous, ranging from pH=7.4 to pH=6.0, and is caused by the limited oxygen diffusion of 10 cell diameters (100-200 µm) and poor perfusion (Gatenby et al. 2007). An additional source of intratumoural acidosis is tumour metabolism itself. Poor perfusion in combination with enhanced glycolysis leads to the accumulation of lactic acid and H^+ generated during anaerobic glycolysis and glutaminolysis (Helmlinger et al. 2002; Newell et al. 1993; Yamagata et al. 1998; Reitzer et al. 1979), and CO_2 derived from the pentose phosphate pathway or mitochondrial respiration (Helmlinger et al. 2002). Importantly, cancer cells deficient of glycolysis still generate acidity by switching to the PPP (Helmlinger et al. 2002). Independent from metabolism-derived acidosis, cancer cells actively increase intracellular pH (pH_i) above the physiological pH ~7.0 while acidifying pH_e via the activation of carbonic anhydrases (Li et al. 2009; Li et al. 2011; Švastová et al. 2004).

1.6.1 The alkalinisation of pH_i is mediated by ion transport along the cell membrane

Tumour cells adapt to acidosis by increasing pH_i while further acidifying pH_e (Chiche et al. 2009; Parks et al. 2016; Reshkin et al. 2000). Tumour cell pH_i alkalinisation and pH_e acidification is realised by H^+ extrusion and bicarbonate re-uptake mediated by the concerted action of membrane-bound ion carriers of the solute carrier superfamily (SLC family) and by carbonic anhydrases (CAs) (Lee et al. 2014; Orlowski et al. 2012; Pouyssegur et al. 1984; Swietach et al. 2014; Spitzer et al. 2002)(Fig. 1.7).

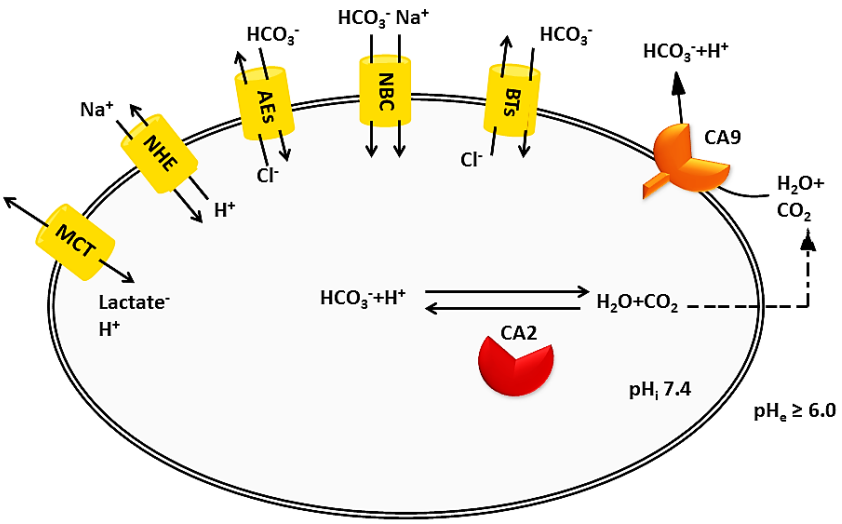

Fig. 1.7: Tumour cells actively regulate intratumoural pH. Intracellular alkalinisation is mediated by ion transport along the cell membrane, whereas pH_e is actively acidified by carbonic anhydrases. This enables tumour cell survival in acidosis and drives tumour progression. The image is based on (Pastorekova & Ratcliffe 2008; Swietach et al. 2007; Thiry et al. 2006).

MCTs belong to the SLC16 family and contribute to H^+ extrusion as they transport lactate together with H^+ along the cell membrane (Dimmer et al. 2000; reviewed by (Halestrap & Price 1999)). As discussed before, MCT4 is overexpressed in hypoxic cancers and plays a central role in glycolysis-derived lactate extrusion, thereby maintaining glycolytic flux; (Baenke et al. 2015; Ullah et al. 2006). The members of the SLC9 family comprises of Na^+/H^+ exchangers which play a central role in pH regulation (Bookstein et al. 1997; Brown et al. 2003; Nakamura et al. 2005; Orlowski & Grinstein 2004). NHE1 expression in cancer cells mediates intracellular alkalinisation, which is not only an adaptive reaction but crucial for malignant transformation as NHE1 inhibition alone prevents tumour formation *in vitro* and *in vivo* (Pouysstgur et al. 1984; Reshkin et al. 2000). NHE1 expression also contributes to tissue invasion *in vitro* and *in vivo* (Denker et al. 2000; Meima et al. 2009) as well as to paclitaxel resistance in triple negative breast cancer cells (Amith et al. 2015). In agreement with these findings, the alkaline shift following increased activity of NHE1 is larger in metastatic breast cancer cell lines compared to *in situ* lines (Reshkin et al. 2000).

The carbonic anhydrases CA9 or CA12 generate bicarbonate in the extracellular space (Chiche et al. 2009). The re-uptake into the cell is mediated by Na^+-dependent Na^+/HCO_3^- co-transporters (NBCs) or by Na^+–independent Cl^-/HCO_3^- anion exchangers (AEs) of the SLC subfamily SLC4 (Groeger et al. 2012; Lee et al. 2014; Lee et al. 2016; Morgan et al. 2007; Romero et al. 2013). In the cytoplasm, CA2 converts HCO_3^- and H^+ into CO_2 and H_2O which passively diffuse into the extracellular space where they are utilized as substrates for CA9 or CA12, and thus maintain bicarbonate flux (Chiche et al. 2009; Musa-Aziz et al. 2014; Švastová et al. 2004).

Additionally to NHE1 expression, NBCn1 (SLC4A7) expression is required to maintain an alkaline pH_i and thereby promotes breast cancer growth and progression *in vivo* (Lee et al. 2016). NBCn1 mediates tumour growth and progression by preventing the acidification of pH_i in an MTC1-dependent manner (Lee et al. 2016). NBCn1 is overexpressed together with NHE1 in primary and metastatic breast cancer tissue, compared to matched healthy breast tissue. However, they distinguish in their respective distribution. NBCn1 is evenly expressed across breast tumours, whereas NHE1 is expressed at peripheral and well-perfused areas (Boedtkjer et al. 2013). However, all ion transporters require the presence of the mobile carbonic buffer system to facilitate the diffusion of extruded H^+ and to prevent the inhibition of H^+ efflux due to the accumulation of extracellular H^+ (Hulikova et al. 2011). This process is supported by the activity of carbonic anhydrases (Spitzer et al. 2002).

1.6.2 The carbonic buffer system

The carbonic buffer system is a systemic system of acid/base regulation that sustains pH_e around pH=7.4 by adjusting CO_2 and HCO_3^- concentrations. The Henderson-Hasselbach equation describes the relationship between pCO_2 (mm of mercury) and HCO_3^-, whereby 0.03 describes the solubility coefficient of CO_2 in plasma (reviewed by (Hamm et al. 2015)):

Equation 1: Henderson-Hasselbach equation

$$pH = 6.1 + \log \frac{HCO_3^-}{0.03 \times pCO_2}$$

The pCO_2 is controlled via respiration, whereas HCO_3^- concentrations are regulated in the kidneys via the reabsorption of filtered HCO_3^- or by producing new HCO_3^- (Hamm et al. 2015). However, without catalysis this reaction would be too slow. Therefore, carbonic anhydrases (CAs) are central parts of carbonic pH regulation (Hulikova et al. 2011; Spitzer et al. 2002). CAs are metalloenzymes and reversibly hydrate CO_2 into HCO_3^- and H^+. The three major classes of CAs are α (mammals), β (plants and some prokaryotes) and γ (archaea bacteria). Human α-CAs comprise of 12 catalytic isoforms which differ in tissue location and catalytic activity (reviewed by (Aggarwal et al. 2013)).

This thesis focuses on CA9, as it is a HIF-target gene that is commonly overexpressed in cancers. It is associated with aggressive tumour growth and poor prognosis. CA9 is a transmembrane-spanning enzyme that forms homodimers (Fig. 1.8).

.

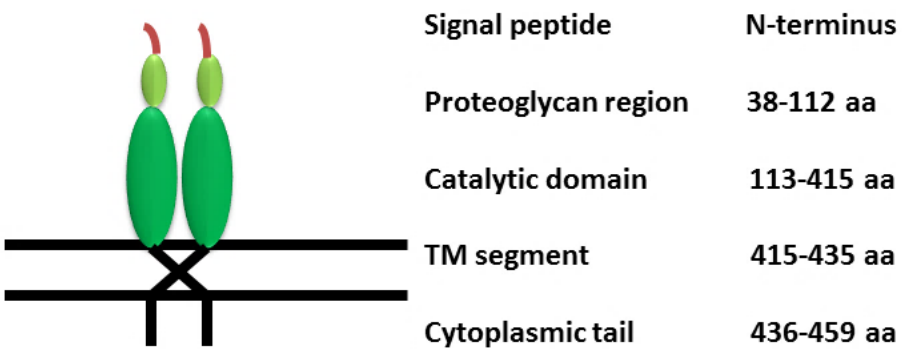

Fig. 1.8: CA9 is a transmembrane-spanning carbonic anhydrase with an extracellular facing catalytic domain. CA9 forms homodimers. The cytoplasmic tail is required for the localisation of CA9 in the cell membrane, CA9 function and signal transduction (Hulikova et al. 2009; Dorai et al. 2005). The transmembrane segment anchors CA9 in the membrane. The catalytic domains mediated the hydration of CO_2 whereas the proteoglycan region and the signal peptide mediate the CA9-specific activation at low pH_e (Innocenti et al. 2009). The image is based on (Alterio et al. 2009).

Therefore, CA9 consists of two catalytic domains which are stabilized by a disulphide bond. The two active sites face the extracellular space and bind one Zinc ion. At the N-terminal end, there is a proteoglycan region (PG) and a signal peptide. The PG region is only expressed in CA9 and therefore enables its unique activity at pH ~ 6.5. This is mediated by acidic residues of aspartic acid and glutamine as they act in a buffer-like manner (Innocenti et al. 2009). The transmembrane-spanning segments are hydrophilic and serve as C-terminal anchor. The cytoplasmic tail is required for localising CA9 in the cell membrane and for extracellular acidification in hypoxia (Hulikova et al. 2009). Phosphorylation of the cytoplasmic tail by signalling proteins additionally regulates CA9 function in hypoxia (Ditte et al. 2011; Dorai et al. 2005).

CA9 acidifies pH_e while it contributes to the alkalinisation of pH_i via bicarbonate synthesis. This process is crucial for pH regulation in hypoxia and tumour progression. Tumour cells only acidify medium in hypoxia, but not in normoxia (Švastová et al. 2004). Additionally, low pH_e is associated with enhanced CA9 activity in MDA-MB-231, further contributing to tumour acidification (Li et al. 2011). Also, CA9 expression and activity increase with tumour aggressiveness and correlate with a highly glycolytic phenotype (Li et al. 2009). CA9 and CA12 jointly maintain an alkaline pH_i thereby enabling tumour growth in an acidic pH_e by sustaining ATP levels and proliferation. This is further increased by hypoxia (Chiche et al. 2009).

Important for sustained CA9 activity is the re-transport of bicarbonate back into the cell by bicarbonate transporters as the inhibition of Na^+-dependent bicarbonate transporters induces apoptosis and acidification of pH_i in MDA-MB-231 spheroids, and reduces xenograft growth *in vivo* (McIntyre et al. 2016). Increased CA9 expression also promotes invasion and metastasis (Lou et al. 2011; Shin et al. 2010; Radvak et al. 2013).

CA9 overexpression is characteristic for aggressive tumour types such as basal-like breast cancer, where CA9 overexpression correlates with tumour size, high histopathologic grade and oestrogen receptor (ER) negativity. CA9 overexpression also significantly correlates with reduced disease-free survival and overall survival (Tan et al. 2009). Murine metastatic breast cancer models have also shown that CA9 expression promotes invasion of distant organs and colonisation of the lung which is reversed by pharmacological and genetic inhibition of CA9 (Lou et al. 2011). This is potentially mediated via Rho-GTPase-mediated EMT, leading to the re-organisation of the cytoskeleton, the weakening of cell adhesion, and increased cell motility (Shin et al. 2010). Hypoxia-induced CA9 also supports invasion by re-locating to the lamellipodia, where it co-localises with NBCn1 and AE2 to acidify pH_e at the leading edge of migrating tumour cells (Svastova et al. 2012).

Hypoxia-induced CA9 expression also contributes to the suppression of the host's anti-tumour immune response. In hypoxic breast cancers, CA9 is required for the production of granulocyte colony stimulating factor (G-CSF). G-CSF mediates the migration of myeloid-derived suppressor cells (MDSCs) to the lung where they prepare the metastatic niche. This process is mediated by NFκB signalling (Chafe et al. 2015).

Additionally, CA9 expression promotes the expansion of $CD44^{+}/CD24^{-/low}$ cancer stem cells in hypoxia in an mTORC1-dependent manner. The inhibition of CA9 reduces the activity and expression of mTOR *in vivo* as well as the expression of the stem cell marker EpCAM (Lock et al. 2013). Additionally, (Ledaki et al. 2015) identified heterogeneous CA9 induction in hypoxia within a panel of human cancer cell lines. This CA9 induction is independent from HIF-1, as HIF-1 is also stabilized in CA9-negative cells. However, CA9-positive populations differ in their gene signature. CA9-positive cells upregulate pathways involved in stem cell maintenance, including ABC transporters and Wnt and Hedgehog signalling. Silencing of CA9 downregulates these pathways and impairs mammosphere formation. The downregulation of CA9 in the CA9-negative population is accompanied by trimethylation of H3K9 in hypoxia and by reduced HIF-binding. Hypoxia-induced CA9 expression is also associated with resistance to chemotherapy (Zheng et al. 2015).

1.6.3 *CA9* is a HIF-1 target gene

The *CA9* gene is located on chromosome 9 in the p12-p13 region and consists of 11 exons. It is transcribed into one single mRNA, 1.5 kb in length. The *CA9* promoter has a high GC content and contains no TATA box, but has two initiator-like sequences which do not overlap with the start of transcription site. Additionally, there are six *cis*-acting elements of which five are activating and one is inhibitory (Fig. 1.9). The HRE lies -10;-3 upstream of the start of transcription and contains the common core sequence ATGCACGTA required for HIF-binding. This is the most important regulatory element as mutations in this sequence abolish *CA9* activation. However, the binding of additional transcription factors is required to induce *CA9* transcription. Consequently, the *CA9* promoter contains specifity protein (SP) SP1 and SP3 binding sites which are essential for minimal *CA9* induction in hypoxia. Additionally, there are activating protein 1 (AP-1) binding sites which integrate oncogenic signalling via the activation of AP-1 complexes by PI3K-MAPK/ERK signalling, and therefore fine-tune *CA9* expression (Grabmaier et al. 2004; Kaluz et al. 2003; Kaluz et al. 2009).

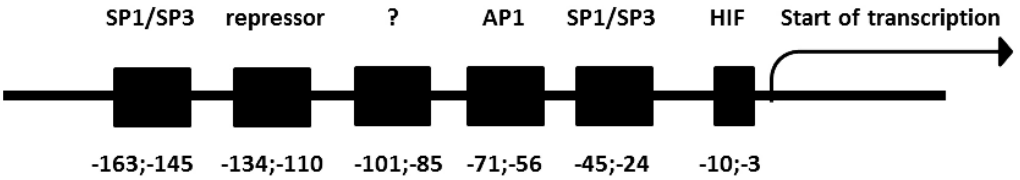

Fig. 1.9: Transcription factors bind regulatory cis-acting elements within the *CA9* promoter and jointly regulate *CA9* transcription. Binding of the transcription factors SP1/3 and HIF-1 is required for *CA9* activation in hypoxia. The binding of transcription factor AP1 enables the integration of PI3K or MAPK-mediated signalling, and therefore amplification of CA9 activation. Position -101;-85 is occupied by an unknown regulatory factor. Regulatory domain -134;-110 is bound by a repressor in a cell type-specific manner (Grabmaier et al. 2004; Kaluz et al. 2003; Kaluz et al. 2009). SP1/SP3, specifity protein 1/3 binding sites; ?, cell type-dependent binding site for unknown regulatory protein; AP1, activating protein 1 binding site; HIF, HIF-1 binding site. The image is based on (Kaluz et al. 2009).

CA9 is strictly regulated by HIF (Grabmaier et al. 2004) and is therefore activated by hypoxia and oxygen-independent factors that stabilise HIF, such as mutations in pVHL in renal carcinomas (Wykoff et al. 2000). Additionally to the regulation of transcription by SP1 and HIF-1, *CA9* expression is also regulated in an epigenetic manner. *CA9* is hypomethylated in CA9 overexpressing renal cancer cells and completely methylated in healthy renal tissue (Cho et al. 2001). CA9 expression is high in the gastric mucosa but drastically reduced in gastric cancer cells and primary gastric tumours which only express CA9 at the invasive front. This difference in expression is independent from HIF-1 but is mediated via the activation of CREB which in turn activates SIRT1 via p300, HDAC1 and DNMT1, leading to deacetylation and methylation of the *CA9* promoter in an oxygen-independent manner (Wang et al. 2015). As already discussed above, (Ledaki et al. 2015) identified a HIF-dependent mechanism of epigenetic regulation of *CA9* expression. Alternatively, *CA9* is induced by high cell density in some cell lines independent from oxygen concentrations via the activation of MAPK or PI3K signalling, inducing basal levels of SP1 and HIF-1 binding (Kaluz et al. 2002; Kopacek et al. 2005).

1.6.4 Hypoxia, the pH regulatory machinery, and its therapeutic implications

Hypoxia and anaerobic metabolism are major contributing factors to extracellular acidosis. However, (Hulikova et al. 2013) demonstrated that NHE1-medaited H^+ extrusion is dominant in normoxia but is inhibited in hypoxia in a broad panel of human breast cancer cell lines. This is mediated by reduced glycosylation of NHE1. However, Na^+-dependent HCO_3^- transport is independent from oxygen levels and cell type, and contributes to intracellular alkalinisation. Therefore, constitutive co-transport of Na^+-HCO_3^-, while inhibiting NHE1-mediated H^+ extrusion, may be protective for hypoxic cancer cells because it prevents overloading the extracellular space with acid.

It remains controversial whether NBCn1 is regulated by hypoxia. In MDA-MB-231 cancer cells, NBCn1 expression is not induced by hypoxia, and impaired pH_i recovery and increased mortality in spheroid growth upon NBCn1 silencing is independent from hypoxia (Parks & Pouyssegur 2015). This agrees with the findings of (Hulikova et al. 2011) who demonstrated that whereas H^+ efflux is variable between cell lines, HCO_3^- flux remains constant. Therefore, bicarbonate uptake acts as "housekeeping "pH regulatory mechanism which highlights its role as essential part of pH_i regulation. Additionally, colorectal cancer spheroids are more sensitive towards NBCn1 inhibition by DIDS with increasing depth as low pH_e inhibits H^+ efflux and impairs proliferation (Hulikova et al. 2011). Consequently, bicarbonate flux fulfils two functions. First, it acts as substrate for ion transporters and secondly, it acts as mobile buffer to reduce H^+ to ensure the sustained efflux of H^+. On the other hand, (McIntyre et al. 2016) demonstrated that there is a highly cell line-dependent induction of SLCA4A4 and SLC4A9 by HIF. The silencing of SLC4A9 acidifies the cores of spheroids as well as pH_i in spheroid cores, and thereby induces apoptosis. *In vivo*, SLC4A9 silencing impairs breast cancer xenograft growth. Further, *SLC4A7* was identified as a breast cancer susceptibility locus in a genome-wide association study (Ahmed et al. 2009). The literature cited above illustrates the importance of bicarbonate transport to tumour progression and pH regulation in hypoxia by maintaining H^+ flux and re-uptake of bicarbonate into the cell.

The active generation and survival of acidosis provides a selective advantage for tumour cell populations and drives invasion (Estrella et al. 2013; Gatenby et al. 2007). However, the buffering capacities within tumours are limited, making tumour cells vulnerable for disruption of their pH regulating system (Estrella et al. 2013; Robey et al. 2009; Parks & Pouyssegur 2015). Consequently, the inhibition of pH regulating mechanisms is of strong clinical interest. However, pH regulating proteins such as NHE1 are systemically expressed (Hachem et al. 2005; Juel 2000; Noel et al. 1996; Yokoyama et al. 2000). Therefore, CA9 is a promising therapeutic target. First, its expression is relative specific as it is induced by hypoxia and it is only expressed in the gastric

mucosa (Beasley et al. 2001; Gut et al. 2002; Ivanov 2001; Wykoff et al. 2000). It is also targetable by small molecule inhibitors as well as by histone modifiers (Ledaki et al. 2015; Lou et al. 2011), and coupled to blocked uptake of bicarbonate, it can induce specific cell death, thereby increasing the success of current cancer therapies (McIntyre et al. 2016). However, pH regulation is complex and its components are often redundant and compensate each other. (Chiche et al. 2009) demonstrated that inhibition of either CA9 or CA12 only minorly reduces xenograft growth *in vivo*, whereas the combined silencing of CA9 and CA12 strongly reduces xenograft growth. The allelic deletion *NHE1* and *CA9* individually reduces xenograft growth *in vivo* but combined silencing leads to compensation by upregulation of CA12 and CA2, supporting xenograft growth (Parks et al. 2016). Alternatively to inhibiting CA9, the inhibition of hypoxia-induced SLC4A4 and SLC4A9 induces apoptosis in spheroids *in vitro* by acidifying pH_i due to hindered bicarbonate uptake (McIntyre et al. 2016). A different approach relies in increasing the buffering capacity of the mobile buffer, impair H^+ diffusion, and to withdraw cancer cells the selective advantage by raising pH_e. In this context, (Estrella et al. 2013) and (Robey et al. 2009) demonstrated that the oral administration of bicarbonate reduces tumour cell invasion *in vivo* which is mediated by acidic tissue remodelling.

1.7 Preliminary work, aims and hypothesis

The previous sections elaborated how hypoxia, glycolysis, and acidosis drive tumour progression. However, the potential role of CtBPs as link between hypoxia-induced glycolysis and the survival of cancer cells in hypoxia-driven acidosis is unknown.

1.7.1 Preliminary work

A preliminary study was performed by the Blaydes group prior to this project. MCF7 breast cancer cells were transfected with siRNA targeting both CtBPs and with non-specific control siRNA and exposed to hypoxia. Consequently, the expression of HIF-dependent target genes was examined in a gene expression study. It was found that under anoxic conditions, and in the absence of CtBP activity or when glycolysis was blocked by 2-deoxyglucose (2-DG), the expression of *CA9* was reduced whereas the expression of *ADM* was increased. This suggests an interaction between HIF and CtBP to ensure cell survival under hypoxic conditions.

1.7.2 Hypothesis

Based on the preliminary findings described above, it is hypothesised that HIF-mediated responses to hypoxia depend on the redox and glycolytic state of a cell and that this response is mediated in an HIF-CtBP dependent manner.

1.7.3 Aims of the study

Therefore this project aims to:

- Determine the impact of glycolytic metabolism and hypoxia on the CtBP-HIF-1-dependent regulation of HIF-target gene expression.
- Shed light onto mechanistic and functional interactions between HIF-1 and CtBPs to regulate HIF target gene expression.
- Investigate the role of CtBPs and HIF-1 interaction in breast cancer cell survival of hypoxia-induced acidosis.

1.7.4 Significance of the study

This work experimentally determines a novel functional interaction between glycolysis and CA9 via the activation of CtBPs, which in conjunction with p53 potentially promotes survival of hypoxia-induced acidosis in MCF7 breast cancer cells. This regulation is unique for CA9. Further, this thesis supports the growing body of evidence that CtBPs also function as co-activators of gene expression, and underlines the role of CtBPs as versatile co-regulators of transcription. All in all, this study further strengthens CtBPs as therapeutic target and highlights the role of glycolysis-mediated gene regulation in the survival of hypoxia-induced acidosis.

Chapter 2: Material and Methods

This chapter is concerned with the methodology that was applied to address the research questions stated in the previous chapter and to test the research hypothesis. This was achieved by performing gene expression studies and protein expression analysis in human cancer cell lines. The chapter is divided into two thematic sections. The first section elaborates basic methodology that was applied throughout the study and includes cell culture, gene expression analysis, and the determination of protein expression. The second section describes specific experiments that were performed to address research aims stated earlier and to test the research hypothesis.

2.1 General methodology

2.1.1 Cell culture

The role of the CtBP-HIF axis in cancer cell survival was studied in the human breast cancer cell lines MCF7 (ATCC), MDA-MB-231 (ECACC), and SkBR3 (Cancer Research UK), and in the pVHL-defective renal carcinoma lines A498 (ATCC) and 786-O (ATCC) (Tab. 2.1). Additionally, the impact of glycolysis and CtBPs on HIF-1 target gene expression was experimentally determined in MCF7 which were modified by members of the Blaydes group. MCF7 breast cancer cells were engineered to either express an empty control vector (MCF7.Control) or to overexpress wild-type CtBP2 (MCF7.CtBP2). The third MCF7–derived cell line (MCF7.CtBP-Mutant) expresses CtBPs exhibiting mutations in the dehydrogenase domain which hinders dimerization of CtBP monomers, and thus activation of CtBPs. These modified cells are adapted to either grow in 10 mM fructose-containing medium or 25 mM glucose-containing medium. Fructose-adapted MCF7.Control cells exhibit similar metabolic adaptions to fructose-grown HeLa cells described by (Reitzer et al. 1979) which includes downregulated glycolysis, and the reliance on the PPP and glutaminolysis for energy generation. Glucose-adapted MCF7.CTBP2 and MCF7.CtBP-Mutant were applied to determine the impact of CtBP expression on the regulation of HIF-1 target genes. All MCF7-derived cell lines were grown in Dulbecco's modified eagle medium (DMEM) that was prepared in house as described below.

2.1.1.1 Maintenance of cell lines

Cells were grown in a humidified incubator at 37 °C and in 10% v/v CO_2 and maintained in DMEM (gibco® by life technologies, UK) which was supplemented with 10% fetal calf serum (FCS) (GE Healthcare, Austria), 1% Penicillin/ Streptomycin (SIGMA Life Sciences, USA) and 1% glutamine (Sigma-Aldrich, UK) (complete DMEM). To ensure sufficient supply with nutrients, cell culture medium was renewed every 48 hours (h). Upon confluence, cells were sub-cultured in T75 cell culture flasks (Corning Incorporated, USA) in a ratio not higher than 1:10 by using trypsin-EDTA (Sigma-Aldrich, USA). The 786-O renal cancer cells were grown at 37 °C in 5% v/v CO_2 in RPMI medium (SIGMA Life Science, UK) supplemented with 10% FCS, 1% Penicillin/ Streptomycin and 1 % glutamine (SIGMA Life Science, UK). The engineered MCF7-derived cell lines were grown in complete DMEM that was either containing 10 mM fructose or 25 mM glucose but was prepared in house. For this, DMEM medium was prepared from 4.15 g/ 500 ml DMEM powder (SIGMA ALDRICH, UK), 1.85 g/ 500 ml sodium bicarbonate (SIGMA ALDRICH, USA), 10% FCS, 1% glutamine, 1% penicillin/ streptomycin, 1% sodium pyruvate (SIGMA ALDRICH, UK) and either 10 mM D(-) fructose (SIGMA ALDRICH, USA) or 25 mM glucose (Corning, USA). Both media were sterile filtered with 0.2 µm syringe filters (BD Plastipak™, Spain) before they were added onto the cells.

2.1.1.2 Harvesting cells for protein or gene expression analysis

To harvest cells after the termination of an experiment, cells were washed with ice-cold sterile PBS. Subsequently, 1 ml of ice-cold PBS was added and cells were dislodged by using the end of a plunger of a syringe (BD Plastipak™, Spain). The suspension was transferred to Eppendorf tubes and centrifuged at 3000 rounds per minute (rpm) (900 G) for 5 minutes (min) at 4 °C. Cell pellets were snap-frozen in liquid nitrogen and stored at -70 °C until further use. All the work was performed on ice.

Tab. 2.1: Overview over the characteristics of the cancer cell lines used in this study

Cell line	Classification	Differentiation	Receptor profile	Reference
MCF7	Luminal Adenocarcinoma of the mammary gland	Preserved characteristics of differentiated epithelium	Oestrogen Receptor (ER)$^{+}$ Progesterone Receptor (PR)$^{+/-}$ HER2^{-}	ATCC-HTB-22 (Prat et al. 2013)
MDA-MB-231	Basal Adenocarcinoma of the mammary gland, Claudin-low, Similar to mammary stem cells/ progenitor cells	Poor (form grade III adenocarcinomas)	ER^{-} PR^{-} HER2^{-}	ATCC-HTB-26 (Prat et al. 2013)
SKBR3	Luminal Adenocarcinoma of the mammary gland	Poor	HER2^{+} ER^{-} PR^{-}	ATCC-HTB-30 (Neve *et al.* 2006)
A498	Primary renal carcinoma with unclear histology	Moderately	pVHL^{-} frameshift in codon 213	ATCC-HTB-44 (Brodaczewska et al. 2016; Gnarra et al. 1994)
786-O	Metastatic clear cell renal cell carcinoma	poor	pVHL^{-} frameshift in codon 175	ATCC-CRL-1932 (Brodaczewska et al. 2016; Gnarra et al. 1994)

2.1.2 Determination of gene expression

In order to determine gene expression by either TaqMan™ reverse-transcription PCR or by Roche library-based reverse-transcription PCR, RNA was extracted from cell pellets and consequently transcribed into cDNA. Gene expression was determined by the comparative C_T method and by ANOVA and uncorrected Fisher's LSD test.

2.1.2.1 RNA extraction for gene expression analysis

RNA was extracted to study gene expression by utilizing the ReliaPrep™ RNA Cell Miniprep System kit (Promega, USA). Frozen cell pellets were lysed by adding 100 µl BL+TG buffer and subsequent vortexing. Immediately, 35 µl of 100% isopropanol (Scientific Fisher, UK) was added and the lysate was vortexed for 5 s. In the following, one minicolumn per sample was placed into a collection tube. The cell lysates were transferred into the minicolumns and centrifuged for 30 s at 10500 rpm at room temperature. The liquid in the collection tube was discarded and the pellet was washed by adding 500 µl of RNA wash solution to the minicolumn. The samples were centrifuged under the same conditions as described earlier and the run through liquid was discarded. To avoid DNA contamination, a DNase I incubation mix was prepared as a mastermix (Tab. 2.2) of which 30 µl were directly added onto the membrane of each minicolumn. Consequently, the DNase I mix was incubated on the columns for 15 min at room temperature.

Tab. 2.2: Pipetting scheme for the preparation of DNase I incubation mastermix

Solution	Volume per sample [µl]	x number of preps	= Total volume
Yellow Core Buffer	24		
$MnCl_2$ 0.09 M	3		
DNase I	3		

Following the incubation with DNase I, 200 µl of Column Wash Solution was added and samples were centrifuged for 15 s at 10,500 rpm at room temperature, followed by another washing step with 500 µl RNA Wash Solution. The collection tube was replaced by a fresh one and the samples were once more washed with 300 µl RNA wash solution and centrifuged for 2 min at 10,500 rpm at room temperature. To elute the RNA, 15 µl of nuclease-free water was added to the minicolumn membrane and the samples were centrifuged for 1 min under the conditions described above. RNA concentration was measured by using a nanodrop 1000 spectrophotometer (Thermo Scientific, UK) and samples were stored at -70 °C until further use.

2.1.2.2 cDNA synthesis for reverse transcription PCRs

To perform reverse transcription qPCR, the extracted RNA had to be transcribed into cDNA. The assay was performed on ice and in 0.5 ml thin walled PCR tubes. RNA samples were diluted with nuclease-free water to give a RNA concentration of 250-1000 ng in 26.25 µl in total. Subsequently, 13.75 µl of a mastermix containing MMLV reverse transcriptase, oligo dT 15 primer and dNTPs (all Promega, USA) were added to the diluted RNA to give a final volume of 40 µl (Tab. 2.3). Samples were gently mixed by pipetting up and down and incubated in a PCR thermocycler (flexigene, UK) at 37 °C for 1 h followed by 5 min at 94 °C. The synthesised cDNA was stored at -20 °C until further use.

Tab. 2.3: Pipetting scheme for mastermix for cDNA synthesis

Reagents (all Promega, UK)	Volume per sample [µl]
5x Reverse Transcriptase Buffer	8
dNTPs- 10 mM	1
Oligo dT 15 primer	1
MMLV Reverse transcriptase	0.75

2.1.2.3 Evaluation of *ADM* and *CA9* expression by TaqMan® qPCR

CA9 and *ADM* expression was evaluated by reverse-transcription TaqMan® qPCR. The TaqMan® assay is based on the 5' endonuclease activity of Taq DNA polymerase cleaving an oligonucleotide probe which results in a detective fluorescent signal (Fig. 2.1). Compared to other quantitative PCR assays, it is more specific due to the utilisation of one forward and one reverse primer, a target-specific oligonucleotide probe and also by the addition of a minor grove binder (Applied Biosciences only) (National Centre for Biotechnology Information (NCBI), USA, 2014). In the annealing phase, both the primers and the probe bind and the fluorescent light emitted by the reporter dye is absorbed by the quencher dye. Next, the probe is displaced by the DNA polymerase while extending the primer. Finally, the probe is degraded, leading to the release of the reporter dye and the emission of a detectable fluorescent signal (NCBI, 2015) (Fig. 2.1).

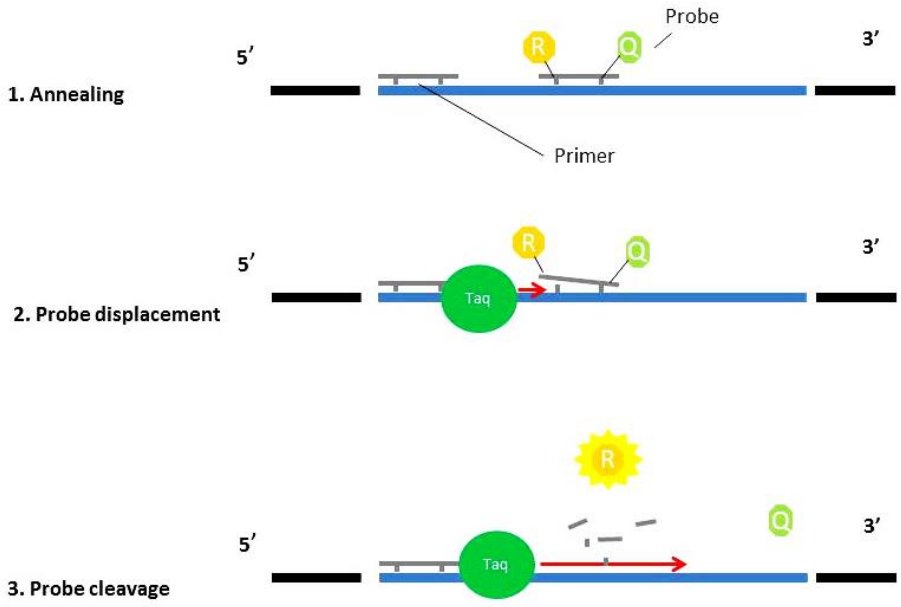

Fig. 2.1: The three phases of an amplification cycle in TaqMan® qPCR exemplarily shown at the 5' forward strand. After double strand denaturation at 95 °C, the target specific primers as well as the reporter and quencher dye-labelled oligonucleotide probe bind to the target gene at 60 °C. During the extension phase (72 °C) the Taq DNA polymerase adds dNTPs to the free 3'end of the primer. Double strand synthesis consequently leads to probe displacement and degradation. This causes the release of the reporter dye and hence the emission of a fluorescent signal which is detected after each cycle. R= reporter dye. Q= quencher dye, Taq= Taq DNA polymerase. This image was modified after NCBI (2014).

First, the cDNA was diluted with nuclease-free water to give a concentration of 1 ng/µl. In the next step, a mastermix containing the probe for the gene of interest, the TaqMan® universal mix, and nuclease-free water was prepared (Tab. 2.4). Both steps were performed on ice.

Tab. 2.4: Pipetting scheme for TaqMan® mastermix preparation

Reagents (all Applied Biosciences, USA)	Volume per sample [µl]
TaqMan® Universal Mix	10
Probe (x20 mix)	1
Actin (4326315E)	
***ADM* (Hs00969450_g1)**	
***CA9* (Hs00154208_m1)**	
Nuclease-free water	4

A MicroAmp® optical 96 well plate (life technologies, USA) was loaded with 15 µl mastermix per well followed by 5 µl of cDNA or nuclease-free water for the non-template control. Each sample

was loaded in duplicates. After all samples were loaded onto the plate it was sealed with a ThermalSeal RT2RR™ (alphalaboratories, UK) and centrifuged for 1 min at 2000 rpm at room temperature. TaqMan® quantitative real-time qPCR was performed using a 7500 real-time PCR system (Applied Bioscience). There were 40 amplification cycles performed, resulting in one C_T value for each reaction.

2.1.2.4 Evaluation of gene expression of further HIF-1 targets by semi-quantitative reverse transcription PCR

It was evaluated whether the CtBP-mediated regulation of gene expression is unique for *CA9* or whether other HIF-1 target genes are also regulated in a CtBP dependent manner. Consequently, samples treated with 2-DG, MTOB and siRNA were also analysed for the hypoxia- or dimethyloxalylglycine-induced (DMOG) expression of *PDK1, EGLN3, INSIG2, FAM162A* and *TMEM45A*. Gene expression of these selected HIF-target genes was determined by reverse-transcription PCR, which was similar to TaqMan™ reverse-transcription PCR, but the TaqMan® system was replaced by Roche library primers and probes (Tab. 2.5). These HIF-target genes were chosen based on their expression in the preliminary microarray analysis. In anoxic MCF7 with silenced CtBP 1/2 expression, the HIF-1 target genes selected displayed a more than threefold change in gene expression. The experiment was performed in MCF7 as wells as in MDA-MB-231 breast cancer cells. Furthermore, MCF7.Control, MCF7.CtBP2 and MCF7.CtBP-Mutant cells were also screened for the DMOG- and hypoxia-induced expression of these HIF-1 target genes.

Tab. 2.5: Mastermix for one reaction for semi-quantitative real-time PCR with Roche library primers and probes against further HIF-1 target genes

Reagent	Volume [µl]
Universal mix	10
Primer L 10µM	1.2
Primer R 10µM	1.2
***PDK1*: #20 10 µM**	0.4
***INSIG2*: #67 10 µM**	0.4
***FAM162A*: #44 10 µM**	0.4
***EGLN3:* #61 10 µM**	0.4
***TMEM45A*: #24 10 µM**	0.4
DNase and RNase free water	2.2

2.1.2.5 Data analysis of reverse-transcription PCR by the comparative C_T method

Gene expression was analysed by applying the comparative C_T method as described by (Livak & Schmittgen 2001). Briefly, for each sample the mean C_T value was calculated, followed by the calculation of the change in C_T values (ΔC_T) by subtracting the C_T value of the housekeeping gene from the C_T value of the target gene:

Equation 2: Calculation of ΔCT

$$\Delta C_T = \mathrm{C_{T\ target}} - \mathrm{C_{T\ housekeeping}}$$

Consequently, the change in ΔC_T ($\Delta\Delta C_T$) was calculated by subtracting the ΔC_T of the negative control from the ΔC_T of the sample:

Equation 3: Calculation of ΔΔCT

$$\Delta\Delta\mathrm{CT} = \Delta_{\mathrm{C_{T\ sample}}} - \Delta_{\mathrm{C_{T\ negative\ control}}}$$

Finally, relative expression was calculated by the following formula:

Equation 4: Relative gene expression

$$\mathrm{relative\ expression} = 2^{\Delta\Delta\mathrm{CT}}$$

All data analysed by the comparative C_T method was analysed by applying a template provided by the Blaydes group.

2.1.2.6 Statistical analysis

Each experiment was performed in three independent repeats unless stated otherwise and all data was analysed and displayed by using the statistics software Graph Pad Prism version 6.01. Furthermore, all data is represented as mean values ± standard error of the mean (SEM) throughout the thesis unless stated otherwise. Statistical significance was determined by applying ANOVA and Fisher's uncorrected LSD test. The level of significance was defined as $p < 0.05$.

2.1.3 Analysis of protein expression

2.1.3.1 Cells lysis and determination of protein concentration for Western blotting

In order to evaluate the expression of the proteins of interest, harvested cells (see 2.1.1.2) were lysed by denaturising urea whole cell lysis. First, cell pellets were placed on ice and 20 µl of urea lysis buffer was added (Tab. 2.6). The buffer was stored in single use aliquots at -20 °C.

Tab. 2.6: Urea lysis buffer for whole cell lysis

Reagent	Final concentration	Volume for 1 ml
8M urea (Fisher Scientific, UK)	7M	880 µl
10% Triton X-100 (SIGMA, Switzerland)	0.05%	5 µl
5M NaCl (Fisher Scientific, UK)	25 mM	5 µl
1M HEPES pH 7.6 (SIGMA)	20 mM	20 µl
1M DTT in 0.1M NaAC pH 5.2	100 mM	100 µl

In the following, cells were lysed for 15 min on ice including a brief vortex after 8 min in order to break up the pellet. Following lysis, the lysate was centrifuged for 10 min at 4 °C at 10500 rpm. The supernatant which contained the cell lysate was snap frozen in liquid nitrogen and either stored at -70 °C until further use or subsequently quantified by Bradford assay. For quantification, BioRad protein assay dye concentrate (BioRad, Germany) was diluted 1:5 with sterile de-ionised water. 1 ml of the solution was aliquoted into plastic cuvettes (VWR, Belgium) and 1 µl of cell lysate per cuvette was added. Each sample was measured in duplicate. The samples were mixed by gently inverting the cuvette and the absorbance at wavelength= 595 nm was immediately measured by using a spectrophotometer (Pharamspec UV 1700, Shimadzu). Final protein concentration was calculated from linear regression of a standard curve which derived from samples of known bovine serum albumin (BSA) concentrations (Fig. 2.2). The standard curve was created by Charles Birts and used by other members of the laboratory due to a ready-made, commercially available Bradford reagent being used.

Protein concentration was calculated using the following equation:

Equation 5: Protein concentration of cell lysates $\text{protein concentration } x = y/0.0639$

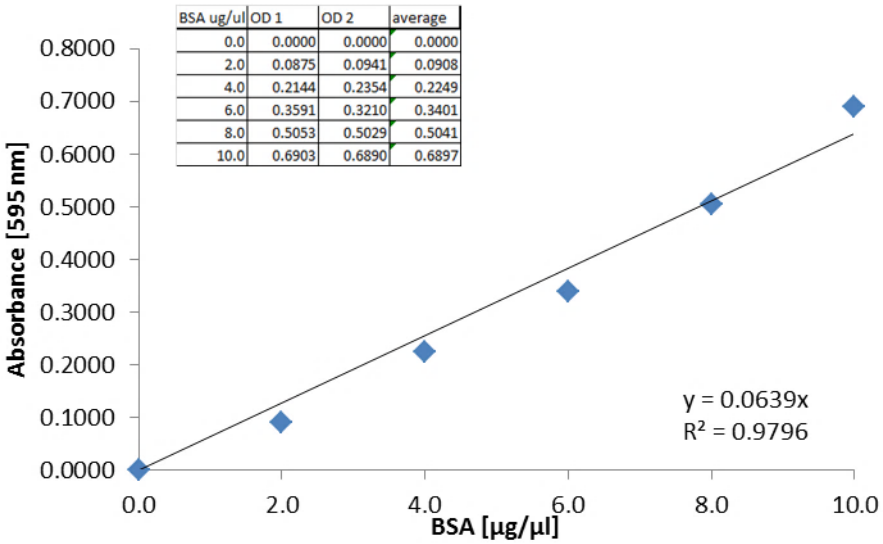

Fig. 2.2: Standard curve to determine the protein concentrations of whole cell lysates. A standard curve was created by performing a Bradford assay on samples with known BSA concentrations. Linear regression of the curve enabled the calculation of protein concentration by using the obtained equation. The standard curve was created by Charles Birts and was also used by other members of the laboratory as the Bradford reagent involved was ready-made and commercially available.

2.1.3.2 Evaluation of protein expression

The expression of proteins of interest was evaluated by Western blot. First, Sodium Dodecyl Sulphate Polyacrylamide Gel Electrophoresis (SDS-PAGE) was performed with the quantified whole cell lysates. Applying electric current, SDS-PAGE separates the proteins within the lysate by the virtue of their molecular weight. For this, a 10% acrylamide gel was prepared. The running gel was prepared by gently mixing 2.5 ml of 40% Acrylamide-Bis 29:1 (SIGMA Life Science, USA), 4.8 ml sterile de-ionised water, 2.5 ml 1.5 M Tris pH 8.8 (Fisher Scientific, UK) and 100 µl 10% SDS (Fisher Scientific, UK) in water. To prepare the stacking gel, 1 ml 40% Acrylamide-Bis 29:1, 6.3 ml water, 2.5 ml 0.5 M Tris pH 6.8 (Fisher Scientific, UK) and 100 µl 10% SDS in water were gently mixed. The running gel was polymerized by adding 100 µl 10% ammonium persulphate (SIGMA Life Science, Japan) and 5 µl TEMED (SIGMA Aldrich, China) to the mixture. Quickly, around 3 ml of running gel solution per gel were pipetted into the BioRad Mini-gel apparatus (BioRad) and topped off with water. After the running gel polymerised, the stacking gel was polymerised by adding 100 µl 10% ammonium persulphate and 10 µl TEMED. Subsequently, the water was removed and the stacking gel was layered on top, a comb was inserted to create wells and the gel was allowed to polymerise. Once the stacking gel polymerised, the gel could be stored, wrapped in moist cling film, up to 48 h at 4 °C until further use.

During polymerisation, the samples for Western blot were prepared by adding 4x SDS sample buffer to the demanded volume of cell lysate (Tab. 2.7). The 4xSDS sample buffer was stored at room temperature and 1M DTT was added before use to result in a final concentration of 200 mM. Once DTT was added, the buffer was stored at -20 °C. To give a final volume of 12 µl, de-ionised water was added. Subsequently, the samples were denatured at 95 °C for 5 min, centrifuged, and stored on ice until needed. Once the gels were polymerised they were inserted into the apparatus and the reservoirs were filled with running buffer (Tab. 2.8) until covered. The gels were loaded with 12 µl of the prepared samples. Empty lanes were loaded with 4xSDS sample buffer alone. To determine protein size, one lane was also loaded with 1 µl of protein ladder (Thermo Scientific, UK). The gels were run at 150 V for 1 h or until the SDS sample buffer reached the bottom of the gels.

Tab. 2.7: 4x SDS sample buffer for sample preparation for Western blot

Reagent	Concentration
EDTA (Fisher Scientific, UK)	10 mM
SDS (Fisher Scientific, UK)	4%
Glycerol	20%
Tris pH 6.8 (Fisher Scientific, UK)	20 mM
Bromophenol Blue (Bio-Tad Laboratories, USA)	To colour

Tab. 2.8: 10x concentrated stock of running buffer for gel electrophoresis

Reagent	Amount required for 1 l
Tris Base	30g
Glycine (Fisher Scientific)	144g
SDS	10g
De-ionised H_2O	To 1 l

Next, the separated proteins were transferred from the gel onto a membrane by using electric current. For this, the sponges of the clamp apparatus were soaked in transfer buffer. To prepare the transfer buffer, 100 ml TG (Tab. 2.9), 700 ml of de-ionised water, and 200 ml ethanol were mixed in the order mentioned in order to prevent the precipitation of TG.

Tab. 2.9: Protocol for the preparation of TG

Reagent	Amount required for 1 l
Tris Base	29 g
Glycine	145 g
Ethanol (Fisher Scientific, UK)	20%
De-ionised H_2O	To 1 l

Two layers of Whatman™ paper (GE Healthcare, UK) soaked in transfer buffer were placed on top followed by one ™Hybond ECL membrane (GE Healthcare, Germany). The acrylamide gel was carefully placed on top followed by two more layers of Whatman™ paper soaked in transfer buffer, and a sponge. The clamps were closed and transferred into the blotting apparatus, the membrane facing the anode. The chamber was filled with transfer buffer and the transfer was performed overnight at 0.02 V. To ensure the protein bands were transferred from the gel onto the membrane, Indian ink staining was performed. For this, the membrane was incubated on a waver for 5-10 min in 200 µl of Indian ink (Parker, France) diluted in PBS-tween. Excess ink was removed by washing the membranes with washing buffer three times for 5 min. The washing buffer was prepared from PBS (Tab. 2.10) and 0.1% Tween 20 (Fisher Bioreagents, USA).

Tab. 2.10: Protocol for the preparation of 30x PBS

Reagent	Amount required for 2.5 l
NaCl	600 g
KCl	15 g
Na_2HPO_4	108 g
KH_2PO_4	18 g
De-ionised H_2O	To 2.5 l

Following the transfer step, membranes were blocked for 1 h with 5% milk (Marvel, Ireland) in PBS-tween (0.1%) (PBS-T). This was performed on a waver at room temperature. In order to detect the protein of interest, primary antibodies were diluted in 3% milk-PBS-T (Tab. 2.11). Each membrane was inserted into a falcon tube with the protein side facing inwards and incubated with 3 ml of primary antibody solution overnight at 4 °C. The following day, excess antibody solution was removed by washing the membranes three times for 5 min with PBS-tween. To detect the protein of interest, horseradish peroxidase (HRP)-conjugated secondary antibodies which recognised the primary antibody were added at an appropriate concentration (Tab. 2.11) to 3 ml of 3% milk-PBS-T per membrane and incubated at room temperature for 1 h. Excess antibody solution was removed by washing with PBS-T for 15 min and twice for 10 min. The binding of the secondary antibody was visualised by using supersignal west pico chemiluminescent substrate reagent (Thermo Scientific, USA) which consists of luminol enhancer and a stable peroxide solution in equal parts. The signal was measured with BioRad FluoroS multimanager, using an exposure time of 10 s. To ensure equal loading of the gel, the membranes were additionally probed for actin. Subsequently, the membranes were incubated over night at 4 °C with rabbit anti-actin antibody (SIGMA, USA) and detected by HRP-conjugated goat anti-rabbit IgG as described above (Tab. 2.11).

Tab. 2.11: Overview of the antibodies used, their concentrations (c) and (catalogue numbers)

Target	Primary Antibody	µg/ ml	Supplier	Secondary Antibody	µg/ ml	Supplier
CtBP1	Mouse anti-human CtBP1IgG	0.5	Santa Cruz Biotechnology, UK (SC-177759)	Sheep anti-mouse IgG, HRP-conjugated (NA931)	0.53	GE Health-care, UK
CtBP2	Mouse anti-human CtBP2 IgG	0.09	BD Transduction Laboratories, USA (612044)	Sheep anti-mouse IgG, HRP-conjugated (NA931)	0.53	GE Health-care, UK
CtBP2-E16	Polyclonal goat anti-human CtBP2 (E16)	0.67	Santa Cruz Biotechnology, USA	Rabbit-anti-goat IgG, HRP-conjugated (P0449)	0.5	Dako, DK
CA9	Polyclonal goat anti-human CA9 IgG	1.0	R& D systems, UK (AF2188)	Rabbit-anti-goat IgG, HRP-conjugated (P0449)	0.5	Dako, DK
p53	Monoclonal rabbit anti-human p53 IgG	0.33	Cell signalling, USA (#2527)	Goat anti-rabbit IgG, HRP-conjugated (P0448)	0.53	GE Health-care, UK
GLUT-1	Polyclonal rabbit anti- human GLUT-1IgG	0.5	abcam®, UK (ab15309)	Goat anti-rabbit IgG, HRP-conjugated (P0448)	0.5	Dako, DK
LDH-A	Rabbit anti-human LDH-A IgG	1:3000 (supplier does not specify)	Cell signalling, UK (3582S)	Goat anti-rabbit IgG, HRP-conjugated (P0448)	0.5	Dako, DK
Actin	Rabbit-anti human actin IgG	2.8	SIGMA, USA (A5060)	Goat anti-rabbit IgG, HRP-conjugated (P0448)	0.5	Dako, DK

2.2 Experimental procedures performed for hypothesis testing

2.2.1 Analysis of *ADM* and *CA9* expression after increasing exposure to hypoxia

To determine the earliest time point of induction of *ADM* and *CA9* gene expression, $0.5x10^6$ of MCF7, SKBR3 or $0.4x10^6$ MDA-MB-231 cells were plated in 60 mm cell culture dishes (Corning Incorporated, USA) in 3 ml complete DMEM, 24 h prior to hypoxia exposure. Consequently, cells were incubated for 2, 5, 7 and 17 h at either normoxic (20% O_2) or hypoxic conditions (1% O_2) within a hypoxic chamber (billups-rothenberg, USA). To achieve an atmosphere with 1% O_2, cells were exposed to a gas consisting of 1% O_2, 5% CO_2 and 94% N for 5 min. The hypoxic chamber was immediately returned to the cell culture incubator. The procedure was repeated after 1 h. Cells were incubated at 1% O_2 for the indicated time point and immediately harvested with ice-cold sterile phosphate-buffered saline (PBS) and stored at -70 °C until further use. Gene expression was determined by reverse-transcription TaqMan® PCR. The experiment was repeated twice.

2.2.2 Determination of the impact of glycolysis on HIF-1 gene expression

MCF7, MDA-MB-231, A498 and 786-O cells were seeded in complete DMEM at a concentration of $2.2x10^5$/2 ml in 6 well plates (Corning Incorporated, USA). 24 h later, the medium was exchanged. 48 h post-plating, cell culture medium was exchanged again and replaced by complete DMEM supplemented with 10 mM 2-DG (SIGMA-ALDRICH, UK). 2-DG is a glucose analogue which has the second hydroxyl group replaced by hydrogen. Therefore, 2-DG acts as competitive inhibitor of glucose hexokinase and inhibits the reaction of glucose into glucose-6-phosphate. Consequently, glucose cannot be kept within the cell and glycolysis is inhibited (Yamaguchi *et al.*, 2011). The applied concentration of 10 mM compared to 25 mM glucose only reduces glycolysis rather than completely inhibiting it. In order to induce HIF-1 target gene expression, the breast cancer cells MCF7, SkBR3 and MDA-MB-231 were incubated at either 1% or 20% O_2 for 18 h as described above. The renal carcinoma cell lines A498 and 786-O were incubated at 20% O_2 for 18 h. Protein expression was analysed by Western blot. However, it suggested to also probe for HIF-1 expression in the future, in order to confirm the stabilisation of HIF-1 by hypoxia. This accounts for all experiments in which HIF-1 is activated by hypoxia. Gene expression was determined by TaqMan® PCR or Roche library reverse-transcription PCR.

The glycolytic rate is determined by measuring the extracellular acidification rate (ECAR) with a seahorse analyser (Parks et al. 2013). Therefore, it is suggested to include the measurement of

the ECAR in 2-DG treated cells in future experiments, in order to initially demonstrate the impact of 2-DG on glycolysis.

2.2.3 Transient transfection of human cancer cell lines

In order to evaluate the impact of CtBP expression on HIF-target gene expression, cells were transfected with either a single siRNA which targeted both CtBP isoforms (CtBP 1/2 siRNA), with two individual CtBP1 and CtBP2-targeting siRNAs (CtBP 1+2) or with a non-silencing control siRNA. 24 h prior to transfection, MCF7 and MDA-MB-231 breast cancer cells were seeded in complete DMEM in 6 well plates at a concentration of $2.2x10^5$/2 ml. The following day, 50 nM of siRNA (Tab. 2.12) was mixed with OPTI-MEM® (gibco® by life technologies, UK) and INTERFERin® (Polyplus Transfection™, France) (Tab. 2.13), vortexed for 10 s and incubated for 10 min at room temperature. Subsequently, the volume of DMEM was reduced to 1.3 ml and 200 µl of transfection mix was added to each well. After 4 h of incubation at 37 °C, the transfection mix was replaced by 2 ml fresh DMEM. All work was performed under sterile conditions in a cell culture hood.

Tab. 2.12: Sequences of CtBP-targeting siRNAs and of non-silencing control siRNA

Target	siRNA	Supplier	Sense strand (5'→3')	Antisense strand (5'→3')
Non-human RNA	Silencer® negative control No1	Ambion, Applied Biosystems	No sequence provided	
CtBP1		Quiagen	ACGACUUCACCGUCAAGCATT	UGCUUGACGGUGAAGUCGUTT
CtBP2		Quiagen	GCGCCUUGGUCAGUAAUAGTT	CUAUUACUGACCAAGGCGCTT
CtBP1/2		Ambion, Applied Biosystems	GGGAGGACCUGGAGAAGUUTT	AACUUCUCCAGGUCCUCCCTT

Tab. 2.13: Pipetting scheme for one transfection. The volumes refer to a 20 pmol/ µl stock solution of siRNA constructs and included a" buffer" of x1.05 for pipetting errors.

Target	25 nM [µl]	50 nM [µl]	Optimem [µl]	INTERFERin® [µl]	Culture vessel	Transfection volume [ml]
NS	-	3.94	210	10.5	6 well	1.3
CtBP1/2+ NS	1.97 1.97	-	210	10.5	6 well	1.3

48 h post-transfection, the medium was replaced and cells were transferred to either 1% O_2 or 20% O_2 for 18 h. Subsequently, cells were immediately transferred onto ice and pelleted as described before. The cell pellets were either lysed by urea whole cell lysis buffer for determination of protein expression by Western blot or for the analysis of HIF-1 target gene expression by TaqMan® reverse-transcription PCR as described earlier.

Additionally, CtBP expression was inhibited by a combination of four CtBP1- and CtBP2 siRNAs targeting different sequences of CtBP mRNA (smartpool) to further determine the role of CtBPs in the regulation of hypoxia-induced CA9 expression. The smartpool of CtBP1 and CtBP2 siRNAs (Quiagen (gene solution), UK) was kindly provided by Jason Fleming and was sufficient to perform one experiment. Alas, the individual siRNA sequences are not provided by the manufacturer. Therefore, product codes are given as reference instead (Tab. 2.14). To transfect MCF7 cells with smartpool siRNA, MCF7 were plated at a concentration of $2.2x10^5$/2 ml in complete DMEM and in 6 well plates. 24 h post-plating, cells were transfected with smartpool siRNAs or control siRNA as described above, however with adjusted volumes for siRNA and Optimem (Tab. 2.15). 48 h post-transfection, DMEM was replaced and cells were either incubated at 20% or 1% O_2 for 18 h. CA9 protein expression was determined by Western blot.

Tab. 2.14: Product codes for a smartpool of CtBP-targeting siRNAs (QIAGEN (gene solution)).

Target	Allocated siRNA #	Product code
CtBP1	5	s103211201
CtBP1	6	s104142082
CtBP1	7	s104301325
CtBP1	8	s104347749
CtBP2	7	s104139933
CtBP2	8	s104162473
CtBP2	9	s104214301
CtBP2	10	s104238052

Tab. 2.15: Pipetting scheme for one transfection with a smartpool of siRNAs.

Target	Control [µl]	CtBP1+ CtBP2 [µl/siRNA]	Optimem [µl]	INTERFERin® [µl]	Culture vessel	Transfection volume [ml]
Non-silencing control	1.65	-	201.85	10	6 well	1.3
CtBP1+CtBP2	-	1.65	190.3	10	6 well	1.3

2.2.4 Titration of 2-DG concentrations in human cancer cell lines

It was evaluated whether the effect of 2-DG on CA9 expression is dose-dependent and whether a higher dose of 2-DG causes further reduction in CA9 expression. Additionally, CA9 protein is very stable in A498 cells. Therefore, it was aimed to determine whether CA9 expression could be decreased by higher doses of 2-DG. Consequently, 4.4 x10^5 MCF7, MDA-MB-231 and A498 cells were plated in 4 ml DMEM and in 6 cm dishes as described. 24 h later, the medium was replaced by DMEM supplemented with either 0 mM, 25 mM, 50 mM, 75 mM or 100 mM 2-DG and cells were either incubated at 1% or 20% O_2 for 18 h. To evaluate CA9 expression, SDS gels were loaded with 14 µg whole cell lysate and protein expression was determined by Western blot.

In order to confirm the dose-dependent impact of 2-DG on glycolysis, it is suggested to also determine the ECAR in future dose-titration experiments. Therefore, the impact of 2-DG on hypoxia-induced glycolysis would have been sufficiently demonstrated, and would not be required to be measured in follow-up experiments, again.

2.2.5 Time- and dose-dependent titration of 2-DG in renal carcinoma cell lines

To determine whether CA9 expression could be decreased over time with higher 2-DG concentrations, 4.4x10^5 cells were plated in 4 ml of complete DMEM and in 6 cm dishes. 24 h later, DMEM was exchanged and supplemented with 0 mM, 50 mM or 100 mM 2-DG. The experiment was terminated 18 h, 24 h, 48 h, 72 h, 96 h, and 120 h after adding 2-DG to the cell culture medium. CA9 protein expression was determined by Western blot.

2.2.6 Investigating the impact of CtBP expression on HIF-1 target gene regulation in renal carcinoma cell lines

To determine the impact of CtBPs on CA9 expression in A498 and 786-O, cells were transfected with 50 nM siRNA as described above and harvested 48 h post-transfection. CtBP, CA9 and LDH-A protein expression was evaluated by Western blot as described before.

2.2.7 Time-dependent impact of CtBP expression in renal cancer cell lines

In order to determine whether CA9 expression can be modulated by increasing the incubation time of CtBP 1/2 siRNA, the renal cancer cell lines A498 and 786-O were transfected with 50 nM non-silencing control siRNA and CtBP 1/2 siRNA. In the next step, cells were incubated with siRNA for 24 h, 48 h, 72 h, 96 h, and 144 h. The experiment was terminated after the indicated time points and Western blot was applied to evaluate CtBP1, CtBP2 and CA9 expression. Additionally,

CA9 expression was evaluated by TaqMan™ reverse-transcription PCR. The experiment was performed once.

2.2.8 The impact of cell density on CA9 expression in normoxia in MCF7 and MDA-MB-231 breast cancer cells

Density-induced expression of CA9 was evaluated by plating MCF7 and MDA-MB-231 in 5 ml complete DMEM cell culture medium in 6 cm cell culture dishes at increasing cell concentrations (Tab. 2.16).

Tab. 2.16: Plating of MCF7 and MDA-MB-231 cells for evaluation of density-induced CA9 expression

Cell number [x10^6]	**Plating volume [ml]**	**Cell number [x10^6]/ml**
0.44	5	0.088
0.88	5	0.175
1.75	5	0.35
3.5	5	0.7
7	5	1.4
14	5	2.8

For plating, cells were harvested as described and a stock solution at a concentration of 2.8x10^6 cells/ml was prepared by re-suspending the cell pellet in complete DMEM. In order to achieve the desired cell numbers, a serial dilution was performed where each step consisted of a 1:2 dilution. Per cell number, one dish for counting cells upon termination of the experiment and one dish for the evaluation of CA9 expression by Western blot was plated. The medium was changed the following day. Cells were imaged at days two and three using phase contrast microscopy (Olympus IX81). Furthermore, cells were harvested at day 4 and either counted to determine growth behaviour and cell numbers upon termination or lysed with urea lysis buffer. Protein concentration was determined by Bradford assay. The SDS gel was loaded with 15 µg whole cell lysate. CA9 expression was evaluated by Western blot.

2.2.9 The role of glycolysis in HIF-target gene expression in hypoxia-treated fructose-adapted MCF7.Control cells

First, glucose- and fructose-adapted MCF7.Control cells were plated at a concentration of $4.4x10^5$/ 4 ml in a 6 cm dish and the corresponding media were exchanged 24 h and 72 h post-plating. On day 3, cells were either incubated at 1% or 20% O_2 for 18 h. Protein expression was determined by Western blot and gene expression was analysed by TaqMan® reverse-transcription PCR and Roche library-based reverse-transcription PCR. For future experiments, it suggested to also confirm the role of glycolysis in the regulation of HIF-target genes by determining the ECAR.

2.2.10 Validation of DMOG-induced CA9 expression

To confirm that the hypoxia-induced expression of CA9 and other HIF-target genes is HIF-dependent, hypoxia was replaced by incubating cells in 1 mM DMOG (SIGMA-Aldrich, UK) at 20% O_2 for 18 h. DMOG activates HIF-1 by inhibiting the activity of prolyl hydroxylases (PHDs). Therefore, HIF-1α dimerizes with HIF-1β in the nucleus, leading to the activation of HIF-1 target genes in normoxia (Fig. 2.3).

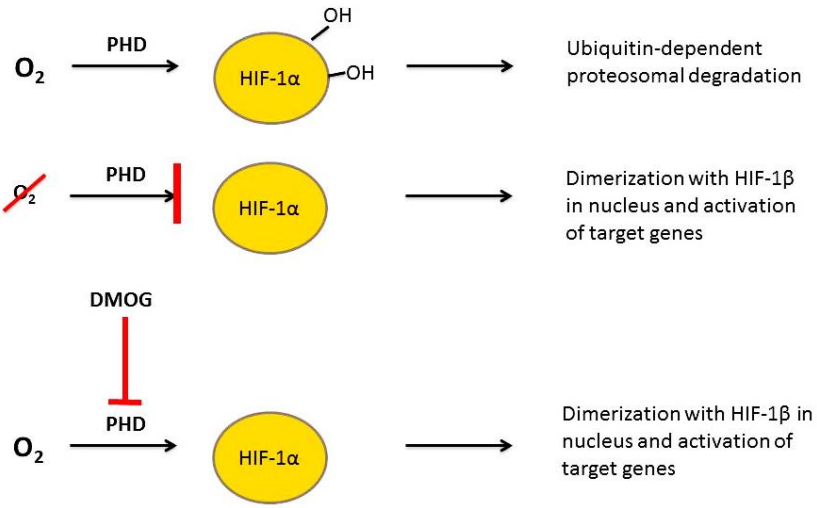

Fig. 2.3: DMOG inhibits the activity of prolyl hydroxylases which leads to the normoxic activation of HIF-1. In the presence of physiological O_2 levels, HIF-1α is hydroxylated by PHDs and degraded by ubiquitin-dependent proteosomal degradation (top). In sub-physiological O_2 levels, PHDs are inactivated, allowing HIF-1α to dimerize with HIF-1β and to activate HIF-target genes in the nucleus. DMOG mimics this process in normoxia (bottom).

To evaluate whether the suggested concentration of 1 mM (Hulikova et al. 2013) is sufficient to induce CA9 protein expression, a preliminary experiment was performed. First, MCF7 cells were plated at a concentration of $7.0x10^5$/ 4 ml in complete DMEM and in 6 cm dishes. 24 h later, when cells were ~ 80-100 % confluent, fresh DMEM containing either 1 mM DMOG, 0.1% DMSO, or DMEM alone was added to the cells and incubated for 18 h at 20% O_2. Following the incubation period, cells were pelleted immediately and CA9 protein expression was determined by Western

blot. Additionally, the DMOG-induced expression of HIF-1 should be confirmed by Western blot in future experiments. This accounts for all experiments in which DMOG is applied to activate HIF-1.

2.2.11 The impact of 2-DG on DMOG-induced HIF-target gene expression

MCF7 cells were plated in complete DMEM at a concentration of $2.2x10^{5}$/2 ml in 6 well plates. 48 h post-plating, DMEM was replaced by complete DMEM alone or supplemented with 10 mM 2-DG, 0.1% DMSO, 1mM DMOG or 1 mM DMOG and 10 mM 2-DG. Subsequently, cells were incubated for 18 h in 20% O_2. Following the incubation period, cells were pelleted and protein expression was analysed by Western blot whereas HIF-1 target gene expression was determined by TaqMan® qPCR or Roche library semi-quantitative reverse transcription PCR. Similar to the treatment with hypoxia, the impact of 2-DG on the DMOG-induced upregulation of glycolysis should be initially confirmed by measuring the ECAR in future experiments.

2.2.12 The role of fructose-adapted metabolism in the regulation of DMOG-induced HIF-target genes

To further determine whether the impact of glycolysis on HIF-1 target gene expression is mediated by HIF-1, glucose- and fructose-adapted MCF7.Control cells were plated at a concentration of $4.4x10^{5}$/ 4 ml in a 6 cm dish in either glucose- or fructose-containing DMEM as described before. The corresponding media were exchanged 24 h and 72 h post-plating. On day 3, cells were either incubated in 0.1% DMSO or 1 mM DMOG for 18 h. Consequently, cells were pelleted and either lysed for analysis of protein expression by Western blot, or RNA was extracted and transcribed into cDNA for the analysis of HIF-1 target gene expression by TaqMan® reverse-transcription PCR or Roche library reverse-transcription PCR. As described for hypoxia, the role of glycolysis in the DMOG-induced expression of HIF-target genes in fructose- versus glucose-adapted MCF7 cells should be initially confirmed by evaluating the ECAR in future experiments.

2.2.13 Analysing the impact of the CtBP inhibitor MTOB on hypoxia-induced HIF-1 target gene expression

For further determination of how CtBPs interact with HIF-1 to regulate the expression of HIF-1 target genes, CtBP activity was inhibited by the methionine pathway intermediate 2-keto-4-methylthio-2-oxo butyrate (MTOB). MTOB was discovered to act as substrate for the CtBP dehydrogenase domain (Achouri et al. 2007). Additionally, MTOB was identified to inhibit CtBP activity at high concentrations (mM) by inducing conformational changes in the PXDLS binding pocket which reduces recruitment to the target gene promoter (Di et al. 2013; Straza et al. 2010).

First, MCF7 breast cancer cells were plated in 6 well plates in complete DMEM at a concentration of $2.2x10^5$/ 2 ml. 24 h post-plating, medium was replaced by DMEM containing 4 mM MTOB (SIGMA-ALDRICH, UK). 48 h later, medium was exchanged by fresh MTOB-containing DMEM. Consequently, cells were either transferred to 1% or 20% O_2 for 18 h. In the following, cells were pelleted as described. Cell pellets were lysed by urea lysis and analysed by Western blot for the determination of protein expression, or RNA was extracted and transcribed into cDNA for the determination of HIF-1 target gene expression by reverse-transcription PCR.

2.2.14 The role of modified CtBP expression on hypoxia-induced HIF-target genes

First, glucose-adapted MCF7.Control, MCF7.CtBP2 and MCF7.CtBP-Mutant cells were plated in 6 well plates at a concentration of $2.2x10^5$/ 2 ml. 24 h and 72 h later, medium was renewed and cells were either incubated at 20% or 1% O_2 for 18 h. Immediately after expose to hypoxia, cells were harvested on ice as described before and HIF-1 target gene expression was analysed by reverse-transcription PCR, whereas CA9 protein expression was evaluated by Western blot.

2.2.15 The impact of CtBP-targeting siRNA on DMOG-induced HIF-1 target gene expression

To confirm that the hypoxia-induced expression of HIF-1 target genes was mediated by HIF-1, hypoxia was replaced by incubating cells with 1 mM DMOG in 20% O_2. MCF7 breast cancer cells were plated in complete DMEM in 6 well plates at a concentration of $2.2x10^5$/ 2 ml. 24 h later, cells were transfected with 50 nM non-silencing siRNA, or a combination of CtBP 1/2-targeting and non-silencing siRNA. 48 h post-transfection, DMEM was renewed and supplemented with either 1 mM DMOG or 0.1 % DMSO which was used as negative control. Cells were incubated for 18 h at 20% O_2 and harvested immediately. Induction of CA9 and reduction of CtBP protein expression was determined by Western blot, whereas HIF-1 target gene expression was analysed by (TaqMan™) reverse-transcription PCR.

2.2.16 Investigating the impact of MTOB on DMOG-induced HIF-1 target gene expression

To further assess the potential interaction between HIF-1 and CtBPs, CtBP expression was inhibited by MTOB. First, MCF7 breast cancer cells were plated in complete DMEM at a concentration of $2.2x10^5$/ 2 ml in 6 well plates. 4 h later, medium was replaced with medium containing 4 mM MTOB. 48 h later, medium was exchanged and 4 mM MTOB as well as 1 mM DMOG or 0.1% DMSO was added to the cells. In the following, cells were incubated for 18 h and immediately harvested on ice for protein analysis by Western blot and determination of HIF-1 target gene expression by (TaqMan™) reverse-transcription PCR.

2.2.17 The impact of engineered CtBP expression on DMOG-activated HIF-1 target genes

MCF7.Control, MCF7.CtBP2 and MCF7.CtBP-Mutant cells were plated at a concentration of 2.2x105/ 2 ml in 6 well plates, and in glucose-containing DMEM which was prepared in-house. The medium was exchanged 24 h post-plating. 72 h post-plating, fresh medium containing either 1 mM DMOG or 0.1% DMSO was added to the cells. 18 h later, cells were immediately harvested and protein expression was evaluated by Western blot, whereas HIF-1 target gene expression was determined by (TaqMan™) reverse-transcription PCR. Three independent experiments were performed.

2.2.18 Dissecting the mechanism of interaction between CtBPs and HIF-1

In order to dissect the mechanism by which CtBPs and HIF-1 interact, chromatin immunoprecipitation was performed with the Invitrogen™ MAGnify™ chromatin immunoprecipitation system (UK). However, immunoprecipitations remained unsuccessful, even after several adaptions. Therefore, the experimental procedure and outcomes are discussed in Appendix B.

2.2.19 Optimisation of experimental conditions to determine CtBP-mediated survival of hypoxia-induced acidosis

It was hypothesised that hypoxia-induced and CtBP-regulated CA9 expression promotes the survival of breast cancer cells within an acidic environment, caused by hypoxia and up-regulated glycolysis. In order to determine the impact of CtBP and CA9 on long-term survival, an experiment based on (Parks et al. 2013) was performed. Briefly, MCF7 cancer cells were plated at a concentration of $2.2x10^5$/ 2 ml to reach a confluency of 30-50% 24 h post-plating. The following day, DMEM was constituted with 1 mM DMOG or 0.1% DMSO for 24 h. On day 3, DMEM was replaced by bicarbonate-free medium which was adjusted to either pH 7.4 or pH 6.3 and which contained either 1 mM DMOG or 0.1% DMSO. 24 h later, cells should be harvested for determination of CA9 protein and mRNA expression, and to re-plate cells for colony forming assay to determine long-term survival. However, cells did not survive 48 h incubation in 1mM DMOG (data not shown). Therefore, experimental conditions were optimised as elaborated below.

2.2.19.1 Preparation of bicarbonate-free and pH-adjusted cell culture medium

The bicarbonate/CO_2 buffer system used in DMEM to buffer pH around pH 7.6 masks the activity of CA9. Therefore, cells had to be grown in an air-buffered system that was free from bicarbonate. To prepare bicarbonate-free cell culture medium, 0.84 g DMEM powder, 10 ml FCS, 1 ml sodium pyruvate, and 1 ml glucose to result in a final glucose concentration of 25 mM, 1 ml glutamine and 1 ml penicillin/ streptomycin were dissolved in 100 ml deionized water. To adjust pH, either 30 mM HEPES (Sigma, UK) to calibrate pH to 7.4 or 30 mM MES (Sigma, UK) to adjust pH to 6.3 was added to the medium. Calibration was performed on medium that was preheated to 37 °C by using a Corning pH meter 220. Consequently, the pH-adjusted bicarbonate-free media were sterile-filtered and stored at 4 °C for maximum two days. Before the medium was applied to the cells, it was pre-warmed to 37 °C by using a water bath. Furthermore, cells grown in bicarbonate-free medium were incubated in an air-buffered cell culture incubator (Shel Lab) at 37 °C as the medium was air-buffered.

2.2.19.2 Trypan blue exclusion assay and colony forming assay

In order to determine the impact on short-term survival, cells were stained by trypan blue exclusion assay before re-plating for colony forming assay. First, cells were washed with 1 ml HBSS and trypsinized with 500 µl of trypsin+EDTA as described before. Consequently, cells were re-suspended in 1.5 ml complete DMEM and isolated by pipetting up and down. 100 µl of the suspension was transferred into a sterile Eppendorf tube and an equal volume of trypan blue (SIGMA-ALDARICH, UK) was added. The suspension was mixed by gently pipetting up and down and 10 µl were transferred into a haemocytometer for counting. Trypan blue only passes through damaged cell membranes and therefore selectively stains dead cells blue whereas viable cells remain bright. Blue and white cells were counted separately.

Total cell numbers for re-plating for colony forming assay, number of dead cells, as well as percentage of dead cells were calculated by applying the following formulae, where "2" is the dilution factor when cells were diluted with trypan blue:

Equation 6: dead cells/ml

$$\text{dead cells/ml} = \left(\frac{\text{number of dead cells counted}}{\text{number of squares counted}}\right) \times 2 \times 10^4$$

Equation 7: total cell count/ml

$$\text{total cell count/ml} = \left(\frac{\text{dead cells} + \text{living cells}}{\text{number of squares counted}}\right) \times 2 \times 10^4$$

Equation 8: cell death [%]

$$\text{percentage death} = \left(\frac{\text{number of dead cells}}{\text{total number of cells}}\right) \times 100$$

For colony forming assay, total cell numbers were determined and cells were plated in 6 well plates at a concentration of $2x10^2$/ 2 ml complete DMEM by serial dilution. First, a cell suspension was prepared with the concentration of $1X10^4$/ ml and a total volume of 2 ml. In the following, this suspension was further diluted to achieve a concentration of $1x10^2$/ml and a total volume of 10 ml. This suspension was used to plate 2 ml resulting in $2x10^2$ cells per well. Cells were plated in triplicates and incubated at 37 °C in 10% CO_2 for 10 days. After 10 days, colonies were visualized by crystal violet staining. For staining, DMEM was removed by aspiration and colonies were fixed by adding 800 µl 100% ethanol (Fisher Scientific, UK) to each well. After 10 min of incubation at room temperature, ethanol was removed and 800 µl 0.1% crystal violet (SIGMA ALDRICH, China) dissolved in 20% ethanol was added to the colonies and was incubated for 15 min at room temperature. Finally, colonies were washed with tap water to remove excessive staining solution and air-dried for 24 h. The following day, colonies were examined under a light microscope and all colonies consisting of ≥ 50 cells were included in the count. For counting, colonies were first imaged with the GelDoc-It™ Imaging system. Photographs were saved in TIF format and colonies were manually counted by using the plugin "multipoint analysis" of the open source software ImageJ (version May 2016).

2.2.19.3 Titration of cell numbers

The appropriate cell numbers to be seeded in a colony forming assay were determined by plating MCF7 breast cancer cells in DMEM medium at day 1 in 6 well plates at a concentration of $2.2x10^5$/2 ml. The cells were seeded in triplicates to ensure abundant cell concentrations further downstream of the assay. 24 h post-plating, DMEM medium was replaced by bicarbonate-free medium which was pH-adjusted to either pH 7.4 or to pH 6.3. MCF7 breast cancer cells were incubated at either pH 7.4 or pH 6.3 for 5 h. Following the incubation time in bicarbonate-free medium, cells were trypsinized and re-plated in triplicates in DMEM medium at a concentration of $1x10^4$/2ml, $1x10^3$, $1x10^2$ or 3x103/2 ml and $3x10^2$/2ml by performing a serial dilution. 10 days post-seeding, the colonies were visualised by crystal violet staining and imaged as described.

2.2.19.4 Determination of optimum incubation times in hypoxia and acidosis

The impact of CtBP expression on long-term survival in hypoxia at low pH as well as the time of maximum CA9 induction was evaluated in two experiments. In experiment 1, cells were incubated in hypoxia for 18 h followed by either 7 h or 24 h in bicarbonate-free medium at either pH 7.4 or pH 6.3 and 20% O_2. In experiment 2, cells were exposed to 1% O_2 for 48 h in total. After 18 h, DMEM medium was replaced by bicarbonate-free medium which was adjusted to either pH 6.3 or pH 7.4.

To conduct experiment 1, cells were plated in DMEM in 6 well plates at a concentration of $2.2x10^5$/ 2 ml. 24 h later, cells were transfected with 50 nM non-silencing siRNA or CtBP-targeting siRNA, as previously described, or left untreated as control. 48 h post-transfection, medium was renewed and cells were incubated at either 1% or 20% O_2 for 18 h. Following the incubation in either 1% or 20% O_2, cells were either harvested to confirm CA9 induction and CtBP silencing by Western blot or transferred into bicarbonate-free medium at either pH 7.4 or pH 6.3. After either 7 h or 24 h at pH 7.4 or pH 6.3, cells were re-seeded in DMEM in 6 well plates at a concentration of $2x10^2$/ 2 ml. The colony forming assay was performed in triplicates. 10 days post-seeding, colonies were visualised by crystal violet staining and analysed by counting colonies as described above.

Experiment 2 was performed by plating and transfecting MCF7 breast cancer cells as described in experiment 1. Additionally, untreated cells were included as intrinsic control. On day 3, DMEM was renewed and cells were transferred to either 20% or 1% O_2 for 18 h. After 18 h, DMEM was quickly replaced by bicarbonate-free medium adjusted to either pH 7.4 or pH 6.3 and cells were transferred back into hypoxia. 24 h later, cells were re-seeded for colony forming assays as described earlier. Colonies were visualised and counted 10 days post-seeding.

2.2.19.5 Determination of CA9 stability following re-oxygenation

In order to determine whether CA9 is still expressed and potentially active when cells were transferred into bicarbonate-free medium at 20% O_2, a reoxygenation time course was performed. For this, MCF7 cancer cells were plated in complete DMEM at a concentration of $6x10^5$/ 4 ml in 6 cm dishes. 24 h later, medium was exchanged and cells were transferred into 1% O_2 for 18 h. In the following, cells were transferred back to 20% O_2 and harvested for either RNA extraction or urea lysis 0 h, 2 h, 5 h, 7 h or 24 h post-reoxygenation. To determine CA9 protein expression Western blot was performed. *CA9* gene expression was analysed by TaqMan™ reverse-transcription PCR.

2.2.19.6 Determination of CA9 induction by acidosis in normoxia

To further characterise CA9 expression at low pH, it was determined whether low pH induces CA9 expression at 20% O_2, as described for glioblastoma cells (Ihnatko et al. 2006). First, $2.2x10^5$ cells/ 2 ml were seeded in 6 well plates in complete DMEM. 24 h later, DMEM was replaced by bicarbonate-free medium adapted to pH 7.4 or to pH 6.3 and cells were transferred to an air-buffered incubator and harvested 5 h, 7 h, 18 h and 24 h after incubation at either pH 7.4 or pH 6.3. *CA9* mRNA expression levels were determined by TaqMan™ reverse-transcription PCR and CA9 protein expression was evaluated by Western blot.

2.2.19.7 The impact of CtBP expression on survival of acidosis in MCF7

In order to determine the role of CtBPs in CA9-mediated survival of hypoxia-induced acidosis, MCF7 breast cancer cells were plated in complete DMEM at a concentration of $2.2x10^5$/ 2 ml in duplicates. 24 h later, cells were transfected with either 50 nM non-silencing control siRNA or CtBP 1/2 siRNA. Non-transfected cells were used as intrinsic control to determine cell viability. 48 h post-transfection, medium was exchanged and cells were either incubated at 1% or 20% O_2 for 18 h. In the following, one set of cells was harvested for determination of CtBP and CA9 protein expression by Western blot, whereas the other set was transferred to bicarbonate-free medium adjusted to either pH 6.3 or pH 7.4 for 24 h at 20% O_2. The next day, cells were re-plated in complete DMEM in triplicates at a concentration of $2x10^2$/ 2 ml by performing serial dilution. 10 days later, colonies were visualised by crystal violet staining and colonies consisting of ≥ 50 cells per colony were counted by the software ImageJ.

2.2.19.8 Investigating the role of p53 in the survival of acidosis in MCF7 and MDA-MB-231

To dissect the role of p53 in CtBP-regulated CA9-mediated long-term survival in low pH, MCF7 breast cancer cells were plated in duplicates in complete DMEM in 6 well plates at a concentration of $2.2x10^5$/ 2 ml. 24 h later, cells were either transfected with 50 nM non-silencing siRNA or with a combination of 25 nM p53-targeting and 25 nM non-silencing siRNA or left non-transfected to be used as intrinsic control for cell viability. 48 h post-transfection, medium was replaced by fresh complete DMEM and cells were either incubated at 1% or 20% O_2 for 18 h to induce CA9 expression. Subsequently, one set of cells was harvested and lysed by urea whole cell lysis to determine p53 and CA9 protein expression by Western blot. In the second set, complete DMEM was replaced by bicarbonate-free medium which was adjusted to either pH 7.4 or pH 6.3 or fresh DMEM, and cells were incubated at either pH 7.4 or pH 6.3 for 24 h in an air-buffered cell culture incubator at 36.8 °C or in 10% CO_2 at 37 °C when cells were grown in DMEM. The following day, short term survival was determined by trypan blue staining and cells were re-plated for colony forming assay in complete DMEM in 6 well plates at a concentration of $2x10^2$/ 2 ml. Cells were plated in triplicates. 10 days post-seeding, colonies were stained with a 0.1% crystal violet solution and imaged with the GelDoc-It™ Imaging system. Colonies were manually counted by using the plugin “multipoint count” of the software ImageJ. Statistical significance was determined by Fisher’s LSD test. Two independent experiments were performed.

The acidosis experiment was repeated in MDA-MB-231 as described for MCF7. However, to dissect the role of CtBP and CA9 expression in long-term survival of hypoxia-induced acidosis, CtBP and CA9 expression was silenced by transfection with 25 nM CtBP 1/2 and 25 nM non-silencing control siRNA or 25 nM CA9 and 25 nM non-silencing siRNA respectively. Furthermore, as MDA-MB-231 do not form colonies cell viability was determined by measuring the absorbance of crystal violet at 595 nm with a spectrophotometer. Briefly, crystal violet staining was performed as described and plates were air-dried overnight. The following day, 800 µl 20% acetic acid (Fisher Scientific, UK) was added to each well and crystal violet was dissolved by scraping the cells with a disposal Eppendorf pipette tip. Consequently, three times 200 µl from each well were transferred into 96 well plate wells, therefore measuring each well in triplicates. Consequently, each sample was measured in nine technical repeats. 20% acetic acid was used as blank which was also measured in triplicates. Absorbance at 595 nm was measured by the plate reader Varioskan™ by Thermo Fischer Scientific. To analyse the raw data, the mean of the blank was subtracted from each measurement. In the next step, the mean of nine technical repeats was calculated for each sample. Whether the means were statistically different from each other was determined by Fisher’s LSD test. Three independent experiments were performed.

2.2.20 Dissecting the roles for CtBPs, CA9 and p53 in the long-term survival of hypoxia-induced acidosis

MCF7 breast cancer cells were plated at concentration of $4.4x10^5$/ 4 ml in complete DMEM in 6 cm dishes and in triplicates, to be transfected with 50 nM siRNA targeting p53, CtBPs and CA9 individually or in combination (Tab. 2.17 and Tab. 2.18). One set was allocated to determine CA9 expression by Taqman™ reverse-transcription PCR, one to determine the expression of CtBP and p53 protein expression by Western blot following the transfection with siRNA, and the third set was plated to determine the impact of CtBP, p53 and hypoxia-induced CA9 on long-term survival of low pH. Consequently, 18 6 cm dishes of MCF7 were plated. 24 h later, cells were transfected with 50 nM siRNA as described previously.

Tab. 2.17: Combinations of siRNA resulting in a total concentration of 50 nM per reaction

Reaction	***siRNA combination [50 nM]***
1	Non-silencing control
2	P53 and CtBP 1/2
3	P53 and CA9
4	Non-silencing control and p53
5	Non-silencing control and CtBP 1/2
6	Non-silencing control and CA9

Tab. 2.18: Sequences of p53- and CA9-targeting siRNA

	CA9 siRNA (ThermoFisher Scientific)	**p53 siRNA (Hs_TP53.9)**
Sequence	sequence not specified	5'→ 3'
Sense	Silencer®Select Pre-Designed siRNA (s2269)	AAU UUG CGU GUG GAG UTT
Antisense		ACU CCA CAC GCA AAU UUC CTT

48 h post-transfection, complete DMEM was exchanged and cells were transferred to 1% O_2 for 18 h in order to induce CA9 expression. Next, cells were incubated in bicarbonate-free medium buffered at pH 6.3 for 24 h. Following incubation at low pH, cells were harvested for protein and gene expression analysis and snap frozen with liquid nitrogen for storage at -70 °C until further use, or to be re-plated for colony forming assay. CtBP and p53 protein expression was determined by Western blot (Tab. 2.11). *CA9* expression was determined by TaqMan™ reverse-transcription PCR instead of Western blot in this experiment due to high batch-to batch variations as well as high variability between experiments. Three independent experiments were performed.

Chapter 3: Preliminary experiments

3.1 Introduction

3.1.1 Glycolysis regulates gene networks relevant for breast cancer progression via the activation of CtBPs

An increased flux of glucose through glycolysis is a prominent feature of malignant and benign tumours compared to healthy epithelial tissue (Warburg 1924; Warburg 1956), and correlates with poor prognosis and survival (Groheux et al. 2012; Vleugel et al. 2005). It is now established that cancer cells upregulate glycolysis to ensure the fast generation of macromolecules, ATP, and reducing equivalents such as NADH, required for the production of biomass and for cell division (reviewed by (Vander Heiden et al. 2009)), or to adapt to low levels of oxygen (Semenza et al. 1994). Increased glycolysis in cancer cells is sustained by oncogenic signalling through Akt (Elstrom et al. 2004), silencing of p53 (Bensaad et al. 2006; Kawauchi et al. 2008; Schwartzenberg et al. 2004) or by the hypoxia-dependent (Semenza et al. 1994; Kim et al. 2006) or independent activation of HIF-1 (Lu et al. 2002).

In return, glycolytic by-products regulate the expression of genes relevant for tumour progression. Increased levels of NADH over NAD^+ activate the transcriptional co-regulators CtBP1 and CtBP2 by inducing their dimerization (Zhang et al. 2002). Consequently, CtBPs bind to transcription factors and chromatin-modifying enzymes via the consensus sequence PXDLS and co-regulate the expression of their target genes (Furusawa et al. 1999; Shi et al. 2003). CtBPs have been demonstrated to be relevant for malignant transformation and tumour progression of breast cancer. CtBP expression is high in triple negative and basal subtypes but low or negative in healthy breast tissue, and is associated with resistance to chemotherapy and decreased overall survival (Birts et al. 2010; Di et al. 2013; Deng et al. 2012). Additionally, (Di et al. 2013) identified CtBP binding sites at promoters of genes which belong to networks important for malignant transformation and progression of breast cancer. This includes genes which regulate responses to DNA damage, cell cycle, proliferation, cell death and adhesion. (Di et al. 2013) also performed microarray studies and chromatin immunoprecipitation (ChIP) sequencing in MCF7 transfected with CtBP siRNA which identified 179 upregulated and 100 downregulated genes. Unsupervised hierarchical cluster analysis of gene expression identified a cluster of genes as CtBP target genes which are downregulated in Claudin-low, basal subtypes. Similarly, reduced metastatic-free survival of breast cancer patients correlated with this CtBP signature in two independent studies (Di et al. 2013). (Di et al. 2013) also demonstrated that altering levels of NADH influences *BRCA1*

gene expression via the activation of CtBPs. Additionally, growing cancer cells in high glucose increases the CtBP-mediated suppression of *BRCA1* whereas low glucose concentrations have the opposite effect. Furthermore, it is well established that CtBPs co-repress the induction of *CDH1* (protein: E-cadherin), and therefore support epithelial-to-mesenchymal transition (Zhang et al. 2013). Other well-characterised CtBP target genes include *CDKN2A* (protein: $p16^{Ink4}$) which mediates the regulation of senescence (Deng et al. 2013; Mroz et al. 2008) and the pro-apoptotic genes *PTEN* and *BAX* (Grooteclaes et al. 2003; Paliwal et al. 2007). The studies cited above all demonstrate the relevance of CtBPs in the regulation of genetic networks important for breast cancer progression. It is known that CtBPs respond to increased levels of NADH in hypoxia to support EMT (Zhang et al. 2006) or the overcoming of cell cycle checkpoints (Mroz et al. 2008), however it is unknown whether CtBPs interact with HIF-1 to regulate the adaptive response to hypoxia.

Oxygen only diffuses for 100-200 µm from the blood vessel into surrounding tissues (Beasley et al. 2001). Tumour cells however grow distant from their blood supply. This creates areas of hypoxia, nutrient deprivation, and low pH as the lack of functional vasculature leads to the accumulation of glycolytic metabolites, CO_2, and H^+ (Gatenby et al. 2007). Adaptive responses are mediated by the transcription factor HIF-1. HIF-1 responsive genes include glucose transporters (e.g. GLUT-1) and glycolytic enzymes to sustain ATP generation in low oxygen concentrations by glycolysis, proteins of the pH regulating machinery such as *CA9,* angiogenic agents including *ADM* and *VEGF* or metastasis-promoting genes such as matrix metalloproteases (reviewed by (Semenza 2012). Whereas the oxygen pressure of healthy breast epithelia lies between 12.5 and 65 mmHg, in 50% of examined cancers the measured intratumoural oxygen pressure is as low as 0-2.5 mmHg (Vaupel et al. 1991). This results in profound negative impacts on therapy outcome. Hypoxia and overexpression of HIF-1 correlates with more aggressive tumour phenotypes (Bos et al. 2001; Vleugel et al. 2005), reduced overall survival and poor responses to chemotherapy (Generali et al. 2006) and radiotherapy as both forms of therapy rely on the cytotoxic generation of free radicals and the targeting of rapidly dividing cells (Gatenby et al. 2007).

To investigate whether CtBPs also regulate the expression of HIF-1 target genes, in collaboration with Dr Ivan, Tufts University, the Blaydes group performed a gene expression analysis of HIF target genes in mRNA from MCF7 exposed anoxia and/or CtBP-targeting siRNA. Additionally, MCF7 were treated with 10 mM 2-DG or left untreated. Following the incubation in anoxia for 18 h, several HIF-1 target genes were identified as potential candidates for CtBP-mediated regulation. The HIF-1 target genes which showed the strongest changes in expression when either CtBP expression or glycolysis was inhibited were *ADM* and *CA9. ADM* mediates the neovascularisation and blood vessel stabilisation in tumours (Kocemba et al. 2013). It was found

to be co-expressed with VEGF at the edge of necrotic areas which indicates a role in angiogenesis (Metellus et al. 2011) . *CA9* on the other hand is a transmembrane-spanning enzyme of the carbonic anhydrase family and catalyses the reversible generation of bicarbonate and protons from water and CO_2. This leads to the acidification of the extracellular space, whereas the intracellular remains alkaline and thus sustains cellular processes (Chiche et al. 2009). However, CA9 expression is associated with increased metastasis as it reduces cell adhesion (Radvak et al. 2013), increases motility (Svastova et al. 2012), and indirectly activates proteases via the acidification of the extracellular environment. In breast cancer, CA9 overexpression was demonstrated to correlate with reduced relapse-free and overall survival (Chia et al. 2001), the acquiring of stem cell like characteristics (Lock et al. 2013), and resistance to chemotherapy due to an increased hypoxic response (Tan et al. 2009).

As determined by the preliminary gene expression study introduced above, in MCF7 with silenced CtBP expression or treated with 2-DG, anoxia-induced *ADM* expression is increased, whereas the expression of anoxia-induced *CA9* is decreased. These findings are in agreement with the current literature as (Natsuizaka et al. 2007) evaluated that *ADM* is strongly induced by hypoxia in different cancer cell lines but that induction of gene expression is even higher when cells were grown in 50 mg/dl (0.5 g/l) glucose instead of 100 mg/ dl (1 g/l). Additionally, *CA9* expression is induced by hypoxia but decreases when combined with glucose deprivation. (Parks et al. 2013) did not investigate CA9 expression in their experiments. However, they demonstrated that the survival of different cancer cell lines in low extracellular pH is improved in hypoxia and that ATP generation under these conditions is preserved by hypoxia-induced glycolysis. Returning to the interaction of CtBPs with HIF-1, (Zhang et al. 2006) described that CtBPs co-regulate the hypoxia-mediated expression of E-cadherin via the NADH-dependent recruitment of CtBPs to the *CDH1* promoter. This recruitment of CtBPs to the *CDH1* promoter is blocked by pyruvate and the silencing of CtBP expression. This results in reduced promoter repression and increased expression of E-cadherin in hypoxia.

3.1.2 Aim and scope of this chapter

As evaluated above, it is established that CtBPs respond to elevated NADH levels in hypoxia to regulate gene expression, thus contributing to EMT and genetic instability. It is unknown however, whether CtBPs interact with HIF-1 to regulate the expression of HIF-1 target genes such as *ADM* and *CA9* to support survival in hypoxia. Further, it is unknown whether this interaction occurs indirectly via the HIF-1-mediated upregulation of glycolysis which leads to an increase in NADH or whether CtBPs and HIF-1 directly interact at the target gene promoter. Therefore, this chapter aims to determine whether glycolysis regulated the hypoxia-induced expression of the HIF-1

target genes *ADM* and *CA9* via the activation of CtBPs. These aims were approached by reproducing the gene expression data described above in MCF7, SkBR3 and MDA-MB-231 breast cancer cells, but anoxia was replaced by hypoxia. Additionally, it was aimed to establish the pVHL-defective renal carcinoma cells lines A498 and 786-O as positive controls (Gnarra et al. 1994). However, later literature research showed, that these cell lines do not express HIF-1.

3.1.3 Overview of this chapter

First, the optimum incubation time in hypoxia was evaluated by incubating MCF7, MDA-MB-231, and SkBR3 breast cancer cells for increasing times in either 1% or 20% O_2. *ADM* gene expression was evaluated by TaqMan® reverse-transcription PCR. Once the optimum incubation time was determined, experiments were performed to validate the gene expression data described above in MCF7, MDA-MB-231, and SkBR3 breast cancer cells. This was realized by incubating these cells, which were either transfected with 50 nM CtBP 1/2-targeting or non-silencing control siRNA or treated with 10 mM 2-DG or left untreated, in 1% or 20% O_2 for 18 h. The impact of CtBP 1/2 siRNA or 2-DG on *ADM* gene expression in hypoxia was evaluated by TaqMan® reverse-transcription PCR. However, two independent experiments showed that *ADM* is not regulated in a glycolysis-CtBP-dependent manner; therefore the preliminary findings were not reproduced. Consequently, the focus turned to *CA9* which was also identified in the same microarray study. Similar to *ADM*, optimum incubation time in hypoxia was evaluated first by analysing the same samples for *CA9* expression. After the incubation time in hypoxia was established for *CA9*, the hypoxia experiment was repeated in the same way as described above but also including samples for the determination of CA9 protein expression in hypoxia. To further characterize the glycolysis-mediated regulation of CA9 protein expression, titration experiments with increasing concentrations of 2-DG were performed in MCF7 and MDA-MB-231 breast cancer cells. Cell density is discussed as an alternative mechanism to induce CA9 expression in normoxia. To address whether density plays a role in the regulation of CA9 protein expression in breast cancer cells, MCF7 and MDA-MB-231 breast cancer cells were grown in normoxia at increasing cell concentrations.

The pVHL-defective renal carcinoma cell lines A498 and 786-O were applied to study the impact of CtBPs and glycolysis on CA9 expression in normoxia. Similar to the breast cancer cell lines, the role of glycolysis in the regulation of CA9 protein expression was determined by performing time course and titration experiments with increasing 2-DG concentrations in A498 and 786-O cells. To determine whether glycolysis also regulates CA9 protein expression via the activation of CtBPs, the renal cancer cell lines were transfected with 50 nM CtBP 1/2 siRNA and time course experiments were performed.

3.2 *ADM* expression after increasing exposure to hypoxia

To evaluate the optimum incubation time in hypoxia, MCF7, MDA-MB-231, and SkBR3 breast cancer cells were either incubated at 1% or 20% O_2 for 2 h, 5 h, 7 h or 17 h and *ADM* expression was determined by TaqMan™ reverse-transcription PCR. *ADM* is a well characterized HIF-1 target gene which is unambiguously induced by hypoxia (Garayoa et al. 2000; Natsuizaka et al. 2007). Therefore, this experiment was only performed twice to determine the optimum incubation time in hypoxia for further experiments to achieve robust and clear induction of gene expression.

Induction of *ADM* expression in hypoxia is the strongest in MCF7 (Fig. 3.1). In MCF7, *ADM* expression is significantly different from expression in normoxia after 5 h ($p = 0.034$), and is upregulated by 9.11-fold (SD = 2.65). Induction of *ADM* expression after 7 h is not significantly different from expression in normoxia. The incubation in hypoxia for 17 h induced *ADM* by 19.07-fold (SD = 8.01) which is significantly different from expression in normoxia ($p < 0.001$). Induction of *ADM* expression in MDA-MB-231 in hypoxia is not significantly different from expression in normoxia. However, expression became more stable over time as the standard deviation decreased and is the smallest after 17 h. In SkBR3, the hypoxia-induced expression of *ADM* is highly variable which potentially masks significant differences in induction of gene expression between normoxia and hypoxia. The only significant difference is detected after 5 h where *ADM* expression is induced by 3.55-fold (SD = 0.70; $p = 0.04$). Consequently, 17 h of incubation in hypoxia was chosen as an appropriate time point to study *ADM* expression in hypoxia.

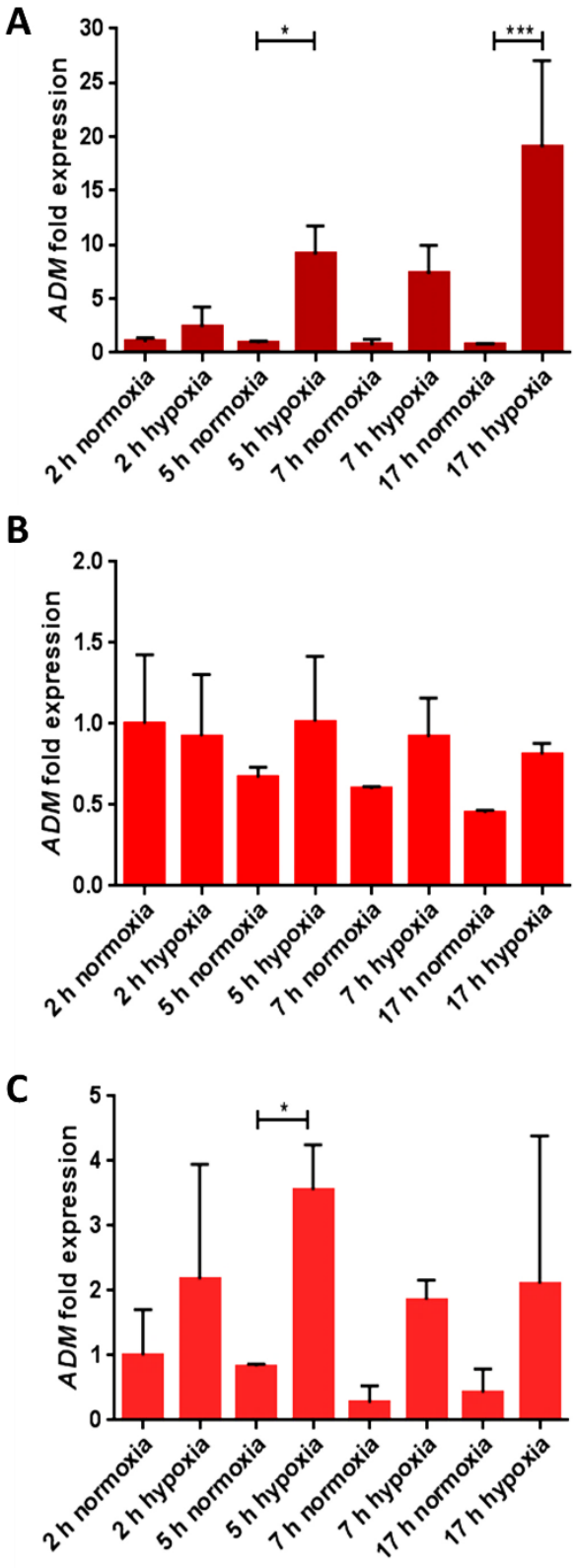

Fig. 3.1: Fold induction of *ADM* in MCF7 (A), MDA-MB-231 (B), and SkBR3 (C) breast cancer cells after 2 h, 5 h, 7 h and 17 h of incubation at 1% and 20% O_2. Cells were harvested immediately after termination of the experiment and gene expression was analysed by TaqMan™ reverse-transcription PCR. Actin was used as housekeeping gene. The means of two experiments and their SD are shown in the figure above. Data were normalized to the time point 2 h in normoxia. Statistical significance was determined by Fisher's LSD test.

3.3 *ADM* is regulated in a glycolysis-dependent manner

With the aim of verifying the preliminary findings that reduced CtBP levels and inhibited glycolysis increase *ADM* expression in hypoxia, breast cancer cells were transfected with CtBP 1+2 and 1/2 siRNA or treated with 10 mM 2-DG, exposed to hypoxia and gene expression was determined by reverse-transcription TaqMan™ PCR.

3.3.1 Confirmation of CtBP knockdown

CtBP expression levels were evaluated by Western blot. In all three cell lines CtBP expression is reduced upon transfection with 1/2 siRNA (Fig 3.2). However, SkBR3 express lower levels of CtBP than MCF7 and MDA-MB-231 cells (Fig. 3.2A), and transfection is not well tolerated. Therefore, and because of unreliable induction of *ADM* expression in hypoxia, SkBR3 cells are excluded from further experiments. Moreover, other members of the group (Jason Fleming, personal communication) also noticed that the 1+2 siRNA exhibited adverse effects on gene expression and was therefore not included in the analysis.

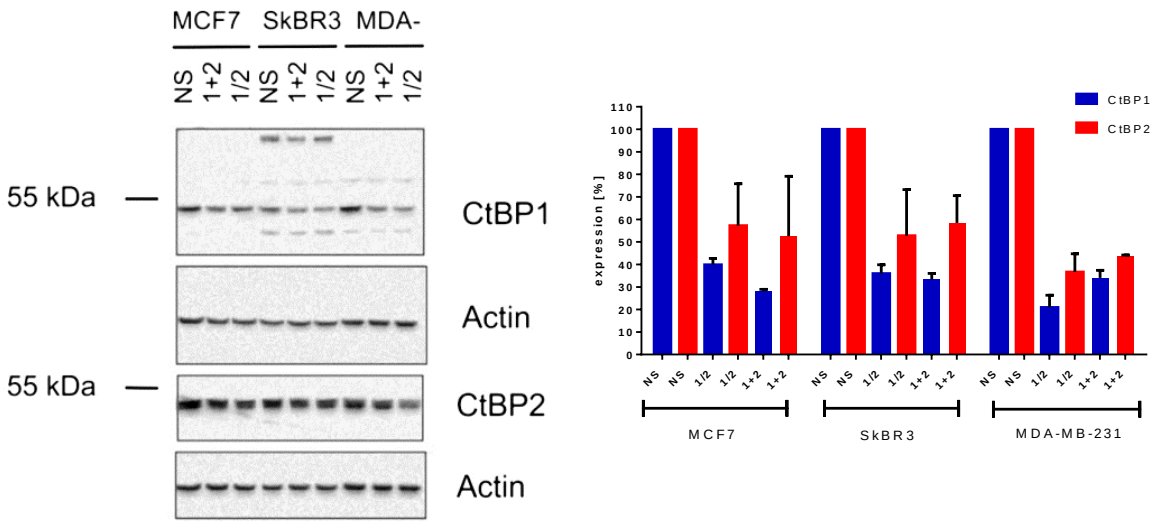

Fig 3.2: CtBP knockdown was evaluated by Western blot. A: Western blot showing CtBP expression in MCF7, SkBR3, and MDA-MB-231 (MDA-) breast cancer cells. The gel was loaded with 20 µg of whole cell lysate. Actin was used as a loading control. One representative Western blot comparing levels of CtBP expression in all three breast cancer cell lines is shown. **B**: CtBP knockdown was quantified by using the software "Quantity One". Shown are the means of three experiments and their SEM. NS: Non-silencing siRNA, 1/2: CtBP 1/2 siRNA, 1+2: CtBP1+ CtBP2 siRNA.

3.3.2 *ADM* expression is regulated by glycolysis

In MCF7 transfected with non-silencing siRNA, *ADM* is strongly induced by hypoxia as its expression is significantly increased by 26.71-fold (SEM = 8.41) ($p = 0.002$), compared to expression in normoxia. In untreated cells, expression is also significantly increased in hypoxia by 20.39-fold (± 2.58) ($p = 0.009$), compared to expression in normoxia. There is no significant effect of siRNA or 2-DG treatment on *ADM* expression in normoxia. However, transfection with CtBP 1/2 siRNA significantly reduces *ADM* expression in hypoxia ($p = 0.037$), whereas the treatment with 10 mM 2-DG significantly increases *ADM* expression ($p < 0.001$) (Fig. 3.3).

In MDA-MB-231 cells, induction of *ADM* expression in hypoxia is less than in MCF7, but yet significantly different from expression in normoxia. *ADM* is induced by 1.43-fold (± 0.24) in cells transfected with non-silencing siRNA ($p=0.044$) and by 1.95-fold (± 0.09) in untreated cells ($p = 0.01$). However, 2-DG and siRNA treatment has no significant effect on *ADM* expression in neither normoxia nor hypoxia (Fig. 3.3).

Consequently, the preliminary finding that both, reduced CtBP expression and glycolytic activity increases *ADM* expression in hypoxia was only partially reproduced. *ADM* appears to be regulated in a glycolysis-dependent manner whereas CtBPs are potentially required for sustaining *ADM* expression in hypoxia. Therefore, *ADM* was excluded from further studies as the regulation of *ADM* expression in this manner contradict the preliminary findings, and was also only produced in one cell line.

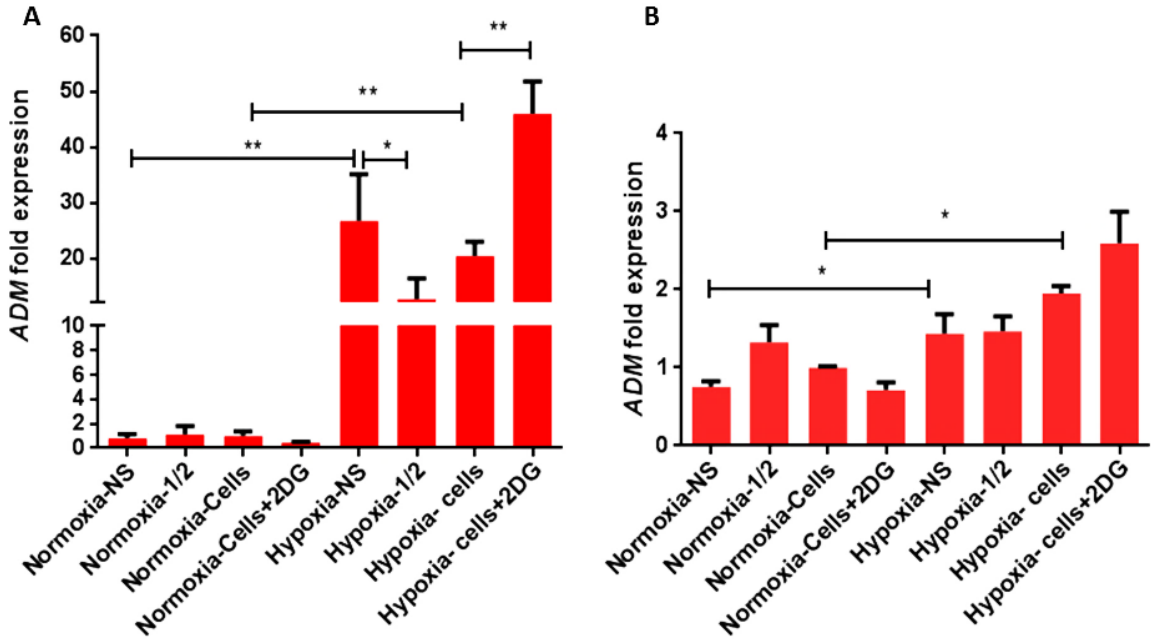

Fig. 3.3: *ADM* is regulated in a glycolysis-dependent manner in MCF7 (A) but not in MDA-MB-231 (B) breast cancer cells. Cells were plated at a concentration of $2.2x10^5$/ 2 ml in 6 well plates in complete DMEM. 24 h later, cells were transfected with 50 nM non-silencing or CtBP 1/2-targeting siRNA. 72 h post-plating, non-transfected cells were treated with 10 mM 2-DG and both, transfected cells and cells treated with 2-DG, were incubated at either 1% or 20% O_2 for 18 h. *ADM* expression was determined by TaqMan™ reverse-transcription PCR. Expression was normalized to untreated cells in normoxia and statistical significance was determined by Fisher's uncorrected LSD test. Shown are the means of two independent experiments and their SEM.

3.4 *CA9* expression after increasing exposure to hypoxia

After *ADM* was excluded as its expression is not regulated in a CtBP-HIF-1-dependent manner, it was decided to focus on *CA9* as the same gene expression study which identified *ADM* as potential CtBP-HIF-1-regulated target also identified *CA9* as potential target. Therefore, the samples obtained from the time point experiment performed for *ADM* were also analysed for *CA9* expression in MCF7 and MDA-MB-231 breast cancer cells.

In MCF7, *CA9* expression is significantly different from normoxia for the first time after 7 h in hypoxia ($p = 0.008$) when it is induced by 5.60-fold (SD = 1.96) (Fig. 3.4). *CA9* induction is the highest after 17 h of incubation in hypoxia when its expression is increased by 32.12-fold (SD = 2.76). This difference in gene expression, compared to expression in normoxia, is strongly significant ($p < 0.001$). In MDA-MB-231 breast cancer cells, *CA9* induction in hypoxia is lower than in MCF7 (Fig. 3.4). Similar to MCF7, *CA9* expression in hypoxia is significantly different to expression in normoxia after 7 h of incubation in hypoxia ($p = 0.03$). *CA9* is induced by 1.43-fold (SD = 0.34), after 7 h of incubation in hypoxia. After 17 h of incubation in hypoxia, *CA9* expression is induced by 4.42-fold (SD = 0.17) which is significantly different from expression in normoxia ($p < 0.001$). Consequently, it was decided to incubate cells for 17 h in hypoxia in future experiments as *CA9* induction is the highest and significantly different from expression in normoxia after this time point.

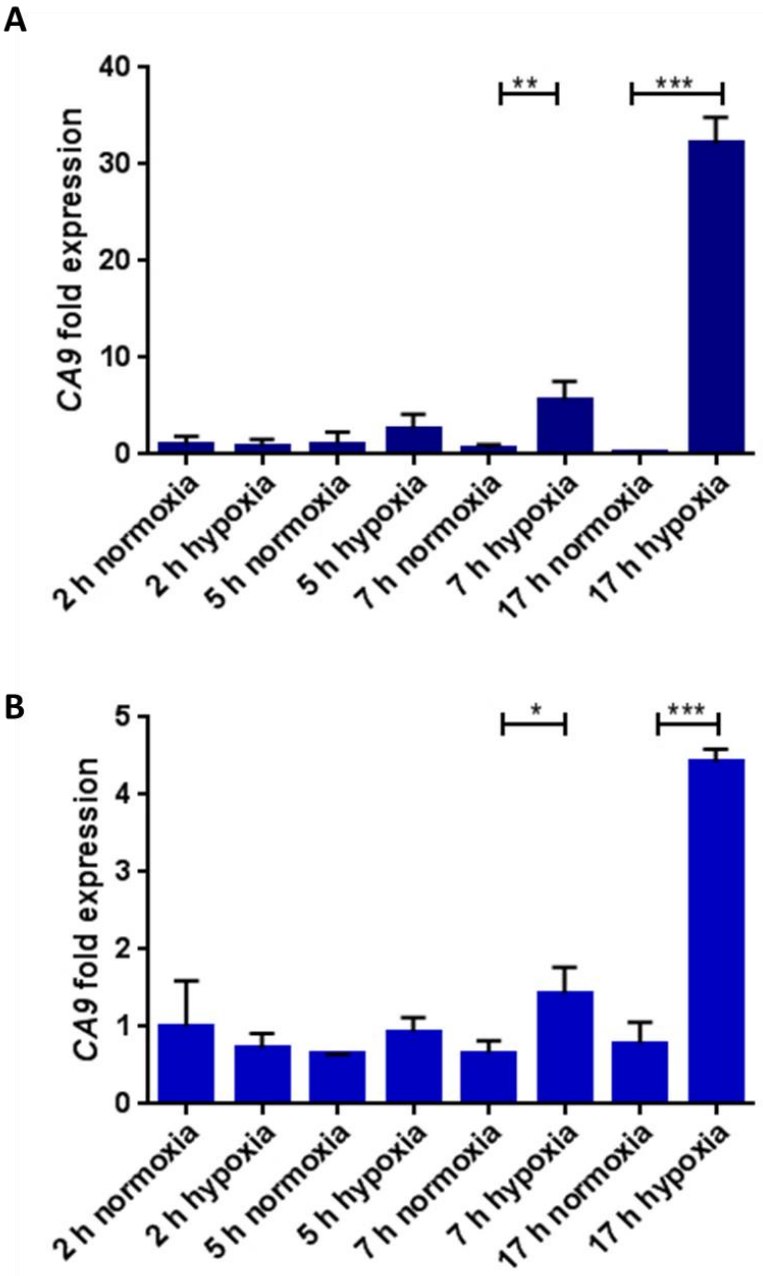

Fig. 3.4: Fold induction of *CA9* in MCF7 (A) and MDA-MB-231 (B) breast cancer cells after 2 h, 5 h, 7 h and 17 h of incubation at 1% and 20% O_2. Cells were harvested immediately after termination of the experiment and gene expression was analysed by TaqMan™ reverse-transcription PCR. Actin was used as housekeeping gene. The means of two experiments and their SD are shown in the figure above. Data were normalized to the time point 2 h in normoxia. Statistical significance was determined by Fisher's LSD test.

3.5 *CA9* gene expression is regulated in a CtBP- and glycolysis-dependent manner

CA9 is induced by hypoxia in both MCF7 and MDA-MB-231 (Fig. 3.5). In MCF7, *CA9* expression is increased in hypoxia by 30.61-fold (SEM = ± 5.81-fold). This is significantly different from expression in normoxia ($p < 0.001$). The treatment with 10 mM 2-DG significantly reduces *CA9* expression in hypoxia, compared to expression in normoxia ($p < 0.001$) (Fig. 3.5A). In untreated MDA-MB-231, hypoxia-induced *CA9* expression is 12.28-fold (± 2.11-fold). This change in *CA9* expression is significant ($p \leq 0.001$). In hypoxic MDA-MB-231, the treatment with 2-DG reduces *CA9* expression by 10.89-fold (± 1.60-fold); a trend that is not significant. Therefore, the partial inhibition of glycolysis by 2-DG reduces *CA9* gene expression in MCF7 but not in MDA-MB-231 breast cancer cells.

In order to establish the impact of CtBPs on *CA9* mRNA expression levels, CtBP expression was inhibited by the transfection of MCF7 and MDA-MB-231 breast cancer cells with 50 nM siRNA. In MCF7, transfection with siRNA specifically reduces CtBP1 and CtBP2 expression in three independent experiments (Fig 3.2). In MCF7 transfected with non-silencing siRNA, hypoxia-induced *CA9* expression is significantly upregulated by 24.23-fold (± 3.90-fold), compared to expression in normoxia ($p < 0.001$). The treatment with 50 nM 1/2 siRNA significantly reduces *CA9* expression in hypoxia (Fig. 3.5A) ($p = 0.004$), compared to expression levels in non-transfected cells, as its induction was 11.09-fold (± 3.09-fold). In MDA-MB-231 transfected with non-silencing control siRNA, hypoxia-induction of *CA9* is 11.65-fold (± 3.12-fold) ($p \leq 0.001$) (Fig. 3.5B). In hypoxic MDA-MB-231 transfected with 1/2 siRNA, *CA9* expression is reduced by 5.32-fold (± 0.40-fold). This difference in *CA9* expression is significant ($p = 0.007$).

In MCF7, these results reproduce findings of the preliminary gene expression study, and indicate that *CA9* gene expression is regulated by enhanced glycolysis in hypoxia via the activation of CtBPs. However, in MDA-MB-231, the treatment with 10 mM 2-DG has no impact on hypoxia-induced *CA9* expression, thereby only partially reproducing preliminary findings. Consequently, in the next step, the impact of 2-DG and CtBP 1/2 siRNA was also determined on the protein level (discussed in the following section). To address the question whether the concentration of 10 mM 2-DG is insufficient to decrease *CA9* gene expression in MDA-MB-231, and to determine the dose-dependent impact of 2-DG on CA9 expression, a titration experiment was performed which is discussed in section 3.7.

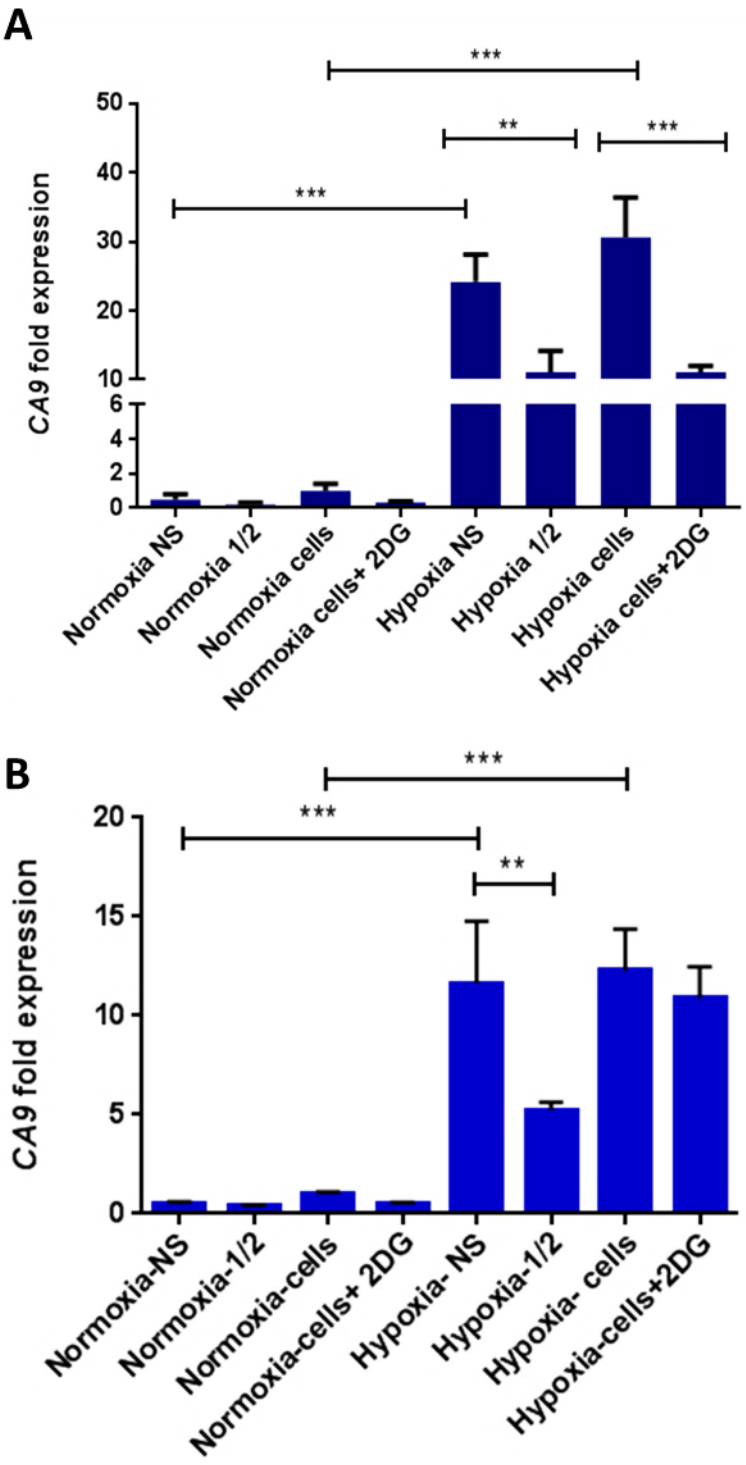

Fig. 3.5: The partial inhibition of glycolysis reduces hypoxia-induced *CA9* gene expression in MCF7 (A) but not in MDA-MB-231 (B) breast cancer cells, whereas the transfection with 50 nM CtBP 1/2 siRNA reduces hypoxia-induced *CA9* expression in both cell lines. Cells were plated at a concentration of $2.2x10^5$/ 2 ml in 6 well plates in complete DMEM. 24 h post-plating, cells were transfected with 50 nM non-silencing or CtBP 1/2-targeting siRNA. 48 h post-plating, cells were treated with 10 mM 2-DG and all conditions were incubated at either 1% or 20% O_2 for 18 h. *CA9* expression was determined by TaqMan™ reverse-transcription PCR. Expression was normalized to untreated cells in normoxia and statistical significance was determined by Fisher's uncorrected LSD test. Shown are the means of three independent experiments and their SEM.

3.6 CA9 protein expression is regulated in a glycolysis-CtBP-dependent manner

Following the demonstration that 2-DG and CtBP 1/2 siRNA decrease *CA9* gene expression in hypoxia, their impact on CA9 protein expression was evaluated by Western blot. CA9 expression is induced by hypoxia in MCF7 and MDA-MB-231 and this induction is reduced upon treatment with 10 mM 2-DG in both cell lines (Fig. 3.6). Reduction in CA9 expression is stronger in MDA-MB-231 than in MCF7. This contradicts the impact of 10 mM 2-DG on hypoxia-induced *CA9* mRNA expression. For future experiments, it is suggested to confirm the downregulation of glycolysis by 2-DG, by also determining the ECAR. Additionally, the stabilisation of HIF-1 in hypoxia, and thus the specific induction of CA9 expression, should be demonstrated, by detecting HIF-1 expression by Western blot. This accounts for all experiments in which CA9 expression was induced by hypoxia.

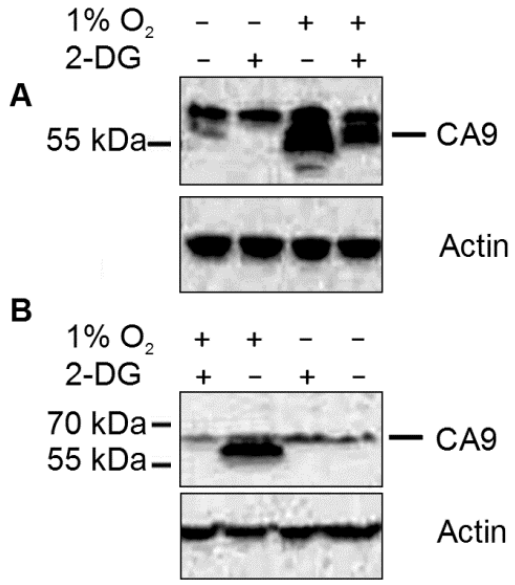

Fig. 3.6: 2-DG inhibits CA9 protein expression in MCF7 (A) and MDA-MB-231(B) breast cancer cells. Cells were plated at a concentration of $2.2x10^5$/ 2 ml in 6 well plates in complete DMEM. 48 h post-plating, cells were treated with 10 mM 2-DG and incubated at either 1% or 20% O_2 for 18 h. CA9 expression was analysed by Western blot. Gels were loaded with 50 µg of whole cell lysate.

Evaluating the impact of CtBPs on CA9 protein expression, it was experimentally determined that hypoxia-induced CA9 protein expression is strongly reduced in MCF7 transfected with 50 nM CtBP 1/2 siRNA (Fig. 3.7A). In MDA-MB-231, transfection with 50 nM 1/2 siRNA also decreases CA9 protein expression, however not as strongly as in MCF7 (Fig. 3.7B). In order to evaluate whether the impact of reduced CtBP expression on hypoxia-induced CA9 is specific for CA9, the impact of CtBP expression on the HIF-target genes LDH-A and GLUT-1 was also determined. In MCF7, LDH-A expression is up-regulated in hypoxia. However, baseline expression in normoxia is already high and CtBP expression levels do not influence LDH-A expression in neither normoxia nor hypoxia. GLUT-1 is induced by hypoxia but siRNA treatment also does not influence its expression (Fig. 3.7A). In MDA-MB-231, baseline expression of CA9, LDH-A and GLUT-1 is higher than in MCF7 but transfection with CtBP 1/2 siRNA also has no impact on LDH-A and GLUT-1 expression in MDA-MB-231 (Fig. 3.7B).

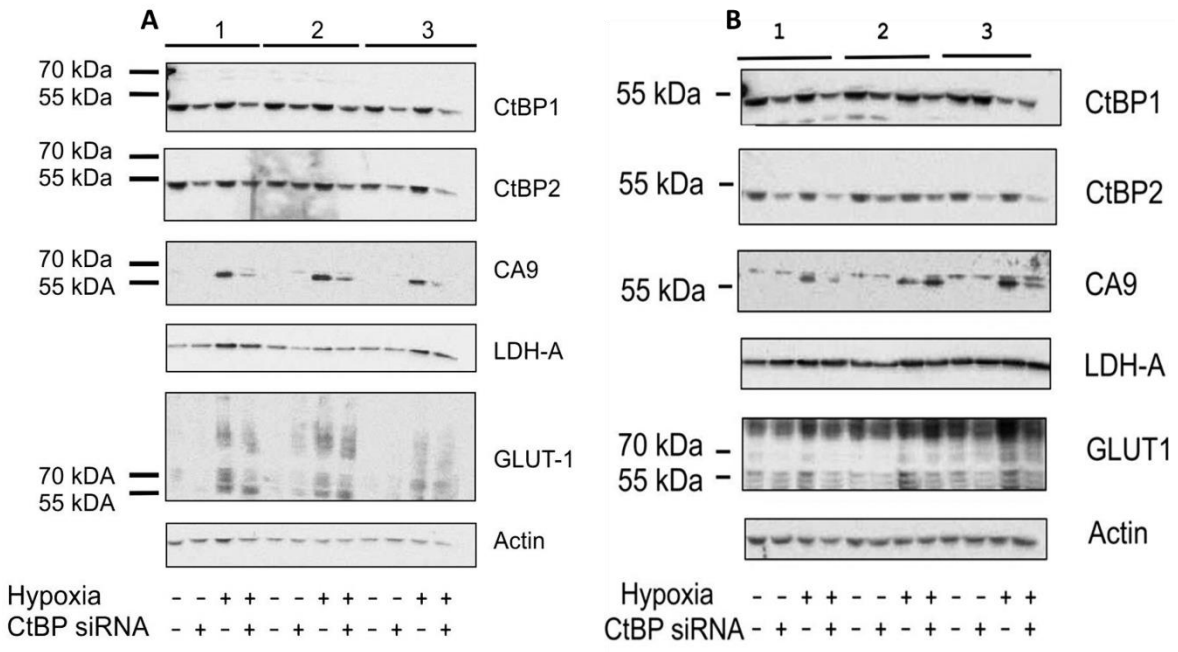

Fig. 3.7: Hypoxia-induced CA9 expression is inhibited when MCF7 (A) and MDA-MB-231 (B) breast cancer cells are transfected with 50 nM CtBP 1/2 siRNA. Cells were plated at a concentration of $2.2x10^5$/ 2 ml in 6 well plates in complete DMEM. 24 h post-plating, cells were transfected with 50 nM non-silencing or CtBP 1/2-targeting siRNA. 48 h later, cells were transferred to either 1% or 20% O_2 and incubated for 18 h. Following the incubation in hypoxia or normoxia, cells were immediately pelleted. CtBP1, CtBP2, CA9, LDH-A, and GLUT-1 expression of three independent experiments (1-3) was determined by Western blot. The gel was loaded with 30 µg of whole cell lysate.

Additionally, MCF7 breast cancer cells were transfected with a combination of CtBP1 and CtBP2 siRNAs targeting different sequences of CtBP mRNA (smartpool) and Western blot was performed to evaluate the impact on hypoxia-induced CA9 protein expression. As expected, hypoxia induction of CA9 is inhibited when cells were transfected with CtBP 1/2 siRNA (Fig. 3.8). When cells were transfected with a smartpool of CtBP-targeting siRNA, CA9 expression in hypoxia is reduced but not as strongly as in cells which were transfected with CtBP 1/2 siRNA. Combining these results with the significant data generated with CtBP 1/2 siRNA, there is experimental evidence that points towards a potential role for CtBPs in the regulation of hypoxia-induced CA9 expression. Summarizing the results described above, it was also confirmed on the protein level that the treatment with 2-DG and CtBP 1/2 siRNA reduces CA9 expression in hypoxia. This suggests a novel, activating role for CtBPs in the regulation of hypoxia-induced CA9 expression via the upregulation of glycolysis. Experiments which further characterise the interaction between glycolysis, CtBPs, and HIF-1 in the regulation of CA9 gene and protein expression, as well as potential consequences for survival in hypoxia-induced acidosis were performed and will be discussed in the following chapters.

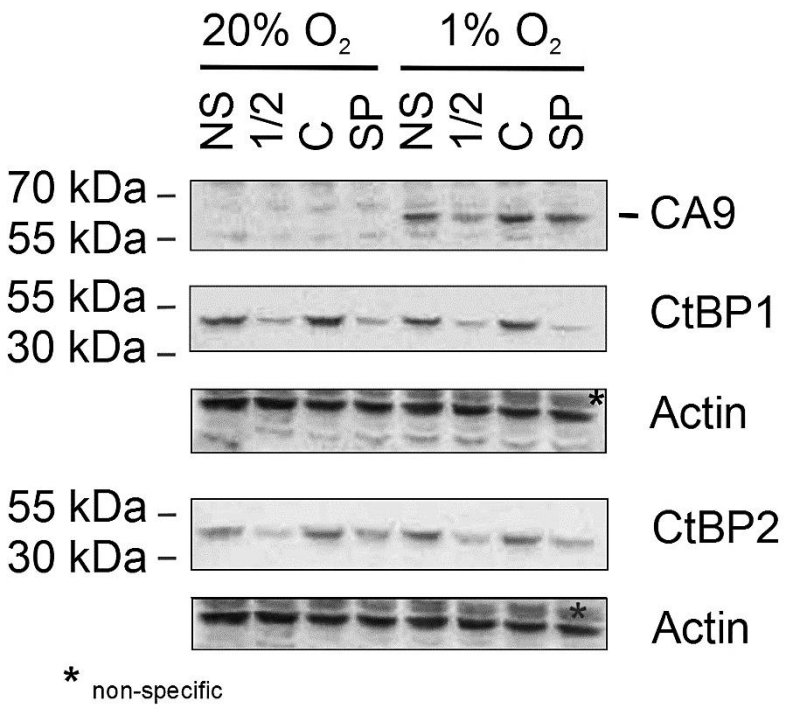

Fig. 3.8: Transfection of MCF7 breast cancer cells with a smartpool of different CtBP1- and CtBP2-targeting siRNAs reduces hypoxia-induced expression of CA9. MCF7 breast cancer cells were plated at a concentration of $2.2x10^5$/ 2 ml in 6 well plates in complete DMEM. 24 h post-plating, cells were transfected with 50 nM non-silencing or CtBP 1/2-targeting siRNA or combination of CtBP1 and CtBP2 targeting siRNAs with different sequences (smartpool). 48 h later, cells were transferred to either 1% or 20% O_2 and incubated for 18 h. CA9 and CtBP expression was determined by Western blot. Gels were loaded with 25 µg whole cell lysate. Key: * nonspecific signal; SP, smartpool.

3.7 CA9 expression in MCF7 breast cancer cells is inhibited by 2-DG in a dose-dependent manner

After CA9 was evaluated as potential target for CtBP-HIF-1-mediated regulation, it was determined whether the effect of 2-DG on CA9 expression is dose-dependent and mediated by enhanced down-regulation of glycolysis at increasing concentrations of 2-DG. In MCF7, CA9 expression in hypoxia continuously decreases in a dose-dependent manner. In MDA-MB-231, the exposure to 25 mM 2-DG inhibits protein expression beyond detection (Fig. 3.9). Therefore, it was concluded that in MCF7, but not in MDA-MB-231, CA9 expression is reduced by 2-DG in a dose-dependent manner, potentially due to increased down-regulation of glycolysis at higher concentrations of 2-DG. This dose-dependent impact of 20DG on hypoxia-induced glycolysis could be confirmed by measuring the ECAR by applying a seahorse analyser.

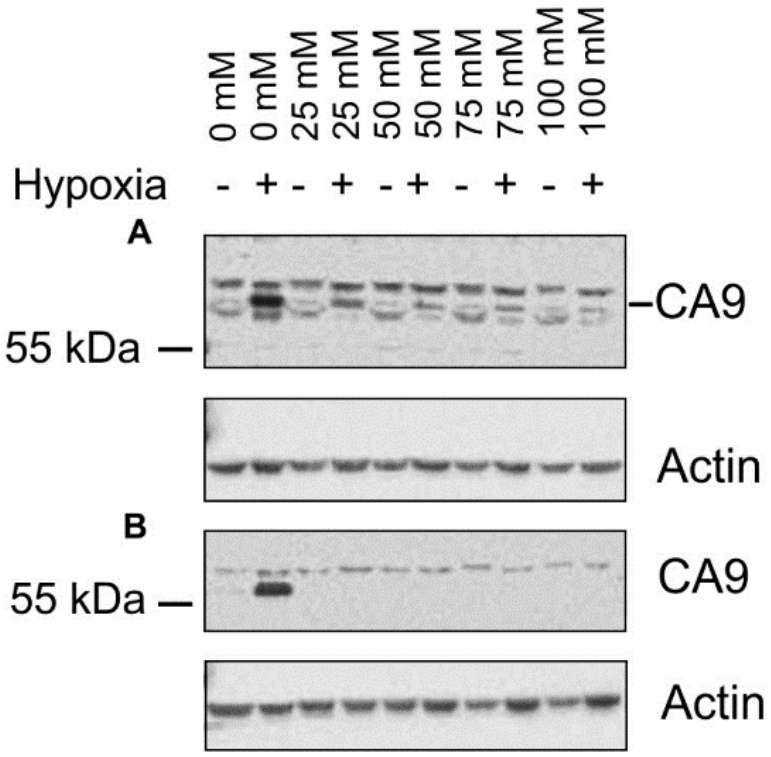

Fig. 3.9: CA9 protein expression is dose-dependent in MCF7 (A) but not in MDA-MB-231 (B) breast cancer cells. Cells were either incubated with 0 mM, 25 mM, 50 mM, 75 mM or 100 mM in 20% or 1% O_2 for 18 h. Whole cell lysates were obtained by lysis with urea lysis buffer. CA9 expression was evaluated by Western blot. Gels were loaded with 14 µg of whole cell lysate. The specific band for CA9 in MCF7 was marked with a dash.

3.8 CA9 is induced by cell density in MDA-MB-231 but not on MCF7 breast cancer cells

Hypoxia is not the only environmental factor which induces CA9 expression. It is reviewed by the literature (Kaluz et al. 2002; Kopacek et al. 2005) that CA9 is also induced under normoxic conditions at high cell densities. In order to study density-induced CA9 expression, MCF7 and MDA-MB-231 cells were plated at increasing densities and harvested 72 h later (Fig. 3.11 and Fig. 3.12). CA9 expression was evaluated by Western blot and cell growth was evaluated by cell counting and phase contrast microscopy.

MCF7 grow slower than MDA-MB-231 and the growth rate is slowed down at cell numbers higher than $4.5x10^6$ cells (Fig. 3.10). MDA-MB-231 cells on the other hand grow faster in the beginning and reduce growth at cell numbers exceeding $1\text{-}4x10^6$ cells. The reduced cell count at high densities may also be caused by the loss of cells upon trypsinizing as MDA-MB-231 cells are not strictly adhesive.

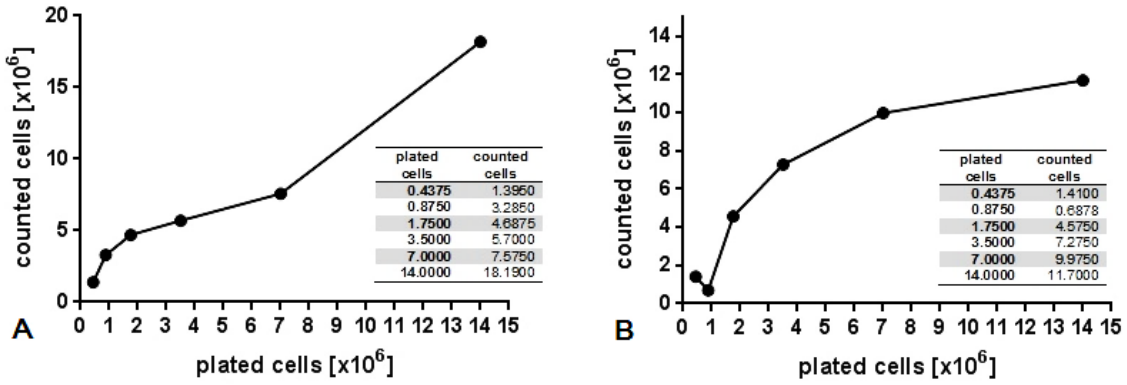

Fig. 3.10: Cell density curves of MCF7 (A) and MDA-MB-231 cells (B). Cells were plated at the indicated densities and cultured at 20% O_2 for 72 h. For counting, cells were washed with PBS-T, treated with trypsin-EDTA, centrifuged at 3000 rpm for 5 minutes and then re-suspended in 1 ml of cell of complete DMEM culture medium. Subsequently the cells were counted using a haemocytometer.

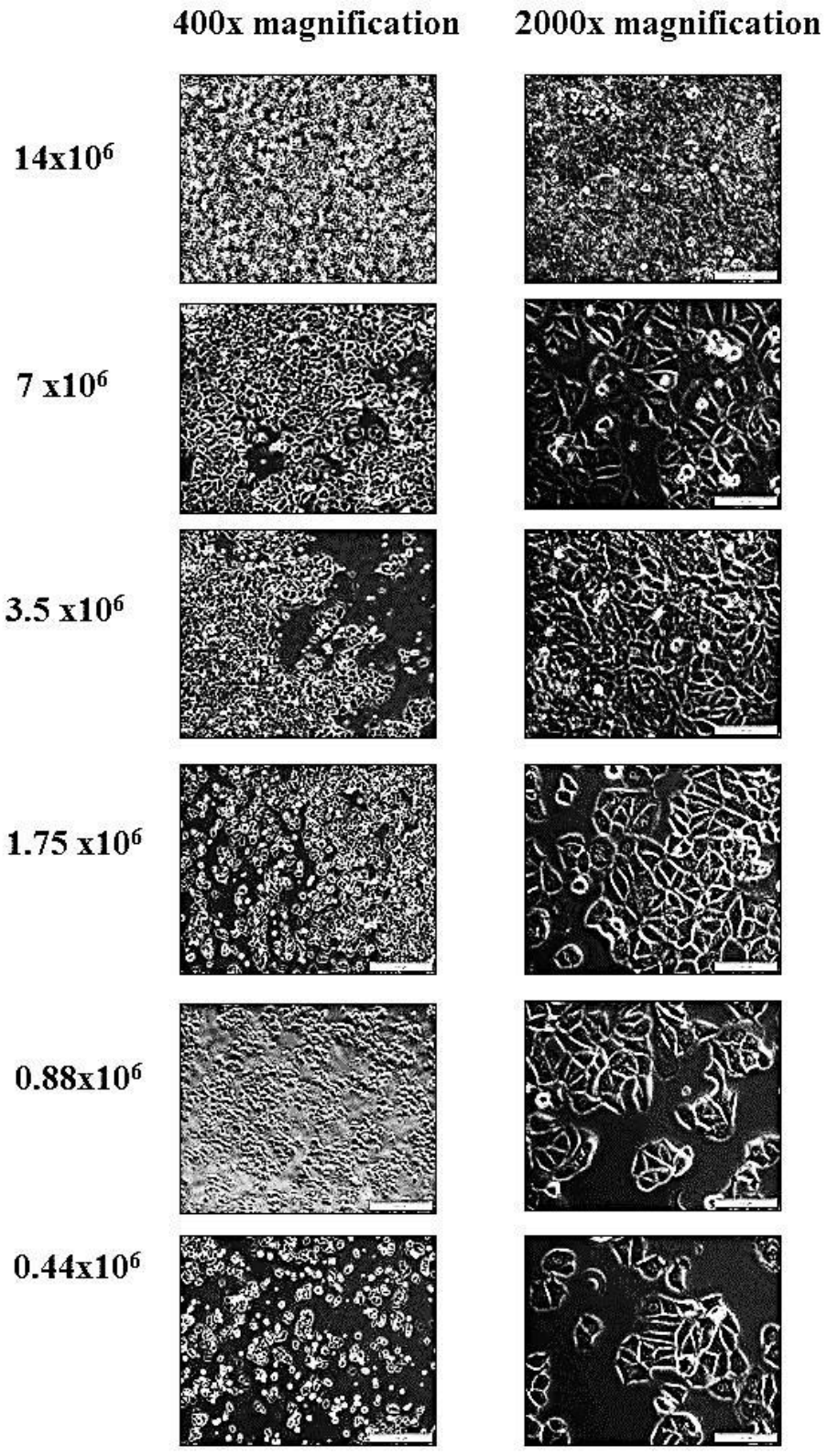

Fig. 3.11: Growth of MCF7 breast cancer cells at different cell densities. To evaluate density-induced expression of CA9 in normoxia, cells were plated at the indicated densities and phase contrast pictures were taken with a light microscope 72 h later. Scale bars represented 500 µm at 400x magnification and 100 µm at 2000x magnification.

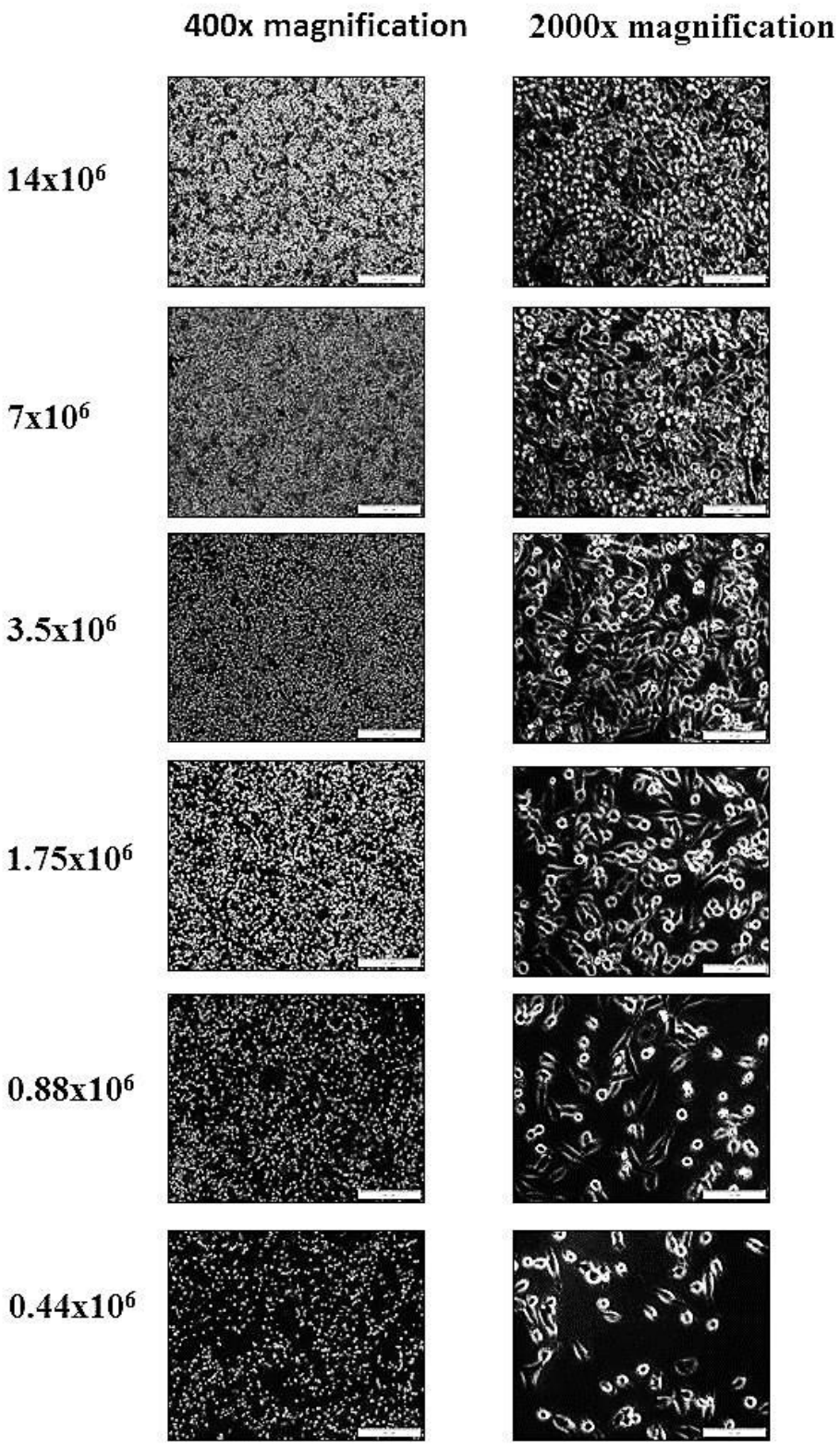

Fig. 3.12: Growth of MDA-MB-231 breast cancer cells at different cell densities. To evaluate density-induced expression of CA9 in normoxia, cells were plated at the indicated densities and phase contrast pictures were taken with a light microscope 72 h later. Scale bars represented 500 µm at 400x magnification and 100 µm at 2000x magnification.

CA9 expression is induced in MDA-MB-231 by densities exceeding $1.61x10^6$ plated cells which corresponds to around $4x10^6$ cells after 72 h in culture, but not in MCF7 (Fig. 3.13). It would have been of interest to also determine HIF-1 expression, in order to investigate whether the density-mediated induction of CA9 expression in MDA-MB-231 is accompanied by HIF-1 stabilisation.

MDA-MB-231 cells exhibit higher levels of glycolysis and HIF-1 expression levels than MCF7 (Robey et al. 2005) and also do not show density-induced growth arrest. Therefore, it may be more important for MDA-MB-231 cells to counteract increasing acidosis by upregulating CA9 expression, whereas MCF7 induce growth arrest and rely on hypoxia-mediated activation of HIF-1 for the induction of CA9 protein expression. Therefore, density as an additional factor for CA9 regulation in MCF7 breast cancer cells is omitted and was not studied in further experiments.

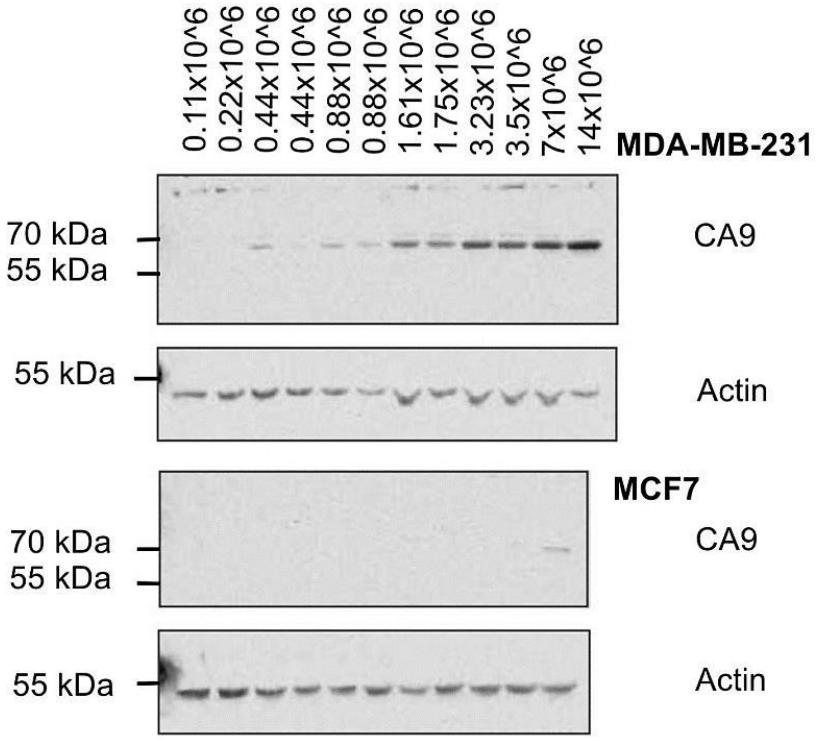

Fig. 3.13: Density induces CA9 expression in MDA-MB-231 but not in MCF7 under normoxic conditions. To determine density-induced CA9 expression in normoxia, cells were plated at the cell numbers indicated above and harvested 72 h later. CA9 expression was studied by Western blot. The gel was loaded with 15 µg of whole cell lysate and actin was used as a loading control.

3.9 CA9 regulation in pVHL-defective renal carcinoma cell lines is independent from HIF-1

Renal clear cell carcinoma cell lines are deficient in the expression of von Hippel-Lindau protein (Gnarra et al. 1994). This results in the constitutive expression of HIF-1α and/or HIF-2α subunits, and in the constitutive expression of CA9 in HIF-1 expressing clear cell carcinomas (Turner et al. 2002; Wykoff et al. 2000). In this light, the pVHL-defective renal carcinoma cell lines A498 and 786-O were selected to determine the role of CtBPs and HIF-1 in the regulation of CA9 in the context of this background. However, literature search performed at a later stage showed that 786-O express only truncated HIF-1α mRNA and lack the expression of HIF-1α protein, but express HIF-2α mRNA and protein (Brodaczewska et al. 2016; Shinojima et al. 2007). A498 express detectable levels of HIF-1α mRNA whereas the expression of HIF-1α protein is controversial (Lau et al. 2007; Shinojima et al. 2007). Similar to 786-O, A498 express HIF-2α mRNA and protein (Shinojima et al. 2007). In this light, the data presented below have to be interpreted with caution (see discussion for further details). Determining HIF-1 protein expression levels by Western blot may have also clarified the role of HIF-1 in these cell lines.

A498 and 786-O renal carcinoma cells were treated with 10 mM 2-DG and 50 nM CtBP 1/2 siRNA as described for MCF7 and MDA-MB-231 breast cancer cells, with the difference that cells were grown in normoxia.

3.9.1 Time- and dose-dependent impact of 2-DG on CA9 in renal cancer cells

In order to characterise the impact of glycolysis on CA9 expression in A498 and 786-O renal cancer cells, a time course with 0 mM, 50 mM and 100 mM 2-DG was performed (Fig. 3.14). Furthermore, the renal carcinoma line 786-O was included in the experiment. In A498, CA9 expression increases over time at 0 mM 2-DG. This density-mediated effect disappears upon exposure to 2-DG, suggesting that 2-DG has a cytostatic effect. In 786-O cells, CA9 expression is induced at 48 h (Fig. 3.14). There is no induction of CA9 upon 2-DG treatment in 786-O cells. Due to high cell death, no samples for Western blot could be obtained for the 96 h and 120 h time points in 786-O cells at 50 mM 2-DG, the 120 h time point in A498 cells at 100 mM 2-DG as well as for the 96 h and 120 h time points at 100 mM 2-DG in 786-O cells. 2-DG appears to have a cytostatic effect at first and becoming cytotoxic at high concentrations, affecting overall viability rather than reducing CA9 expression in a glycolysis-dependent manner. Consequently, CA9 protein expression is strongly regulated by cell density in these lines as demonstrated at 0 mM 2-DG.

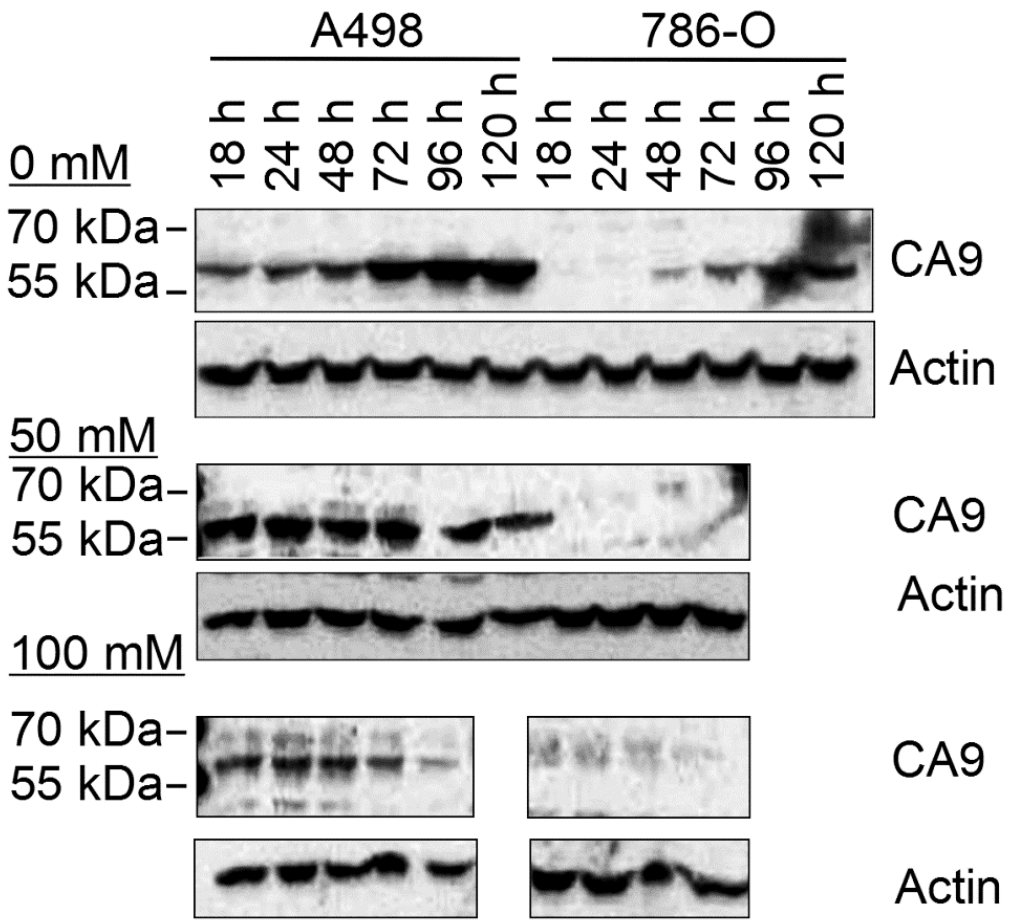

Fig. 3.14: CA9 expression over time and at increasing 2-DG concentrations in A498 and 786-O renal carcinoma cells. Cells were incubated with either 0 mM, 50 mM or 100 mM 2-DG for 18 h, 24 h, 48 h, 72 h, 96 h or 120 h. The experiment was terminated by harvesting cells in cold PBS and lysis in urea lysis buffer. Gels were loaded with 30 µg whole cell lysate.

3.9.2 Incubation of CtBP siRNA for 48 h does not impact on CA9 in renal carcinoma cell lines

In the renal carcinoma cell lines A498 and 786-O, CtBP expression is reduced upon transfection with 50 nM 1/2 siRNA (Fig. 3.15). However, the treatment with siRNA does not reduce CA9 expression in A498 cells in two out of three experiments. Transfection with CtBP 1/2 has also no effect on LDH-A expression. In 786-O cells, CA9 is not detected, and siRNA treatment also has no impact on LDH-A (Fig. 3.15).

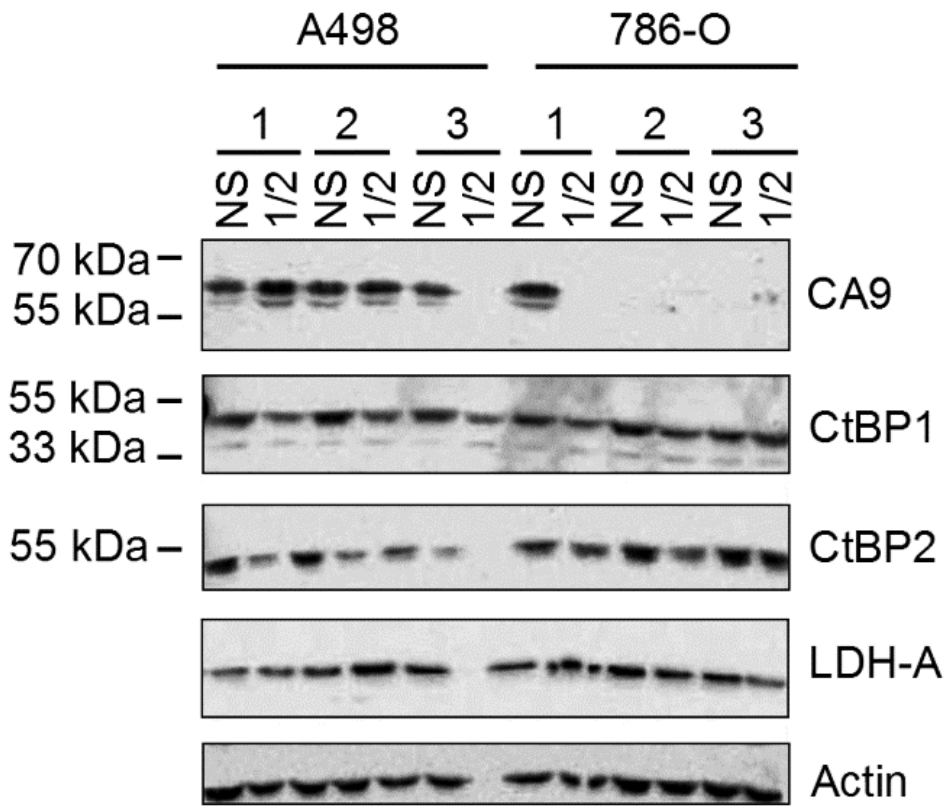

Fig. 3.15: Treatment with 50 nM CtBP 1/2 siRNA does not decrease CA9 expression in A498 and 786-O cells. Cells were treated with 50 nM control or 1/2 siRNA and. CtBP1, CtBP2, CA9, LDH-A, GLUT-1 expression of three independent (1-3) experiments was determined by Western blot. The gel was loaded with 30 µg of whole cell lysate.

3.9.3 Time-dependent impact of CtBP expression in renal cancer cell lines

CA9 expression is very stable in A498 cells. Therefore, the incubation time of CtBP 1/2 siRNA was increased in order to evaluate whether a longer incubation time would reduce CA9 expression. The highest reduction in CtBP1 expression occurs after 72 h. CtBP2 expression is the lowest 96 h post-transfection and increases at later time points. CA9 expression increases over time, confirming previous findings (Fig. 3.14). However, despite the impact of cell density, transfection with CtBP-targeting siRNA decreases CA9 expression at 96 h and 144 h (Fig. 3.16), but not at earlier time points. These findings are confirmed on the mRNA level (Fig. 3.17). *CA9* mRNA expression levels are inhibited by CtBP 1/2 siRNA at time points exceeding 48 h post-transfection. However, the impact of cell density on CA9 expression is also detectable at the mRNA level. Additionally, findings presented in Fig. 3.17 are the result of one PCR which was performed in duplicates and may not be representative. However, this PCR and other findings presented above demonstrate that CtBP expression may impact the regulation of CA9 in A498 renal carcinoma cells but cell density appears to be a dominant mechanism of CA9 regulation in this cell line.

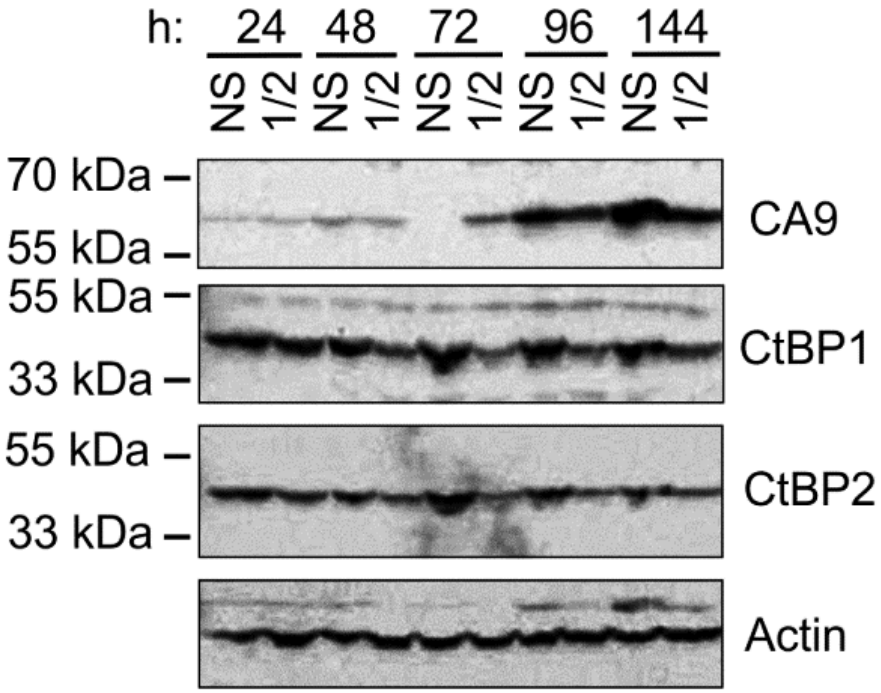

Fig. 3.16: CA9 expression in A498 cells after transfection with 50 nM CtBP-targeting siRNA for 24 h, 48 h, 72 h, 96 h and 144 h in 20% O_2. Cells were transfected with 50 nM of either control or 1/2 siRNA and harvested 24 h, 48 h, 72 h, 96 h or 144 h post-transfection. Cells were lysed with urea lysis buffer and protein expression was studied by Western blot. The gel was loaded with 30 µg of whole cell lysate.

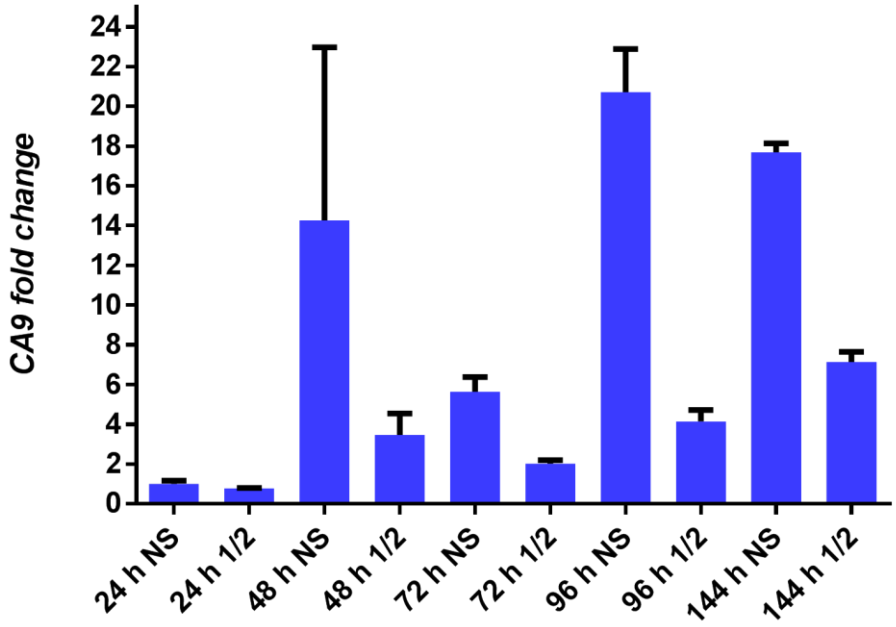

Fig. 3.17: *CA9* expression is inhibited in A498 renal carcinoma cells following the transfection with 50 nM CtBP 1/2 siRNA. A498 renal carcinoma cells were transfected with 50 nM of either control (NS) or 1/2 siRNA (1/2) and harvested 24 h, 48 h, 72 h, 96 h or 144 h post-transfection. The experiment was performed at 20% O_2. CA9 mRNA expression levels were quantified by TaqMan™ reverse-transcription PCR. The figure shows the mean of one set of duplicates with the corresponding SEM. The experiment was performed once.

In 786-O cells, CtBP expression is very stable (Fig. 3.18). Additionally, CA9 expression is not induced prior to 72 h post-transfection. This is also the point of peak expression. Transfection with CtBP 1/2 siRNA decreases CA9 expression at 72 h. Furthermore, CA9 expression is reduced after 72 h. The highest reduction of CtBP expression occurs after 96 h post-transfection (Fig. 3.18). However, cell viability was already affected at this stage as the cell culture medium turned yellow and dead cells were present in the cell culture dish. Moreover, detection of CA9 was inconsistent in this cell line and therefore conclusions about the impact of CtBP expression on CA9 are difficult to draw.

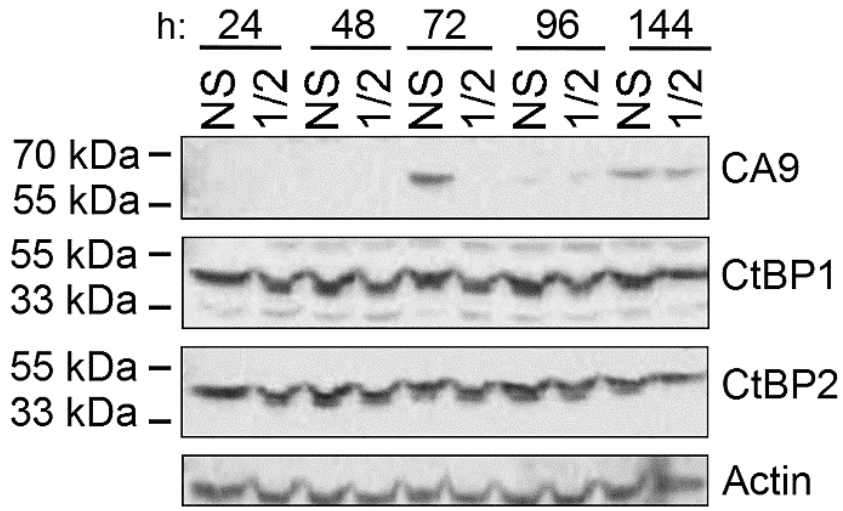

Fig. 3.18: CA9 expression in 786-O after transfection with 50 nM 1/2 siRNA for 24 h, 48 h, 72 h, 96 h and 144 h in 20% O_2. . Cells were transfected with 50 nM of either control or 1/2 siRNA and harvest 24 h, 48 h, 72 h, 96 h or 144 h post-transfection. Cells were lysed with urea lysis buffer and protein expression was studied by Western blot. The gel was loaded with 30 µg of whole cell lysate.

CtBP expression in both renal cancer cell lines is very stable, and 786-O cells do not tolerate transfection. However, most importantly, 786-O renal clear cell carcinoma cells are deficient in HIF-1α protein expression. Additionally, the expression of HIF-1α protein in A498 renal carcinoma cells is highly controversial. Therefore, A498 and 7686-O were omitted from further experiments.

3.10 Summary of preliminary experiments

Initially, it was aimed to evaluate whether *ADM* expression in hypoxia was regulated in a glycolysis-CtBP-dependant manner as suggested by gene expression data generated prior to the start of this project. First, a time course experiment was performed to determine the optimum incubation time in 1% O_2 in order to achieve reliable induction of *ADM* expression. Applying TaqMan™ reverse-transcription PCR, it was evaluated that *ADM* expression in MCF7 is significantly different from expression in normoxia after 17 h of incubation in normoxia. In MDA-MB-231, there is no significant difference in *ADM* expression in normoxic and hypoxic cells, whereas differences in induction of gene expression are masked by high standard deviations in SkBR3. Based on these results, 17 h was chosen as incubation time in 1% O_2 for future experiments. Most importantly, it was experimentally determined that *ADM* expression in hypoxia is not regulated by glycolysis via the activation of CtBPs. This conclusion was based on the result that *ADM* expression in MCF7 in hypoxia is inhibited by CtBP 1/2 but is increased when cells were incubated with 2-DG. In MDA-MB-231, neither the treatment with 2-DG nor the treatment with CtBP 1/2 had an impact on *ADM* expression in hypoxia. Therefore, *ADM* was excluded from further experiments and the preliminary findings discussed in the introduction were not reproduced.

The focus shifted to *CA9,* which was also identified as potential candidate for glycolysis-CtBP-mediated regulation of gene expression. Again, optimum incubation times for robust induction of *CA9* expression was determined by re-analysing the samples generated in the time course experiment. SkBR3 cells were excluded from analysis as they exhibit strong variation in induction of gene expression and naturally low levels of CtBP expression. In MCF7, *CA9* expression is significantly different from expression in normoxia after 7 h. However, induction is the highest after 17 h. The same accounts for MDA-MB-231, but the induction of *CA9* expression is lower than in MCF7. Therefore, cells were incubated for 17 h in hypoxia in all further experiments. To determine the impact of glycolysis and CtBP expression on *CA9* expression, samples generated for the evaluation of *ADM* expression were re-analysed by TaqMan™ reverse-transcription PCR. In MCF7, *CA9* is regulated in a glycolysis-CtBP dependent manner, as induction of *CA9* expression in hypoxia is reduced when cells were treated with either 2-DG or CtBP 1/2 siRNA. These findings were confirmed on the protein level, too. Additionally, titration of 2-DG further highlights the role of glycolysis in hypoxia-induced CA9 expression as the inhibition of CA9 expression is dose-dependent in MCF7. In MDA-MB-231, 2-DG does not impact *CA9* gene expression. Additionally, the impact of 2-DG on CA9 protein expression is not dose-dependent in this cell line. However, the transfection with CtBP 1/2 siRNA reduces *CA9* gene and protein expression.

The role of cell density in the induction of CA9 expression in MCF7 was ruled out, and therefore density as another factor regulating CA9 expression in this cell lines was omitted and not studied further. However, density induces CA9 expression in MDA-MB-231. MDA-MB-231 cells are more glycolytic and therefore more acidic than MCF7. Therefore, density appears to play a role in more acidic environments.

The renal carcinoma cells lines A498 and 786-O exhibit mutations in the von Hippel-Lindau protein. Therefore, it was planned to determine the glycolysis-CtBP-dependent regulation in these lines in normoxia and apply them as positive controls. However, 2-DG acted cytostatic and cytotoxic at high concentrations rather than regulatory. Furthermore, cell density strongly impacts CA9 expression. Additionally, 786-O cells lack HIF-1α protein expression and in A498, HIF-1α expression is unclear. Therefore, these cell lines were excluded from further experiments.

Consequently, this chapter demonstrated that *ADM* is not regulated in a glycolysis-CtBP-dependent manner. However, hypoxia-induced CA9 was identified as potential target for glycolysis-CtBP-mediated gene regulation in breast cancer cells, but not in renal carcinoma cells with constitutive HIF-1 activation. These findings raised the question whether CA9 is uniquely regulated by glycolysis via the activation of CtBPs or whether other HIF-1 target genes are regulated in the same manner, too. Additionally, it was aimed to further determine the role of glycolysis and CtBPs in the regulation of CA9, whether this interaction is dependent on HIF-1, and if so, whether there is an interaction between CtBP and HIF-1 at the *CA9* promoter. These questions were addressed in experiments discussed in the following chapter.

Chapter 4: Hypoxia-induced glycolysis regulates *CA9* expression via the activation of CtBPs

4.1 Introduction

The previous chapter established hypoxia-induced CA9 as potential target for glycolysis-CtBP-mediated gene regulation in breast cancer cells. These findings raised the question whether CA9 is uniquely regulated by glycolysis via the activation of CtBPs, or whether other HIF-1 target genes are regulated in the same manner. Therefore, this chapter addresses the role of glycolysis and CtBPs in the regulation of *CA9* and other HIF-1 target genes, the question whether this interaction is dependent on HIF-1, and if so, whether CtBPs and HIF-1 interact at the *CA9* promoter.

4.1.1 Context of this chapter

To determine whether CA9 is uniquely regulated by glycolysis via the activation of CtBPs, further HIF-1 target genes were included in the study. The genes were selected because they showed a higher than 3-fold change in gene expression in the preliminary gene expression study discussed in Chapter 3:, and because of their relevance to cancer biology (Tab. 4.1).

Tab. 4.1: Overview of the HIF-1 target genes analysed in this chapter

HIF-1 target gene	Function	Reference
CA9	Regulation of pH	McIntyre et al. 2016; Robertson et al. 2004
PDK1	Flux of glucose-derived pyruvate to lactate, reduction of mitochondrial metabolism	Kim et al. 2006
EGLN3	Oxygen sensing and control of the hypoxic response, rapid HIF-1 degradation upon re-oxygenation	Henze et al. 2010; Marxsen et al. 2004
FAM162A	Promotion of hypoxia-induced apoptosis	Lee et al. 2004; Kim et al. 2006
TMEM45A	Protection from chemotherapy-induced apoptosis in hypoxia	Flamant et al. 2012; Guo et al. 2015
INSIG2	Potentially supports invasion and resistance to chemotherapy-induced Bax-mediated apoptosis	Li et al. 2008

PDK1 (pyruvate dehydrogenase kinase 1) actively attenuates mitochondrial respiration by phosphorylating PDH. This leads to the inactivation of PDH and the feeding of glucose-derived pyruvate into the conversion into lactate instead of the TCA cycle and oxidative phosphorylation. Consequently, this causes the inhibition of mitochondrial metabolism and the switch to glycolysis for ATP generation in hypoxia. Additionally, levels of hypoxia-induced ROS are reduced, thus preventing hypoxia-induced apoptosis (Kim et al. 2006). *PDK1* also plays a role in liver metastatic breast cancer cells as the increased expression of HIF-1α and PDK1 in liver metastases correlates with the increased flux of glucose-derived pyruvate into lactate and reduced mitochondrial respiration. The silencing of *PDK1* reduces the numbers of liver metastases in balb/c mice. Further, breast cancer patients show increased immunohistochemistry staining for PDK1 in liver metastases compared to primary tumour. Lung and bone marrow metastases on the other hand do not overexpress HIF-1 and PDK1 and rely on oxidative phosphorylation (Dupuy et al. 2015).

EGLN3 (egl9 family hypoxia inducible factor 3) or PHD3 contains a HRE (Pescador et al. 2005) and is therefore also induced by HIF-1α in hypoxia (Marxsen et al. 2004). The activation of *EGLN3* in hypoxia by HIF-1α leads to its own degradation and consequently provides a vital control mechanism of the hypoxic response. It is thought that the HIF-1-induced activation of EGLN3 expression supports the rapid degradation of HIF-1α after re-oxygenation (Marxsen et al. 2004). Alternatively, PHD3 activation in hypoxia may provide a self-regulatory mechanism to sustain tumour growth and progression in prolonged hypoxia. (Henze et al. 2010) showed that in glioblastoma the treatment with hypoxia and DMOG sensitised cancer cells for Tumour necrosis factor-related apoptosis-inducing ligand (TRAIL)-induced apoptosis. Consequently, PHD3 expression potentially protects glioblastoma cells from hypoxia-induced cell death, which may be an adaptive mechanism to spatially and temporally fluctuating oxygen concentrations within glioblastomas (Henze et al. 2010). However, the role of PHD3 expression in tumour progression and survival appears to be highly context-dependent and tissue-specific. In this light, the nuclear and cytoplasmic expression of EGLN3/PHD3 is commonly found in healthy epithelial tissues, whereas the expression of EGLN3 in tumour cells of human breast carcinomas is reduced to low to moderate expression (Soilleux et al. 2005). Similarly, (Radhakrishnan et al. 2016) described in the context of colon cancer that expression levels of EGLN3 mRNA as well as protein are reduced in cancerous tissue, compared to healthy mucosa. The reduced expression of PHD3 in these patients also correlates with the presence of distant metastases and the reduction in overall survival. These findings were reproduced *in vitro*, and in mouse models in which the silencing of PHD3 causes an increase in tumour volume, tumour weight, and increased liver metastasis. Conversely, the overexpression of PHD3 leads to reduced tumour volume, reduced number of liver metastases, and increased overall survival. Decreased PHD3 expression was further linked

with the increased expression of myeloid cell leukaemia sequence 1 (MCL-1) and increased ATP production via mitochondrial respiration (Radhakrishnan et al. 2016). Independently, (Luo et al. 2011) described that the silencing of PHD3 in hypoxia increases oxygen uptake while reducing glucose uptake and lactate production. Additionally, they suggested a co-activating role for PKM2 by hydroxylating proline residue 403/408 which resulted in enhanced binding of HIF-1α and p300 to the HRE of the HIF-1 target genes *PDK1*, *LDH-A* and *GLUT1*, thereby promoting a glycolytic phenotype. Furthermore, the re-activation of PHD3 in hypoxia, *e.g.* via α-ketoglutarate derivates causes cell death by ATP depletion in hypoxic but not normoxic cells. This is mediated by the downregulation of glycolysis (Tennant et al. 2009; Tennant & Gottlieb 2010). In the light of the findings discussed above however, re-activation of PHD3 as therapeutic strategy requires further research as the role of PHD3 in cancer cell survival appears to be diverse and highly context-specific.

FAM162A (Family with sequence similarity 162 member A) is overexpressed in cervical (Cho et al. 2010) and gastric cancers (Cho et al. 2009) but not in matched control mucosa. This suggests a role in tumorigenesis. FAM162A is responsive to HIF-1α, exerts pro-apoptotic functions and is of mitochondrial location. (Lee et al. 2004) further suggest a mechanism by which FAM162A interacts with voltage-dependent anion channels (VDAC) from the mitochondrial permeability transition pore (PTP) which leads to permeability transition and consequently to release of cytochrome c into the cytoplasm and the activation of caspase 3 and 9. This was confirmed by suppressing FAM162A, which rescues cells from hypoxia-induced apoptosis, and no cytochrome c release was detected (Lee et al. 2004). (Kim et al. 2006) suggested that translocation of FAM162A to the mitochondrion is mediated by heat shock protein 90 (Hsp90). However, the pro-apoptotic properties of FAM162A remain poorly understood.

Similarly, *TMEM45A* (Transmembrane protein 45A) was described to be induced by hypoxia but its functions and regulation are also poorly understood. In the breast cancer cell line MDA-MB-231, TMEM45A expression protects from Taxol-induced apoptosis in hypoxia which is reversed when TMEM45A expression is silenced by siRNA. Upregulated expression of TMEM45A is associated with reduced relapse-free survival of breast cancer patients (Flamant et al. 2012). In glioma (Sun et al. 2015) and ovarian cancer (Guo et al. 2015) tissues, TMEM45A is overexpressed compared to healthy control tissue. In both cancer models, the silencing of TMEM45A reduces proliferation and causes the cell cycle to arrest at the transition from G_1 to S phase. Further, invasion and migration is reduced as demonstrated in transwell migration assays. In ovarian cancer cells, the reduced adhesion to fibronectin is suggested to be mediated by the inhibition of the focal adhesion pathway following the silencing of TMEM45A via reducing RhoA and Rock2 expression. Both, RhoA and Rock2 were determined as downstream targets of TMEM45A by gene

enrichment analysis of the Cancer Genome Atlas (TCGA) ovarian cancer dataset and subsequent validation by real-time PCR and Western blot (Guo et al. 2015). However, all experiments were performed in normoxia. Therefore, it remains unclear whether the overexpression of TMEM45A is HIF-1-dependent in these cancer models or whether the overexpression of TMEM45A in normoxia is unique to the glioma and ovarian cancer data sets and cell lines studied by the authors as TMEM45A requires hypoxia and therefore HIF-1 for its induction in models of breast and liver cancer (Flamant et al. 2012).

INSIG2 (Insulin inducible gene 2) is another poorly understood HIF-1 target gene which was discovered by (Yabe et al. 2002) as part of lipid metabolism. The translocation of sterol regulatory-binding proteins (SREBPs) from the endoplasmatic reticulum (ER) to the Golgi apparatus is a central event in lipid homeostasis. SREBPs are synthesised at the ER membrane where they bind to SREBP cleavage-activating proteins (SCAP) which exhibit sterol-sensing domains. In sterol-deprived cells, SCAPs guide SREBPs to the Golgi apparatus where they are activated by protease cleaving. The active domains are released into the cytosol and consequently enter the nucleus to activate the transcription of genes encoding for enzymes involved in the synthesis of cholesterol, fatty acids, triglycerides and phospholipids. In high sterol concentrations, SCAPs undergo conformational changes and consequently remain in the ER membrane which leads to the downregulation of lipid synthesis. INSIG2 binds to SREBPS, thus preventing its relocation to the Golgi apparatus and its activation (reviewed by (Goldstein et al. 2006)). Therefore, INSIG2 provides an important negative control mechanism for lipid homeostasis. However, its role in obesity is discussed controversially (Krapivner et al. 2008; A. J. P. Smith et al. 2007) and its role in cancer is unclear. It was described by (Kayashima et al. 2011) that *INSIG2* is upregulated in pancreatic cancer cell lines following 24 h of incubation at 1% O_2. However, how *INSIG2* is regulated by HIF remains elusive. INSIG2 is overexpressed in lesions of pancreatic intraepithelial neoplasia and invasive ductal carcinoma (Kayashima et al. 2011) and colon cancer (Li et al. 2008; Sun et al. 2016) compared to their matched non-cancerous control. However, INSIG2 expression is not linked with areas of hypoxia or HIF expression in these studies. Therefore, it is not clear whether the overexpression of INSIG2 is mediated by HIF or hypoxia. In pancreatic cancer, the overexpression of INSIG2 correlates with increased number of metastases in lymph nodes and distant organs as well as with higher tumour grades (TNM stages) but has no significant impact on overall survival (Kayashima et al. 2011). Additionally, (Kayashima et al. 2011) described reduced proliferation and invasion when INSIG2 is inhibited by siRNA. In colon cancer, the overexpression of INSIG2 significantly reduces overall survival (Li et al. 2008; Sun et al. 2016). As described for pancreatic cancer by (Kayashima et al. 2011), (Li et al. 2008) experimentally determined that the overexpression of INSIG2 in the human colon cancer cell line HCT116 leads to

increased cell growth and invasion as well as anchorage-independent growth in soft agar compared to the mock-transfected control. The overexpression of INSIG2 further leads to increased resistance against apoptosis induced by the chemotherapeutic agents Actinomycin D and staurosporine. This was suggested to be mediated by the binding of INSIG2 to pro-apoptotic Bax and therefore preventing its translocation to the mitochondrion. Agreeing with these findings, (Sun et al. 2016) described reduced invasion and migration in colon cancer cells when INSIG2 expression was silenced by siRNA. This was suggested to be mediated by epithelial-to-mesenchymal transition as cells transfected with INSIG2 siRNA also express reduced levels of the mesenchymal markers N-Cadherin, Vimentin and Snail. The role of INSIG2 in forming metastases is supported by *in vivo* findings in a nude mice model where cells transfected with INSIG2 siRNA form less liver metastases than control cells. Summarizing, the role of INSIG2 in cancer progression as well as its regulation by HIF remains elusive. It may protect from Bax-mediated apoptosis and support invasion by supporting the expression of mesenchymal markers. In this light, to determine the impact of glycolysis and CtBP expression on the HIF-1-induced expression of *INSIG2* should shed more light onto the function of INSIG2 in cancer progression and adaption to hypoxia.

To determine whether hypoxia-induced glycolysis regulates the expression of CA9 and potentially other HIF-1 target genes via the activation of CtBPs in a HIF-1 dependent manner, hypoxia was replaced with the PHD inhibitor dimethyloxalylglycine (DMOG). DMOG is a cell permeant 2-oxoglutarate analogue which inhibits prolyl and asparagyl hydroxylases in whole cell systems (Baader et al. 1994) and *in vitro* (Epstein et al. 2001), and therefore activates HIF-1 in an oxygen-independent manner (Elvidge et al. 2006). DMOG is widely used in cancer research to investigate HIF-dependent mechanisms such as HIF-1-dependent intracellular pH regulation in hypoxia (Hulikova et al. 2013), the impact of genetic variation on HIF-binding to MYC enhancers in clear cell renal cell carcinoma (Grampp et al. 2016) or the HIF-dependent reprogramming of cancer cell metabolism (Golias et al. 2016; Kuo et al. 2016). Additionally, DMOG is a suitable HIF-1 activator in MCF7, the breast cancer cell line mainly used in this thesis, as MCF7 express all PHD isoforms. PHD1 is constitutively expressed, whereas the expression of PHD2 and PHD3 is oxygen-dependent. Most importantly however, there is a broad overlap of hypoxia- and DMOG-induced target genes in MCF7 which includes the HIF-1-specific target gene *CA9* (Elvidge et al. 2006).

However, DMOG also exhibits side effects. Importantly, DMOG was described to inhibit mitochondrial respiration in a HIF-1α-independent manner as demonstrated by the application of pharmacological HIF- 1 inhibitors and siRNA. This occurs before the activation of HIF-1 target genes by DMOG and is mediated by the de-esterified version of DMOG, NOG. Consequently, DMOG-treated cells become more vulnerable for the disruption of glycolysis as these cells are not

able to compensate disrupted mitochondrial metabolism with the upregulation of glycolysis (Zhdanov et al. 2015).

To determine the role of CtBPs in coupling hypoxia-induced glycolysis to the HIF-1-dependent regulation of *CA9* and potentially other HIF-1 target genes, CtBP activity was pharmacologically inhibited by MTOB. This method was chosen as an additional approach to transient transfection of siRNA. MTOB is an intermediate of the methionine salvage pathway and was identified by (Achouri et al. 2007) as substrate for CtBP1, acting as inhibitor at concentrations in the mM range. However, the mechanism is still unknown. (Zhao & Chinnadurai 2010) suggested that the binding of MTOB by CtBPs induces a conformational change in the PXDSL-binding cleft in the CtBP dimer which consequently prevents the binding to transcription factors and DNA-modifying enzymes, and therefore inhibits CtBP-mediated co-regulation of target gene transcription. This change in conformation has not been demonstrated, however. Nevertheless, in agreement with this suggestion it was demonstrated that MTOB prevents the binding of CtBPs to the promotors of target genes such as *Bik* which induces apoptosis in human colorectal cancer cell lines (Straza et al. 2010). Additionally, MTOB expels CtBPs from the promoter of target genes in breast cancer cell lines which reversed the mesenchymal phenotype to an epithelial phenotype as defined by re-expression of E-cadherin (Di et al. 2013). It remains also unclear whether the high concentrations of MTOB used *in vivo* do not exert off-target effects. (Tang et al. 2006) reported that high concentrations of MTOB (8 mM) inhibit the activity of the enzyme ornithine decarboxylase (ODC), which is the initial enzyme in the polyamine biosynthetic pathway. This effect is post-translational as expression levels of mRNA are not affected. Further, the specific ODC inhibitor DMFO induces cell growth arrest and apoptosis to a lesser extent than MTOB and in a p53- and caspase 3/7-dependent manner, whereas MTOB-induced apoptosis is p53-independent and does not involve the activation of caspase 3/7. The addition of polyamines also only mildly rescues growth inhibition and apoptosis caused by MTOB. Therefore, ODC does not play a major role in MTOB-induced inhibition and apoptosis, however it cannot be excluded. Even though its exact mechanism is still unknown MTOB is a *bona fide* CtBP inhibitor widely used in the literature.

Furthermore, small molecule inhibitors of CtBPs have been developed based on MTOB and NAD^+-binding, leading to the inhibition of its dehydrogenase activity in a competitive manner. Its specifity to highly glycolytic cells (Birts et al. 2013) and cells with a higher degree of transformation as well as its p53-independent mode of action (Tang et al. 2006) makes the inhibition of CtBPs by small molecules a potential therapeutic target (Korwar et al. 2016).

Cultured transformed mammalian cells metabolize high amounts of glucose and rely on glycolysis as the main pathway for biomass production as HeLa cells grown in high concentrations of glucose

(10 mM) produce high concentration of lactate (Reitzer et al. 1979). Further, 80% of glucose-derived carbon is detected in glycolysis-derived lactate which is mainly utilized to form macromolecules and metabolic intermediates. Only 5% of glucose-derived carbon is fed into the TCA cycle. However, HeLa cells are also able to grow in lower glucose concentrations, which lead to the decreased generation of lactate, indicating compensatory metabolism. Interestingly, (Reitzer et al. 1979) demonstrated that the growth rates of fructose- and galactose-grown HeLa cells are comparable to glucose-grown cells. However, cells grown in 10 mM glucose consume 100-times more sugar molecules per minute than HeLa cells grown in 2 mM fructose. However, fructose-grown cells exhibit low levels of lactate, indicating reduced glycolytic rates, and 90% of fructose-derived carbon is metabolized to CO_2 through the oxidative arm of the pentose phosphate pathway. These cells rely heavily on the oxidation of glutamine to generate ATP. Despite of reduced glycolysis, ATP levels are not reduced compared to glucose-grown cells. The fructose-adapted MCF7 cells described in this thesis were derived on the basis of this work on HeLa cell metabolism. These cells have been extensively characterised by other members of the laboratory and show similar properties than the fructose-grown HeLa cells described by (Reitzer et al. 1979) which include low rates of glycolysis and proliferation equivalent to cells grown in glucose. Therefore, fructose-adapted MCF7 were applied as additional approach to the partial inhibition by 2-DG to determine the impact of glycolysis on the hypoxia- and HIF-1-dependent induction HIF-1 of target gene expression.

4.1.2 Aim of this chapter

This chapter aims to dissect the role of glycolysis and CtBPs in the regulation of HIF-induced *CA9* expression. Further, it is aimed to determine whether *CA9* is uniquely regulated in a HIF-1-CtBP-dependent manner and whether other HIF-1 target genes are regulated in a similar fashion. Therefore, the HIF-1 target genes introduced above were included in the study and their expression was analysed by Roche library reverse-transcription PCR.

4.1.3 Overview of this chapter

First, it was experimentally determined how glycolysis impacts the extended HIF-1 response in MCF7 and MDA-MB-231 breast cancer cells. Therefore, the impact of 2-DG on the hypoxia-induced expression of *EGLN3*, *PDK1*, *FAM162A*, *TMEM45A* and *INSIG2* was evaluated by Roche library reverse-transcription PCR. To further dissect the role of glycolysis in the regulation of *CA9* and other HIF-1 target genes, the hypoxia-induced gene expression in fructose-grown MCF7.Control cells was compared to the hypoxia-induced expression in MCF7.Control cells grown in glucose. Next, to confirm the activation of these genes by HIF-1, hypoxia was replaced by the

prolyl-4 hydroxylase inhibitor DMOG which activates HIF-1 in the presence of O_2. It was first demonstrated that the incubation in 1 mM DMOG for 18 h is sufficient to induce CA9 protein expression in MCF7 breast cancer cells. Therefore, this concentration was applied in all further experiments involving DMOG. To confirm whether the glycolysis-mediated and hypoxia-induced expression of CA9 and of other HIF-1 target genes is induced by HIF-1, MCF7 breast cancer cells were incubated with 2-DG and DMOG in normoxia. Additionally, fructose- and glucose-adapted MCF7.Control cells were incubated with 1 mM DMOG. Consequently, the role of CtBPs in this regulatory mechanism was dissected next. First, the impact of transfection with CtBP 1/2 siRNA on the broader HIF-1 response was determined in MCF7 and MDA-MB-231 breast cancer cells. The role of CtBPs as potential coupling mechanism between glycolysis and the hypoxia-induced expression of HIF-1 target genes, especially of CA9, was additionally investigated by inhibiting CtBP activity with MTOB, and in MCF7-derived cell lines which overexpress wildtype CtBP2 (MCF7.CtBP2), mutant CtBP monomers (MCF7. CtBP-Mutant) and an empty control vector (MCF7.Control). For confirming whether the CtBP-mediated induction of HIF-1 target gene expression is induced by HIF-1, these experiments were repeated with the HIF-1 activator DMOG. Additionally, it was planned to determine how CtBPs and HIF-1 interact at the *CA9* promoter by applying chromatin immunoprecipitation. However, due to technical problems the outcome of this experiment is discussed in Appendix B.

4.2 Glycolysis differentially regulates the expression of HIF-1 target genes

4.2.1 The partial inhibition of glycolysis by 2-DG increases hypoxia-induced *PDK1* expression but has no impact on other HIF-1 target genes

In order to determine whether glycolysis also impacts the expression of other HIF-1 target genes or whether the impact of glycolysis is specific for *CA9*, the same samples described in Chapter 3: (Fig. 3.5), were analysed by performing reverse-transcription PCR that utilises a Roche® probe library system.

In MCF7 breast cancer cells, partial inhibition of glycolysis by 2-DG only impacts the expression of *PDK1*. In contrast to *CA9*, the treatment with 2-DG increases the hypoxia-induced *PDK1* expression in MCF7 breast cancer cells, similar to *ADM*, which indicates that glycolysis differentially regulates the expression of these HIF-1 target genes (Fig. 4.1). This conclusion is based on the findings elaborated below.

In greater detail, the hypoxia-induced expression of *ELGN3* ($p < 0.001$), *PDK1* ($p = 0.002$), *TMEM45A* ($p < 0.001$), and *INSIG2* ($p = 0.005$) is significantly different from expression in normoxia (Fig. 4.1). *EGLN3* expression is significantly increased by 5.77-fold (± 0.60) in hypoxia, compared to expression in normoxia. The treatment with 10 mM 2-DG has no significant impact on induction in hypoxia as its expression is decreased by 5.09-fold (± 0.72). Compared to induction of gene expression in normoxia, *PDK1* expression is significantly increased in hypoxia by 2.84-fold (± 0.22). Further, the treatment with 2-DG significantly increases *PDK1* expression in hypoxia by 4.04-fold (± 0.29) ($p = 0.015$), compared to untreated MCF7 in hypoxia.

There is no significant induction of *FAM162A* expression in hypoxia compared to normoxia as its expression is increased by 1.34-fold (± 0.42). 2-DG also does not significantly impact *FAM162A* expression in hypoxia as its expression is reduced by 1.18-fold (± 0.31). *TMEM45A* expression is significantly upregulated in hypoxia by 6.40-fold (± 0.96), compared to induction of gene expression in normoxia. The treatment with 2-DG increases the hypoxia-induced expression of *TMEM45A* by 7.05-fold (± 0.65). However, this change in *TMEM45A* expression is not significant. *INSIG2* is significantly induced in hypoxia by 3.42-fold (± 0.55), compared to the normoxic control. The treatment with 2-DG only insignificantly increases *INSIG2* expression by 3.85-fold (± 0.60).

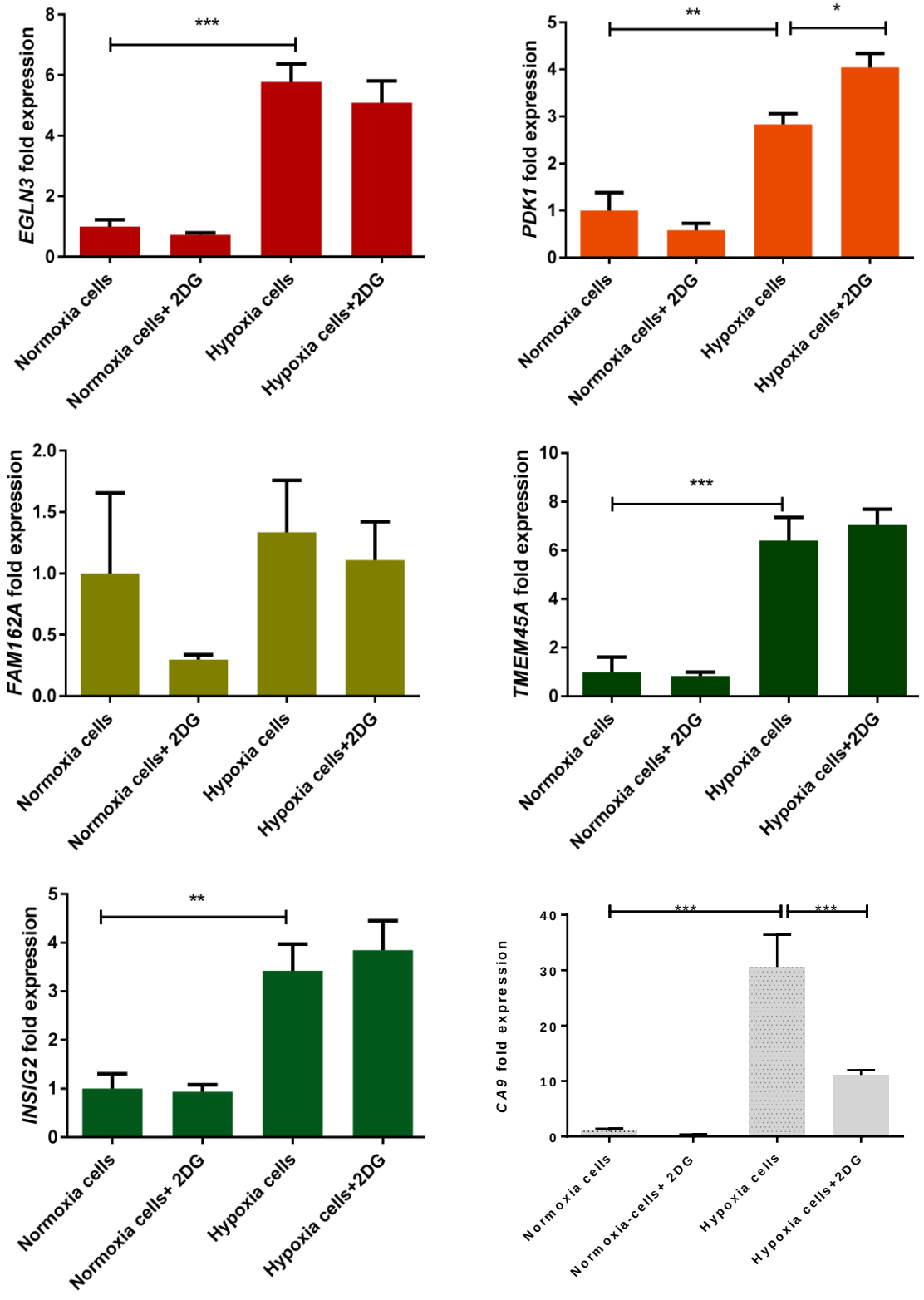

Fig. 4.1: Partial inhibition of glycolysis by 10 mM 2-DG increases *PDK1* gene expression in MCF7 breast cancer cells. MCF7 breast cancer cells were plated at a concentration of $2.2x10^5$/ 2 ml in 6 well plates in complete DMEM. 48 h post-plating, cells were treated with 10 mM 2-DG and incubated at either 1% or 20% O_2 for 18 h. HIF-1 target gene expression was determined by Roche® library reverse-transcription PCR. Expression was normalized to untreated cells in normoxia and statistical significance was determined by Fisher's uncorrected LSD test. Shown are the means of three independent experiments and their SEM. The data for *CA9* are the same as presented in Fig. 3.5 and are shown for comparison.

In MDA-MB-231 breast cancer cells, *PDK1* ($p = 0.001$), *FAM162A* ($p < 0.001$), and *INSIG2* ($p = 0.006$) expression is significantly induced in hypoxia, compared to expression in normoxia (Fig. 4.2). The induction of *EGLN3* expression in hypoxia is 3.98-fold (± 3.154). *EGLN3* expression increases by 6.43-fold (± 4.76) when hypoxic MDA-MB-231 were treated with 2-DG. Both, the induction of gene expression in hypoxia, and increased expression upon treatment with 2-DG are insignificant. Hypoxia significantly induces *PDK1* expression by 3.98-fold (± 0.55). Additionally, the treatment with 2-DG significantly increases the hypoxia-induced *PDK1* expression by 7.71-fold (± 0.57) ($p < 0.001$), compared to untreated MDA-MB-231 in hypoxia.

FAM162A expression is significantly increased by 2.1-fold (± 0.12) in hypoxia compared to normoxia, and treatment with 2-DG also significantly increases hypoxia-induced expression by 3.25-fold (± 0.11) ($p < 0.001$). *INSIG2* expression is significantly upregulated by 6.93-fold (± 1.82) in hypoxia compared to normoxia, whereas the treatment with 2-DG does not significantly impact I*NSIG2* expression in hypoxia as *INSIG2* expression is only insignificantly increased by 8.65-fold (± 0.99). The 22.74-fold (± 7.65) induction of *TMEM45A* in hypoxia as well as the upregulation upon 2-DG treatment by 48.64-fold (± 19.66) is also insignificant.

Therefore, when glycolysis was partially inhibited by the treatment with 2-DG, the hypoxia-induced expression of *PDK1* and *FAM162A* is significantly increased which points towards a glycolysis-mediated regulation of these HIF-1 target genes in MDA-MB-231 breast cancer cells. Similar to MCF7 breast cancer cells, the upregulation of these genes is in contrast to the inhibition of hypoxia-induced *CA9* expression by 2-DG. Consequently, HIF-1 target genes are differentially regulated by glycolysis when induced by hypoxia.

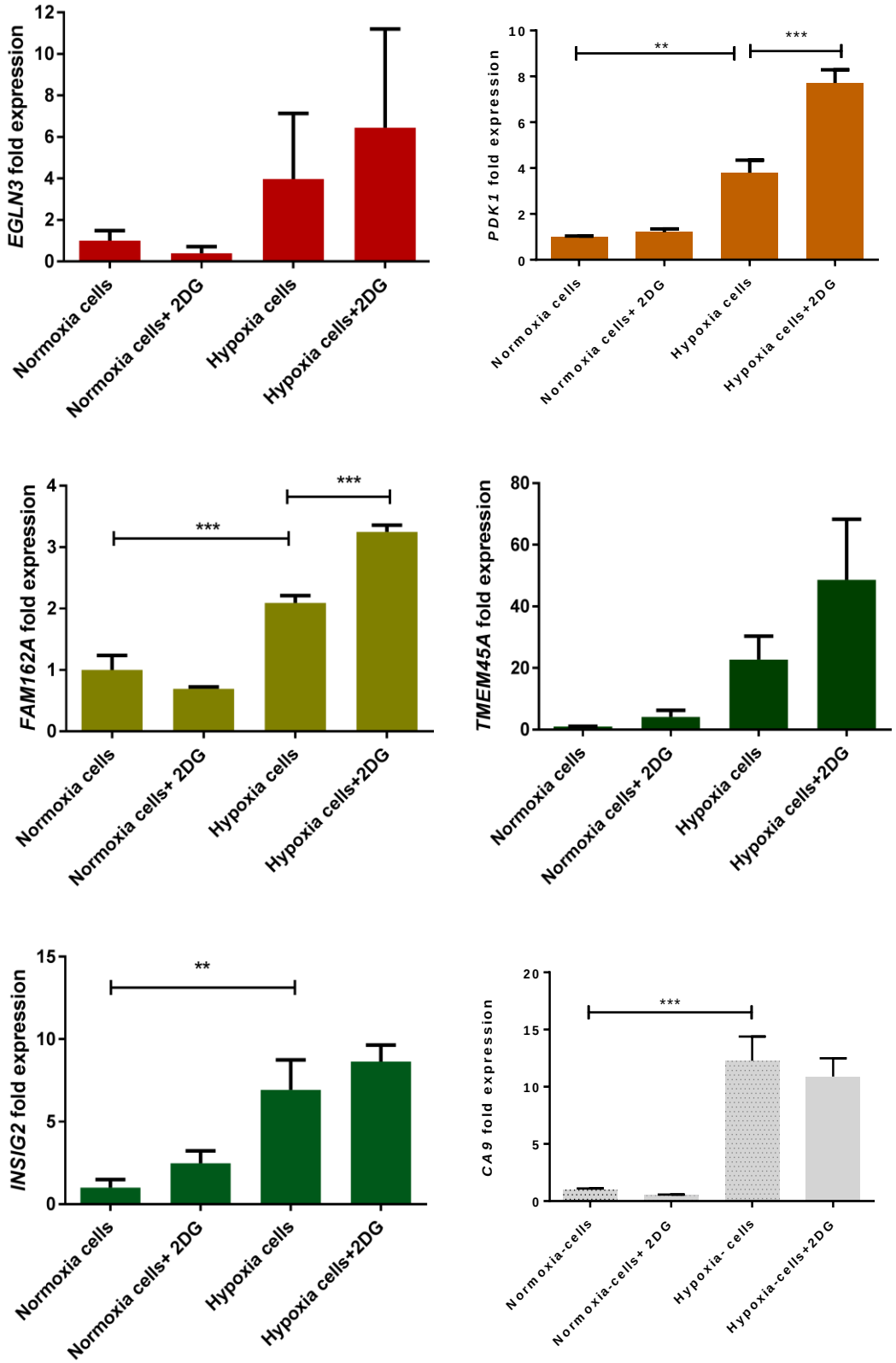

Fig. 4.2: The partial inhibition of glycolysis by 10 mM 2-DG increases *PDK1* and *FAM162A* gene expression in MDA-MB-231 breast cancer cells. MDA-MB-231 breast cancer cells were plated at a concentration of $2.2x10^5$/ 2 ml in 6 well plates in complete DMEM. 48 h post-plating, cells were treated with 10 mM 2-DG and incubated at either 1% or 20% O_2 for 18 h. HIF-1 target gene expression was determined by Roche® library reverse-transcription PCR. Expression was normalized to untreated cells in normoxia and statistical significance was determined by Fisher's uncorrected LSD test. Shown are the means of three independent experiments and their SEM. *CA9* is shown as comparison and displays the same data presented in Fig. 3.5.

4.2.2 Cultivation in fructose reduces the hypoxia-induced expression of *CA9* and other selected HIF-1 target genes

The impact of glycolysis on the regulation of hypoxia-induced CA9 protein and mRNA expression was investigated in greater detail by including MCF7.Control cells in the study. As introduced in 2.1.1, Fructose-adapted MCF7.Control cells exhibit similar metabolic adaptions to fructose-grown HeLa cells described by (Reitzer et al. 1979). This includes the strong downregulation of glycolysis, and the reliance on the PPP and glutaminolysis for energy generation. HIF-target gene expression was compared to glucose-grown MCF7.Control cells which exhibit unchanged levels of glycolysis.

In fructose-adapted MCF7.Control cells, hypoxia-induced CA9 protein expression is strongly decreased compared to MCF7.Control cells grown in glucose-containing DMEM (Fig. 4.3A). *CA9* mRNA expression is significantly induced in hypoxia, compared to normoxia in glucose-grown MCF7.Control cells ($p < 0.001$) (Fig. 4.3B). Hypoxia-induced *CA9* expression is upregulated by 193.5-fold (± 4.30) in glucose-adapted MCF7.Control cells. In fructose-adapted MCF7.Control cells *CA9* expression is only induced by 20.99-fold (± 3.81). This reduction of *CA9* induction in fructose-grown MCF7.Control cells compared to glucose-adapted MCF7.Control cells is highly significant ($p < 0.001$). Combining both data sets for CA9, generated from the treatment with 2-DG and from MCF7 grown in fructose- versus glucose-containing DMEM, there is experimental evidence that glycolysis may be required for CA9 protein and gene expression in hypoxia. In order to confirm the role of glycolysis in the hypoxia-induced expression of HIF-target genes, the glycolytic rate could be measured by determining the ECAR in fructose- and glucose-adapted MCF7.

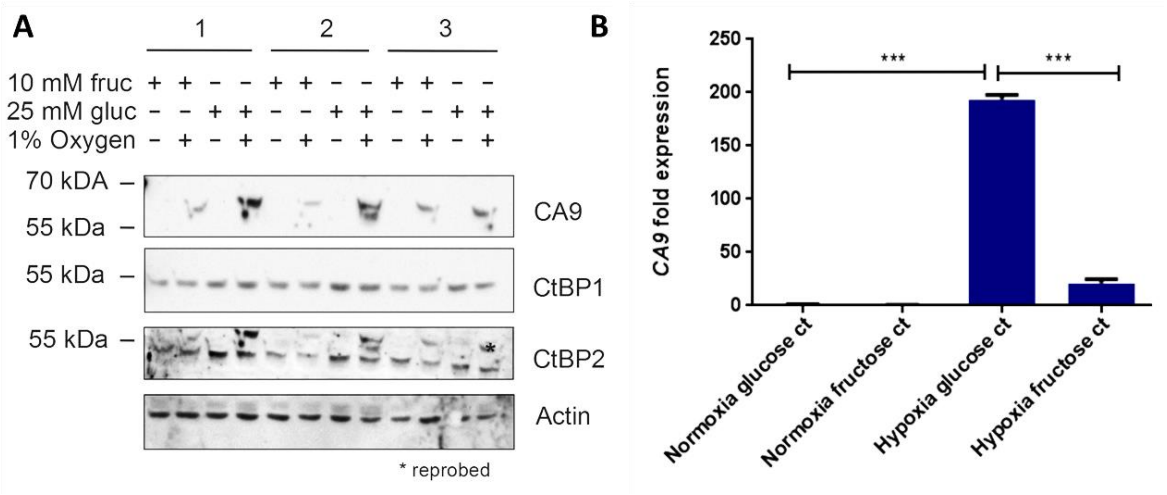

Fig. 4.3: Inhibition of glycolysis in fructose-adapted MCF7.Control cells reduces hypoxia-induced CA9 expression. MCF7.Control cells were plated at a concentration of $2.2x10^5$/ 2 ml in 6 well plates in DMEM that was prepared in house and supplemented with 10 mM fructose or 25 mM glucose. 48 h post-plating, medium was renewed and cells were incubated at either 1% or 20% O_2 for 18 h. **A**: CA9 protein expression was evaluated by Western blot. Gels were loaded with 20 µg whole cell lysate. CA9 expression of three independent repeats was evaluated on one membrane (1-3). **B**: *CA9* gene expression was determined by TaqMan® quantitative reverse-transcription PCR. Expression was normalized to glucose-adapted MCF7.Control cells (ct) in normoxia and statistical significance was determined by Fisher's uncorrected LSD test. Shown are the means of three independent experiments and their SEM.

To further determine whether glycolysis impacts the broader HIF-1-mediated response to hypoxia, the hypoxia-induced expression of *EGLN3*, *PDK1*, *FAM162A*, *TMEM45A* and *INSIG2* in glucose- and fructose-adapted MC7.Control cells was evaluated by Roche® library reverse-transcription PCR (Fig. 4.4).

In contrast to the treatment with 2-DG, hypoxia-induced gene expression of all HIF-1 target genes evaluated in this experiment is strongly reduced in fructose-adapted MCF7.Control cells, compared to their glucose-grown counterparts (Fig. 4.4). In glucose-adapted cells, *EGLN3* expression is significantly induced in hypoxia by 4.29-fold (± 0.18) ($p < 0.001$), compared to normoxia. *EGLN3* expression in hypoxia is strongly reduced in cells grown in fructose-containing DMEM compared to their glucose-adapted counterparts, as induction in hypoxia is only 2.27-fold (± 0.12). This difference in induction of gene expression is highly significant ($p < 0.001$).

In glucose-adapted cells, *PDK1* is also significantly induced in hypoxia by 6.21-fold (± 0.34) ($p < 0.001$), compared to induction in normoxia. In fructose-adapted cells, hypoxia-induced expression of *PDK1* is clearly reduced as induction is only 3.76-fold (± 0.39) which is significantly different from the induction of *PDK1* expression in glucose-adapted cells ($p < 0.001$). In glucose-adapted cells, *FAM162A* is significantly induced in hypoxia by 6.43-fold (±0.34) ($p < 0.001$), compared to normoxia. The induction of *FAM162A* in fructose-adapted MCF7.Control cells in hypoxia is 2.69-fold (± 0.14). This reduction in gene expression is highly significant ($p < 0.001$).

In glucose-grown MCF7.Control cells, *TMEM45A* expression is increased in hypoxia by 6.95-fold (± 0.21) ($p < 0.001$), compared to their normoxic counterparts. In fructose-adapted MCF7.Control cells, *TMEM45A* is induced by 2.50-fold (± 0.12) in hypoxia which is significantly different from hypoxia-induction in glucose-grown MCF7.Control cells ($p < 0.001$). Hypoxia increases *INSIG2* expression by 4.40-fold (± 0.23) in glucose-adapted cells which is significantly different from expression in normoxia ($p < 0.001$). In fructose-adapted cells, *INSIG2* is upregulated in hypoxia by 2.02-fold (± 0.28). This reduction of *INSIG2* expression is strongly significant ($p < 0.001$).

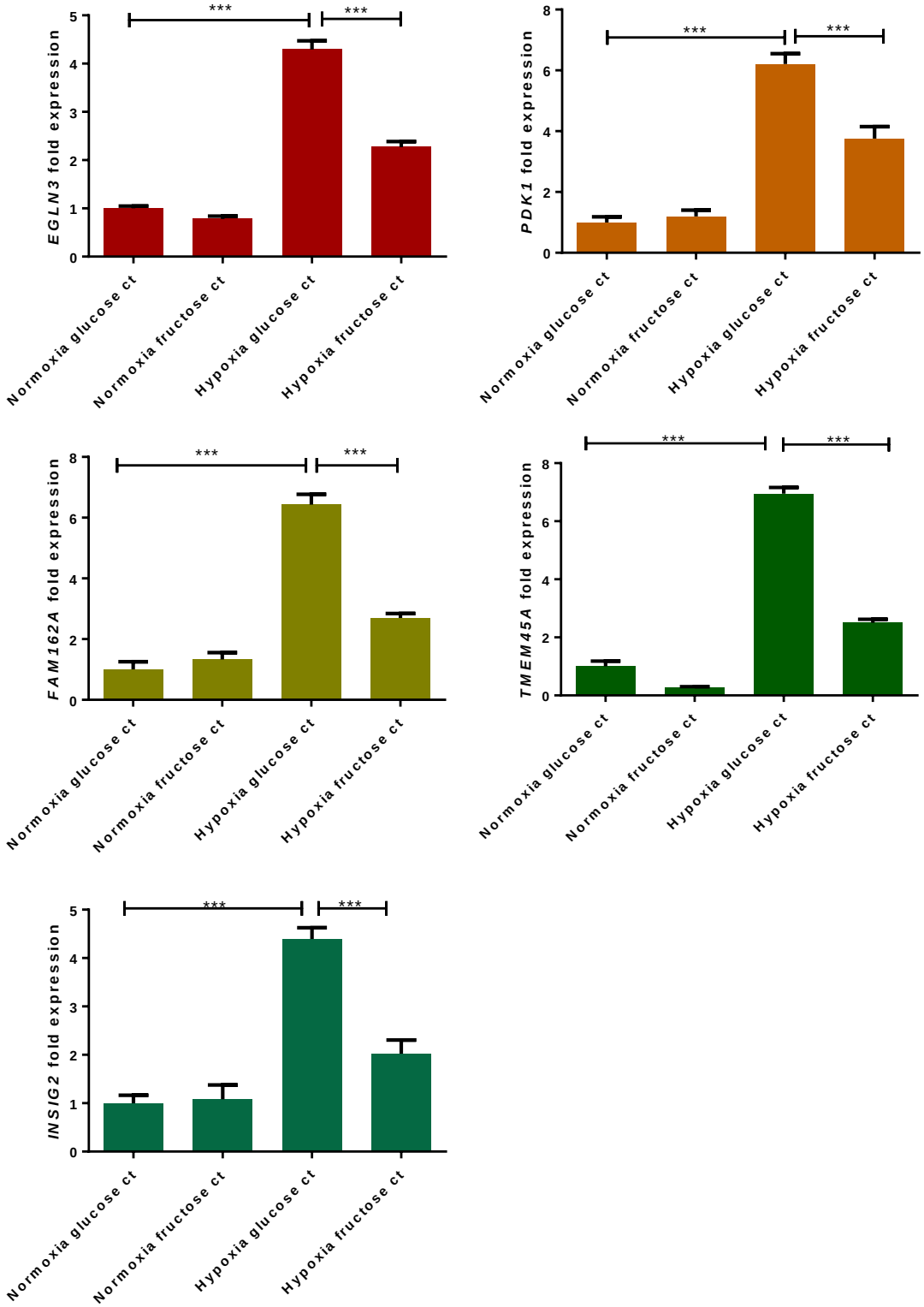

Fig. 4.4: Impaired glycolysis decreases HIF-1 target gene expression in MCF7.Control cells grown in fructose-containing DMEM. MCF7.Control cells were plated at a concentration of $2.2x10^5$/ 2 ml in 6 well plates in DMEM that was prepared in house and supplemented with 10 mM fructose or 25 mM glucose. 48 h post-plating, medium was renewed and cells were incubated at either 1% or 20% O_2 for 18 h. HIF-1 target gene expression was determined by semi-quantitative reverse-transcription PCR. Expression was normalized to glucose-adapted MCF7.Control cells (ct) in normoxia and statistical significance was determined by Fisher's uncorrected LSD test. Shown are the means of three independent experiments and their SEM.

4.3 Glycolysis regulates the DMOG-induced expression of CA9 and of other HIF-1 target genes

Hif-1 target gene expression is differentially regulated when glycolysis is reduced by the treatment with 2-DG or inhibited by growth in fructose-containing DMEM. To confirm the HIF-dependent activation of these genes, hypoxia was replaced by incubating cells in the PHD inhibitor DMOG for 18 h in 20% O_2.

4.3.1 DMOG induces CA9 expression in normoxia

First, it was evaluated whether the concentration suggested by (Hulikova et al. 2013) was sufficient to induce CA9 protein expression in MCF7. For this, MCF7 were either incubated with 1 mM DMOG, 0.1% DMSO or left untreated for 18 h. Protein expression was determined by Western blot. Both, the incubation time of 18 h and the concentration of 1 mM are sufficient to induce CA9 expression in the presence of O_2 (Fig. 4.5). Therefore, incubation time and concentration were applied to all further experiments involving DMOG. However, it would have been useful to confirm the DMOG-induced stabilisation of HIF-1 expression by Western blot. This accounts for all following Western blots, which show the DMOG-induced expression of CA9.

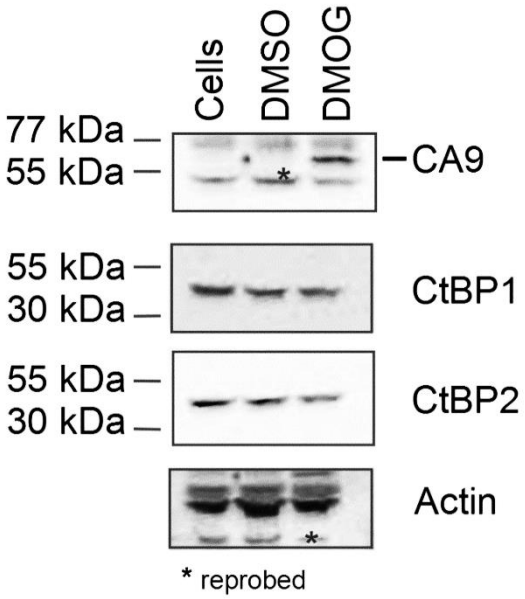

Fig. 4.5: CA9 protein expression is induced by 1 mM DMOG. MCF7 breast cancer cells were plated in 6 cm dishes in complete DMEM at a concentration of $7x10^5$/ 4 ml. 24 h post-plating, cells were either incubated with medium alone (cells), 0.1 % DMSO (DMSO) or 1 mM DMOG (DMOG) for 18 h. CA9 and CtBP protein expression was determined by Western blot. Gels were loaded with 20 µg whole cell lysate. Specific CA9 expression was labelled with a dash.

4.3.2 2-DG reduces the DMOG-induced expression of CA9 but differentially impacts the expression of other HIF-1 target genes

MCF7 breast cancer cells were incubated with 10 mM 2-DG as described and hypoxia was replaced by either 1 mM DMOG or 0.1% DMSO. Untreated MCF breast cancer cells were included as intrinsic control. In three independent experiments, CA9 protein expression is induced by 1 mM DMOG and is strongly reduced when cells were additionally treated with 2-DG (Fig. 4.6A). DMOG significantly upregulates *CA9* gene expression by 210.8-fold (± 4.71) ($p < 0.001$), compared to untreated cells, or cells treated with 0.1% DMSO (Fig. 4.6B). Upon treatment with 2-DG, hypoxia-induced *CA9* expression is strongly reduced as induction is only 91.36-fold (± 3.96). This is significantly different from *CA9* expression in DMOG-treated cells ($p < 0.001$). Therefore, it is concluded that the HIF-dependent induction of CA9 expression is impaired by the partial inhibition of glycolysis through 2-DG. This conclusion can be confirmed by determining the ECAR with a seahorse analyser.

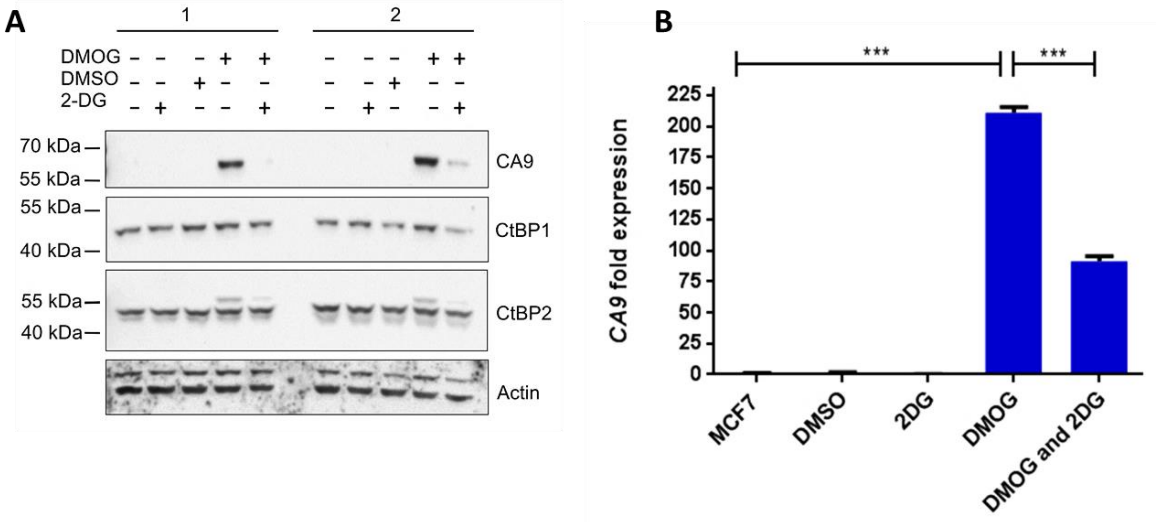

Fig. 4.6: Partial inhibition of glycolysis reduces DMOG-induced CA9 protein (A) and gene expression (B) in MCF7 breast cancer cells. Cells were plated at a concentration of $2.2x10^5$/ 2 ml in 6 well plates in complete DMEM. 48 h post-plating, cells were treated with 10 mM 2-DG and incubated in either complete DMEM, 0.1% DMSO, 1 mM DMOG or in 1 mM DMOG and 10 mM 2-DG in 20% O_2 for 18 h. **A**: CA9 protein expression was determined by Western blot. Gels were loaded with 15 µg whole cell lysate. Displayed is one representative image of three independent repeats showing membranes where experiment 1 and 2 were analysed. **B**: *CA9* expression was determined by TaqMan® quantitative reverse-transcription PCR. Expression was normalized to untreated cells in normoxia and statistical significance was determined by Fisher's uncorrected LSD test. Shown are the means of three independent experiments and their SEM.

The DMOG-induced expression of other HIF-1 targets included in this study is differentially affected by the treatment with 2-DG (Fig. 4.7). It was determined that DMOG induces the expression of all HIF-1 target genes included in this experiment. However, only the expression of *EGLN3*, *FAM162A* and *TMEM45A* is decreased when cells were additionally treated with 2-DG, whereas the expression of *PDK1* and *INSIG2* is not affected.

Illustrating these results in greater detail, *EGLN3* expression is significantly induced by DMOG ($p < 0.001$), compared to DMSO- or untreated MCF7, as its expression is increased by 25.98-fold (± 1.92). The induction of *EGLN3* expression is decreased by 10.87-fold (± 1.34) when cells were additionally treated with 2-DG. This decrease in *EGLN3* expression is strongly significant ($p < 0.001$). In DMOG-treated MCF7, *PDK1* expression is upregulated by 9.79-fold (± 1.38). This induction of gene expression is significantly different from the expression in untreated cells ($p < 0.001$). In cells which were additionally treated with 2-DG, *PDK1* expression is increased by 9.10-fold (± 0.80) and is not significantly different from *PDK1* expression in DMOG-treated MCF7.

DMOG-induced *FAM162A* expression is significantly upregulated by 12.10-fold (± 0.76) ($p < 0.001$), compared to expression in untreated cells. *FAM162A* is upregulated by 9.02-fold (± 0.48) when cells were additionally treated with 2-DG. This means a significant reduction in *FAM162A* expression ($p = 0.003$). In DMOG-treated MCF7, the expression of *TMEM45A* is induced by 29.95-fold (± 1.95) which is significantly different to *TMEM45A* expression in untreated cells ($p < 0.001$). The treatment with 2-DG significantly reduces *TMEM45A* expression by 14.61-fold (± 0.71) ($p = 0.005$). The expression of *INSIG2* is significantly increased by 9.90-fold (± 1.12) ($p < 0.001$) when cells are treated with 1 mM DMOG, compared to the untreated control. There is a minor increase in *INSIG2* expression by 10.15-fold (± 0.63) when cells were additionally treated with 2-DG. This is not significantly different from *INSIG2* expression in DMOG-treated cells.

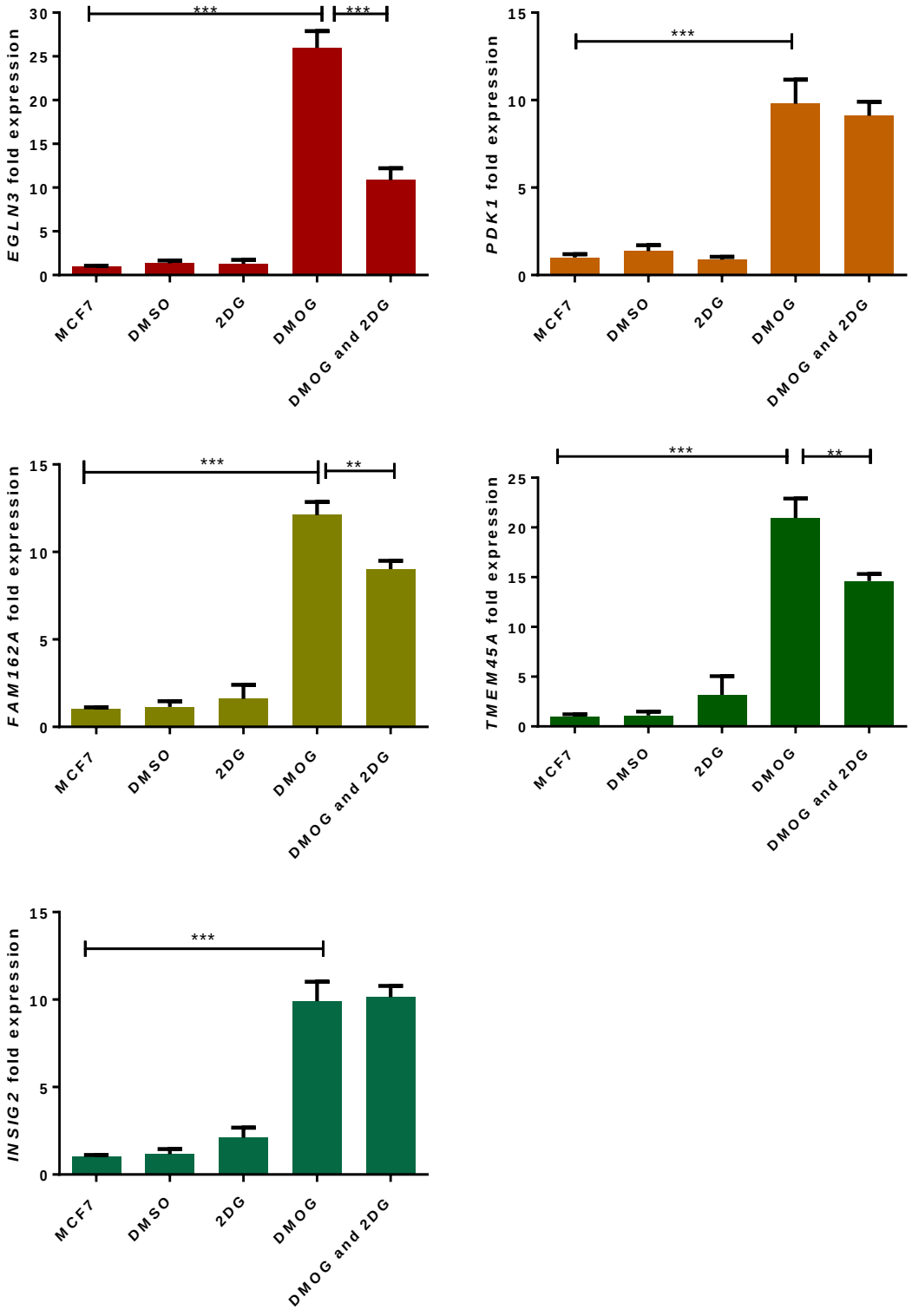

Fig. 4.7: The Partial inhibition of glycolysis by 10 mM 2-DG reduces the DMOG-induced expression of *EGLN3*, *FAM162A* and *TME45A* in MCF7 breast cancer cells. MCF7 breast cancer cells were plated at a concentration of $2.2x10^5$/ 2 ml in 6 well plates in complete DMEM. 48 h post-plating, cells were treated with either complete DMEM alone (MCF7), 0.1% DMSO, 1 mM DMOG or 1 mM DMOG and 10 mM 2-DG and incubated at 20% O_2 for 18 h. HIF-1 target gene expression was determined by semi-quantitative reverse-transcription PCR. Expression was normalized to untreated cells in normoxia and statistical significance was determined by Fisher's uncorrected LSD test. Shown are the means of three independent experiments and their SEM.

4.3.3 Cultivation in fructose reduces DMOG-induced CA9 expression

For further determination of the glycolysis- and HIF-1-mediated regulation of the HIF-1 response, HIF-1 was specifically activated in normoxia by treating glucose- and fructose-adapted MCF7.Control cells with 1 mM DMOG for 18 h. It is suggested to determine the ECAR in future experiments, in order to demonstrate the role of glycolysis in DMOG-induced HIF-target gene expression in fructose- versus glucose-adapted MCF7.Control cells.

In three independent experiments, DMOG-induced CA9 protein expression is strongly reduced in fructose-adapted cells, compared to cells grown in glucose (Fig. 4.8A). DMOG increases the expression of *CA9* in glucose-adapted MCF7.Control cells by 121.6-fold (± 13.41) (Fig. 4.8B). This is significantly different from the induction of *CA9* expression in untreated MCF7.Control cells ($p < 0.001$). In fructose-adapted cells, induction of *CA9* expression in DMOG-treated MCF7.Control cells is 56.05-fold (± 13.22). This difference in DMOG-induced *CA9* expression between fructose- and glucose-adapted cells is highly significant ($p < 0.001$).

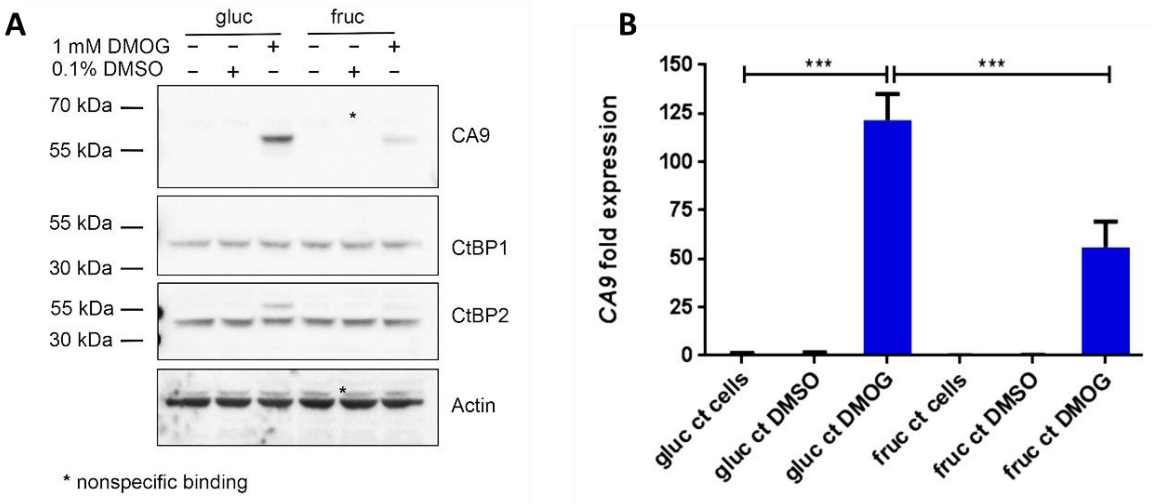

Fig. 4.8: Inhibition of glycolysis in fructose-adapted MCF7.Control cells reduces DMOG-induced CA9 expression. MCF7.Control cells were plated at a concentration of $2.2x10^5$/ 2 ml in 6 well plates in DMEM that was prepared in house and supplemented with 10 mM fructose or 25 mM glucose. 48 h post-plating, medium was renewed and cells were incubated in either complete DMEM, 0.1% DMSO or 1 mM DMOG at 20% O_2 for 18 h. **A**: CA9 protein expression was evaluated by Western blot. Gels were loaded with 20 µg whole cell lysate. Displayed is one representative experiment. **B**: *CA9* gene expression was determined by TaqMan® quantitative reverse-transcription PCR. Expression was normalized to untreated glucose-adapted MCF7.Control cells (ct and statistical significance was determined by Fisher's uncorrected LSD test. Shown are the means of three independent experiments and their SEM.

Downregulated glycolysis in fructose-adapted MCF7.Control cells reduces the DMOG-induced expression of *EGLN3*, *PDK1* and *TMEM45A* but has no impact on *INSIG2* and *FAM162A* expression (Fig. 4.9). This was concluded based on the findings described in the following paragraph.

In DMOG-treated glucose-adapted cells, *EGLN3* expression is significantly upregulated by 4.67-fold (± 0.39) ($p < 0.001$), compared to *EGLN3* expression in untreated controls (Fig. 4.9). In fructose-grown cells, *EGLN3* expression is induced by 2.70-fold (± 0.11). This difference in induction of *EGLN3* expression is highly significant ($p < 0.001$). In glucose-adapted cells, *PDK1* expression is significantly induced by DMOG by 5.78-fold (± 0.63). This induction of *PDK1* expression is significantly different from induction in untreated MCF7.Control cells ($p < 0.001$). In fructose-adapted cells, DMOG induces *PDK1* by 4.52-fold (± 0.41) which is significantly different from *PDK1* expression in glucose-adapted MCF7.Control cells ($p = 0.03$). *FAM162A* expression is significantly induced by 5.18-fold (± 0.84) by DMOG in glucose-grown MCF7.Control cells, compared to *FAM162A* expression in untreated MCF7.Control cells ($p < 0.001$). In fructose-adapted cells, *FAM162A* is upregulated by DMOG by 5.53-fold (± 1.24). However, the difference in DMOG-induced *FAM162A* expression between glucose- and fructose-adapted MCF7.Control cells is not significant.

In glucose-adapted MCF7.Control cells, DMOG significantly induces *TMEM45A* expression by 4.28-fold (± 0.36), compared to induction of gene expression in untreated MCF7.Control cells ($p < 0.001$). In fructose-adapted MCF7.Control cells, *TMEM45A* is only induced 1.60-fold (± 0.46). The difference in *TMEM45A* induction between the two cell lines is highly significant ($p < 0.001$). *INSIG2* is increased by 2.53-fold (± 0.23 fold) by DMOG in glucose-adapted cells which is significantly different from induction of *INSIG2* expression in untreated MCF7.Control cells ($p = 0.006$). The 1.58-fold induction of *INSIG2* expression (± 0.23) in fructose-adapted MCF7.Control cells is not significantly different from the DMOG-induced expression of *INSIG2* in glucose-adapted MCF7.Control cells.

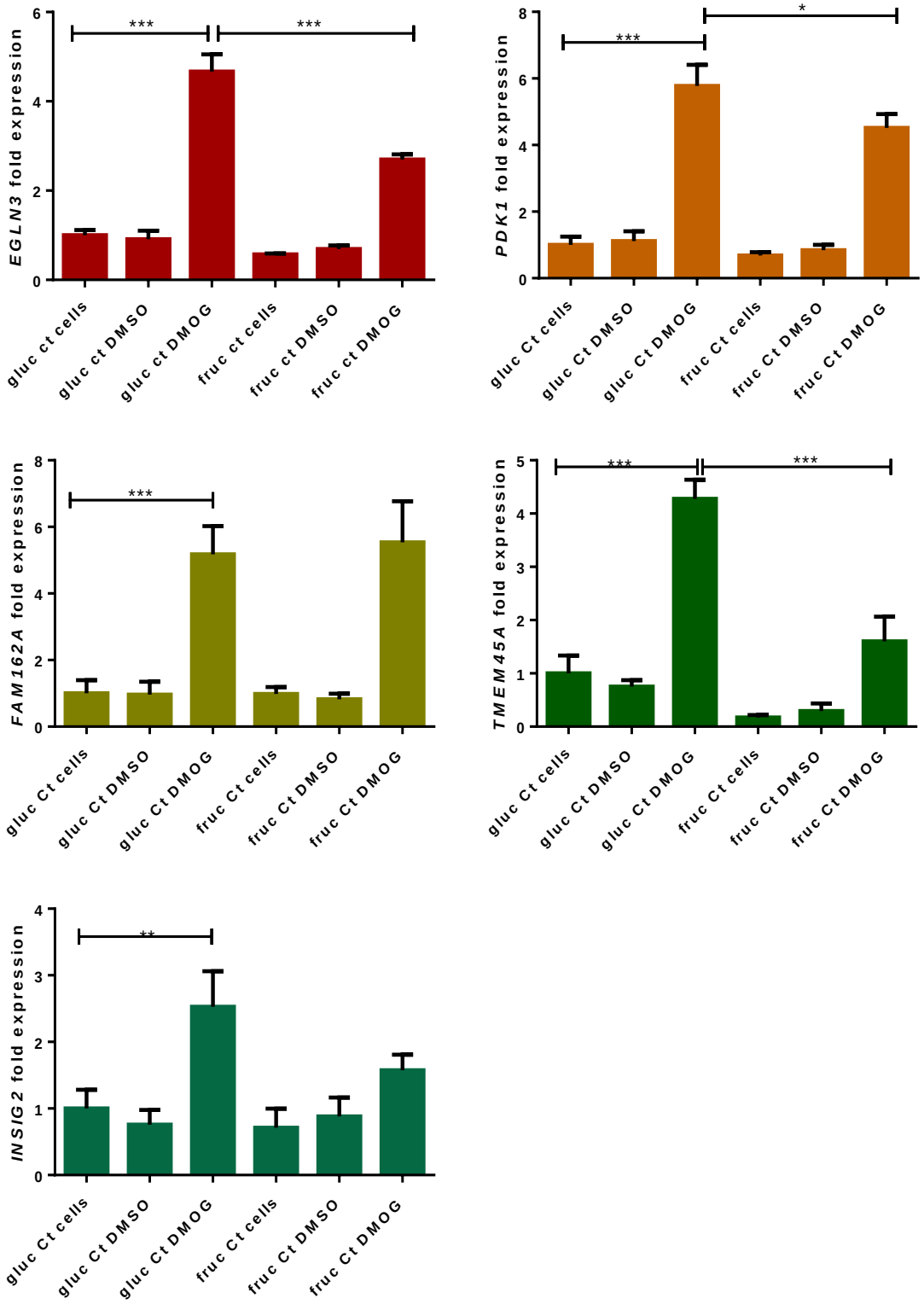

Fig. 4.9: *EGLN3*, *PDK1* and *TMEM45A* expression is reduced in fructose-grown MCF7.Control cells. MCF7.Control cells were plated at a concentration of $2.2x10^5$/ 2 ml in DMEM that was supplemented with 10 mM fructose or 25 mM glucose. 48 h post-plating, cells were incubated in either complete DMEM, 0.1% DMSO or 1 mM DMOG for 18 h at 20% O_2. Gene expression was determined by semi-quantitative reverse-transcription PCR. Expression was normalized to untreated glucose-adapted MCF7.Control cells (ct) in normoxia and statistical significance was determined by Fisher's uncorrected LSD test. Shown are the means of three independent experiments and their SEM.

4.4 Glycolysis mediates the regulation of hypoxia-induced HIF-1 target genes- summary

MDA-MB-231 breast cancer cells hardly respond to hypoxia or DMOG as they express high basal levels of HIF-1. MDA-MB-231 also do not respond to treatment with 2-DG. Therefore, they were excluded from further experiments.

As Tab. 4.2 illustrates, CA9 expression is induced by hypoxia and DMOG. Moreover, its hypoxia- and DMOG-induced expression is inhibited when MCF7 breast cancer cells were treated with 2-DG or grown in fructose-containing DMEM. Consequently, based on these data it is suggested that the HIF-dependent expression of CA9 is regulated by glycolysis.

Next, it was investigated whether CA9 is uniquely regulated by glycolysis or whether the expression of other HIF-1 target genes is mediated by glycolysis as well. *EGLN3*, *PDK1*, *FAM162A*, *TMEM45A* and *INSIG2* are induced by hypoxia and DMOG. However, the reaction to different treatments is more diverse. *PDK1* expression increases when treated with 2-DG whereas it is decreased in fructose-adapted MCF7. 2-DG has no impact on *PDK1* expression, when MCF7 were incubated with DMOG, but DMOG-induced expression in fructose-adapted cells is reduced. *INSIG2* expression in hypoxia is not influenced by 2-DG but is inhibited in fructose-grown cells. In DMOG on the other hand, neither 2-DG nor growth in fructose-containing medium has an impact on *INSIG2* expression.

The expression of *FAM162A*, *TMEM45A* and *EGLN3* is not impacted by 2-DG in hypoxia but is reduced when cells were grown in fructose-containing medium. However, 2-DG reduces the expression of those genes in DMOG, whereas only the expression of *TMEM45A* and *EGLN3* is reduced when cells were grown in fructose-containing medium. Therefore, it is argued that CA9 is the only HIF-1 target gene included in the analysis that is jointly regulated by glycolysis and HIF-1. Further experiments were performed to determine how glycolysis mediates the expression of hypoxia-induced HIF-1 target genes. Therefore the following section is concerned with how glycolysis may regulate HIF-1 target gene expression via the activation of CtBPs.

Tab. 4.2: Glycolysis differentially regulates the DMOG- and hypoxia-induced expression of HIF-1 target genes in MCF7 breast cancer cells

	Induction by hypoxia	Impact of 2-DG	Reduction in fructose medium	Induction by DMOG	Impact of 2-DG	Reduction in fructose medium
CA9	Yes	Reduced	Yes	Yes	Reduced	Yes
EGLN3	Yes	No Impact	Yes	Yes	Reduced	Yes
PDK1	Yes	Increased	Yes	Yes	No impact	Yes
FAM162A	Yes	No impact	Yes	Yes	Reduced	No impact
TMEM45A	Yes	No impact	Yes	Yes	Reduced	Yes
INSIG2	Yes	No impact	Yes	Yes	No impact	No impact

4.5 Glycolysis differentially regulates HIF-1 target gene expression via the activation of CtBPs

In the previous section it was evaluated that glycolysis activates CA9 protein and gene expression in hypoxia in a HIF-1-dependent manner, and that other selected HIF-1 target genes are differentially regulated by glycolysis. CtBPs are activated by NADH and therefore provide an important link between glycolysis and regulation of gene expression. However, it was not known whether CtBPs also link glycolysis and the regulation of HIF-1 target genes, as suggested by the preliminary gene expression data discussed in previous chapters. Therefore, it was of particular interest whether CA9 expression is regulated by glycolysis via the activation of CtBPs. The following section addresses this research question by inhibiting CtBP expression by siRNA and MTOB as well as by including MCF7-derived cell lines MCF7.CtBP2 and MCF7.CtBP-Mutant and MCF7.Control cells into the study (introduced in section 2.1.1). To determine whether the hypoxia-induced expression of *CA9* and other HIF-target genes, under the conditions described above, is dependent on HIF, hypoxia was replaced by DMOG.

4.5.1 Silencing of CtBP expression differentially impacts HIF-1 target gene expression in MCF7 and MDA-MB-231 breast cancer cells

The impact of transient transfection with CtBP 1/2 siRNA on hypoxia-induced expression of *EGLN3*, *PDK1*, *FAM162A*, *TMEM45A* and *INSIG2* in MCF7 and MDA-MB-231 was determined by Roche® library reverse-transcription PCR (Fig. 4.10). It was found that only the hypoxia-induced expression of *PDK1* and *INSIG2* in MCF7 transfected with non-silencing siRNA is significantly different from induction of gene expression in their normoxic counterparts. The inhibition of CtBP expression by 1/2 siRNA only significantly decreases the hypoxia-induced expression of those genes but has no impact on *EGLN3*, *FAM162A* and *TMEM45A* expression. Consequently, based on the data elaborated below, HIF-1 target genes are differentially impacted by CtBP expression.

EGLN3 expression is upregulated by 3.85-fold (± 0.53) in hypoxic MCF7 breast cancer cells which were transfected with non-silencing siRNA. This induction of *EGLN3* expression is not significantly different from expression in normoxia. The transfection with CtBP 1/2 siRNA insignificantly reduces *EGLN3* expression to 3.18-fold (± 0.36), compared to *EGLN3* expression in hypoxic MCF7 transfected with non-silencing siRNA.

In cells transfected with non-silencing siRNA, *PDK1* expression is significantly induced by 18.46-fold (± 0.50), compared to normoxic MCF7 transfected with non-silencing siRNA ($p < 0.001$). In hypoxic MCF7 transfected with CtBP 1/2 siRNA, *PDK1* is induced by 10.13-fold (± 0.22). This reduction in hypoxia-induced *PDK1* expression is significantly different to *PDK1* expression in hypoxic MCF7 transfected with non-silencing siRNA ($p = 0.003$).

In MCF7 transfected with non-silencing control siRNA, *FAM162A* is upregulated in hypoxia by 9.83-fold (± 2.36). This trend is not significant ($p = 0.053$). Upon transfection with CtBP 1/2 siRNA, *FAM162A* expression is induced by 7.19-fold (± 1.95). This difference in *FAM162A* induction is not significant.

In MCF7 transfected with non-silencing siRNA, the hypoxia-induced upregulation of *TMEM45A* by 26.48-fold (± 4.09) is also not significantly different from *TMEM45A* expression in normoxia. The inhibition of CtBP expression by 1/2 siRNA also has no significant effect on *TMEM45A* expression in hypoxia as it is induced by 26.53-fold (± 0.09).

However, in MCF7 transfected with non-silencing siRNA, the hypoxia-induced upregulation of *INSIG2* by 7.05-fold (± 0.99) is significantly different from *INSIG2* expression in normoxia ($p = 0.001$). Furthermore, the transfection with 1/2 siRNA significantly reduces the hypoxia-induced expression of *INSIG2* by 3.69-fold (± 0.0072), compared to expression in hypoxic MCF7 transfected with non-silencing siRNA ($p = 0.007$).

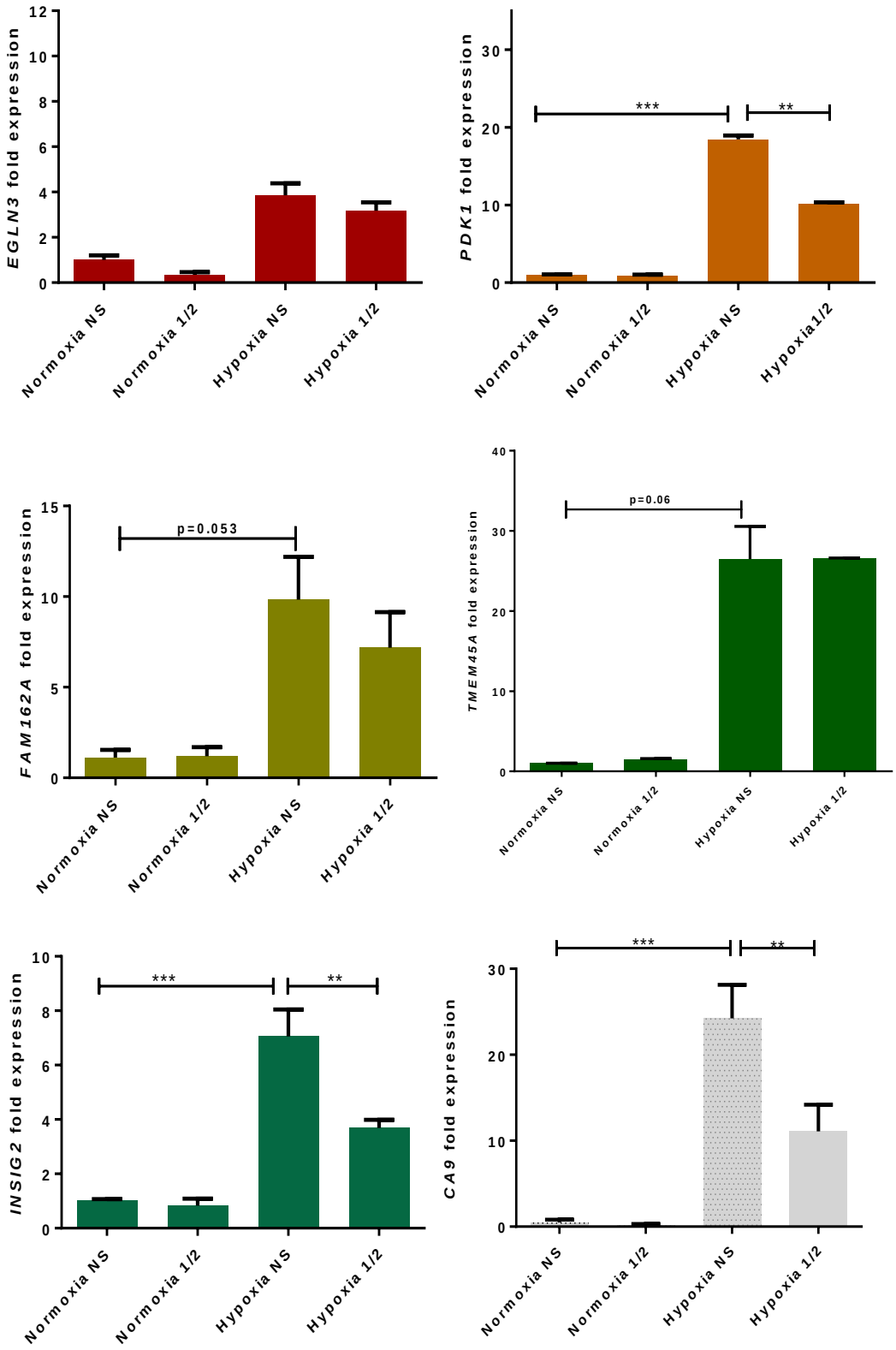

Fig. 4.10: CtBP expression differentially impacts HIF-1 target gene expression in MCF7 breast cancer cells. MCF7 were plated at a concentration of $2.2x10^5$/ 2 ml in 6 well plates in complete DMEM. 24 h post-plating, cells were transfected with 50 nM of either non-silencing siRNA, CtBP1-, CtBP2-, a combination of CtBP1 and CtBP2 siRNA or CtBP 1/2 siRNA. 48 h later, cells were incubated at either 1% or 20% O_2 for 18 h and immediately pellet. HIF-1 target gene expression was determined by semi-quantitative reverse-transcription PCR. Expression was normalized to MCF7 transfected with non-silencing siRNA in normoxia and statistical significance was determined by Fisher's uncorrected LSD test. Shown are the means of three independent experiments and their SEM. The data for *CA9* are the same as presented in Fig. 3.5 and are shown for comparison.

In MDA-MB-231 breast cancer cells, CtBP expression does not impact the broader HIF-1 response (Fig. 4.11). In greater detail, in MDA-MB-231 transfected with non-silencing siRNA, *EGLN3* is induced by hypoxia by 10.64-fold (± 2.84). This induction of *EGLN3* expression significantly differs from induction of gene expression in normoxia ($p = 0.016$) (Fig. 4.11). Moreover, when CtBP expression is reduced by siRNA, *EGLN3* expression is only induced by 3.61-fold (± 0.94). This trend is not significantly different from *EGLN3* expression in hypoxic MDA-MB-231 transfected with non-silencing siRNA. *PDK1* expression is significantly induced in hypoxic cells transfected with non-silencing siRNA by 2.36-fold (± 0.03), compared to MDA-MB-231 in normoxia ($p < 0.001$). The transfection with CtBP 1/2 siRNA has no significant impact on *PDK1* expression in hypoxia. *PDK1* expression is induced by 1.94-fold (± 0.003) in these cells.

The upregulation of *FAM162A* expression in hypoxia by 2.02-fold (± 0.36) is not significant in MDA-MB-231 transfected with non-silencing siRNA. CtBP 1/2 siRNA insignificantly reduces *FAM162A* expression in hypoxia by 1.63-fold (± 0.12), compared to expression in hypoxic MDA-MB-231 transfected with non-silencing siRNA. In hypoxia, *TMEM45A* is significantly induced by 6.47-fold (± 0.22), compared to MDA-MB-231 transfected with non-silencing siRNA in normoxia ($p = 0.004$). In hypoxic MDA-MB-231 treated with CtBP 1/2 siRNA, *TMEM45A* is insignificantly upregulated by 9.43-fold (± 0.32). In hypoxia, *INSIG2* expression is significantly upregulated by 2.31-fold in cells transfected with non-silencing siRNA (± 0.09), compared to the normoxic control ($p = 0.008$). Upon treatment with CtBP1/2 siRNA, *INSIG2* expression is reduced by 1.86-fold (± 0.01) in hypoxia. This trend is not significant.

Summarising the data described above, it was determined that the HIF-target genes analysed in this study are not regulated in a CtBP-dependent manner in MDA-MB-231. Further, induction of HIF-1 target genes is low in this cell line. Thus, MDA-MB-231 cells were excluded from further experiments.

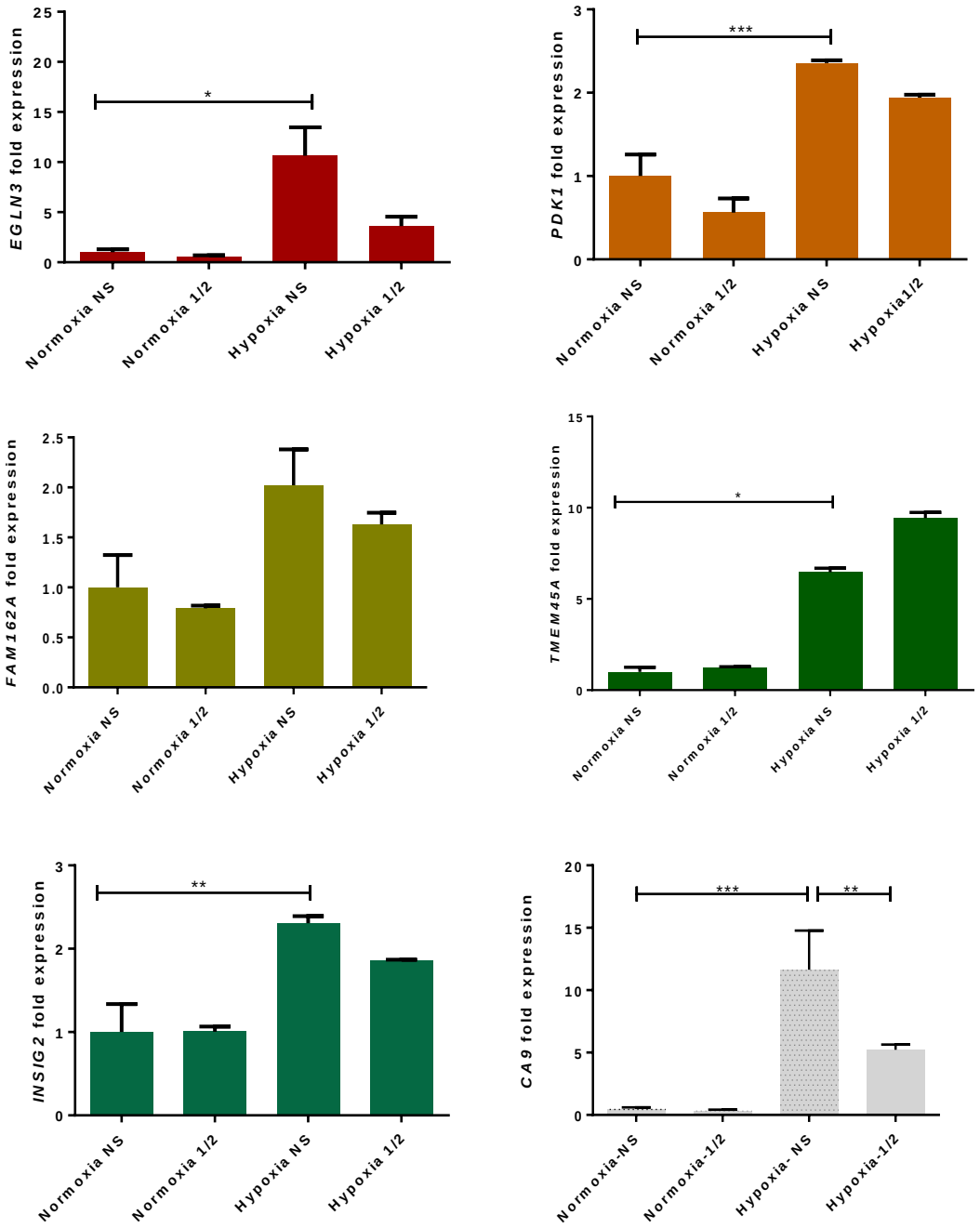

Fig. 4.11: CtBP expression differentially impacts HIF-1 target gene expression in MDA-MB-231 breast cancer cells. MDA-MB-231 breast cancer cells were plated at a concentration of $2.2x10^5$/ 2 ml in 6 well plates in complete DMEM. 24 h post-plating, cells were transfected with 50 nM of either non-silencing siRNA, CtBP1-, CtBP2-, a combination of CtBP1 and CtBP2 siRNA or CtBP 1/2 siRNA. 48 h later, cells were incubated at either 1% or 20% O_2 for 18 h and immediately pellet. HIF-1 target gene expression was determined by semi-quantitative reverse-transcription PCR. Expression was normalized to MDA-MB-231 transfected with non-silencing siRNA in normoxia and statistical significance was determined by Fisher's uncorrected LSD test. Shown are the means of three independent experiments and their SEM. *CA9* expression was added for comparison.

4.5.2 MTOB reduces hypoxia-induced HIF-1 target gene expression

To further evaluate the role of CtBPs in the regulation of hypoxia-induced CA9 expression, CtBP activity was inhibited by the inhibitor MTOB. CA9 expression was determined by Western blot and TaqMan® quantitative real-time PCR. In three independent experiments, CA9 protein expression is reduced when hypoxic MCF7 breast cancer cells were treated with 4 mM MTOB (Fig. 4.12A). Analysis of *CA9* mRNA expression levels confirms the impact of MTOB on CA9 protein expression on the level of mRNA expression (Fig. 4.12B). In hypoxic MCF7, *CA9* gene expression is significantly induced by 293.7-fold (± 1.65), compared to *CA9* expression in normoxia ($p < 0.001$). In MCF7 which were treated with 4 mM MTOB, hypoxia-induced expression of *CA9* is reduced by 35.69-fold. This is significantly different from induction of *CA9* expression in hypoxia alone ($p < 0.001$).

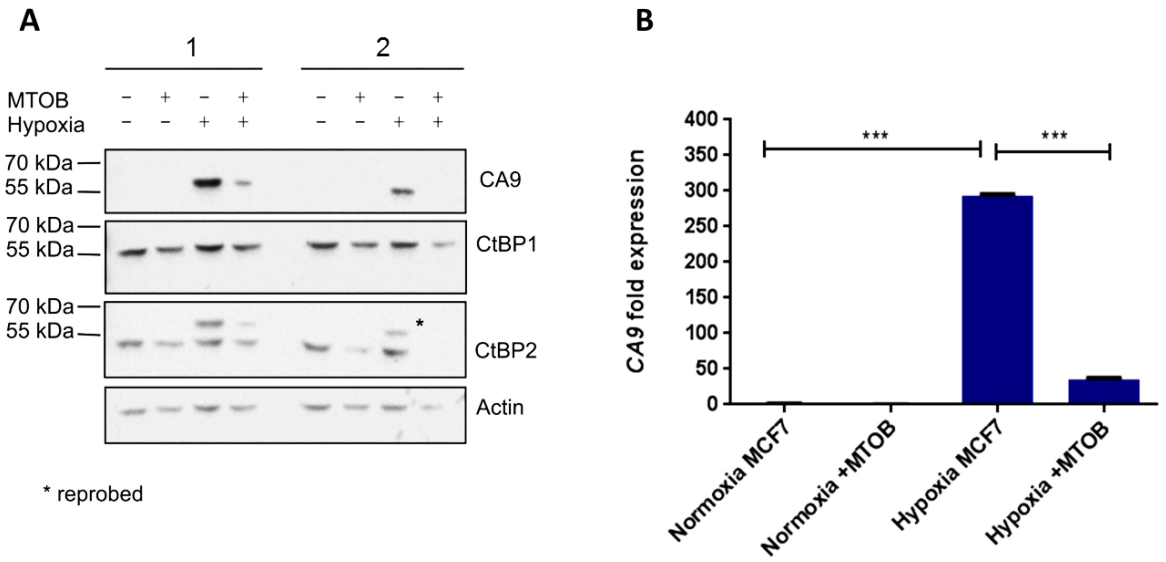

Fig. 4.12: MTOB reduces hypoxia-induced CA9 protein (A) and gene (B) expression in MCF7 breast cancer cells. Cells were plated at a concentration of $2.2x10^5$/ 2 ml in 6 well plates in complete DMEM. 24 h post-plating, cells were incubated with 4 mM MTOB. 48 h later, fresh MTOB was added and cells were transferred to either 1% or 20% O_2 and incubated for 18 h. Following the incubation in hypoxia or normoxia cells were immediately pelleted. **A:** The impact of MTOB on hypoxia-induced CA9 expression was determined by Western blot. The gel was loaded with 20 µg of whole cell lysate. Shown is one representative image displaying two out of three independent experiments. **B**: *CA9* gene expression was determined by TaqMan® quantitative reverse-transcription PCR. Expression was normalized to untreated cells in normoxia and statistical significance was determined by Fisher's uncorrected LSD test. Shown are the means of three independent experiments and their SEM.

Turning now to the impact of MTOB on the broader HIF-1 response, it was determined that CtBPs potentially play a role in the regulation of *CA9* and other HIF-1 target genes as MTOB reduces the hypoxia-induced expression of the HIF-1 target genes included in this study (Fig. 4.13).

The hypoxia-induced expression of the HIF-1 target genes *EGLN3* ($p < 0.001$), *PDK1* ($p < 0.001$), *FAM162A* ($p < 0.001$), *TMEM45A* ($p < 0.001$) and *INSIG2* ($p < 0.001$) is significantly different from expression in normoxia (Fig. 4.13). In hypoxia, *EGLN3* expression is induced by 8.69-fold (± 0.56) and is significantly reduced by 4.19-fold (± 0.76) ($p = 0.002$) in MCF7 treated with MTOB, compared to untreated MCF7 in hypoxia. The hypoxia-induced expression of *FAM162A* is 12.06-fold (± 1.41). The treatment with MTOB significantly reduces *FAM162A* expression in hypoxia by 5.66-fold (± 1.42) ($p = 0.002$). *PDK1* expression is increased by 10.44-fold (± 0.14) in hypoxic MCF7 cells. This upregulation of gene expression is significantly different from expression in normoxia ($p < 0.001$). In MCF7 treated with MTOB, hypoxia-induced *PDK1* expression is significantly reduced to 2.76-fold (± 0.40) ($p < 0.001$). *INSIG2* is upregulated in hypoxia by 7.13-fold (± 1.17) which is significantly different from expression in normoxia ($p < 0.001$). In MCF7 treated with MTOB, the hypoxia-induced expression of *INSIG2* is significantly reduced by 2.49-fold (± 0.98) ($p = 0.003$). The hypoxia-induced expression of *TMEM45A* is 42.37-fold (± 0.74) which is significantly different from induction of gene expression in normoxia ($p < 0.001$). In MCF7 treated with 4 mM MTOB, hypoxia-induced expression is 10.19-fold (± 0.94). This reduction in hypoxia-induced *TMEM45A* expression is significant ($p < 0.001$).

The results described above contrast to the findings generated for the treatment with CtBP 1/2 siRNA as MTOB reduces the expression of all HIF-1 target genes. This raises the question whether MTOB has negative off-target effects. Consequently, these data have to be interpreted with caution.

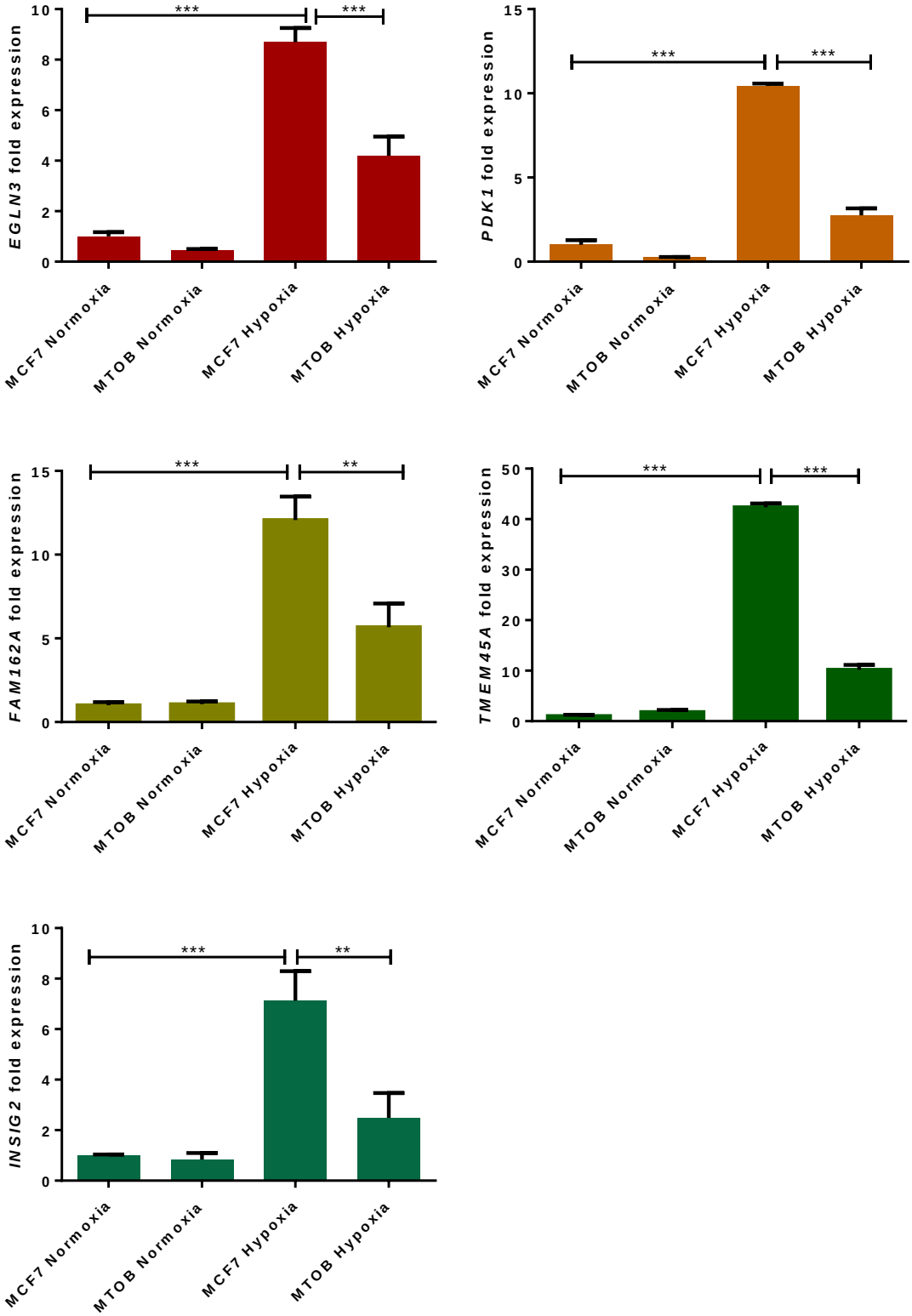

Fig. 4.13: MTOB reduces hypoxia-induced HIF-1 target gene expression in MCF7 breast cancer cells. Cells were plated at a concentration of $2.2x10^5$/ 2 ml in 6 well plates in complete DMEM. 24 h post-plating, cells were incubated with 4 mM MTOB. 48 h later, fresh MTOB was added and cells were transferred to either 1% or 20% O_2 and incubated for 18 h. Following the incubation in hypoxia or normoxia, cells were immediately pelleted. HIF-1 *target* gene expression was determined by semi-quantitative reverse-transcription PCR. Expression was normalized to untreated cells in normoxia and statistical significance was determined by Fisher's uncorrected LSD test. Shown are the means of three independent experiments and their SEM.

4.5.3 CtBP overexpression increases hypoxia-induced HIF-target gene expression

The role of CtBPs in the regulation of HIF-1 target gene expression was experimentally determined in MCF7 cells which were engineered by members of the Blaydes group to either express an empty control vector (MCF7.Control) or to overexpress wild-type CtBP2 (MCF7.CtBP2). The third MCF7–derived cell line (MCF7.CtBP-Mutant) expresses CtBPs exhibiting mutations in the dehydrogenase domain which hinders dimerization of CtBP monomers, and thus activation of CtBPs (section 2.1.1).

CA9 protein expression was determined by Western blot, whereas *CA9* mRNA expression levels were evaluated by TaqMan® quantitative reverse-transcription PCR. In three independent experiments, CA9 protein expression is increased in hypoxia, when either wildtype CtBP2 was overexpressed or when cells were expressing mutated CtBP (Fig. 4.14A). Similarly, *CA9* gene expression is significantly increased in cells overexpressing wildtype CtBP2 ($p < 0.001$) or expressing mutant CtBP ($p = 0.006$). In MCF7.Control cells, *CA9* is significantly induced in hypoxia by 199.5-fold (± 21.97), compared to MCF7.Control cells grown in normoxia ($p = 0.03$). Hypoxia increases *CA9* gene expression by 624.0-fold (± 106.2), when wildtype CtBP2 was overexpressed. This increase in CA9 expression compared CA9 expression in hypoxic MCF7.Control cells is significant ($p < 0.001$). Overexpression of mutant CtBP causes an upregulation of *CA9* in hypoxia by 465.2-fold (± 87.27) which is also significantly different from CA9 expression in hypoxic MCF7.Control cells ($p = 0.006$) (Fig. 4.14B).

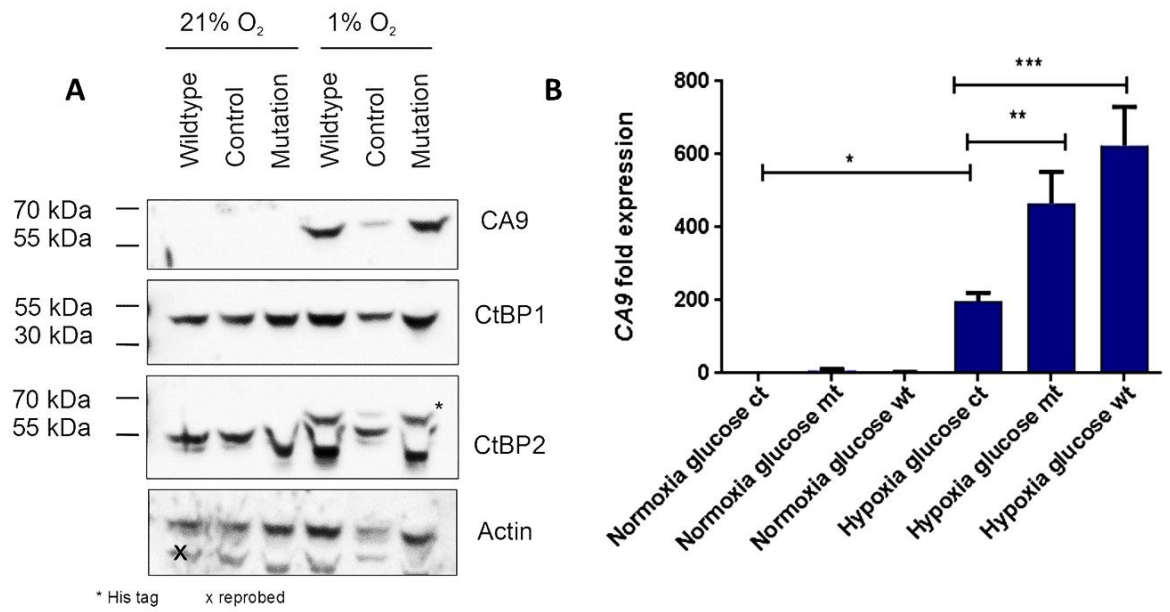

Fig. 4.14: Overexpression of wildtype CtBP2 increases hypoxia-induced CA9 protein (A) and gene (B) expression in glucose-adapted MCF7.CtBP2 and MCF7.CtBP-Mutant cells. MCF7.CtBP2 and MCF7.CtBP-Mutant cells were plated at a concentration of $2.2x10^5$/ 2 ml in 6 well plates in DMEM that was prepared in house and supplemented with 25 mM glucose. 48 h post-plating, medium was renewed and cells were grown at 1% or 20% O_2 for 18 h. **A**: CA9 protein expression was evaluated by Western blot. Gels were loaded with 20 µg whole cell lysate. Displayed is one representative image of three independent repeats. **B**: *CA9* gene expression was determined by TaqMan® quantitative reverse-transcription PCR. Expression was normalized to MCF7.Control cells in normoxia and statistical significance was determined by Fisher's uncorrected LSD test. Shown are the means of three independent experiments and their SEM.

Evaluating the impact of CtBP expression on the wider HIF-1 response, altered CtBP expression in hypoxia has no impact on *EGLN3* and *FAM162A* expression, whereas the overexpression of wildtype CtBP2 increases the hypoxia-induced expression of *TMEM45A* (Fig. 4.15). In MCF7 expressing mutant CtBP, the hypoxia-induced expression of *PDK1*, *TMEM45A* and *INSIG2* is increased compared to cells expressing the empty control vector. Elaborating these results in greater detail, *EGLN3* is significantly induced in MCF7.Control cells in hypoxia by 4.35-fold (± 0.60) ($p = 0.007$). In MCF7.CtBP2 cells, hypoxia-induction of *EGLN3* is 6.06-fold (± 1.11). In MCF7.CtBP-Mutant cells, hypoxia-induced expression of *EGLN3* is 5.84-fold (± 1.22). The difference in *EGLN3* expression in hypoxia between MCF7.Control and cells expressing CtBP variants is not significant (Fig. 4.15).

Hypoxia induction of *PDK1* in MCF7.Control cells is 6.52-fold (± 1.0) and is significantly different from expression in normoxia ($p = 0.005$). In MCF7.CtBP2 cells, *PDK1* is induced in hypoxia by 8.88-fold (± 2.00). In MCF7.CtBP-Mutant cells, *PDK1* is upregulated in hypoxia by 10.10-fold (± 1.53). There is no significant difference between MCF7.Control and MCF7.CtBP2 cells in hypoxia-induced *PDK1* expression. However, the difference in *PDK1* induction between MCF7.Control and MCF7.CtBP-Mutant cells is significant ($p = 0.04$). In MCF7.Control cells, *FAM162A* is upregulated in hypoxia by 7.24-fold (± 1.73) which is a significant difference in gene expression, compared to *FAM162A* expression in normoxia ($p = 0.014$). In wildtype CtBP2 overexpressing MCF7, *FAM162A* induction in hypoxia is 10.28-fold (± 2.73). Further, in MCF7.CtBP-Mutant cells *FAM162A* is induced in hypoxia by 9.73-fold (± 1.90). There is no significant difference in induction of *FAM162A* expression between MCF7.Control and MCF7.CtBP2 and MCF7.Control and MCF7.CtBP-Mutant cells.

TMEM45A is significantly upregulated upon exposure to hypoxia in MCF7.Control cells by 7.19-fold (± 0.81), compared to *TMEM45A* expression in normoxia ($p = 0.05$). In wildtype CtBP2 overexpressing cells, *TMEM45A* is induced in hypoxia by 14.37-fold (± 3.55). In hypoxia, *TMEM45A* is upregulated by 19.41-fold (± 3.10), in mutant CtBP expressing MCF7. Induction of *TMEM45A* expression by hypoxia is significantly different between MCF7.Control cells and MCF7.CtBP2 cells ($p = 0.02$) and between MCF7.Control and MCF7.CtBP-Mutant cells ($p < 0.001$). *INSIG2* is significantly induced by 4.52-fold (±0.48) in hypoxic MCF7.Control cells, compared to cells grown in normoxia ($p = 0.05$). In MCF7.CtBP2, *INSIG2* expression is upregulated in hypoxia by 7.29-fold (± 1.89). *INSIG2* is upregulated in hypoxia by 10.68-fold (± 1.95) in MCF7.CtBP-Mutant cells, the difference in hypoxia-induced *INSIG2* expression between MCF7.Control and MCF7.CtBP2 cells is not significant whereas the difference between MCF7.Control and MCF7.CtBP-Mutant is ($p = 0.002$).

Summarizing the results described above, these results suggest that CtBPs differentially regulate HIF-1 target gene expression in hypoxia and that the regulation of *EGLN3* and *FAM162A* expression is independent from the regulation by CtBPs.

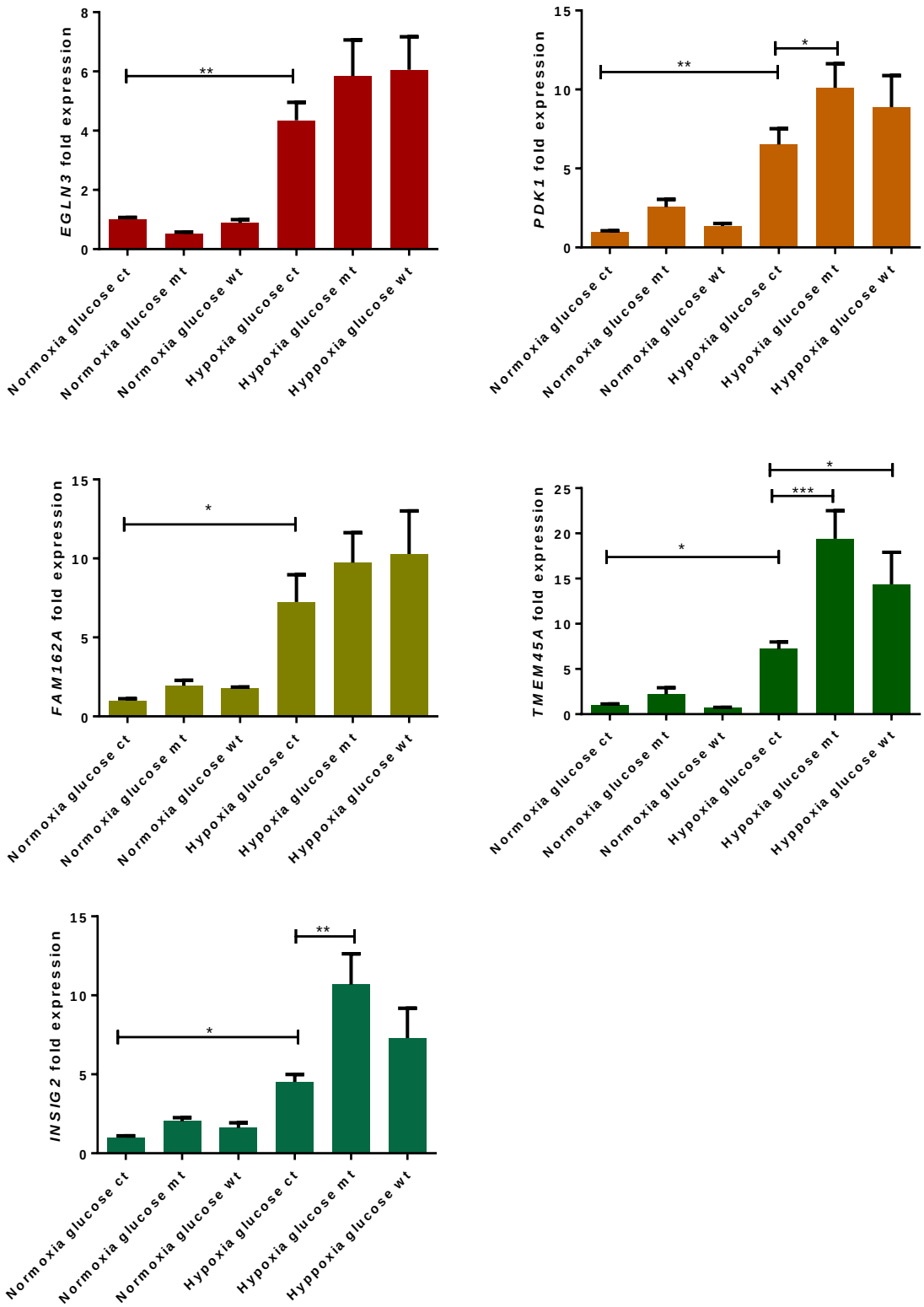

Fig. 4.15: Overexpression of wildtype CtBP2 increases the hypoxia-induced expression of *PDK1*, *TMEM45A* and *INSIG2*. MCF7.Control, MCF7.CtBP2 and MCF7.CtBP-Mutant cells were plated at a concentration of $2.2x10^5$/ 2 ml in 6 well plates in DMEM that was prepared in house and supplemented with 25 mM glucose. 48 h post-plating, medium was renewed and cells were incubated at either 1% or 20% O_2 for 18 h. HIF-1 target gene expression was determined by semi-quantitative reverse-transcription PCR. Expression was normalized to MCF7.Control cells in normoxia and statistical significance was determined by Fisher's uncorrected LSD test. Shown are the means of three independent experiments and their SEM.

4.6 DMOG-induced HIF-target genes are regulated by CtBPs

The following section addresses the question whether the hypoxia-induced HIF-target genes regulated by CtBP expression are induced by HIF. Therefore, hypoxia was replaced by DMOG as described in section 4.3.1.

4.6.1 Transfection with CtBP-targeting siRNA differentially impacts DMOG-induced HIF-1 target gene expression

CA9 protein expression is induced by DMOG in three independent repeats (Fig. 4.16A). DMOG-induced CA9 expression is reduced when CtBP expression was inhibited by siRNA. Similarly, DMOG induces the expression of *CA9* by 362.0-fold (± 36.91). This is significantly different from the expression of *CA9* in MCF7 transfected with non-silencing siRNA (Fig. 4.16B) ($p < 0.001$). In MCF7 transfected with CtBP-targeting siRNA, DMOG-induced *CA9* expression is upregulated by 256.5-fold (± 38.68). This difference in DMOG-induced *CA9* expression is significant ($p = 0.01$). Therefore, the activating role for CtBPs in CA9 protein and gene expression is potentially mediated by HIF-1.

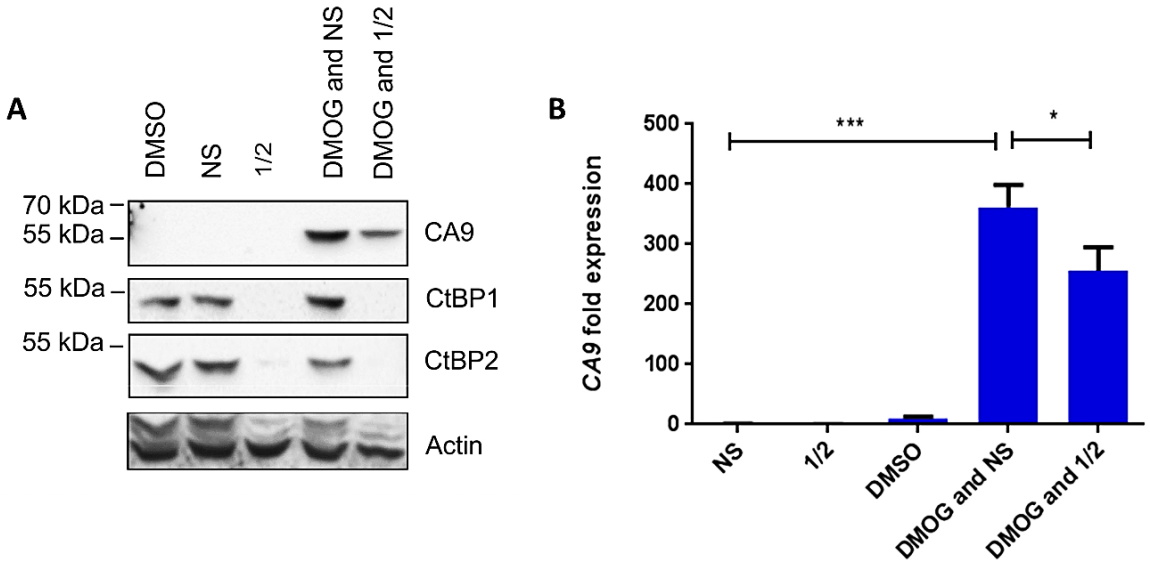

Fig. 4.16: Inhibition of CtBP expression reduces DMOG-induced CA9 protein (A) and mRNA (B) expression. MCF7 breast cancer cells were plated at a concentration of $2.2x10^5$/ 2 ml in complete DMEM. 24 h post-plating, cells were transfected with 50 nM non-silencing or CtBP 1/2 siRNA or left untreated. 48 h later, cells were incubated with either 1 mM DMOG or 0.1% DMSO for 18 h. **A**: CA9 and CtBP protein expression was determined by Western blot. Shown is one representative image of three independent experiments. Gels were loaded with 20 µg whole cell lysate. **B**: *CA9* gene expression was determined by TaqMan® reverse-transcription PCR. *CA9* expression was normalised to normoxic cells transfected with non-silencing siRNA and statistical significance was determined by Fischer's uncorrected LSD test. Shown are the means of three independent experiments and their SEM.

In order to determine whether the hypoxia-induced HIF-target genes which are differentially impacted by CtBP expression are induced by HIF, the samples from the same experiment were also analysed for the expression of *EGLN3*, *PDK1*, *FAM162A*, *TMEM45A* and *INSIG2* (Fig. 4.17).

The inhibition of CtBP expression by siRNA differentially affects the DMOG-induced expression of the HIF-1 target genes analysed in this experiment. Inhibited CtBP expression decreases DMOG-induced *EGLN3* and *PDK1* expression, whereas the expression of *TMEM45A* is increased. There is no effect on *FAM162A* and *INSIG2* expression.

In greater detail, *EGLN3* is induced by DMOG by 16.50-fold (± 3.17) in MCF7 transfected with non-silencing siRNA. This is significantly different from *EGLN3* expression in untreated MCF7 transfected with non-silencing siRNA ($p < 0.001$). In MCF7 transfected with CtBP 1/2 siRNA, the DMOG-induced expression of *EGLN3* is reduced by 9.80-fold (± 3.16). This difference in *EGLN3* induction is significant ($p = 0.04$). Further, DMOG significantly induces *PDK1* expression by 2.97-fold (± 1.95) in MCF7 transfected with non-silencing siRNA, compared to *PDK1* expression in untreated MCF7 transfected with non-silencing siRNA ($p < 0.001$). In MCF7 transfected with CtBP 1/2 siRNA, *PDK1* induction by DMOG is decreased by 15.59-fold (± 1.98) which is significantly different from DMOG-induced *PDK1* expression in MCF7 transfected with non-silencing siRNA ($p = 0.02$). DMOG-induced *FAM162A* expression is 10.67-fold (± 1.88) in MCF7 transfected with non-silencing siRNA. Therefore, *FAM162A* expression in these cells is significantly different from MCF7 transfected with non-silencing siRNA which were not treated with DMOG ($p = 0.001$).

In MCF7 transfected with CtBP 1/2 siRNA, the DMOG-induced expression of *FAM162A* is 14.38-fold (± 2.77) and does not significantly differ from the DMOG-induced expression of *FAM162A* in MCF7 transfected with non-silencing siRNA. DMOG-induced expression of *TMEM45A* is upregulated by 14.47-fold (± 2.20) in MCF7 transfected with non-silencing siRNA and is therefore significantly different from MCF7 which were not treated with DMOG ($p < 0.001$). In MCF7 transfected with CtBP 1/2 siRNA, DMOG induces *TMEM45A* expression by 22.02-fold (± 1.81). This difference in *TMEM45A* induction is significant ($p = 0.002$). *INSIG2* is upregulated by DMOG by 3.65-fold (± 0.41), in MCF7 transfected with non-silencing siRNA. This difference in *INSIG2* expression between DMOG-treated and untreated MCF7 transfected with non-silencing siRNA is significant ($p < 0.001$). In MCF7 treated with CtBP 1/2 siRNA, *INSIG2* expression is 3.96-fold (± 0.52) which is an insignificant change in *INSIG2* induction. Consequently, HIF-1 target genes are differentially regulated by the interaction between CtBP and HIF-1.

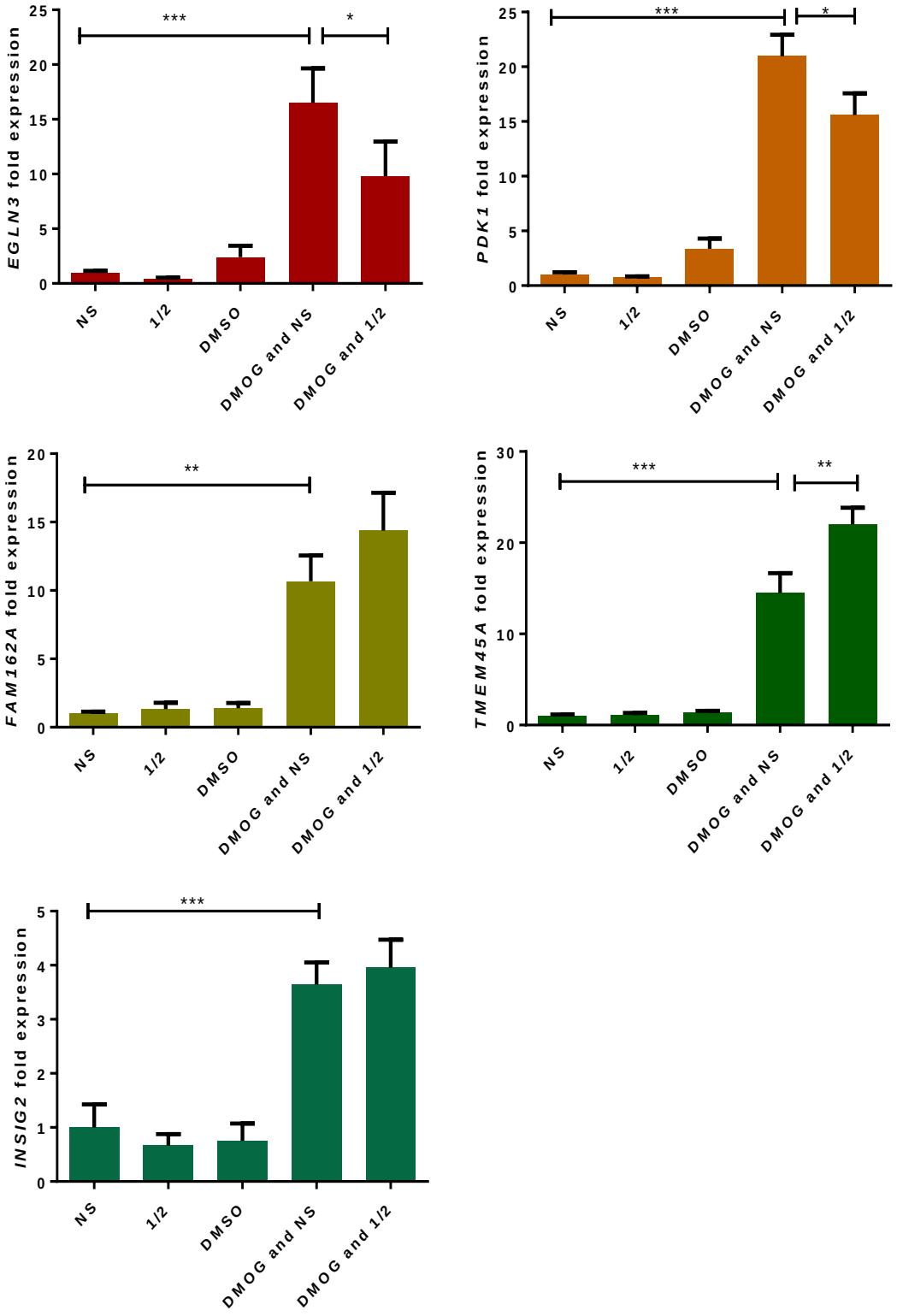

Fig. 4.17: DMOG-induced expression of *EGLN3* and *PDK1* is decreased whereas the expression of TMEM45A is increased when CtBP expression was inhibited by transfection with CtBP 1/2 siRNA. MCF7 breast cancer cells were plated at a concentration of $2.2x10^5$/ 2 ml in 6 well plates in complete DMEM. 24 h post-plating cells were transfected with 50 nM of either non-silencing siRNA or CtBP 1/2 siRNA. 48 h later cells were incubated with either 1 mM DMOG or 0.1% DMSO for 18 h. HIF-1 target gene expression was determined by semi-quantitative reverse-transcription PCR. Expression was normalized to normoxic cells transfected with non-silencing siRNA in normoxia and statistical significance was determined by Fisher's uncorrected LSD test. Shown are the means of three independent experiments and their SEM.

4.6.2 MTOB reduces DMOG-induced HIF-1 target gene expression

As an alternative way to determine whether the regulation of HIF-1-target genes by CtBPs is dependent on HIF-1, CtBP activity was inhibited by 4 mM MTOB. CA9 protein expression induced by DMOG is reduced in three independent experiments in MTOB-treated MCF7 breast cancer cells (Fig. 4.18A). *CA9* gene expression is induced by DMOG by 128.0-fold (± 7.13) and is therefore significantly different from *CA9* expression in untreated MCF7 ($p < 0.001$). The treatment with MTOB reduces *CA9* expression by 22.25-fold. This strong reduction in *CA9* induction is significant ($p < 0.001$) (Fig. 4.18B).

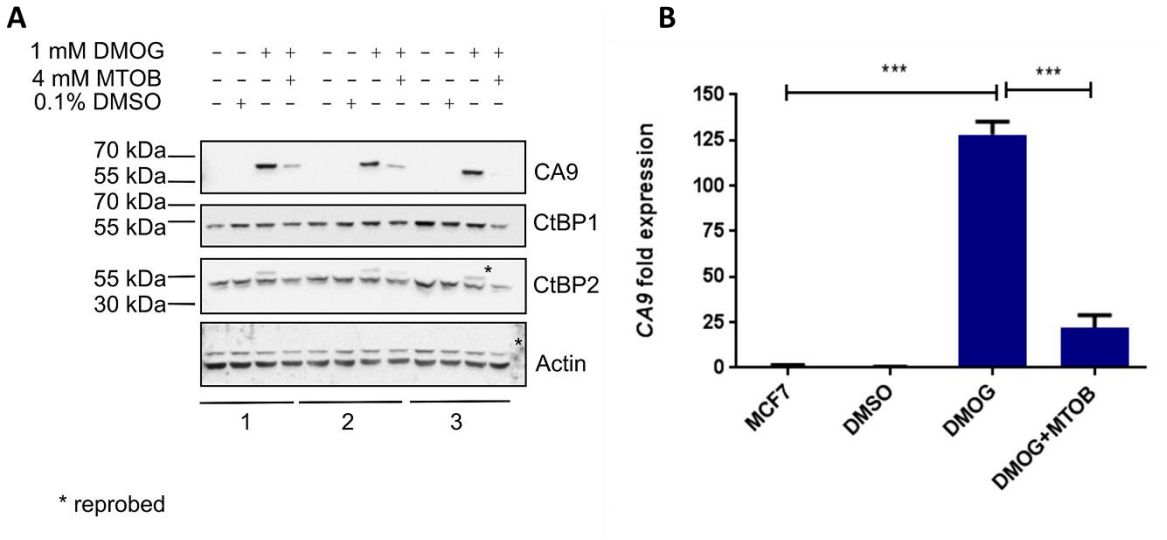

Fig. 4.18: MTOB reduces the DMOG-induced expression CA9 protein (A) and gene (B). MCF7 breast cancer cells were plated at a concentration of $2.2x10^5$/ 2 ml in complete DMEM. 24 h post-plating cells were incubated with 4 mM MTOB. 72 h post-plating MTOB was renewed and cells were additionally incubated with either 1 mM DMOG or 0.1% DMSO at 20% O_2 for 18 h. CA9 protein expression was determined by Western blot in three independent experiments. Gels were loaded with 20 µg whole cell lysate. *CA9* gene expression was determined by TaqMan® quantitative reverse-transcription PCR. Expression was normalized to untreated cells and statistical significance was determined by Fisher's uncorrected LSD test. Shown are the means of three independent experiments and their SEM.

The inhibition of CtBP activity by MTOB inhibits the DMOG-induced expression of all HIF-1 target genes analysed in this experiment (Fig. 4.19). DMOG induces the expression of *EGLN3, PDK1*, *FAM162A*, *TMEM45A* and *INSIG2*. In all cases, DMOG-induced gene expression is significantly different from expression in untreated MCF7 ($p < 0.001$) (Fig. 4.19).

Induction of *EGLN3* by DMOG is 18.97-fold (± 2.68). In cells which were additionally treated with MTOB induction is reduced by 9.33-fold (± 2.1). This is significantly different from *EGLN3* expression in MCF7 treated with DMOG alone ($p = 0.004$). *PDK1* expression is upregulated by DMOG by 19.01-fold (± 1.27). The inhibition of CtBPs by MTOB reduces *PDK1* expression by 3.78-fold (± 0.78). The difference in *PDK1* expression in MCF7 treated with DMOG and MCF7 treated with MCF7 and MTOB is significant ($p < 0.001$). *FAM162A* is induced by DMOG by 16.78-fold (± 1.74). In MCF7 additionally treated with MTOB, *FAM162A* expression is decreased by 5.60-fold (± 1.13). This reduction in DMOG-induced *FAM162A* expression in MTOB-treated cells compared to expression in MCF7 treated with DMOG alone is significant ($p < 0.001$).

TMEM45A is increased by 32.72-fold (± 2.86) in cells treated with DMOG. MTOB inhibited DMOG-induced *TMEM45A* expression as it is reduced to 11.38-fold (± 2.20). This difference in gene expression is significant ($p < 0.001$). In MCF7 breast cancer cells, the treatment with DMOG induces the expression of *INSIG2* by 16.27-fold (± 0.60). In cells that were additionally incubated with MTOB, induction of *INSIG2* expression is significantly reduced to 1.61-fold (± 0.48) ($p < 0.001$).

Therefore, these results contrast to findings obtained from inhibiting CtBP expression by siRNA. Similarly, as already described for the treatment with hypoxia and MTOB, this raises the question whether the impact of MTOB on HIF-1 target genes is non-specific.

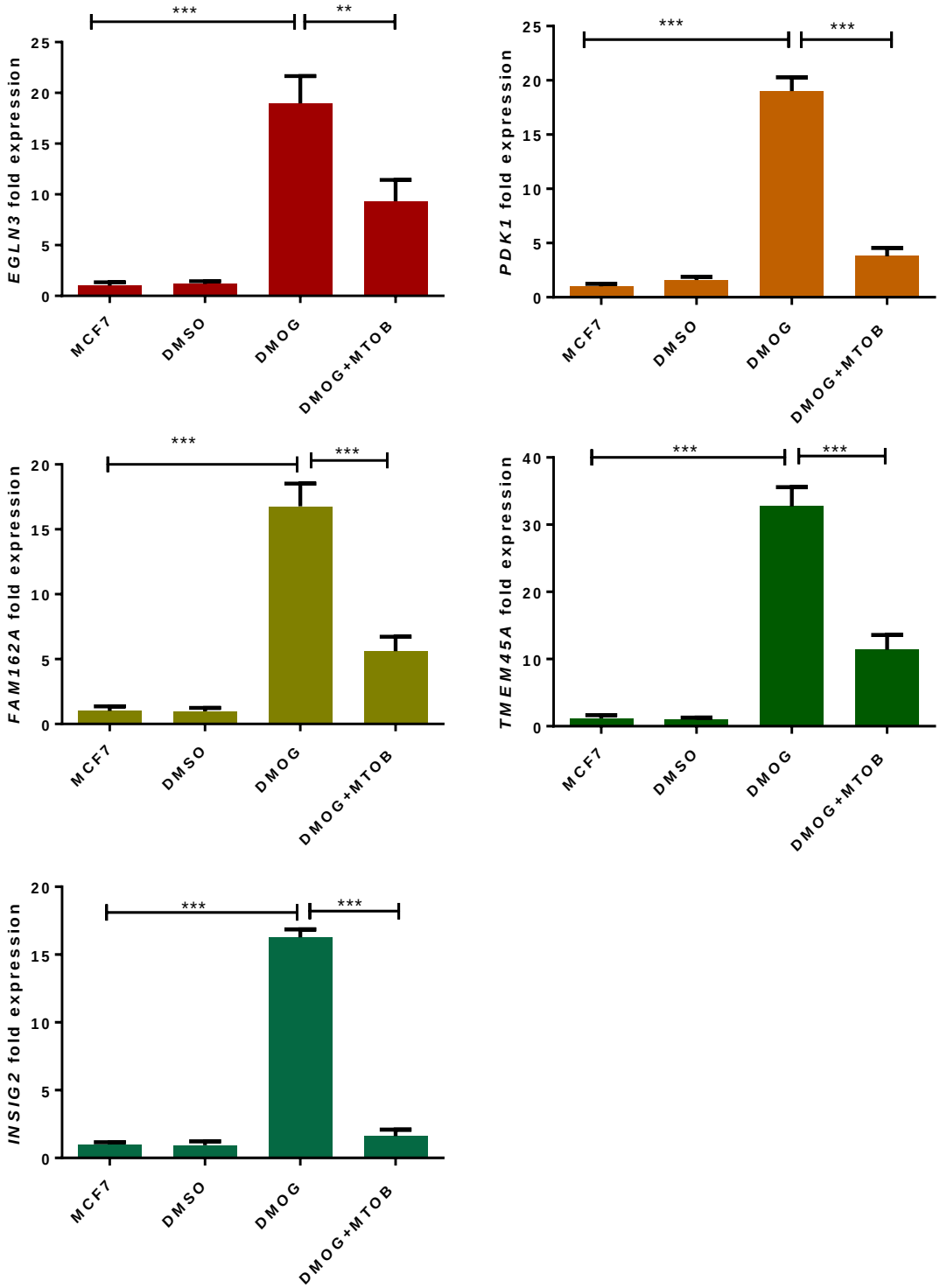

Fig. 4.19: MTOB reduces the DMOG-induced expression of HIF-target genes in MCF7 breast cancer cells. Cells were plated at a concentration of 2.2x10^5/ 2 ml in 6 well plates in complete DMEM. 24 h post-plating cells were incubated with 4 mM MTOB. 48 h later, fresh MTOB was added and cells were transferred to either 1% or 20% O_2 and incubated for 18 h. Following the incubation in hypoxia or normoxia cells were immediately pelleted. HIF-1 *target* gene expression was determined by semi-quantitative reverse-transcription PCR. Expression was normalized to untreated cells in normoxia and statistical significance was determined by Fisher's uncorrected LSD test. Shown are the means of three independent experiments and their SEM.

4.6.3 Overexpression of CtBPs increases HIF-1 target gene expression induced by DMOG

To further determine the impact of CtBPs on the HIF-1-mediated regulation of CA9 expression, CA9 expression was induced by DMOG in MCF7.Control, MCF7.CtBP2, and MCF7.CtBP-Mutant cells grown in glucose-containing medium. In three independent experiments, DMOG-induced CA9 protein expression is increased in cells overexpressing wildtype CtBP2 or mutant CtBP, compared to CA9 expression in MCF7.Control cells (Fig. 4.20A). Therefore, CtBPs potentially regulate CA9 protein expression in a HIF-1-dependent manner. Similar conclusions can be drawn on the mRNA level as induction of *CA9* expression by DMOG is lower in these cells than in cells overexpressing wildtype CtBP2 or mutant CtBP (Fig. 4.20B). In empty vector control cells, *CA9* is induced by 127.0-fold (± 39.56) and therefore *CA9* expression is significantly different from MCF7.Control cells left untreated ($p = 0.009$). In cells overexpressing wildtype CtBP2, *CA9* is induced by DMOG by 577.2-fold (± 70.02) and in mutant CtBP expressing cells DMOG-induced expression of *CA9* is 434.7-fold (± 36.00). Both, the difference in *CA9* expression between MCF7.Control and MCF7.CtBP2 cells, and the difference between MCF7.Control and MCF7.CtBP-Mutant are significant ($p < 0.001$).

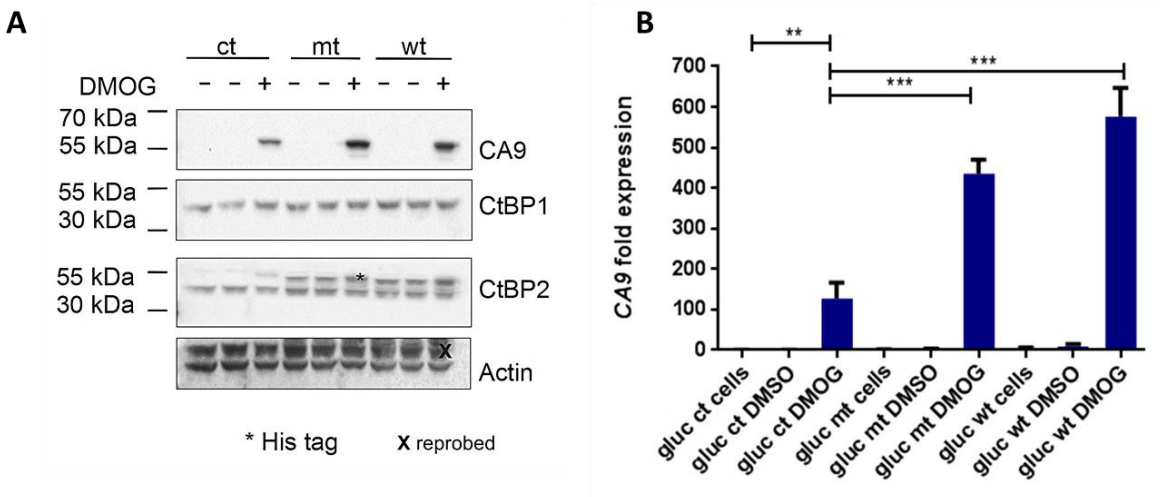

Fig. 4.20: Overexpression of wildtype CtBP2 (wt) and mutant CtBP (mt) increases the DMOG-induced expression of CA9 protein (A) and gene (B) compared to empty vector expressing cells (ct) in glucose adapted MCF7 cells. MCF7.Control, MCF7.CtBP2 and MCF7.CtBP-Mutant cells were plated at a concentration of $2.2x10^5$/ 2 ml in 6 well plates in DMEM that was prepared in house and supplemented with 25 mM glucose. 48 h post-plating, medium was renewed and cells were grown in 1 mM DMOG or 0.1% DMSO for 18 h. **A:** CA9 protein expression was evaluated by Western blot. Gels were loaded with 20 µg whole cell lysate. Displayed is one representative image of three independent repeats. **B**: *CA9* gene expression was determined by TaqMan® quantitative reverse-transcription PCR. Expression was normalized to untreated MCF7.Control cells in normoxia and statistical significance was determined by Fisher's uncorrected LSD test. Shown are the means of three independent experiments and their SEM.

To further determine the impact of CtBPs on the HIF-1 mediated regulation of the broader HIF-1 target genes response, analysis was extended on the other HIF-1 target genes included in this study (Fig. 4.21). It was determined that the expression of *EGLN3*, *PDK1*, *FAM162A* and *INSIG2* is induced by DMOG in MCF7.Control cells. The expression of mutant CtBP leads to an increase in the expression of all HIF-1 target genes analysed in this experiment but the overexpression of wildtype CtBP2 only significantly upregulates the DMOG-induced expression of *EGLN3*, *FAM162A*, *TMEM45A* and *INSIG2.*

Analysing the results in detail, in MCF7.Control cells, *EGLN3* is induced by DMOG by 4.75-fold (± 2.29), and is therefore significantly different from expression in untreated cells ($p < 0.001$). In MCF7.CtBP-Mutant cells, the DMOG-induced upregulation of *EGLN3* is 10.36-fold (± 0.61). DMOG-induced *EGLN3* expression is increased by 10.90-fold (± 0.70) in MCF7.CtBP2 cells. Altered CtBP expression by either overexpressing wildtype CtBP2 or by expressing mutant CtBP significantly increases DMOG-induced *EGLN3* expression in both cases, compared to expression in MCF7.Control ($p < 0.001$). DMOG induces *PDK1* by 6.3-fold (± 1.31) in MCF7.Control cells which is significantly different from *PDK1* expression in untreated MCF7.Control cells ($p < 0.001$). In MCF7.CtBP-Mutant cells, *PDK1* is upregulated by 9.65-fold (± 1.17). The DMOG-induced upregulation of *PDK1* is 8.51-fold (± 1.21), when wildtype CtBP2 was overexpressed. There is a significant difference in DMOG-induced *PDK1* expression between MCF7.Control and MCF7.CtBP-Mutant cells ($p = 0.008$). There is no significant difference between MCF7.Control and MCF7.CtBP2 cells.

FAM162A is induced by 6.42-fold (± 1.44) in MCF7.Control cells treated with DMOG, and therefore *FAM162A* expression is significantly different from expression in untreated MCF7.Control cells ($p = 0.006$). In MCF7.CtBP-Mutant cells, *FAM162A* is increased by DMOG by 9.97-fold (± 2.34). In MCF7.CtBP2 cells, DMOG-induced *FAM162A* expression is 10.90-fold (± 2.16). The difference in expression in MCF7.Control and MCF7.CtBP-Mutant is not significant, whereas the overexpression of wildtype CtBP2 significantly increases the expression of *FAM162A* compared to MCF7.Control cells ($p = 0.002$).

The upregulation of *TMEM45A* by DMOG by 4.15-fold (± 0.81) in MCF7.Control is not significantly different from *TMEM45A* expression in untreated MCF7.Control cells. In MCF7.CtBP-Mutant cells, *TMEM45A* is induced by 14.66-fold (± 3.08). In MCF7.CtBP2 cells, *TMEM45A* is upregulated by 19.07-fold (± 3.08). The difference in DMOG-induced *TMEM45A* expression is significant when mutant CtBP was expressed ($p < 0.001$), and when wildtype CtBP2 was overexpressed ($p < 0.001$). *INSIG2* is upregulated by 2.82-fold (± 0.59) in MCF7.Control cells treated with DMOG. This change in *INSIG2* expression is not significant ($p = 0.06$). In MCF7.CtBP-Mutant cells, DMOG-induced

INSIG2 expression is 7.13-fold (± 1.42). In MCF7.CtBP2, DMOG-induced *INSIG2* expression is 7.5-fold (± 0.89). The difference in *INSIG2* expression between MCF7.Control and MCF7.CtBP-Mutant ($p < 0.001$) as well as the difference between MCF7.Control and MCF7.CtBP2 cells is significant ($p < 0.001$). Consequently, the results described above further support the potential role for CtBPs in the HIF-1 mediated regulation of target genes.

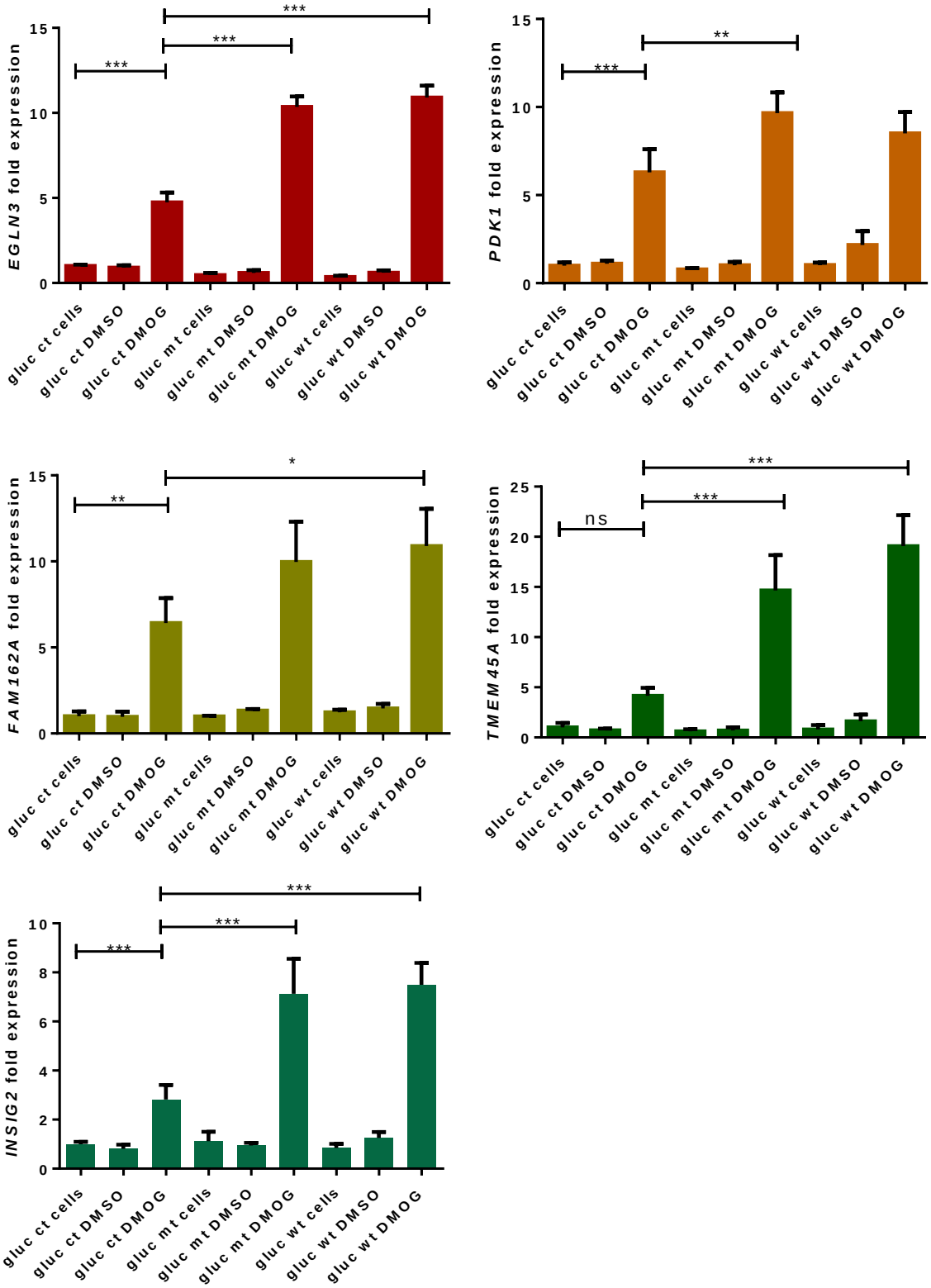

Fig. 4.21: Overexpression of wildtype CtBP2 and mutant CtBP upregulates the DMOG-induced expression of HIF-1 target genes. MCF7.Control, MCF7.CtBP2 and MCF7.CtBP-Mutant cells were plated at a concentration of $2.2x10^5$/ 2 ml in DMEM prepared in house from powder and supplemented with 25 mM glucose. 72 h post-plating cells were incubated in either 1 mM DMOG or 0.1% DMSO or DMEM alone for 18 h. The expression of HIF-1 target genes was determined by semi-quantitative real-time PCR. Expression was normalized to untreated MCF7.Control cells in normoxia and statistical significance was determined by Fisher's uncorrected LSD test. Shown are the means of three independent experiments and their SEM.

4.7 Dissecting the mechanism of interaction between CtBPs and HIF-1

Chromatin immunoprecipitation was performed in order to understand how CtBPs and HIF-1 interact at the *CA9* promoter to upregulate *CA9* expression in hypoxia. Immunoprecipitation with anti-CtBP and anti-HIF-1 antibodies was carried out to evaluate whether CtBPs and HIF-1 directly interact at the *CA9* promoter whereas immunoprecipitation with an anti-RNA polymerase II antibody should confirm the activation of *CA9* expression. However, due to technical difficulties there was no immunoprecipitation detected; neither in MCF7 treated with hypoxia nor with DMOG. Therefore, all results and optimisation steps performed for chromatin immunoprecipitation are discussed in Appendix B.

Tab. 4.3: In MCF7, CA9 is specifically regulated in a HIF-1-glycolysis-dependent manner via the activation of C-terminal binding proteins.

	Induction by hypoxia	Impact of siRNA	Impact of MTOB	Overexpression of wildtype CtBP2	Induction by DMOG	Impact of siRNA	Impact of MTOB	Overexpression of wildtype CtBP2
CA9	Yes	Reduced	Reduced	Increased	Yes	Reduced	Reduced	Increased
EGLN3	Yes	No impact	Reduced	No impact	Yes	Reduced	Reduced	Increased
PDK1	Yes	Reduced	Reduced	No impact	Yes	Reduced	Reduced	No impact
FAM162A	Yes	No impact	Reduced	No impact	Yes	No impact	Reduced	Increased
TMEM45A	Yes	No impact	Reduced	Increased	Yes	Increased	Reduced	No impact
INSIG2	Yes	Reduced	Reduced	No impact	Yes	No impact	Reduced	Increased

4.8 HIF-1 target genes are differentially regulated by CtBPs- summary

In MCF7 breast cancer cells, hypoxia-induced CA9 protein and gene expression is reduced when cells were either treated with CtBP 1/2 siRNA or MTOB, and it is increased when wildtype CtBP2 was overexpressed in MCF7.CtBP2 cells. These findings are reproduced when hypoxia was replaced by DMOG. Consequently, it is argued that *CA9* expression is regulated by glycolysis via the activation of CtBPs (Tab. 4.3) and that this interaction is mediated by HIF-1. Further, CtBP 1/2 siRNA reduces hypoxia-induced *CA9* expression in MDA-MB-231 cells. However, induction of gene expression is low in this cell line. Moreover, there is no impact of CtBP 1/2 siRNA on the other HIF-1 target genes analysed in this experiment. Therefore, MDA-MB-231 cells were excluded from further experiments.

In MCF7, the modification of CtBP expression has controversial effects on the expression of other HIF-1 target genes. *EGLN3* appears not to be regulated by CtBPs in hypoxia, whereas the incubation in DMOG causes upregulation of *EGLN3* in MCF7.CtBP2. The same is true for *FAM162A*. The modification of CtBP expression has no impact on *PDK1* expression whereas the impact on *TMEM45A* and *INSIG2* expression is inconclusive. Consequently, the CtBP and HIF-1 mediated regulation of gene expression is specific for *CA9*. In order to determine the nature of interaction between CtBP and HIF-1 at the *CA9* promoter, ChIP was performed with inconclusive results.

After it was successfully determined that *CA9* expression is specifically regulated by glycolysis via the activation of CtBPs and in a HIF-1-dependent manner, the role of this interaction in CA9-mediated survival of hypoxia-induced acidosis was assessed by colony forming assay.

4.9 Hypoxia-induced glycolysis regulates *CA9* expression via the activation of CtBPs- summary of Chapter 4

This chapter aimed to further determine the role of CtBPs in the regulation of *CA9* expression by hypoxia-induced glycolysis, and whether other HIF-1 target genes are regulated in a similar fashion. Consequently, HIF-1 target genes which showed at least a 3-fold difference in gene expression in the preliminary gene expression study (discussed in chapter 3) were included in the study and were analysed by semi-quantitative reverse-transcription PCR.

Induction of *CA9* expression in hypoxia requires upregulated glycolysis, as inhibition by either 2-DG or growth in fructose decreases hypoxia-induced *CA9* expression on the protein and mRNA level. This activating role of glycolysis is dependent on HIF-1 as demonstrated by specific activation of HIF-1 in normoxia by DMOG, and is potentially mediated by CtBPs as the treatment with MTOB and siRNA inhibited hypoxia- and DMOG-induced expression of CA9 gene and protein expression. However, a direct interaction of HIF-1 and CtBPs at the *CA9* promoter to induce transcription of the *CA9* gene could not be demonstrated due to technical difficulties with chromatin immunoprecipitation.

Investigating the broader hypoxia-response, it was found that hypoxia-induced expression of all HIF-1 target genes is reduced in fructose-grown MC7, whereas the treatment with 2-DG has no impact. Hypoxia-induced expression of all genes is HIF-1 specific as their expression is induced by DMOG. However, the treatment with DMOG increases the susceptibility to 2-DG as the expression of *EGLN3*, *FAM162A* and *TMEM45A* is inhibited in DMOG-treated, but not in hypoxia-treated cells. Consequently, all target genes except from *INSIG2* and *FAM162A* are regulated in a HIF-1-glycolysis-dependant manner. However, the role for CtBPs in the glycolysis-dependent activation of gene expression is unique for *CA9*. It was established that CtBPs potentially couple glycolysis with the hypoxia-induced expression of *CA9* in a HIF-dependent manner. Consequently, it was the next step to determine whether this interaction supports CA9-mediated survival of hypoxia-induced acidosis which is discussed in the next chapter.

Chapter 5: CtBPs promote CA9-mediated survival of hypoxia-induced acidosis in MCF7 breast cancer cells with transient silencing of p53 expression

Thus far this thesis argues that CA9 is potentially regulated by glycolysis via the activation of CtBPs, and that this activation is dependent on HIF-1. This suggests a novel activating role for CtBPs in the regulation of CA9. Consequently, it was investigated next whether this proposed interaction supports breast cancer cell survival in hypoxia-induced acidosis.

5.1 Introduction

5.1.1 Extracellular acidification exerts a strong selection pressure on tumour cell populations

Extracellular acidity in tumours is modulated by the diffusion distance to the closest blood vessel and the metabolic rate (Gatenby et al. 2007) as well as by ion transport across the outer cell membrane (Hulikova et al. 2011). Diffusion distance to the blood vessel plays a major role in intratumoural acidity as many tumours are insufficiently perfused. Further, glycolysis and pentose phosphate pathway are commonly upregulated in cancer cells (Helmlinger et al. 2002; Reitzer et al. 1979; Warburg 1924). This leads to the accumulation of glycolysis-derived lactate and protons during ATP breakdown and of CO_2 generated in the pentose phosphate pathway (Helmlinger et al. 2002). The extrusion of these acidic metabolites to regulate pH_i is strongly affected by pH_e as passive and active ion transport along the cell membrane is inhibited when pH_e is low (Vaughan-Jones & Wu 1990). Therefore, the regulation of both pH_i and pH_e is crucial for cancer cell survival and an appropriate pH sensing and regulating machinery provides cancer cell populations with a selective advantage (Gatenby et al. 2007).

The regulation of pH_i includes the transport of ions across the cell membrane by acid loading and acid extruding transporter proteins. Acid extruding proteins such as Na^+/H^+ exchangers of the SLC4 family or hypoxia-responsive monocarboxylate transporters including MCT4 passively extrude H^+ or H^+-lactate respectively along a gradient. CO_2 freely diffuses out of the cell along a concentration gradient. Acid loading proteins include H^+-ATPase pumps, transporters which produce net bicarbonate influx such as the electroneutral Na^+-HCO_3^- co-transporter NBCn1 (SLC4A7), the electrogenic Na^+-$2HCO_3^-$ co-transporter SLC4A4 or the Na^+-dependent Cl^-/HCO_3^- exchanger SLC4A8 (reviewed by (Swietach et al. 2014)). The active extrusion of H^+ along electrochemical NA^+ or Cl^- gradients remains an energetic burden of already exhausted tumour

cells. Therefore, H^+ extrusion and HCO_3^--transport back into the cell are of central importance in tumour cells exhibiting exhausted buffering capacities (Hulikova et al. 2011; Parks et al. 2016). CA9 catalyses the reaction of CO_2 and H_2O into HCO_3^- and H^+ at the cell surface, and therefore plays a crucial role in pH regulation within tumours and in the interplay between pH_i and pH_e buffer systems (Chiche et al. 2009, Parks & Pouyssegur 2015). Hypoxia-induced upregulation of glycolysis is discussed as one major driving force of intratumoural acidification. Consequently, HIF-1 also induces the expression of pH-regulating genes such as *CA9* (Grabmaier et al. 2004). CA9 is overexpressed in many different cancer types and correlates with poor prognosis (Tan et al. 2009; Wykoff et al. 2000). Importantly, CA9 strongly contributes to the acidification of the extracellular space by generating H^+ (Švastová et al. 2004).

Therefore, the reuptake of CA9-generated bicarbonate into the cell to maintain a physiological pH_i is of crucial importance. This was demonstrated by (Hulikova et al. 2013) who showed that the cell type-specific activity of NHEs is inhibited in hypoxia, whereas the Na^+-dependent co-transport of bicarbonate is constitutive and hypoxia-resistant. The role of CA9-generated bicarbonate reuptake is further highlighted by the finding that the NA^+ / HCO_3^- co-transporter SLC4A4 is co-induced with CA9 in 1% oxygen. The inhibition of SLC4A4 by siRNA also reduces CA9 expression and further leads to impaired pH_i recovery in MDA-MB-231 breast cancer cells (Parks & Pouyssegur 2015). (McIntyre et al. 2016) confirmed the HIF-dependent induction of SLC4A4 expression and also identified SLC4A9 as HIF-target in a broad panel of human cancer cell lines. Conversely, blocking the import of bicarbonate produced by CA9 by inhibiting SLC4A4 and SLC4A9 leads to intracellular acidification and impaired cell growth in cancer cell spheroids. The treatment of spheroids with a small molecule inhibitor of sodium-driven bicarbonate transporters induces apoptosis. Additionally, silencing of SLC4A9 induces apoptosis in spheroids of MDA-MB-231 breast cancer cells and impairs growth of MDA-MB-231 xenografts in mice.

The targeting of pH_e by raising the buffering capacity with bicarbonate showed promising anti-tumour effects as the oral administration of bicarbonate reduces invasion of colon cancer in mice by increasing pH_e (Estrella et al. 2013). Moreover, bicarbonate increases pH_e in tumours and reduces spontaneous metastases in murine models of metastatic breast cancer (Robey et al. 2009). The studies described above highlight the importance of low pH_e as selection pressure on tumour cell populations, resulting in the selection of populations with appropriate pH sensing and regulating machinery. The dependence of tumours on transporting CA9-generated bicarbonate back into the cell to prevent intracellular acidification is therefore a promising therapeutic approach. Importantly, the targeting of hypoxia-inducible bicarbonate transporters or of CA9 is a more tumour-specific approach than targeting Na^+/H^+ exchangers as hypoxia is commonly and almost specifically found in tumours but not in healthy tissues, whereas NHEs are ubiquitously

expressed. However, pH regulating systems are versatile and tumour cells may compensate the blocking of one pH regulator by upregulating another (Parks et al. 2016). Therefore, further research is required to evaluate the pH regulating machinery as therapeutic target.

It is widely established that, by upregulating the expression of glycolytic enzymes, hypoxia contributes to extracellular acidity within tumours. However, a potential protective role for hypoxia-induced glycolysis is less well defined. (Parks et al. 2013) demonstrated that hypoxia protects cancer cells from acidosis-mediated cell death by conserving ATP levels. This protective effect is reversed when glycolysis was inhibited with 2-DG. The treatment with oligomycin which inhibits mitochondrial respiration has no impact on cell viability in hypoxia and acidosis. Based on the work performed by (Parks et al. 2013), it was investigated whether CtBPs, activated by hypoxia-induced glycolysis, support the survival of breast cancer cells in hypoxia-induced acidosis via the activation of CA9.

5.1.2 Aim of this chapter

It was aimed to experimentally determine whether the activation of HIF-1-induced CA9 expression by glycolysis-activated CtBPs supports the survival of MCF7 breast cancer cells in hypoxia-induced acidosis.

5.1.3 Overview over this chapter

It was planned to determine the role of glycolysis-activated CtBPs and CA9 in the survival of breast cancer cells of hypoxia-induced acidosis by following the experimental procedures described by (Parks et al. 2013). However, cells did not survive 48 h incubation in 1 mM DMOG. Therefore, experimental conditions were optimised to avoid incubation times in hypoxia exceeding 24 h. First, titration assays were performed to identify suitable cell concentrations for plating cells for colony forming assays.

In the next step, optimum incubation times in hypoxia and at pH 6.3 were determined. The outcome of these experiments resulted in an incubation time in hypoxia for 24 h followed by 24 h at pH 6.3 in normoxia. In this light, CA9 expression in re-oxygenation was determined as well as the impact of acidosis on the induction of CA9 expression in normoxia. Based on these preliminary data, it was decided to incubate MCF7 with transient knockdown of CtBPs for 24 h in 1% O_2, followed by 24 h at pH 6.3 in normoxia. However, it was demonstrated that CtBP expression has no impact on survival. Therefore, the role of p53 expression in the protection from acidosis-mediated cell death was determined in MCF7 and MDA-MB-231. The outcome of these results led to the final experimental set up. MCF7 breast cancer cells were transfected with combinations of

CtBP 1/2 siRNA, p53 siRNA and CA9 siRNA or individual siRNAs. First, transfected MCF7 were incubated in hypoxia for 24 h to induce CA9 expression, followed by 24 h at pH 6.3 to mimic hypoxia-induced acidosis. The impact of p53, CtBPs and CA9 on long-term survival was determined by colony forming assays.

5.2 Optimisation

As outlined above, the original experiment that was performed to dissect the role of CtBP-activated CA9 in the survival of acidosis required optimisation. Therefore, experiments were performed to identify viable experimental conditions. Findings of these experiments are outlined below.

5.2.1 Titration of cell numbers

First, it was aimed to determine an appropriate cell concentration to seed in the colony forming assay, and to test the impact of acidosis on long-term cell survival of MCF7. Based on colony densities displayed in Fig. 5.1, it was decided to seed cells at a concentration of $2x10^2/2$ ml in future experiments. However, the 5 h incubation time at either pH 7.4 or pH 6.3 was not long enough to detect differences on long-term viability. Therefore, it was decided to elongate the incubation time in bicarbonate-free medium to 7 h which also did not impact long-term viability (data not shown).

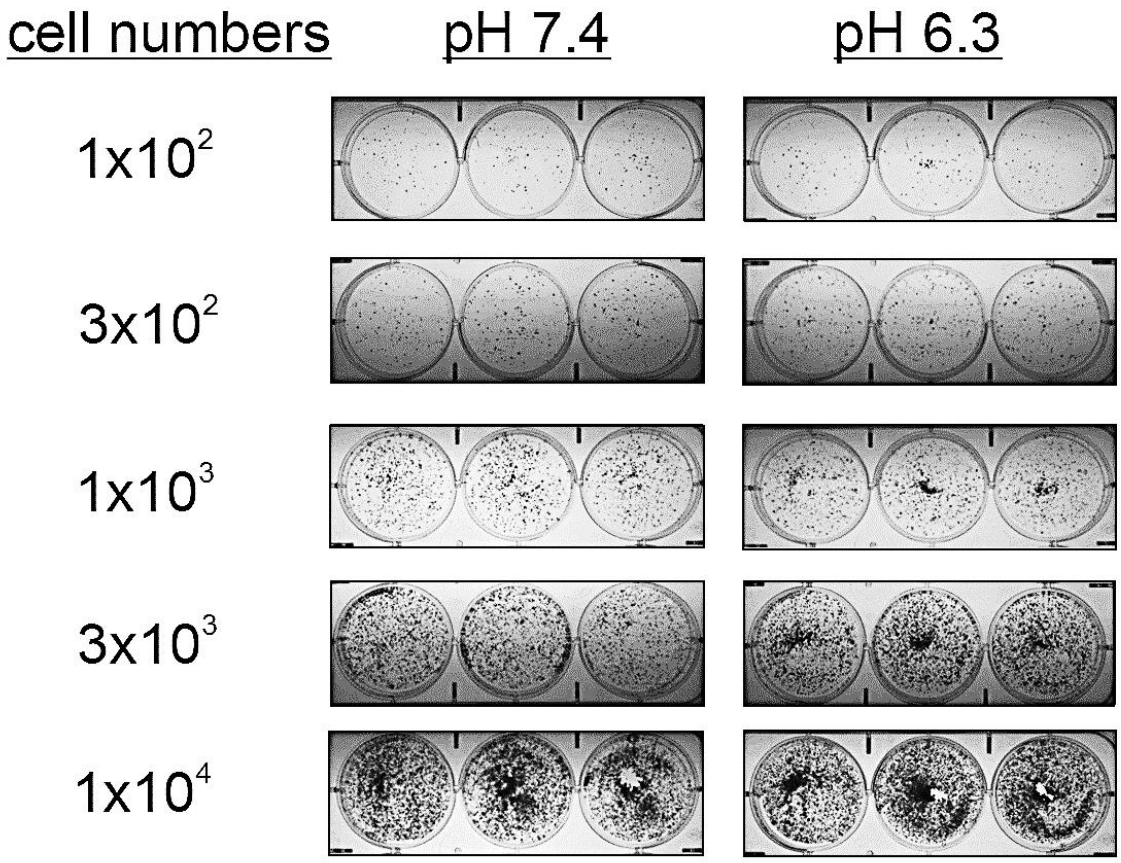

Fig. 5.1: Titration of MCF7 breast cancer cells to determine the concentration of MCF7 cells required for colony forming assay. On day 1, MCF7 breast cancer cells were plated in DMEM medium in 6 well plates in triplicates at a concentration of $2.2x10^5$ cells/ 2 ml. On day 2, MCF7 cells were incubated in bicarbonate-free medium at either pH 7.4 or at pH 6.3 in an air-buffered cell incubator for 5 h. Consequently, MCF7 were trypsinized and re-seeded in DMEM medium in 6 well plates at a concentration of $1x10^4$/ 2 ml, $1x10^3$/ 2 ml, $1x10^2$/ 2 ml or $3x10^3$/ 2 ml and $3x10^2$/ 2 ml by serial dilution. Cell numbers were plated in triplicates. After 10 days, colonies were visualised by crystal violet staining.

5.2.2 Identifying incubation times in hypoxia and acidosis

Following the evaluation of appropriate cell numbers to be plated for colony forming assay, optimum incubation times in hypoxia and acidosis was determined next. Therefore, two experiments were performed. In experiment 1, MCF7 with silenced CtBP expression were incubated in hypoxia for 18 h. Incubation in hypoxia was followed by 7 h or 24 h in pH-adjusted bicarbonate-free medium in 20% O_2. Alternatively, in experiment 2, transfected MCF7 were exposed to 1% O_2 for 48 h in total. After 18 h, DMEM was replaced by pH-adjusted bicarbonate-free medium. Cell viability was monitored by colony forming assays as described.

In experiment 1, CA9 is induced by hypoxia in untreated cells as well as in cells transfected with non-silencing control siRNA. As expected, CA9 protein expression is reduced by CtBP-targeting siRNA. Transfection with 1/2 siRNA successfully silences CtBP1 and CtBP2 expression (Fig. 5.2). Further, there is no difference in colony numbers between cells grown at either pH 6.3 or pH 7.4

for 7 h. There is only a minor increase in colony numbers in hypoxia at pH 6.3. The treatment with siRNA appears to reduce viability. However, O_2 levels and pH does not influence the number of colonies formed by cells transfected with non-silencing siRNA. Transfection with 1/2 siRNA on the other hand reduces colony numbers independent from O_2 levels and pH (Fig. 5.3 and Fig. 5.4). In cells incubated at either pH 7.4 or pH 6.3 for 24 h, there is no difference in numbers of colonies between normoxia and hypoxia at pH 7.4. However, at pH 6.3 there is an increase in colony numbers under hypoxia. At pH 7.4, CtBP 1/2 siRNA reduces cell viability in hypoxia but not in normoxia, whereas at pH 6.3, CtBP 1/2 siRNA reduces cell viability independent from O_2 levels (Fig. 5.5 and Fig. 5.6). Consequently, 24 h at pH 6.3 or pH 7.4 was chosen as time point for further experiments because there is a clear difference between normoxia and hypoxic samples at pH 6.3. However, the treatment with siRNA appears to have a bigger impact on viability than hypoxia. Additionally, the HIF-1-mediated induction of CA9 expression should have been confirmed by Western blot. This also accounts for all further Western blots showing CA9 expression.

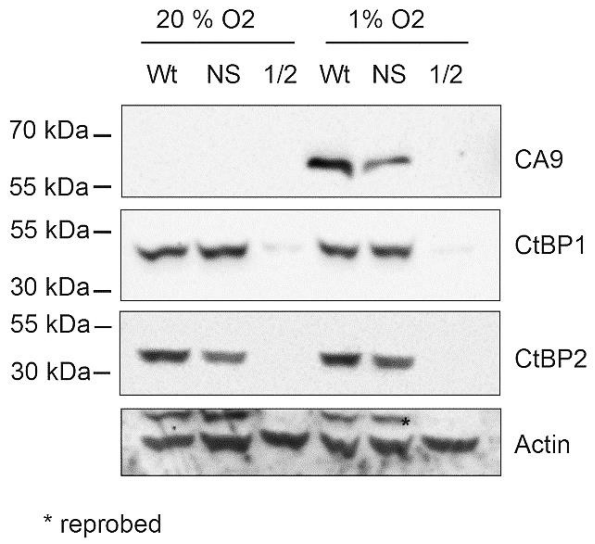

Fig. 5.2: Confirmation of CA9 induction and inhibition of CtBP 1/2 expression by siRNA. MCF7 breast cancer cells were plated at day 1 at a concentration of $2.2x10^5$/ 2 ml. The following day, cells were either transfected with 50 nM non-silencing control siRNA (NS), CtBP 1 and 2-targeting siRNA (1/2) or left untreated as control (wildtype: wt). 48 h post-transfection, cells were exposed to 1% or 20% O_2 for 18 h. Protein expression was analysed by Western blot and gels were loaded with 25 µg whole cell lysate.

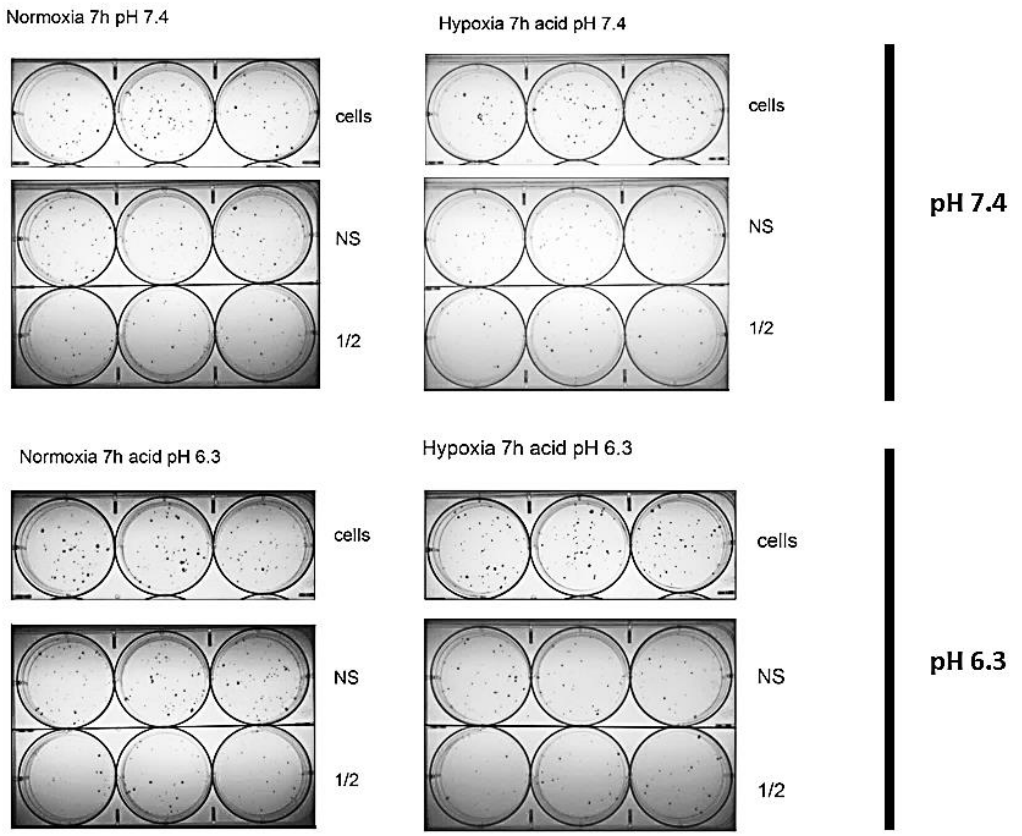

Fig. 5.3: Impact of hypoxia and low pH on long-term viability of MCF7 breast cancer cells. MCF7 breast cancer cells were transfected with 50 nM non-silencing control siRNA (NS) or CtBP1 and 2 targeting siRNA (1/2). Untreated cells were used as controls (cells). 48 h post-transfection, cells were either incubated at 1% O_2 or 20% O_2 for 18 h. Consequently, cells were incubated in bicarbonate-free medium for 7 h that was adjusted to either pH 7.4 or pH 6.3. For colony forming assay, cells were re-seeded in DMEM at a concentration of $2x10^2$/ 2 ml by serial dilution. 10 days post-plating, colonies were visualised by crystal violet staining. The experiment was performed in triplicates.

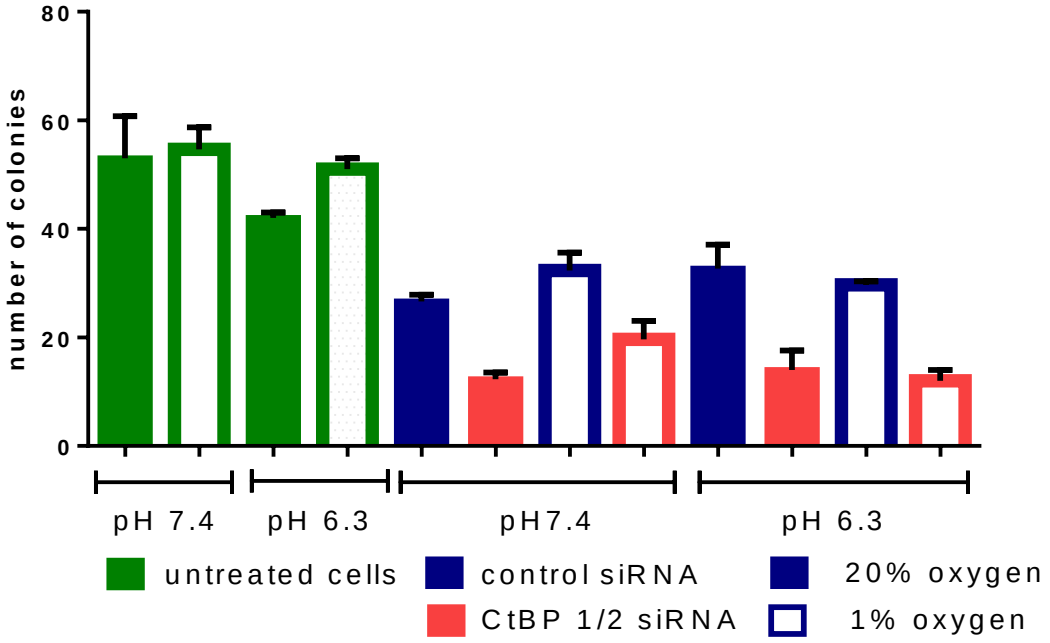

Fig. 5.4: Number of colonies counted after 18 h in hypoxia and 7 h in acidosis. MCF7 breast cancer cells were transfected with 50 nM non-silencing control siRNA (NS) or CtBP1 and 2 targeting siRNA (1/2). Untreated cells were used as controls (cells). 48 h post-transfection, cells were either incubated at 1% O_2 or 20% O_2 for 18 h. Consequently, cells were grown in bicarbonate-free medium for 7 h that was adjusted to either pH 7.4 or pH 6.3.To determine the impact of long-term viability, MCF7 were re-seeded in DMEM by serial dilution at a concentration of $2x10^2$/ 2 ml. 10 days post-plating, colonies were visualised by crystal violet staining. The experiment was performed in triplicates. Error bars represent the SEM. Colonies exceeding 50 cells were included in the count. Images of colonies stained with crystal violet (Fig. 5.3) were imaged and colonies were counted using the multiple cell count tool of the software ImageJ.

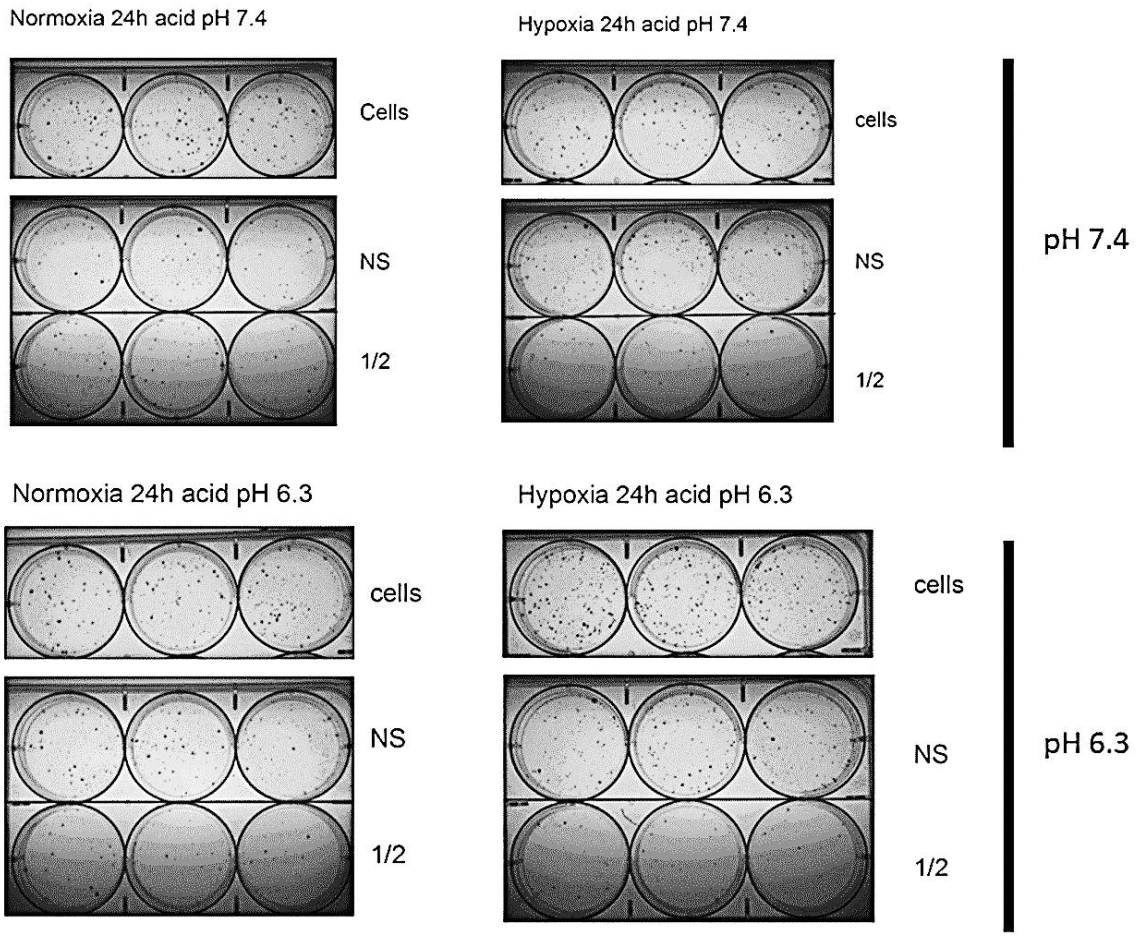

Fig. 5.5: Impact of hypoxia and low pH on long-term viability of MCF7 breast cancer cells. MCF7 breast cancer cells were transfected with 50 nM non-silencing control siRNA (NS) or CtBP1 and 2 targeting siRNA (1/2). Untreated cells were used as controls (cells). 48 h post-transfection, cells were either incubated at 1% O_2 or 20% O_2 for 18 h. Consequently, cells were grown in bicarbonate-free medium for 24 h that was adjusted to either pH 7.4 or pH 6.3. For colony forming assay, MCF7 were re-seeded in DMEM by serial dilution at a concentration of $2x10^2$/ 2 ml. 10 days post-plating, colonies were visualised by crystal violet staining. The experiment was performed in triplicates.

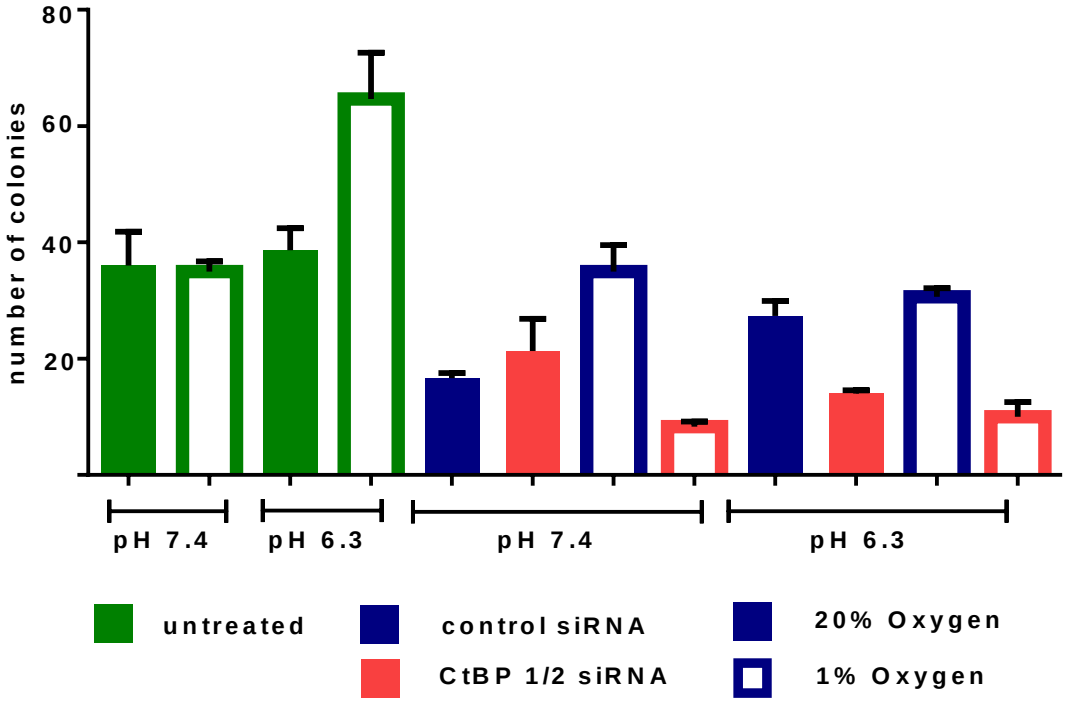

Fig. 5.6: Number of colonies counted after 18 h in hypoxia and 24 h at low pH. MCF7 breast cancer cells were transfected with 50 nM non-silencing control siRNA (NS) or CtBP1 and 2 targeting siRNA (1/2). Untreated cells were used as controls (cells). 48 h post-transfection, cells were either incubated at 1% O_2 or 20% O_2 for 18 h. Consequently, cells were grown in bicarbonate-free medium for 24 h that was adjusted to either pH 7.4 or pH 6.3. For colony forming assay, MCF7 were re-seeded in DMEM by serial dilution at a concentration of $2x10^2$/ 2 ml. 10 days post-plating, colonies were visualised by crystal violet staining. The experiment was performed in triplicates. Error bars show the SEM. Colonies exceeding 50 cells were included in the count. Images of colonies stained with crystal violet (Fig. 5.5) were imaged and colonies were counted using the multiple cell count tool of the software ImageJ.

Evaluating experiment 2, CA9 is induced by hypoxia and its expression is inhibited by CtBP 1/2 siRNA, as expected (Fig. 5.7). However, CA9 expression is negatively influenced by incubation at pH 6.3 for 24 h within total exposure time to hypoxia of 48 h. CtBP expression is not influenced by hypoxia and acidosis, and is successfully downregulated by CtBP 1/2 siRNA. Also, colonies could not be counted as transfected cells did not survive 48 h in hypoxia (Fig. 5.8). Therefore, unlike in (Parks et al. 2013), and based on the outcome of experiment 1, it was decided to incubate cells for 24 h at 1% O_2 to induce CA9, followed by the transfer into pH-adjusted bicarbonate-free medium for 24 h at 20% O_2.

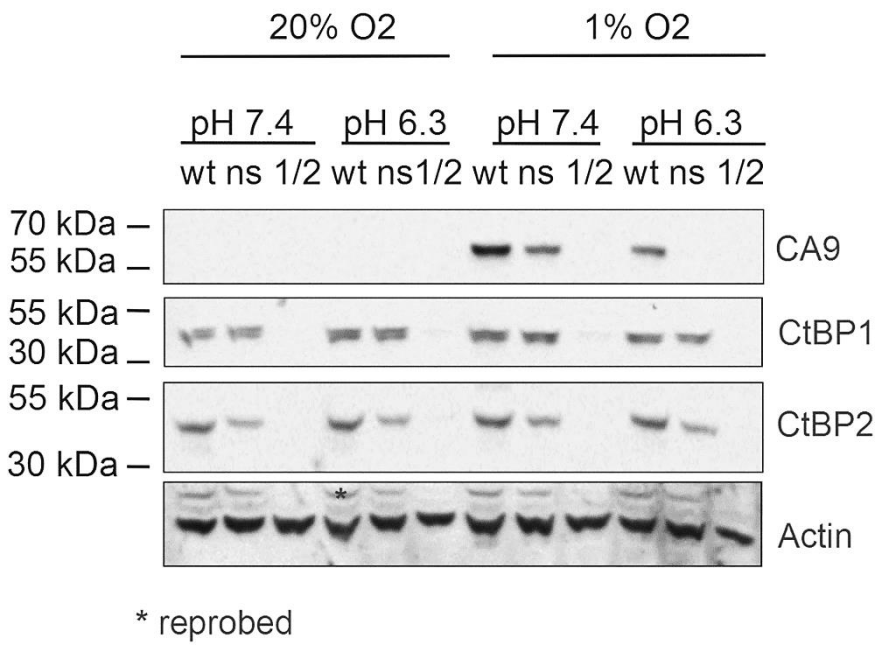

Fig. 5.7: Confirmation of CA9 induction and CtBP inhibition by 50 nM siRNA. MCF7 breast cancer cells transfected with 50 nM CtBP 1/2 siRNA or non-silencing control siRNA, or untreated MCF7 cells (wt) were incubated at either 1% or 20% O_2 for 24 h. Consequently, DMEM was quickly replaced with bicarbonate-free medium calibrated to either pH 7.4 or pH 6.3 and cells were transferred back into either 1% or 20% O_2 for another 24 h. Consequently, cells were harvested and lysed for protein analysis by Western blot. To confirm CA9 induction and downregulation of CtBP expression Western blot was performed with 25 µg whole cell lysate.

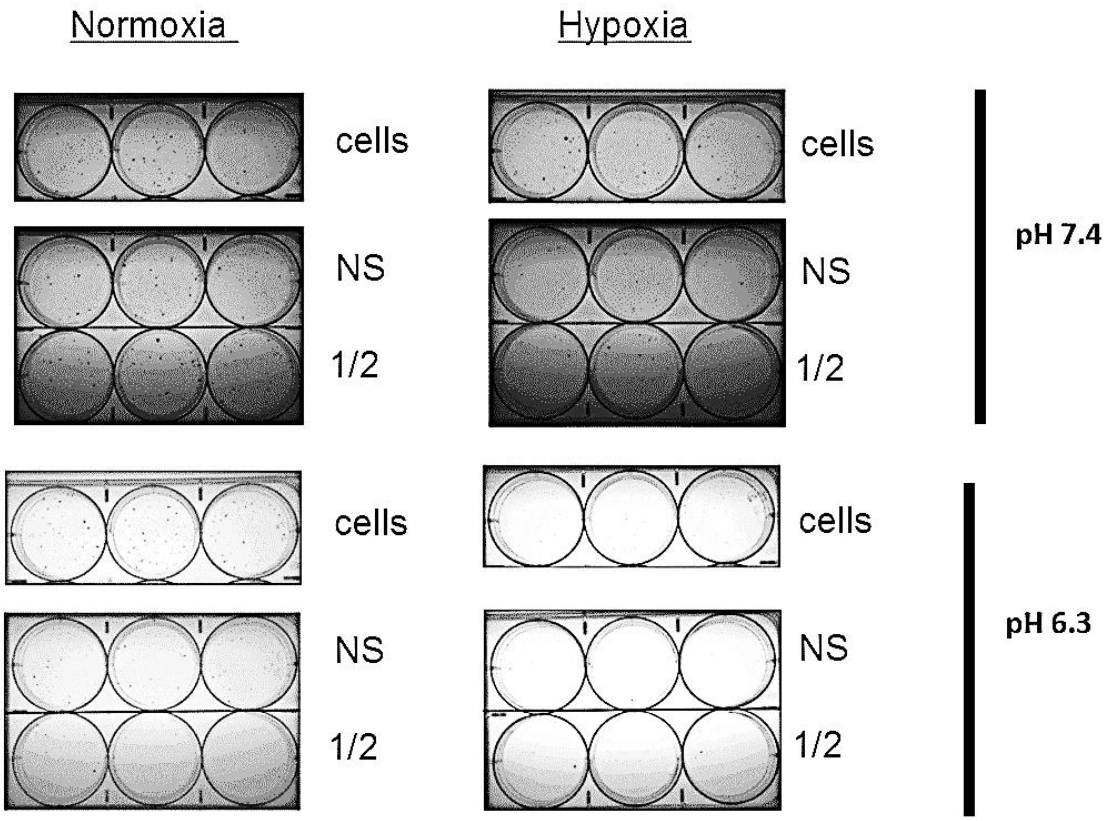

Fig. 5.8: Impact of 48 h hypoxia and 24 h low pH on long-term survival. MCF7 breast cancer cells were transfected with 50 nM non-silencing control siRNA (NS) or CtBP 1/2 siRNA. Untreated cells were used as controls (cells). 48 h post-transfection, cells were either incubated at 1% O_2 or 20% O_2 for 24 h. Consequently, medium was exchanged to bicarbonate-free medium adjusted to either pH 7.4 or pH 6.3 and cells were quickly transferred back into hypoxia for 24 h. The following day, MCF7 were re-seeded in DMEM by serial dilution at a concentration of $2x10^2$/ 2 to determine long-term survival. 10 days post-plating, colonies were visualised by crystal violet staining. The experiment was performed in triplicates.

5.2.3 CA9 protein is expressed 24 h post-re-oxygenation

In next step, the stability of CA9 expression post re-oxygenation was determined by incubating MCF7 in 1 % O_2 for 18 h, followed by 0 h, 2 h, 5 h, 7 h, and 24 h in 20% O_2. CA9 expression was determined by Western blot and TaqMan® quantitative reverse-transcription PCR. CA9 protein is still expressed after 24 h (Fig. 5.9A), but *CA9* mRNA is gradually degraded after re-oxygenation and was not detectable after 24 h (Fig. 5.9B). There is a highly significant difference between 0 h and all other time points ($p < 0.001$). These findings correspond with the literature where CA9 is described as a stable protein (Vordermark et al. 2005). As CA9 is still expressed after 24 h, it potentially remains functional even though *CA9* mRNA is rapidly degraded. Based on these findings, it was decided to incubate cells at pH 6.3 for 24 h at 20% O_2.

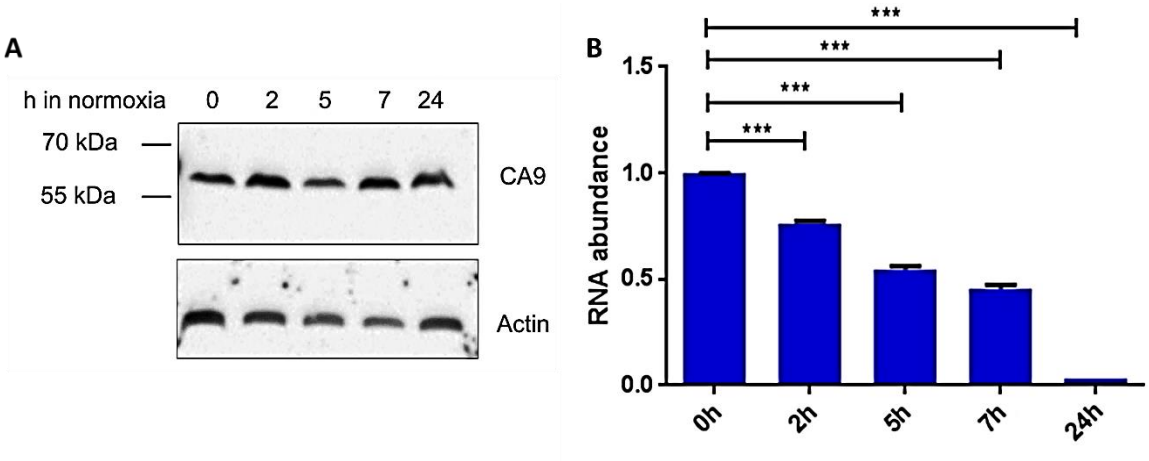

Fig. 5.9: CA9 protein (A) and mRNA (B) stability after re-oxygenation. MCF7 breast cancer cells were plated at a concentration of $6x10^5$/ 4 ml in 6 cm plates and transferred into hypoxia the following day. 18 h post-hypoxia, medium was exchanged and cells were either harvested immediately or 2 h, 5 h, 7 h or 24 h after re-oxygenation. CA9 protein stability was evaluated by Western blot. A 10% SDS gel was loaded with 20 µg whole cell lysate. To determine mRNA stability, TaqMan® quantitative reverse-transcription PCR was performed. Actin was used as housekeeping gene. Data were analysed by the comparative C_T method and expression was relative to the 0 h time point. Displayed are the mean of two duplicates and their SEM.

5.2.4 CA9 is not induced by acidosis in the presence of oxygen

(Ihnatko et al. 2006) suggested that low pH alone is sufficient to induce CA9 expression in glioblastoma cell lines independently from HIF-1. However, HIF-1 has an additive effect on *CA9* gene expression. In order to determine whether low pH at 20% O_2 is sufficient to induce *CA9* gene expression in MCF7 breast cancer cells, cells were incubated in bicarbonate-free medium at either pH 7.4 or pH 6.3 for 5 h, 7 h, 18 h and 24 h. Neither CA9 protein nor mRNA expression is induced at pH 6.3 (Fig. 5.10). Variations in *CA9* mRNA expression are potentially noise as the C_T values for CA9 are extremely low and partially outside of the limit of detection. Consequently, CA9 induction is hypoxia-dependent in MCF7 breast cancer cells which is contradictory to (Ihnatko et al. 2006) but confirms other literature findings (Grabmaier et al. 2004; Wykoff et al. 2000).

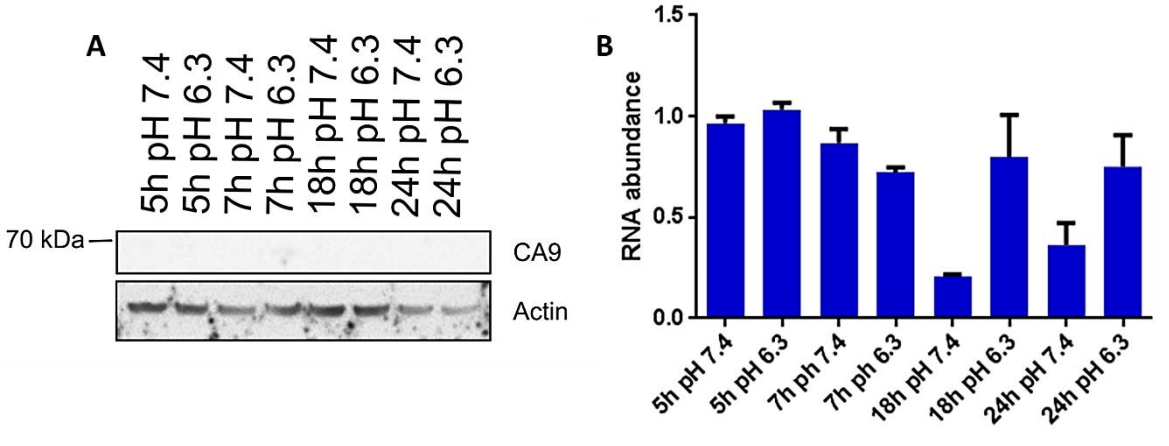

Fig. 5.10: CA9 is not induced by low pH in MCF7 breast cancer cells. To determine whether CA9 protein (A) or gene expression (B) is induced by low pH in normoxia, MCF7 cells were plated in DMEM at a concentration of $2.2x10^5$/ 2 ml in 6 well plates. 24 h later, cells were either transferred to bicarbonate-free medium at pH 7.4 or pH 6.3 for 5 h, 7 h, 18 h and 24 h. CA9 protein expression was determined by Western blot. A 10% SDS gel was loaded with 15 µg whole cell lysate. To determine *CA9* gene induction, TaqMan® quantitative reverse-transcription PCR was performed. Actin was used as housekeeping gene. Data were analysed by the comparative C_T method and expression was relative to the 5 h time point at pH 7.4. Displayed are the mean of two duplicates and their SEM.

5.2.5 The impact of CtBP expression on long-term survival of hypoxia-induced acidosis in MCF7 breast cancer cells

Following the optimisation steps performed earlier, the impact of CtBP expression on survival of acidosis was investigated in MCF7 as elaborated above. Transfection of MCF7 breast cancer cells with CtBP 1/2 siRNA successfully inhibits CtBP1 and CtBP2 protein expression as well as CA9 expression at 1% O_2 (Fig. 5.11). However, there is no difference in colony numbers between transfected or control cells at pH 7.4 and pH 6.3 in 1% or 20% O_2 (Fig. 5.12 and Fig. 5.13). However, epithelial cancer cells are able to induce wildtype p53 to promote survival of adverse conditions (Jackson et al. 2012; Rao et al. 2013; Bertheau et al. 2013). Further, (Parks et al. 2013) only used p53-negative cell lines in their experiments. MCF7 breast cancer cells express wildtype p53. Therefore, it was decided to inhibit p53 expression by transfection with siRNA in order to determine the role of p53 and CtBPs on survival of acidosis. To further determine the role of p53 and CtBPs in CA9-mediated survival of low pH it was also decided to transfect the p53-mutant breast cancer cell line MDA-MB-231 with CtBP 1/2- and CA9-targeting siRNA.

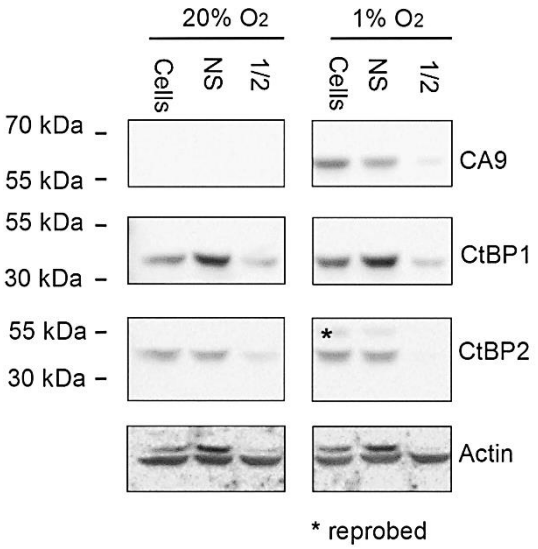

Fig. 5.11: Confirmation of the silencing of CtBP1 and CtBP2 expression following the transfection of MCF7 breast cancer cells with either 50 nM non-silencing control or CtBP 1/2- targeting siRNA. MCF7 breast cancer cells were transfected with 50 nM siRNA to determine the impact of CtBPs on CA9-mediated survival of hypoxia-induced acidosis. 48 h post-transfection, cells were transferred to either 20% or 1% O_2 for 18 h and were harvested for determination of protein expression by Western blot. 10% SDS gels were loaded with 20 µg whole cell lysate.

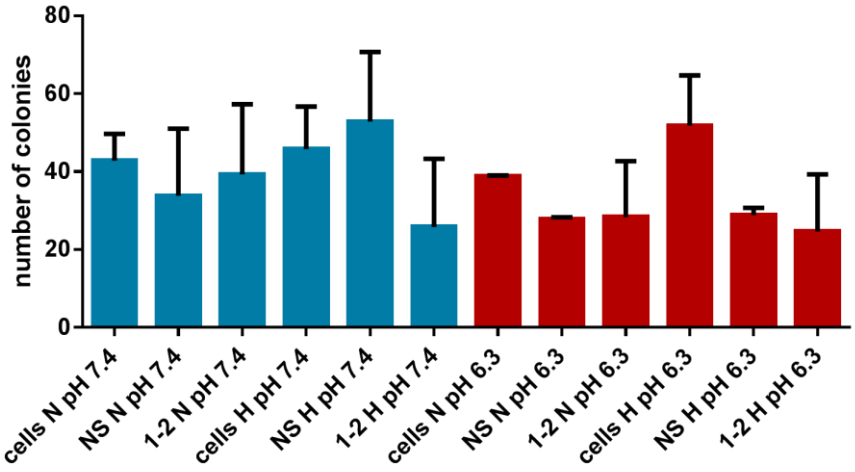

Fig. 5.12: CtBP expression does not impact CA9-mediated long-term survival of hypoxia-induced acidosis in MCF7 breast cancer cells. MCF7 breast cancer cells were transfected with either 50 nM non-silencing or CtBP 1/2-targeting siRNA. 48 h post-transfection, cells were incubated at 20% and 1% O_2 for 18 h. In the following, cells were transferred to bicarbonate-free medium adapted to either pH 7.4 or pH 6.3 for 24 h. To define the impact on long-term survival, cells were re-plated in triplicates in complete DMEM at a concentration of $2x10^2$/ 2 ml in 6 well plates. 10 days post-seeding, colonies were stained by 0.1% crystal violet solution and imaged with the GelDoc-It™ Imaging system. Colonies were counted manually by applying the plugin "multipoint count", whereas all colonies consisting of ≥ 50 cells were included in the count. Displayed are the mean of two independent experiments and their SEM. Statistical significance was determined by Fisher's LSD test.

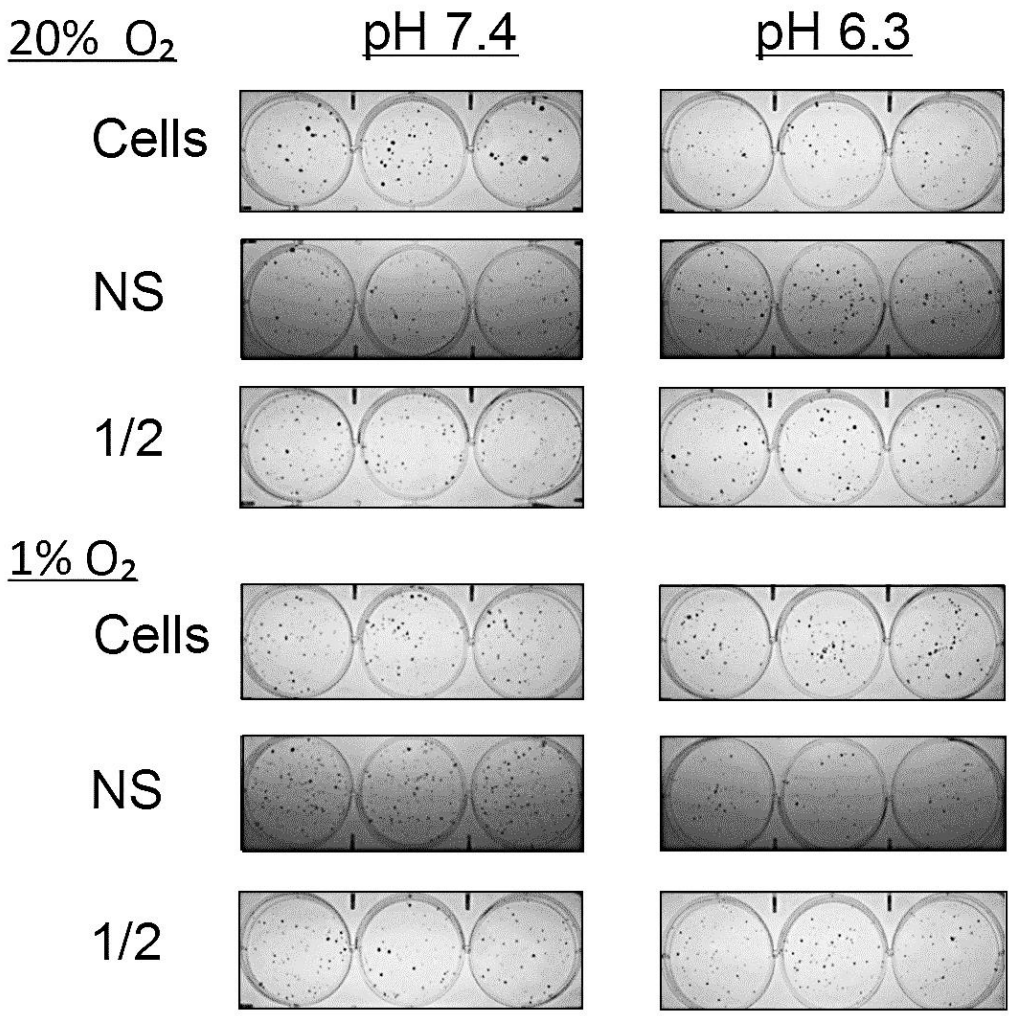

Fig. 5.13: CtBP expression does not impact CA9-mediated long-term survival of hypoxia-induced acidosis in MCF7 breast cancer cells as determined by colony forming assay. MCF7 breast cancer cells were transfected with either 50 nM non-silencing or CtBP 1/2-targeting siRNA. 48 h post-transfection, cells were incubated at 20% and 1% O_2 for 18 h. In the following, cells were transferred to bicarbonate-free medium adapted to either pH 7.4 or pH 6.3 for 24 h. To define the impact on long-term survival, cells were re-plated in triplicates in complete DMEM at a concentration of $2x10^2$/ 2 ml in 6 well plates. 10 days post-seeding, colonies were stained by 0.1% crystal violet solution and imaged with the GelDoc-It™ Imaging system. Shown is one representative image of two independent experiments.

5.2.6 The role of p53 in long-term survival of hypoxia-induced acidosis

The role of wildtype p53 expression on survival of acidic conditions was investigated in wildtype p53-expressing MCF7 and in p53-mutant MDA-MB-231 with silenced CtBP and CA9 expression. Additionally, the impact of p53 (MCF7) and of CtBP and CA9 expression (MDA-MB-231) on short-term survival of hypoxia and acidosis was evaluated by trypan blue staining. There is no difference in cell death between different conditions (Fig. 5.14). Furthermore, the percentage of dead cells varies highly between experiments which may be due to the removal of detached cells during the washes performed for trypsinizing. This may also explain the low percentage of dead cells. There is also no significant difference in total cell numbers between conditions (Fig. 5.15). Total cell numbers were evaluated by combining cell counts for viable and dead cells which only includes attached cells. Therefore, the calculated cell numbers potentially do not reflect the actual impact of p53 expression on short-term survival of hypoxia-induced acidosis.

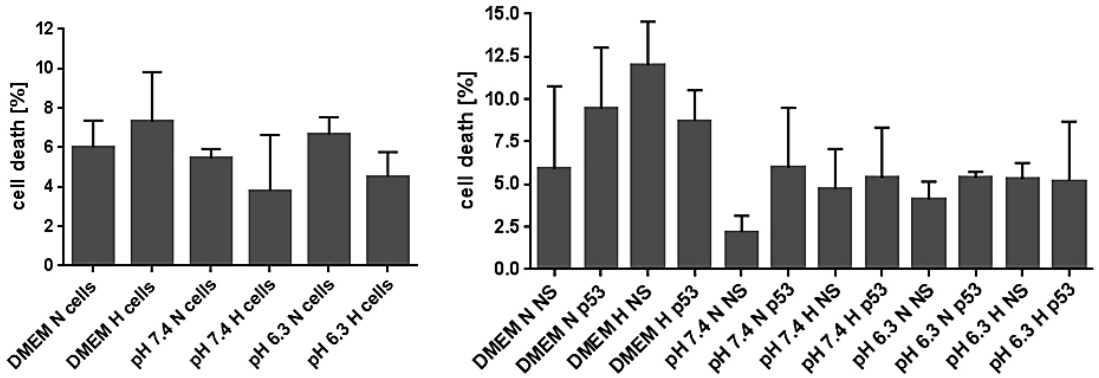

Fig. 5.14: p53 expression has no impact on cell viability of untreated (left) and MCF7 breast cancer cells transfected with p53 siRNA (right) after exposure to hypoxia and low pH. MCF7 breast cancer cells were transfected with 50 nM p53 siRNA or left untreated. 48 h post-transfection, cells were exposed to either 20% (N) or 1% O_2 (H) for 18 h. Incubation time in hypoxia or normoxia was followed by incubation at either pH 7.4 or pH 6.3 in bicarbonate-free medium or in DMEM medium at 10% CO_2 for 24 h. To determine the impact of p53 expression on short-term survival of acidosis, cells were stained with trypan blue. Displayed are the mean of two independent experiments and their SEM. Statistical significance was determined by Fisher's LSD test.

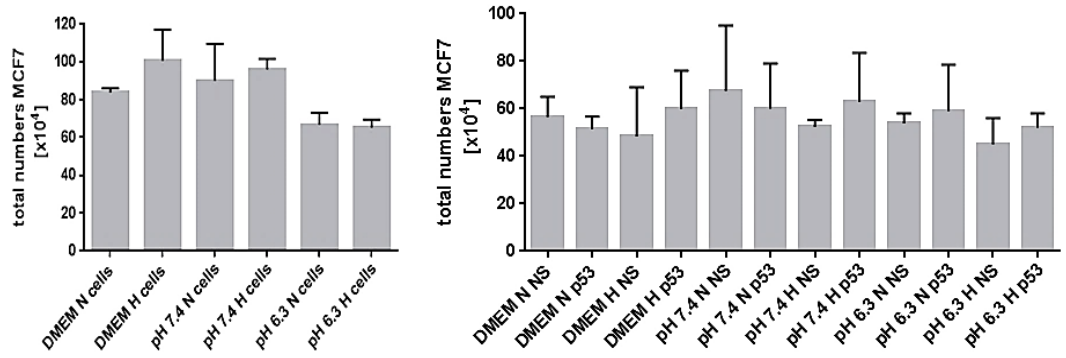

Fig. 5.15: Low pH and p53 expression does not play a role in short-term survival of hypoxia-induced acidosis on untreated MCF7 (left) or MCF7 breast cancer cells transfected with p53 siRNA (right). MCF7 breast cancer cells were transfected with 50 nM p53 siRNA or left untreated. 48 h post-transfection, cells were exposed to either 20% (N) or 1% O_2 (H) for 18 h followed by incubation at either pH 7.4 or pH 6.3 in bicarbonate-free medium or in DMEM medium at 10% CO_2 for 24 h. To evaluate the impact of p53 expression on short-term survival of acidosis, cells were stained with trypan blue. Displayed are the mean of two independent experiments and their SEM. Statistical significance was determined by Fisher's LSD test.

The transfection of MCF7 with p53 siRNA successfully reduces p53 protein expression, and CA9 expression is induced in by 1% O_2 (Fig. 5.16). However, the anti-CA9 antibody did not detect CA9 expression in transfected MCF7 which was problematic and did not reflect previous findings. A similar observation was made in MDA-MB-231 cells. Consequently, it was decided to evaluate *CA9* expression by TaqMan® quantitative reverse-transcription PCR in future experiments.

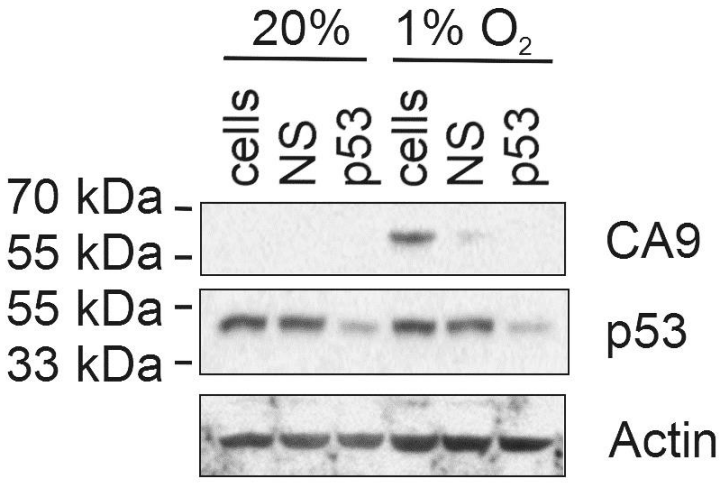

Fig. 5.16: Determination of CA9 and p53 expression in MCF7 breast cancer cells after transfection with 50 nM siRNA. To define the role of p53 and CA9 in long-term survival of hypoxia-induced acidosis, MCF7 breast cancer cells were transfected with 50 nM p53 siRNA. 48 h post-transfection, cells were incubated at either 20% or 1% O_2 for 18 h. Consequently, cells were harvested to confirm induction of CA9 protein expression and downregulation of p53 protein expression by Western blot. Gel electrophoresis was performed with 25 µg whole cell lysate. Shown is one representative image.

As expected, there is no reduction in long-term survival in untreated MCF7 or cells transfected with non-silencing control siRNA in all experimental conditions (Fig. 5.17 and Fig. 5.18). However, there is a significant reduction of colony numbers in cells transfected with p53 siRNA in 1% O_2 in complete DMEM medium compared to cells transfected with non-silencing siRNA alone. There is also a trend towards reduced viability in hypoxia-treated cells transfected with p53 siRNA and grown in bicarbonate-free media which is however not significant. Generally, bicarbonate-free medium appears to reduce viability compared to complete DMEM which may be due to the fact that DMEM is a commercially available and optimised for cell culture medium, whereas the bicarbonate-free media were prepared in-house. This lack of optimisation may have masked potentially significant effects on long-term survival. To further evaluate the role of p53 in the survival of hypoxia-mediated acidosis, the experiment was repeated with the p53-mutant breast cancer cell line MDA-MB-231.

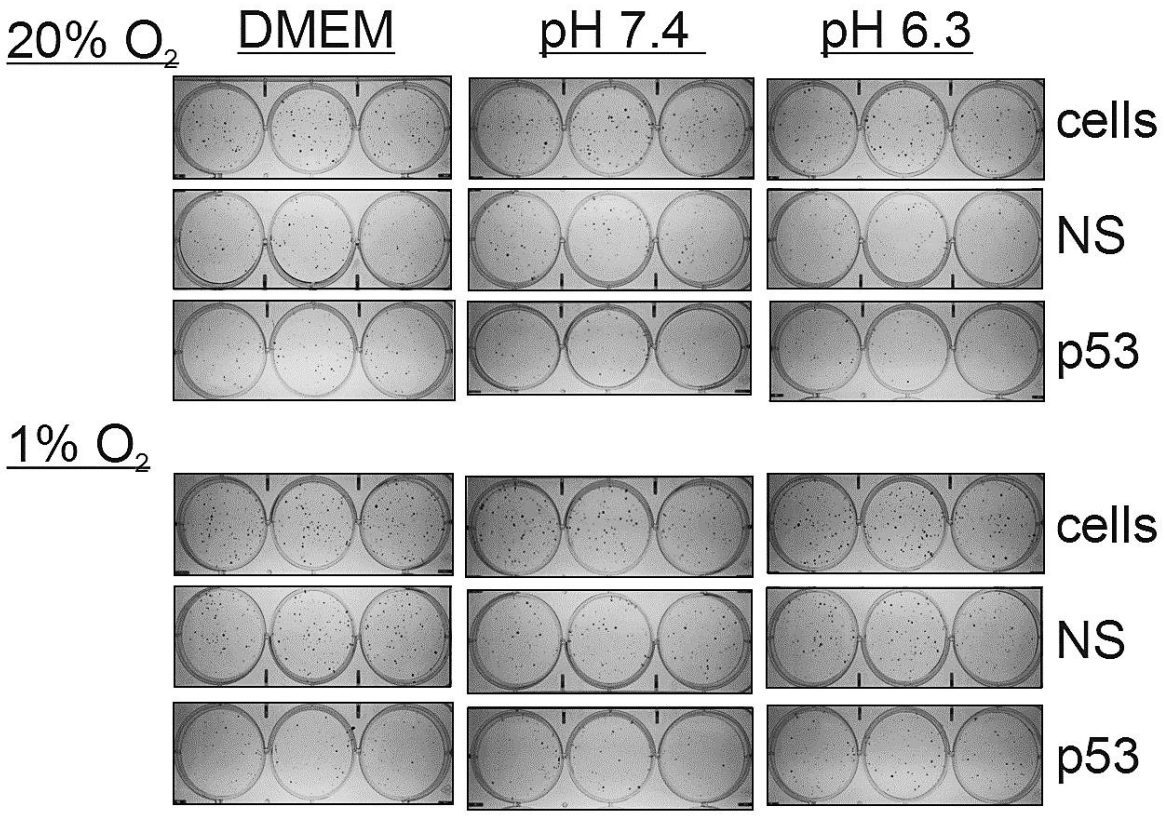

Fig. 5.17: The impact of p53 expression on long-term survival of hypoxia-induced acidosis was determined by the ability to form viable colonies. MCF7 breast cancer cells were transfected with either 50 nM non-silencing or p53-targeting siRNA. 48 h post-transfection, cells were incubated at 20% and 1% O_2 for 18 h. In the following, cells were transferred to either DMEM medium or bicarbonate-free medium adapted to either pH 7.4 or pH 6.3 for 24 h. To define the impact on long-term survival, cells were stained by trypan blue and re-plated at in triplicates in complete DMEM at a concentration of $2x10^2$/ 2 ml in 6 well plates. 10 days post-seeding colonies were stained by 0.1% crystal violet solution and imaged with the GelDoc-It™ Imaging system. Shown is one representative image of two independent experiments.

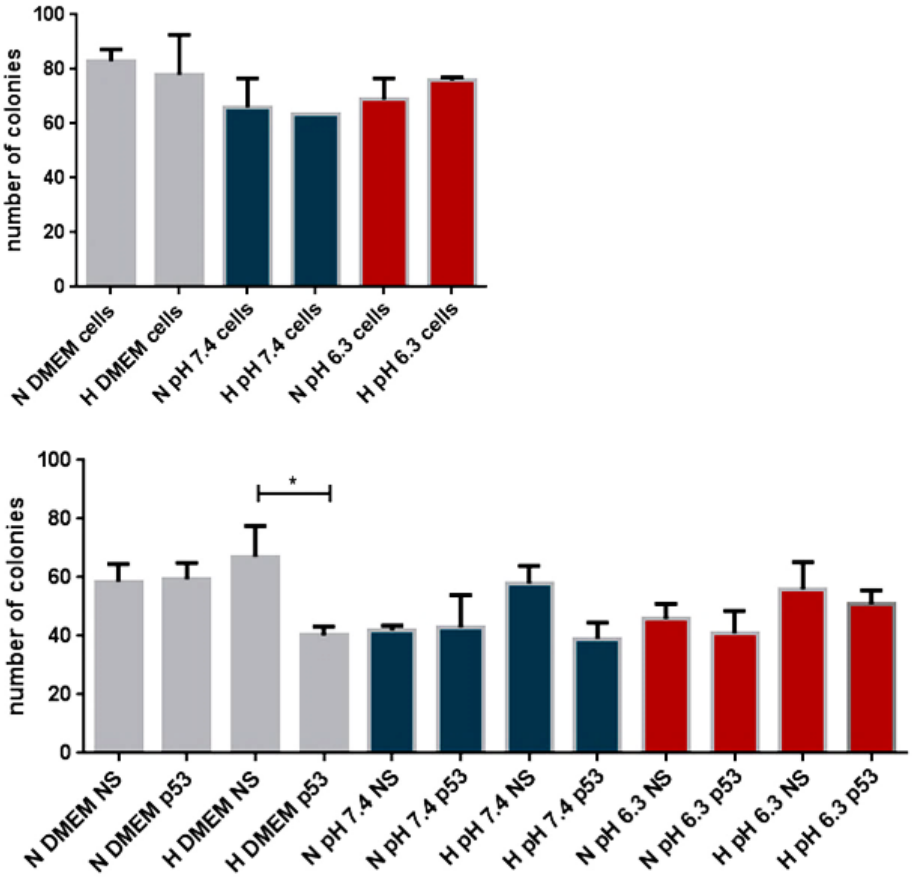

Fig. 5.18: p53 expression protects MCF7 breast cancer cells from hypoxia-induced acidosis (above), whereas transfection with 50 nM p53 siRNA reduces long-term survival (below). MCF7 breast cancer cells were transfected with either 50 nM non-silencing or p53-targeting siRNA or left untreated. 48 h later, cells were incubated at 20% and 1% O_2 for 18 h. In the following, cells were transferred to either DMEM medium or bicarbonate-free medium adapted to either pH 7.4 or pH 6.3 for 24 h. To define the impact on long-term survival, cells were stained by trypan blue and re-plated in triplicates in complete DMEM at a concentration of $2x10^2$/ 2 ml in 6 well plates. 10 days post-seeding, colonies were stained by 0.1% crystal violet solution and imaged with the GelDoc-It™ Imaging system. Colonies were counted manually by applying the plugin "multipoint count", whereas all colonies consisting of ≥ 50 cells were included in the count. Displayed are the mean of two independent experiments and their SEM. Statistical significance was determined by Fisher's LSD test.

In untreated MDA-MB-231, CA9 expression is induced by hypoxia (Fig. 5.19). However, CA9 induction was not detectable in transfected cells. This is contradictory to previous applications of the anti-CA9 antibody. To evaluate whether this is a cell-line specific issue, lysates from hypoxia-treated MCF7 were tested along MDA-MB-231 lysates. As CA9 is detected in hypoxia-treated MCF7 samples as well as in untreated MDA-MB-231 cells, but not in transfected MDA-MB-231 and MCF7 cells, it was concluded that CA9 expression might only be detected in very high abundance by this batch of anti-CA9 antibody which was not observed in previous experiments. Due to the high inter-batch variability it was decided to determine *CA9* expression by TaqMan® quantitative reverse-transcription PCR for reproducible results. On the other hand, CtBP1 and CtBP2 expression levels are successfully reduced by transfection with 50 nM siRNA (Fig. 5.19).

The impact of CtBP and CA9 expression on acute survival of hypoxia and low pH was determined by trypan blue staining in wildtype or transfected cells grown in either DMEM or pH-adjusted bicarbonate-free medium, following the growth in 1% or 20% O_2. There is no effect of CtBP and CA9 expression on cell death (Fig. 5.20). However, as observed in MCF7, there is a strong variability between experiments due to the loss of detached cells during trypsinization. Therefore, the total cell count was included into the determination of CtBP and CA9 impact of short-term survival of hypoxia-induced acidosis. In untreated MDA-MB-231 cells, low pH significantly reduces cell numbers in normoxia (Fig. 5.21).

Furthermore, cell numbers in hypoxia–treated cells are significantly reduced in cells grown in bicarbonate-free medium compared to cells grown in DMEM. Unlike DMEM, bicarbonate-free medium is not optimised and the lack of optimisation may have appeared more prominent in cells stressed by hypoxia than in their normoxic counter parts. However, there is no difference in cell numbers at normoxia and hypoxia at either pH or in DMEM. Therefore, the absence of wildtype p53 expression does not reduce short-term viability in hypoxia, and consequently p53 is not required for short-term survival of hypoxia-induced acidosis in untreated MDA-MB-231 breast cancer cells. In transfected MDA-MB-231 cells, there is a significant impact of CtBP inhibition in DMEM-grown cells as well as on cells grown at pH 6.3 (Fig. 5.21). However, CA9 and CtBP expression does not impact short-term survival of transfected MDA-MB-231 cells in all other conditions.

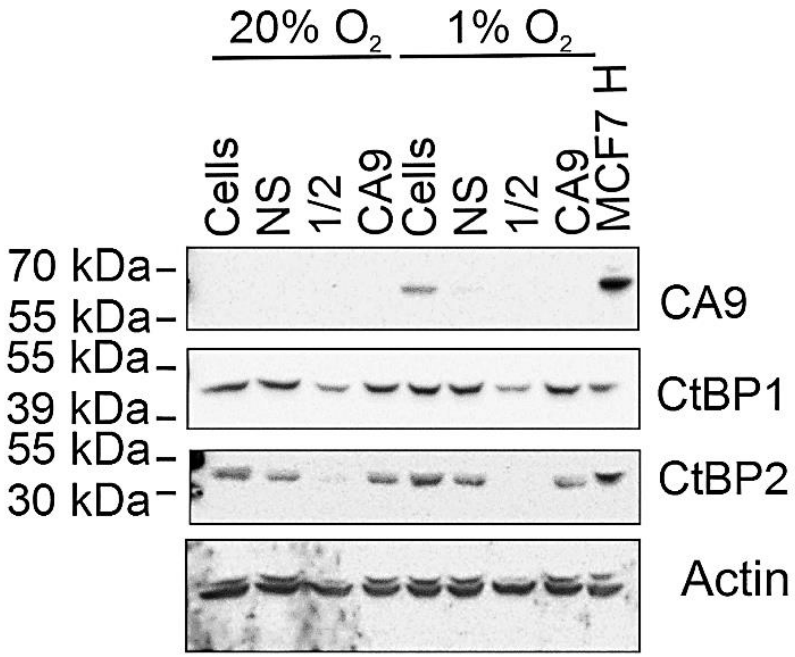

Fig. 5.19: In MDA-MB-231 breast cancer cells, CA9 expression is induced by 1% O_2, and CtBP as well as CA9 protein expression is downregulated by transfection with 50 nM siRNA. MDA-MB-231 cells were transfected with either 50 nM non-silencing or CtBP and CA9-targeting siRNA. 48 h post-transfection, cells were incubated at 20% and 1% O_2 for 18 h. In the following, cells were immediately harvested to determine CA9 and CtBP protein expression by Western blot. Gels were loaded with 25 µg whole cell lysate.

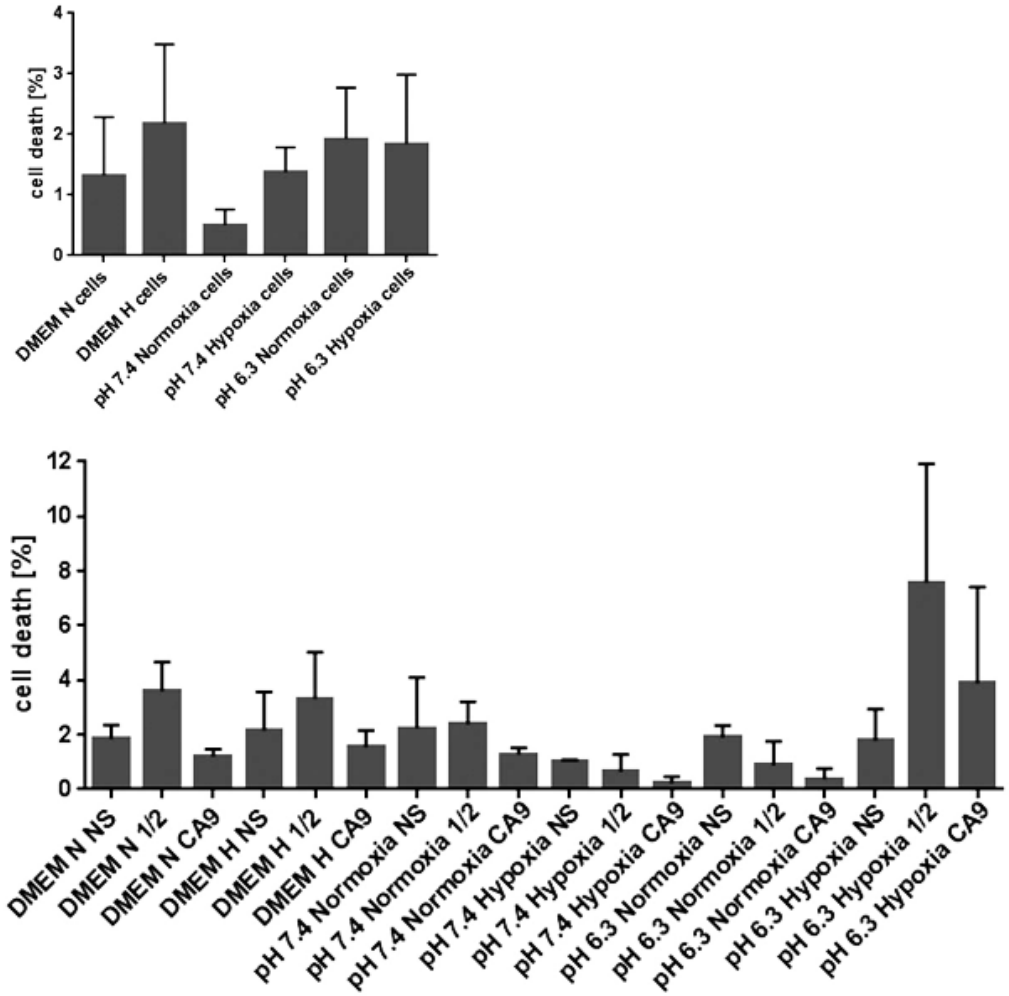

Fig. 5.20: Hypoxia and low pH (above) as well as CtBP and CA9 expression (below) do not impact short-term survival of p53-negative MDA-MB-231 breast cancer cells. MDA-MB-231 cells were transfected with 50 nM non-silencing control, CtBP- and CA9 targeting siRNA or left non-transfected. 48 h later, cells were either incubated at 1% (H) or 20% O_2 (N) for 18 h. Subsequently, cells were either transferred to DMEM or bicarbonate-free medium adjusted at either pH 7.4 or pH 6.3 for 24 h. Cell viability was determined by trypan blue staining and was expressed as percentage of dead cells. The mean of three independent experiments and their SEM are shown above. Significance was determined by Fisher's LSD test.

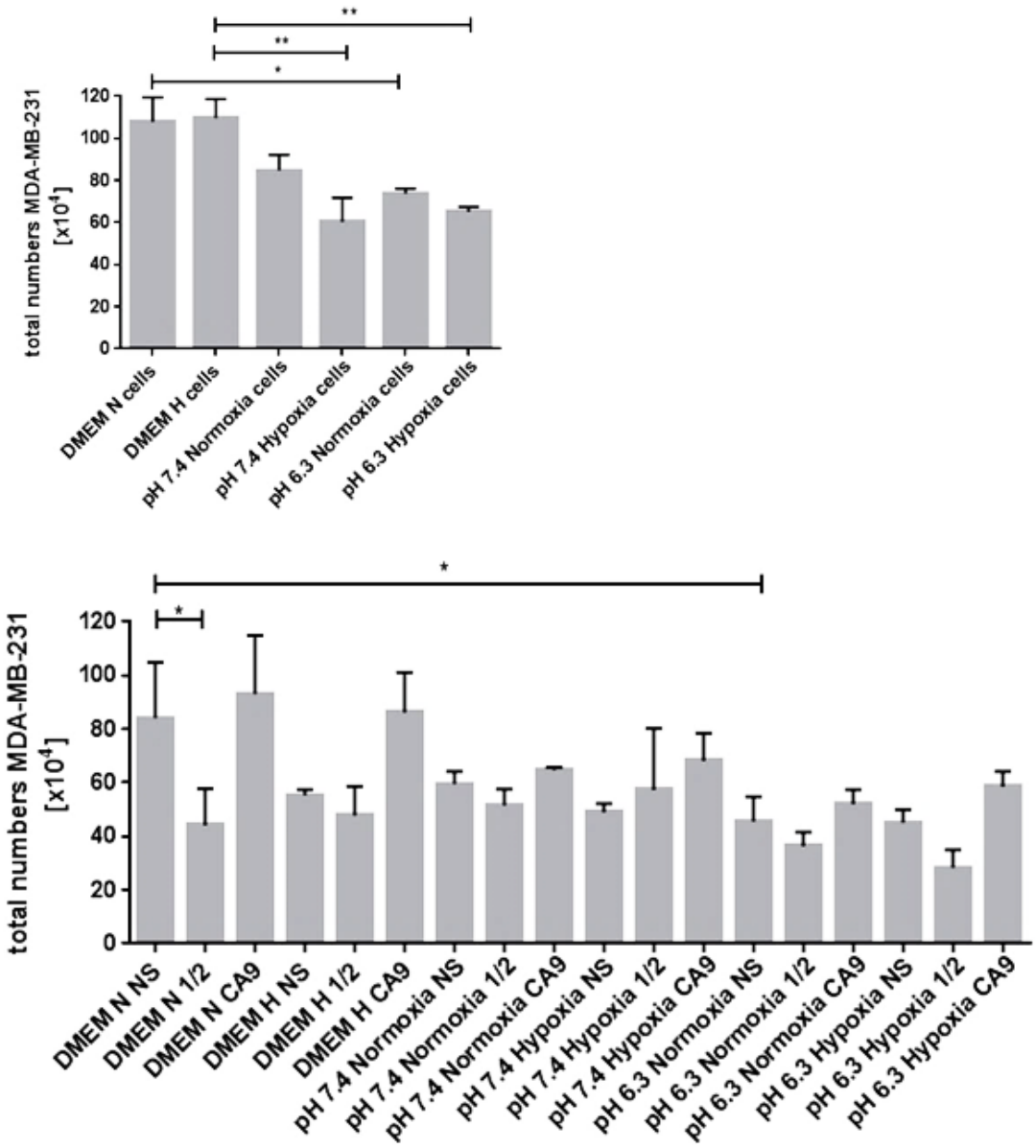

Fig. 5.21: Short-term survival of hypoxia is reduced in bicarbonate-free medium and at low pH in wildtype MDA-MB-231 breast cancer cells (above), whereas acidosis and reduced CtBP expression in normoxia impair short-term viability in transfected MDA-MB-231 cells (below). MDA-MB-231 cells were transfected with 50 nM non-silencing control, CtBP- and CA9 targeting siRNA or left non-transfected. 48 h later, cells were either incubated at 1% (H) or 20% O_2 (N) for 18 h. Subsequently, cells were either transferred to DMEM or bicarbonate-free medium adjusted at either pH 7.4 or pH 6.3 for 24 h. Cell viability was determined by trypan blue staining and it was used to calculate the total number of cells for each treatment. Three independent experiments were performed showing the mean and their SEM. Significance was determined by Fisher's LSD test.

To investigate the role of CtBP and CA9 in the context of a p53-mutant background in long-term survival of hypoxia-induced acidosis, a colony forming assay was performed with wildtype or transfected MDA-MB-231 cells exposed to 1% or 20% O_2 and cultured in either complete DMEM or bicarbonate-free medium at pH 7.4 or 6.3. Survival was indirectly determined by measuring the absorbance at 595 nm of crystal violet in 20% acetic acid. Low pH compared to DMEM significantly reduces survival in wildtype MDA-MB-231 breast cancer cells (Fig. 5.22 and Fig. 5.23). However, there is no difference in survival between normoxia and hypoxia at either pH 7.4 or 6.3 or in DMEM. Therefore, p53 does not play a role in long-term survival of hypoxia-induced acidosis. Furthermore, there is also no difference in survival between cells transfected with control siRNA and CtBP- and CA9-targeting siRNA at either pH. Therefore, CtBP and CA9 expression is not required for survival of hypoxia and low pH in MDA-MB-231 breast cancer cells. Consequently, MDA-MB-231 cells were excluded from further experiments.

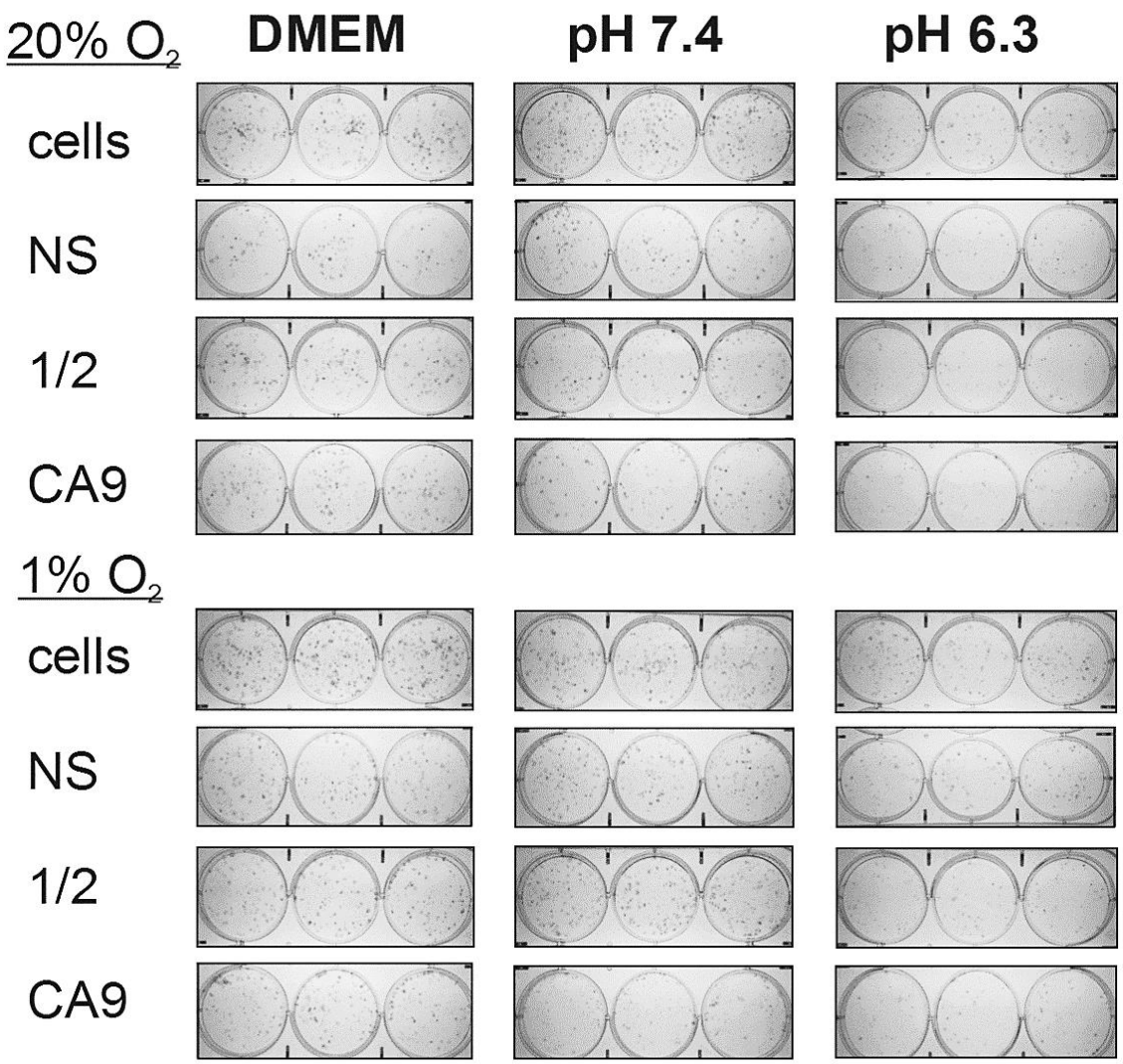

Fig. 5.22: CA9 and CtBP expression does not impact long-term survival of hypoxia-induced acidosis in p53-negative MDA-MB-231 breast cancer cells. MDA-MB-231 breast cancer cells were transfected with either 50 nM non-silencing or CtBP and CA9-targeting siRNA. 48 h post-transfection, cells were incubated at 20% and 1% O_2 for 18 h. In the following, cells were transferred to either DMEM medium or bicarbonate-free medium adapted to either pH 7.4 or pH 6.3 for 24 h. To define the impact on long-term survival, cells were stained by trypan blue and re-plated at in triplicates in complete DMEM at a concentration of $2x10^2$/ 2 ml in 6 well plates. 10 days post-seeding, cells were stained with 0.1% crystal violet solution and imaged with the GelDoc-It™ Imaging system. Shown is one representative image of three independent experiments.

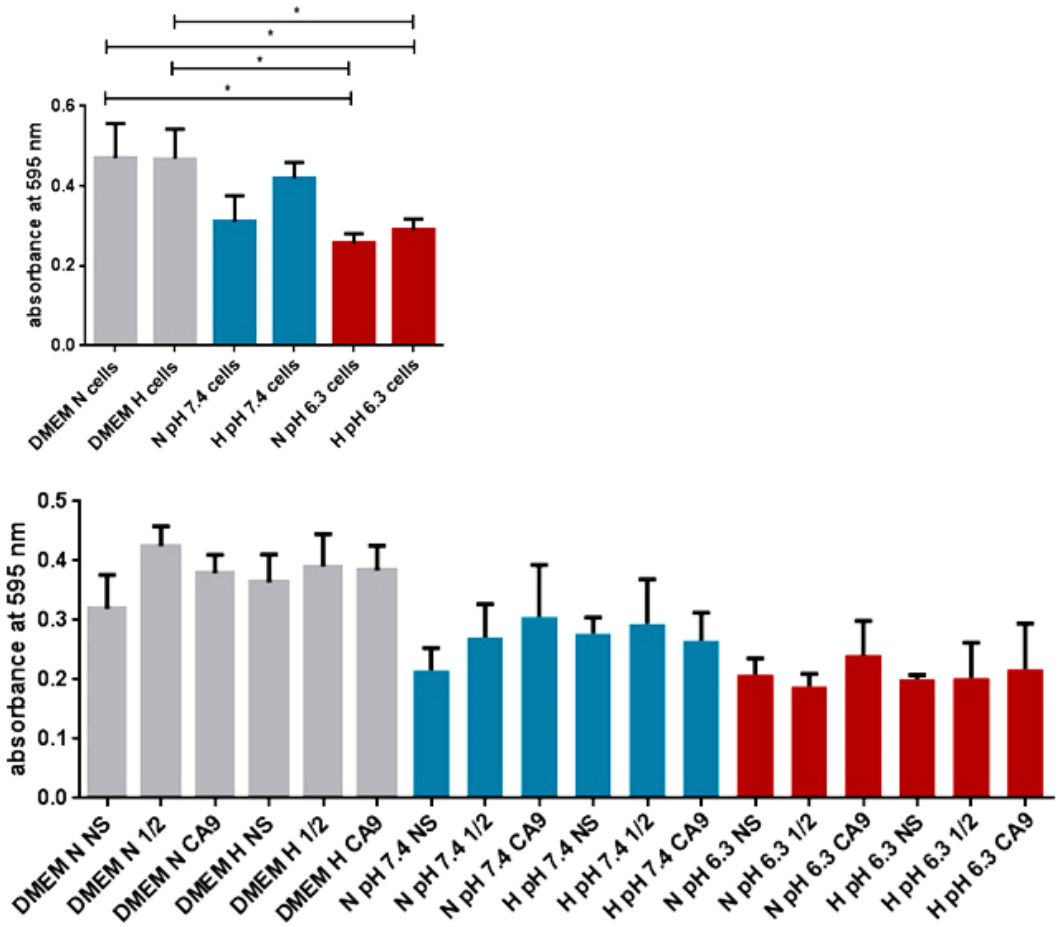

Fig. 5.23: CA9 and CtBPs do not play a role in long-term survival of hypoxia-induced acidosis in p53-negative MDA-MB-231 breast cancer cells. MDA-MB-231 breast cancer cells were transfected with either 50 nM non-silencing or CtBP and CA9-targeting siRNA. 48 h post-transfection, cells were incubated at 20% and 1% O_2 for 18 h. In the following, cells were transferred to either DMEM medium or bicarbonate-free medium adapted to either pH 7.4 or pH 6.3 for 24 h. To define the impact on long-term survival, cells were stained by trypan blue and re-plated at in triplicates in complete DMEM at a concentration of $2x10^2$/ 2 ml in 6 well plates. 10 days post-seeding, cells were stained with 0.1% crystal violet solution and imaged with the GelDoc-It™ Imaging system. Cell viability was determined by measuring absorbance at 595 nm as MDA-MB-231 did not form colonies. Displayed are the mean of three independent experiments and their SEM. Statistical significance was determined by Fisher's LSD test.

5.3 CtBPs and CA9 supported by p53 promote long-term survival in hypoxia-induced acidosis

The optimisation evaluated above led to the question how CtBPs and hypoxia-induced CA9 and p53 promote tumour cell survival in acidosis. Therefore, based on (Parks et al. 2013) an experiment was designed in which MCF7 breast cancer cells where transfected with p53, CtBP and CA9 siRNA, individually or in combination. Following incubation in 1% O_2 for 18 h, cells were grown in bicarbonate-free medium for 24 h which was adjusted to pH 6.3. The impact of CtBP, CA9 and p53 on cell viability was determined by trypan blue staining, whereas the impact on long-term survival was evaluated by colony forming assay.

The transfection of MCF7 breast cancer cells with 50 nM siRNA successfully reduces CtBP and p53 protein expression (Fig. 5.24A). The observation that the silencing of both CtBPs by 1/2 siRNA increased p53 protein expression is in line published findings (Birts et al. 2010). The polyclonal CA9 antibody applied in Western blots showed strong batch-to-batch variations as well as strong variations between assays. Therefore, *CA9* expression was quantified TaqMan® quantitative reverse-transcription PCR. Consequently, transfection with CA9 siRNA significantly reduces *CA9* mRNA expression levels in three independent experiments. There is a highly significant difference in *CA9* expression between cells transfected with non-silencing siRNA, in cells transfected with a combination of p53 and CA9 siRNA ($p < 0.001$), and in cells transfected with CA9 and non-silencing siRNA ($p < 0.001$). As expected, the transfection with CtBP 1/2 and p53 siRNA also significantly reduces CA9 mRNA expression levels ($p = 0.005$) as well as the transfection with CtBP 1/2 and non-silencing siRNA ($p < 0.001$) (Fig. 5.24B).

Before re-plating for colony forming assay, trypan blue exclusion assay was performed in order to determine the impact of hypoxia and acidosis on short-term survival and cell growth. There is no significant difference in total cell numbers and the percentage of dead cells (Fig. 5.26). However, there is a trend towards reduced viability in cells transfected with CtBP 1/2 siRNA in combination with p53 siRNA or non-silencing control siRNA. This may be caused by mitotic stress as CtBPs also play an important role in mitosis (Birts et al. 2011). However, cells detected by trypan blue staining only include attached cells and (dead) cells in suspension could not be detected by the assay as they were removed during trypsinizing. Therefore, the percentage of dead cells detected is highly variable between experiments and lower than expected. Nevertheless, the downregulation of CtBP expression either alone ($p = 0.020$) or in conjunction with p53 ($p = 0.029$) significantly reduces long-term viability whereas silencing of CA9 expression only significantly reduces long-term viability in conjunction with p53 ($p = 0.012$) but not on its own (Fig. 5.26 and

Fig: 5.27). There is a minor trend towards reduced long-term viability in cells transfected with p53 and non-silencing control siRNA which is not significant (p = 0.06). The transfection with CtBP 1/2 reduces total cell numbers due to mitotic stress, selecting cells unaffected by mitotic stress and it was expected that those cells were also unaffected by acid stress as demonstrated in MDA-MB-231. However, reduced CtBP expression still impacts long-term survival, pointing towards a role in hypoxia-induced acidosis. Transfection with CtBP 1/2 siRNA alone reduces long-term viability which was not observed before. However, the impact is stronger when both CtBP and p53 are inhibited. As reduced p53 and CA9, and p53 and CtBP expression impair long-term survival, the hypothesis that those proteins are required for long-term viability in hypoxia-induced acid stress was accepted. Therefore, p53 in conjunction with CtBPs and hypoxia-induced CA9 show protective properties in the survival of acidosis.

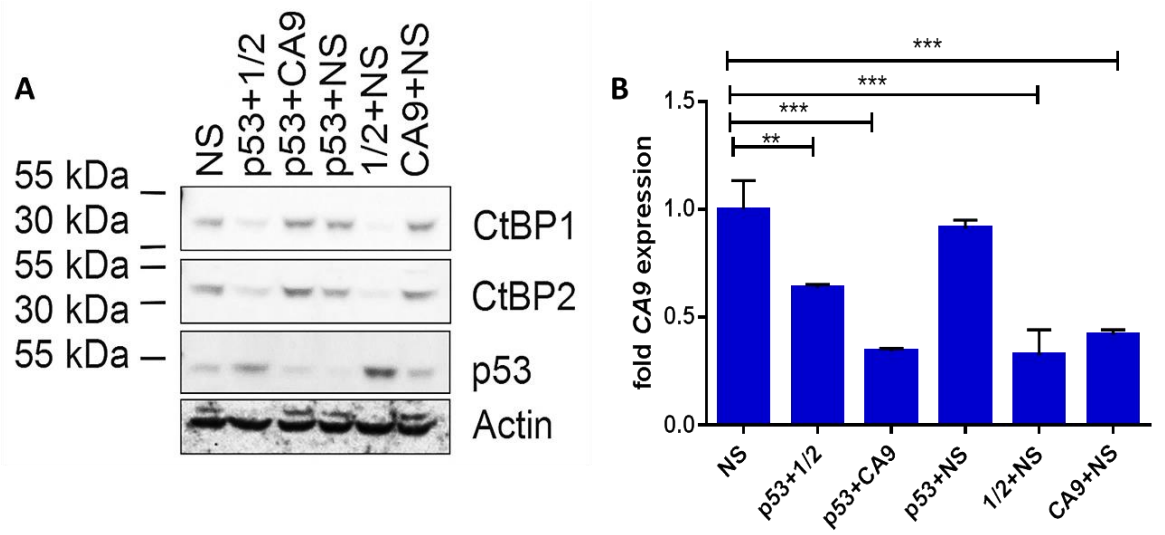

Fig. 5.24: Confirmation of the transient silencing of CtBP1 and 2 and p53 expression by Western blot (A) and confirmation of silenced *CA9* expression by TaqMan® quantitative reverse-transcription PCR (B). MCF7 cells were plated in DMEM at day 1 at a concentration of $4.4x10^5$/ 4 ml in 6 cm dishes. 24 h later, cells were transfected with 50 nM siRNA. 48 h post-transfection, cells were incubated at 1% O_2 for 18 h. **A** CtBP1, CtBP2, and p53 protein expression was determined by Western blot. A 10% SDS gel was loaded with 15 µg whole cell lysate. One representative image is shown. **B**: *CA9* expression was analysed by TaqMan® quantitative reverse-transcription PCR. Data were normalized to the housekeeping gene actin and analysed by the comparative C_T method. Displayed are the means of three independent experiments and their SEM. Statistical significance was determined by Fisher's uncorrected LSD test.

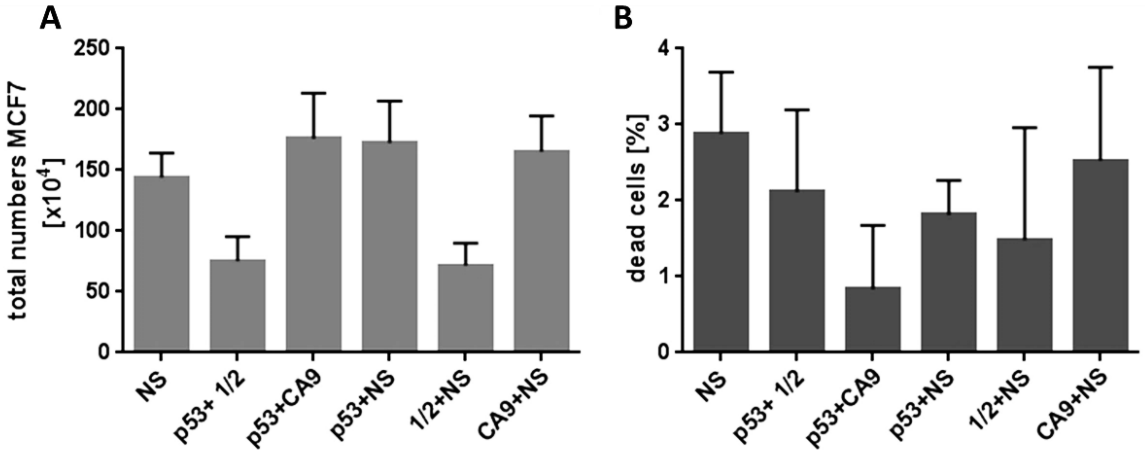

Fig. 5.25: There is no significant difference in total cell numbers (A) and percentage of dead cells (B) between MCF7 transfected with non-silencing control siRNA and combinations of CtBP-, CA9- and p53-targeting siRNAs. To determine the impact of CtBP, CA9 and p53 expression on short-term survival of hypoxia and low pH, MCF7 cells were plated in DMEM at day 1 at a concentration of $4.4x10^5$/ 4 ml in 6 cm dishes. 24 h later, cells were transfected with 50 nM non-silencing, p53 and CtBP 1/2, p53 and CA9, p53 and non-silencing, CtBP 1/2 and non-silencing and CA9 and non-silencing siRNA. 48 h post-transfection, cells were incubated at 1% O_2 for 18 h. Consequently, cells were transferred into bicarbonate-free medium at pH 6.3 and were incubated for 24 h in an air-buffered cell culture incubator. To determine short-term survival, cells were stained with trypan blue and counted before they were re-seeded for colony forming assay at a concentration of $2x10^2$/ 2 ml. Displayed are the means of three independent experiments and their SEM. Statistical significance was determined by Fisher's uncorrected LSD test.

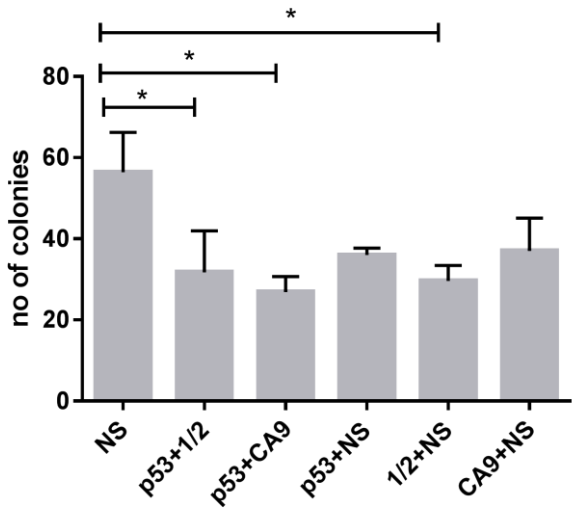

Fig. 5.26: The expression of CtBPs and CA9 is required for long-term survival in low pH and is supported by p53. MCF7 cells were plated in DMEM at day 1 at a concentration of $4.4x10^5$/ 4 ml in 6 cm dishes. 24 h later, cells were transfected with 50 nM non-silencing, p53 and CtBP 1/2, p53 and CA9, p53 and non-silencing, CtBP 1/2 and non-silencing and CA9 and non-silencing siRNA. 48 h post-transfection, cells were incubated at 1% O_2 for 18 h. Consequently, cells were transferred into bicarbonate-free medium at pH 6.3 and were incubated for 24 h in an air-buffered cell culture incubator. To determine long-term survival, cells were re-seeded for colony forming assay as described at a concentration of $2x10^2$/ 2 ml. 10 days post-seeding, colonies were visualised by crystal violet staining and colonies were counted by applying the tool "multicellular count" of the open source software ImageJ. Shown are the means of three independent experiments each performed in triplicates and their SEM. Statistical significance was determined by Fisher's uncorrected LSD test.

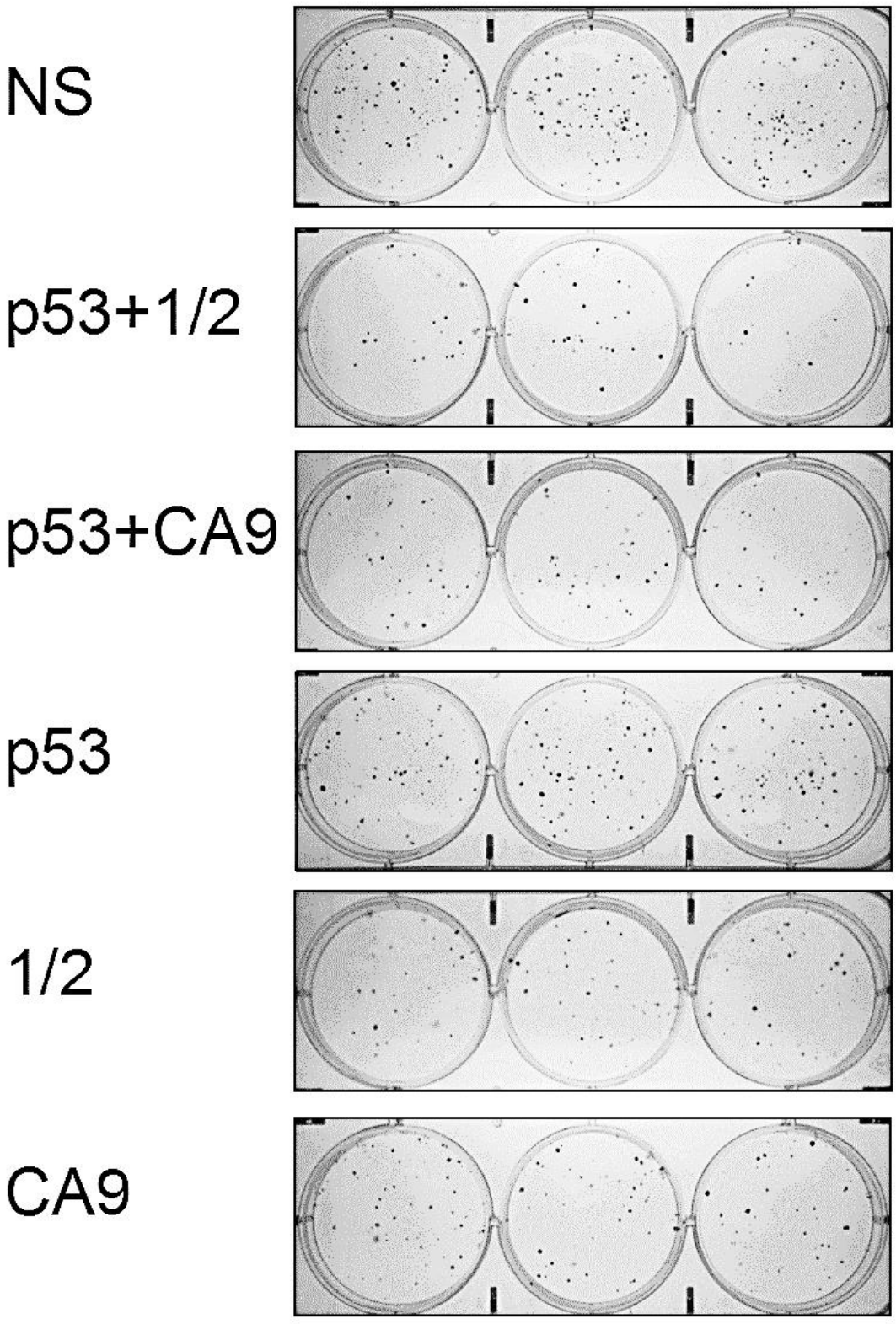

Fig: 5.27: CtBPs and CA9 expression are required for long-term survival in low pH and is supported by p53. MCF7 cells were plated in DMEM at day 1 at a concentration of $4.4x10^5$/ 4 ml in 6 cm dishes. 24 h later, cells were transfected with 50 nM non-silencing, p53 and CtBP 1/2, p53 and CA9, p53 and non-silencing, CtBP 1/2 and non-silencing and CA9 and non-silencing siRNA. 48 h post-transfection, cells were incubated at 1% O_2 for 18 h. Consequently, cells were transferred into bicarbonate-free medium at pH 6.3 and were incubated for 24 h in an air-buffered cell culture incubator. To determine long-term survival, cells were re-seeded for colony forming assay at a concentration of $2x10^2$/ 2 ml. 10 days post-seeding, colonies were visualised by crystal violet staining and imaged 24 h later. One representative image is shown.

5.4 CtBPs promote CA9-mediated survival of hypoxia-induced acidosis in p53-negative MCF7- summary of chapter 5

An optimisation process identified viable experimental conditions for investigating the role of CtBP-activated CA9 in the survival of acidosis. Findings of these preliminary experiments led to the experimental settings in which CA9 is first induced by incubation in hypoxia for 24 h, followed by 24 h at pH 6.3. However, the silencing of CtBP expression has no effect on the survival of acidosis in MCF7. In this context, experiments in MCF7 with transient silencing of p53 and in MDA-MB-231 expressing mutant p53, elaborated a protective role for p53 in the survival of acidosis in MCF7 but not in MDA-MB-231. CA9 expression was further characterised by determining protein stability following re-oxygenation, and induction of CA9 expression by low pH in normoxia. CA9 protein is still expressed 24 h after re-oxygenation, whereas mRNA levels are gradually declining. Moreover, neither CA9 gene nor protein expression is induced by growth at pH 6.3 in 20% O_2. Following the optimisation process, the impact of p53, CtBP, and CA9 expression on the survival of acidosis was determined by transient transfection of individual siRNAs or siRNA combinations. In this light, it was demonstrated that the silencing of CtBPs alone impairs cell survival in low pH, whereas the transfection with CA9 siRNA alone is not sufficient to reduce survival and requires the additional inhibition of p53 expression. Consequently, there is a novel, potential role for CtBPs in promoting tumour cell survival in hypoxia-induced acidosis via the activation of CA9, supported by p53. However, further research is required to learn more about the role of p53 in the protection from acidosis-mediated cell death.

Chapter 6: Discussion and future work

This project determined the potential role of hypoxia-induced glycolysis in the regulation of HIF-target genes via the activation of CtBPs. Additionally, the implications of the potential CtBP-HIF interaction for tumour cell survival in hypoxia-induced acidosis were investigated in MCF7 and MDA-MB-231.

6.1 Preliminary experiments

First, it was aimed to reproduce the findings of a preliminary study performed by the Blaydes group which determined that the hypoxia-induced expression of the HIF-1 target gene *ADM* is regulated by glycolysis in a CtBP-dependent manner. Further, it was aimed to characterise the regulation of HIF-target genes by glycolysis and CtBPs by applying pVHL-deficient renal clear cell carcinoma cells, and to investigate the role of alternative modes of CA9 activation.

6.1.1 Induction levels of *ADM* and *CA9* in a panel of breast cancer cell lines

First, optimum incubation times in hypoxia for the maximum induction of *ADM* was evaluated in the human breast cancer cell lines MCF7 (ER^+), SkBR3 ($Her2^+$) and MDA-MB-231 (TNBC). Induction of *ADM* expression is the highest after 17 h in hypoxia, and only detectable in MCF7. Based on the lack of significant *ADM* induction and low levels of CtBP expression (discussed below) the cell line SkBR3 was excluded from further experiments. Additionally, the same samples were evaluated for *CA9* expression. In MCF7 and MDA-MB-231 breast cancer cell lines, *CA9* expression peaks after 17 h in hypoxia. However, induction of *CA9* expression is almost 10-fold higher in MCF7 than in MDA-MB-231. This difference in induction is potentially mediated by increased basal levels of HIF, accompanied by high levels of glycolysis compared to MCF7 (Blancher et al. 2000). HIF-1α expression also correlates with enhanced glycolysis (Cairns et al. 2011) which causes acidification of the extracellular environment, and consequently up-regulation of *CA9* expression (Kaluz et al. 2002; Kopacek et al. 2005). MDA-MB-231 convert 94% of glucose into lactate whereas MCF7 only utilize 50% of glucose for lactate production (Li *et al.* 2009; Blancher *et al.* 2000). Additionally, CA9 (protein) abundance is subtype-dependent as its expression is linked to basal B and triple negative breast cancers (Li et al. 2009). In this context, (Tan *et al*. 2009) described that 50% of basal-like tumours express HIF-1α and overexpress CA9. CA9 expression further correlates with oestrogen receptor negativity and MDA-MB-231 cells belong to this category. Also, levels of CA9 mRNA and protein expression are lower in MCF7 than in MDA-MB-231 cells (Li et al. 2009). The strong

induction of *CA9* expression following 17 h corresponds to findings described in the literature (Vordermark et al. 2005), and was therefore chosen for all further experiments.

6.1.2 *ADM* is regulated in a glycolysis-dependent manner

The influence of CtBPs on HIF-1 target gene regulation in hypoxia was experimentally determined by the transfection of breast cancer cells with 50 nM non-targeting siRNA, a combination of CtBP1 and CtBP2 siRNA (CtBP 1+2), and one single siRNA targeting both isoforms (CtBP 1/2). CtBP-targeting siRNA specifically reduces CtBP expression. However, there is greater variability between experiments regarding CtBP2 than CtBP1 expression. This may be due to higher protein stability. Comparing the knockdown efficiency of CtBP 1+2 and CtBP 1/2 siRNA, it was found that both treatments cause a similar reduction in CtBP expression. However, it was observed that CtBP1 exerts off-target effects on gene expression which were also experienced by other members of the group (personal communication with Jason Fleming). Therefore, results generated by using this siRNA combination were excluded from analysis. In SkBR3 cells, the treatment with siRNA also causes off-target effects as basal levels of CtBP expression are lower in SkBR3 cells, compared to MCF7 and MDA-MB-231 (Birts et al. 2010). Consequently, this cell line was omitted from further experiments.

The transfection with 50 nM 1/2 siRNA significantly reduces *ADM* expression in MCF7 but not in MDA-MB-231 cells. The treatment with 10 mM 2-DG significantly increases *ADM* expression in MCF7 but has no impact on *ADM* expression in MDA-MB-231. Therefore, the regulation of hypoxia-induced *ADM* is inconsistent between cell lines. In MCF7, impaired glycolysis augments *ADM* expression, potentially to increase glucose and nutrient uptake by upregulating the expression of the pro-angiogenic factor ADM. Reduced glucose availability, which is to a certain extent mimicked by 2-DG, also upregulates *ADM* expression in hypoxia (Natsuizaka et al. 2007), thereby confirming this result. Conflicting with this result, the inhibition of CtBP expression by siRNA reduces *ADM* expression. In MDA-MB-231, neither CtBP expression nor glycolysis impacts on *ADM* expression. MDA-MB-231 cells are more glycolytic than MCF7 (Li et al. 2009). Therefore, the concentration of 10 mM 2-DG may have been too low to influence *ADM* expression. However, as the impact of glycolysis and CtBP expression on *ADM* are inconsistent and contradictory to the preliminary findings, *ADM* was excluded from the study.

6.1.3 *CA9* mRNA and protein expression is regulated in a glycolysis-CtBP-dependent manner

The HIF-target gene *CA9* was also identified in the preliminary gene expression study to be potentially regulated in a CtBP-HIF-dependent manner. Therefore, samples were re-analysed for *CA9* expression. In MCF7 and MDA-MB-231, CtBP expression is required for optimum induction of *CA9* expression in hypoxia. The treatment with 2-DG only impairs hypoxia-induced *CA9* expression in MCF7 but has no effect in the more glycolytic cell line MDA-MB-231. These findings were confirmed on the protein level. However, there is a discrepancy between CA9 mRNA and protein expression levels in MDA-MB-231 cells, following the treatment with 2-DG. The treatment with 2-DG completely abolishes the expression of CA9 in this cell line. This may be due to a lack of sensitivity of the polyclonal antibody used for CA9 detection in this cell line as this antibody displayed high batch-to-batch variations and had to be replaced by TaqMan™ quantitative reverse-transcription PCR eventually. Furthermore, the detection of protein abundance strongly relies on the quality of the antibody used for detection, and on protein abundance (Tuttle *et al.* 2014).

The CtBP-glycolysis mediated regulation which was determined for CA9 was not observed for LDH-A and GLUT-1, indicating that this HIF-CtBP-mediated regulation may be unique for CA9. Additionally, the impact of 2-DG on CA9 expression is dose-dependent in MCF7 which further underlines the role of glycolysis in hypoxia-induced CA9 regulation. These findings correspond with the literature. (Natsuizaka et al. 2007) reported that low glucose impairs hypoxia-induction of *CA9* in different cancer cell lines. Glucose deprivation also abolishes the induction of *CA9* in fibrosarcoma cells in anoxia (Vordermark et al. 2005). A similar observation was made by (Said *et al*. 2013) who described that the blocking of glycolysis reduces *CA9* expression in human glioblastoma cells. Still, the significance of glucose deprivation on *CA9* regulation and its underlying mechanism are unknown. Importantly, the preliminary findings were confirmed on the mRNA and protein level. Based on these findings it was hypothesised that hypoxia-induced glycolysis activates CA9 via the activation of CtBPs to support cancer cell survival in hypoxia-induced acidosis. The experiments designed to test this hypothesis are discussed in the following sections.

6.1.4 CA9 expression in pVHL-deficient renal cancer cells

One important molecular characteristic of renal carcinoma is the presence or absence of functional pVHL (Turner et al. 2002). Clear cell renal cell carcinomas (ccRCCs) are frequently pVHL-defective, leading to the constitutive expression of HIF-1α and/or HIF-2α subunits. However, the role of HIF-1 vs HIF-2 in renal carcinoma is complex and poorly understood. There is evidence that HIF-1 is only active in early stages, whereas HIF-2 is highly expressed in advanced stages. Additionally, HIF-1 is linked with good prognosis, while HIF-2 expression corresponds with poor outcome (Schoedel et al. 2016).

Corresponding with the evidence described above, Immunohistochemical analysis of CA9 in ccRCC tissue demonstrated strong expression in a patient with $pVHL^{-/-}$ syndrome and highly reduced expression in advanced stages of the disease. Additionally, CA9 staining is only present in perinecrotic areas of papillary renal carcinoma tissue (Wykoff et al. 2000). This may be a sign of hypoxia-induced expression. To a certain extent, these findings are reproduced in renal carcinoma cell lines. It was demonstrated that pVHL-defective cell lines constitutively express HIF-1 (and CA9), whereas HIF-1 (and CA9) expression in pVHL-functional cell lines is dependent on hypoxia (Lau et al. 2007; Shinojima et al. 2007; Wykoff et al. 2000). Most importantly, the expression of CA9 in pVHL-defective renal carcinoma cell lines is strictly HIF-1-dependent (Grabmaier et al. 2004; Wykoff et al. 2000).

It was planned to investigate the role HIF-CtBP-mediated regulation of CA9 expression in the pVHL-deficient renal clear cell carcinoma cell lines A498 and 786-O. However, as discussed earlier, 786-O lacks HIF-1α protein expression and its expression in A498 is unclear (Lau et al. 2007; Shinojima et al. 2007). Therefore, it would have been beneficial to also determine HIF-1α protein expression in these lines, especially because CA9 protein expression was detected in A498. 786-O cells are clearly defined as HIF-2α-positive renal clear cell carcinoma cells, whereas it is controversial whether A498 cells are of papillary or of clear cell origin (Brodaczewska et al. 2016). This may cause the contrasting findings on HIF-1α protein expression in this cell line.

Increasing concentrations of 2-DG do not impact CA9 protein expression in A498 and 786-O, but rather exert a cytostatic effect. In untreated controls, CA9 protein expression increases over time, indicating that CA9 expression may be also regulated by cell density in these cell lines. In A498, silencing of CtBP expression reduces CA9 protein and mRNA expression levels at CtBP siRNA incubation time points that exceed 96 h. In 786-O cells, CA9 expression is inconsistent due to the lack of HIF-1 expression. Therefore, results for this cell line are inconclusive. Consequently, both experiments, the treatment with 2-DG and the silencing of CtBP expression by siRNA, may point towards a role for cell density in the regulation of CA9 in these cell lines (discussed in greater

detail below). In the light of the findings discussed above, A498 and 786-O cells are not a suitable model to determine the role of CtBP-HIF-1 mediated regulation of CA9 expression and were therefore omitted from further experiments.

6.1.5 Cell density is an alternative mode of CA9 activation in renal cancer cells and MDA-MB-231 breast cancer cells

Cell density induces CA9 protein expression in the pVHL-deficient renal clear cell carcinoma cell lines A498 and 786-O and in the breast cancer cell line MDA-MB-231, but not in MCF7. The density-induced expression of CA9 potentially depends on the cell type. MDA-MB-231 cells lack density-induced growth arrest and therefore continue growing in high densities and acidic pH (as determined by colour change in DMEM). This may have been caused by mild local hypoxia and nutrient deficiency. Moreover, as previously mentioned, MDA-MB-231 cells are more glycolytic than MCF7 cells which may have caused stronger medium acidification, leading to the induction of CA9 in normoxia. Also, MDA-MB-231 cells exhibit higher CA9 baseline expression than MCF7. MCF7 cells on the other hand induce growth arrest at high cell densities, exhibit low baseline expression of CA9, and are less glycolytic than MDA-MB-231. All these reasons may contribute to reduce acid stress and oxygen consumption in MCF7, and therefore induction of CA9 may have not been required. In the renal clear cell carcinoma cell lines A498 and 786-O, CA9 expression is also augmented by cell density (Fig. 3.14 and Fig. 3.16).

Induction of CA9 expression is fine-tuned by oncogenic signalling which also plays a role in density-induced CA9 expression. In this context, the induction of CA9 expression in normoxia upon high cell densities is HIF-1-dependent and either regulated via Akt and mTOR signalling (Dayan et al. 2009) or via PI3K and MAPK signalling (Kaluz et al. 2002; Kaluz et al. 2009; Kopacek et al. 2005). (Dayan et al. 2009) reported that high cell densities lead to high oxygen consumption and consequently to the Akt and mTOR-dependent stabilisation of HIF-1α and induction of CA9. The inhibition of PI3K also reduces CA9 expression via the down-regulation of HIF-1α (Kaluz et al. 2002). Combined inhibition of both PI3K and MAPK has an augmented negative effect on CA9 expression and promoter activity at high cell densities in HeLa cells. Furthermore, the transcriptional activity of both transcription factors HIF-1 and SP1 is required to activate CA9 transcription at high cell densities in normoxia whereas in hypoxia HIF-1 activity alone is sufficient, but transcription is enhanced by SP1. Consequently, the inhibition of SP1 reduces CA9 expression but the effect is the strongest when additionally MAPK and PI3K are inhibited (Kopacek et al. 2005). This demonstrates that activating mutations in these signalling pathways potentially affect intratumoural CA9 expression, independently from hypoxia.

6.2 Hypoxia-induced glycolysis regulates the HIF-dependent induction of CA9 expression via the activation of CtBPs

The role of glycolysis in the regulation of hypoxia-induced CA9 expression was dissected by additionally growing MCF7.Control cells in fructose-containing DMEM. The impact of CtBP activity on CA9 expression was determined by additionally inhibiting CtBP expression by incubation in 4 mM MTOB, and by including the cell lines MCF7.CtBP2 and MCF7.CtBP-Mutant. MCF7.CtBP2 cells overexpress wildtype CtBP2 whereas MCF7.CtBP-Mutant express mutant CtBP monomers, which are unable to dimerise. Gene expression in these lines was compared to the expression in MCF7.Control cells which express the empty control vector. To confirm that the hypoxia-induced expression of HIF-target genes is dependent on HIF, hypoxia was replaced by the PHD inhibitor DMOG. Additionally, it was determined whether the regulation of CA9 by CtBPs is unique for CA9. Thus, the study was extended by the HIF-target genes *EGLN3*, *PDK1, FAM162A*, *TMEM45A* and *INSIG2*, and their expression was evaluated by semi-quantitative reverse-transcription PCR.

Hypoxia-induced CA9 expression is reduced on the protein and mRNA level when glycolysis was inhibited by either 2-DG or fructose. Additionally, the inhibition of CtBP activity by MTOB or CtBP expression by siRNA reduces CA9 expression in hypoxia, whereas it is increased in MCF7.CtBP2 and MCF7.CtBP-Mutant. These findings were reproduced when hypoxia was replaced by DMOG. Consequently, glycolysis upregulated by hypoxia may activate CtBPs, which together with HIF induce CA9 expression.

All HIF-target genes are induced by hypoxia and DMOG in MCF7, confirming their HIF-dependent activation in hypoxia. MDA-MB-231 cells were excluded from further experiments as HIF-target gene induction by hypoxia and DMOG is low and highly variable. Additionally, MDA-MB-231 are not responsive to 2-DG (in a dose-dependent manner). MDA-MB-231 express high levels of basal HIF and glycolysis, and therefore gene induction is low and the glycolytic phenotype is difficult to experimentally manipulate. Consequently, MCF7 cells were the model of choice as the glycolytic phenotype as well as HIF-target gene expression is inducible by hypoxia and DMOG. Additionally, MCF7 are resistant to acidosis and are able to proliferate at acidic pH.

The criteria for HIF-target genes to be accepted to be co-regulated by CtBPs are that induction of gene expression has to be impacted by the treatment with 2-DG and by growth in fructose. Additionally, gene expression has to be impacted by CtBP 1/2 targeting siRNA, and by the overexpression of wildtype CtBP2. Results generated by the treatment with MTOB are excluded from the discussion as the treatment with MTOB may have caused off-target effects. MTOB is the final component of the methionine pathway and is a *bona fide* CtBP inhibitor (Achouri et al. 2007;

Straza et al. 2010; Tang et al. 2006). Furthermore, MTOB is used as the starting point for the development of small molecule inhibitors (Birts et al. 2013; Hilbert et al. 2014). However, concentrations in the mM range have to be applied in order for MTOB to act as inhibitor (Patel et al. 2014; Straza et al. 2010). Therefore, off-target effects are likely to occur. Additionally, high concentrations of MTOB induce apoptosis by de-repressing CtBP-repressed pro-apoptotic gene *Bik* (Straza et al. 2010), which is independent from p53 expression (Tang et al. 2006). There is no difference in the number of dead cells between controls and samples treated with MTOB, but MTOB may have affected overall viability. However, the concentration of 4 mM is commonly used within the group and corresponds to the concentrations used within the field. Dose titrations are commonly performed to determine the impact of a regulatory molecule and could also be performed in this case to investigate the impact of MTOB on HIF-target gene expression.

Additionally, it is common practise to evaluate the impact of co-regulators such as CtBPs on a gene of interest via the application of different approaches. In this case, the role of CtBPs on HIF-target gene regulation has been determined by siRNA and the overexpression of wildtype CtBP2 in MCF7.CtBP2 cells. Additionally, CtBP activity has been indirectly inhibited by the treatment with 2-DG and by long-term cultivation in fructose. Results generated by these methods deviate from the results obtained with MTOB. It is for these reasons that the impact of MTOB on the HIF-target genes *EGLN3*, *PDK1*, *FAM162A*, *TMEM45A* and *INSIG2* is excluded from discussion and that the criteria for the potential co-regulation of CtBP and HIF are defined as evaluated above. Also excluded are results generated in MCF7.CtBP-Mutant cells. MCF7.CtBP-Mutant cells are engineered to express CtBP monomers that are unable to dimerise due to mutations in the NADH-binding domain. However, CtBP activity is not inhibited in these cells and rather resembles the activity in MCF7.CtBP2 overexpressing cells as determined by the impact of mutant CtBP expression on HIF-target gene expression.

CtBP expression does not impact hypoxia-induced *EGLN3* expression but DMOG-induced gene expression. In hypoxia, 2-DG does not alter *EGLN3* expression, whereas in fructose-adapted MCF7 gene expression is reduced. Additionally, DMOG-induced *EGLN3* expression is inhibited by 2-DG. Therefore, applying the criteria defined above, *EGLN3* is not regulated in a HIF-CtBP-dependent manner. Additionally, only chronic and strong downregulation of glycolysis inhibits *EGLN3* expression as 2-DG has no effect in hypoxia. However, the treatment with DMOG sensitises *EGLN3* to 2-DG-mediated downregulation of glycolysis. The impact of glycolysis and CtBP expression on *PDK1* is conflicting. The only consistent reaction is the downregulation of gene expression in fructose-grown cells in hypoxia and DMOG. Therefore, *PDK1* expression is affected by strong downregulation of glycolysis whereas the treatment with 10 mM 2-DG is not sufficient to inhibit induction of gene expression. Consequently, *PDK1* expression is not regulated in a CtBP-

HIF-dependent manner. *FAM162A* is also not regulated in a HIF-CtBP-dependent manner. The treatment with 2-DG has no effect on hypoxia-induced *FAM162A* expression, whereas in fructose-adapted MCF7 induction of *FAM162A* expression is impaired. Similar to *EGLN3*, DMOG sensitises *FAM162A* expression to 2-DG-induced inhibition of gene expression. CtBP expression has a conflicting impact on *FAM162A* expression as there is no impact of CtBP inhibition on *FAM162A* expression in hypoxia but DMOG-induced *FAM162A* expression is increased in MCF7.CtBP2. Therefore, *FAM162A* expression is not mediated in a HIF-CtBP-dependent manner. *TMEM45A* expression is also not regulated by the interaction of CtBPs with HIF. Findings for the impact of CtBP expression on the induction of *TMEM45A* expression are inconclusive. However, *TMEM45A* expression is strongly inhibited in fructose-adapted MCF7, in hypoxia and in DMOG-treated cells. Interestingly, DMOG also sensitises *TMEM45A* expression to the inhibition by 2-DG. *INSIG2* expression is reduced in hypoxia in a HIF-independent manner in fructose-grown cells. Therefore, *INSIG2* expression is only impaired when glycolysis is strongly inhibited as the incubation with 10 mM 2-DG has no effect. The modulation of CtBP expression also does not impact on *INSIG2* induction. Therefore, the HIF-CtBP-dependent induction of gene expression is unique for *CA9,* and the hypothesis is accepted.

The long-term cultivation of MCF7 in fructose reduces the expression of all HIF-target genes in a HIF-dependent manner, excluding *FAM162A* and *INSIG2*. Fructose-adapted MCF7 are commonly used by members of the Blaydes group to study the impact of metabolism on gene expression. The metabolic adaptions in these cells are comparable with metabolic changes in HeLa cells grown in fructose. In this context, (Reitzer et al. 1979) determined that HeLa cells grown in fructose are 900 times less glycolytic compared to glucose-grown cells and hardly generate glycolytic metabolites. Fructose-derived carbon is fed into the PPP and not utilised for energy production, but for the generation of CO_2. However, fructose and glucose grown cells rely heavily on glutamine to generate macromolecules (18-25%), but also lactate (13%) and CO_2 (35%), thereby preventing ATP deficiency and energy stress. Therefore, fructose-adapted MCF7 cells are a suitable model to evaluate the impact of reduced glycolysis on HIF-target gene expression as energy stress due to high concentrations of 2-DG is avoided.

However, fructose-adapted MCF7 are metabolically different to glucose-grown MCF7 treated with 2-DG. The degree of glycolysis inhibition is dose-dependent (in MCF7), temporary, and high concentrations of 2-DG result in energy stress. Fructose-grown cells on the other hand exhibit highly reduced glycolysis without energy stress as these cells are metabolically adjusted to grow in fructose. Therefore, fructose-adapted cells are suitable to determine long term effects of inhibited glycolysis on gene transcription. The reduction of HIF-target gene induction by HIF and hypoxia in fructose-grown MCF7 demonstrates the importance of glycolytic metabolites in the

activation of HIF-target genes by augmenting their HIF-dependent activation. The expression of *INSIG2* and *FAM162A* is not impacted by glycolysis and thereby may be mediated by other HIF-stabilising factors or HIF-independent oncogenic kinase signalling. CtBPs are activated by an increased NADH:NAD^+ ratio, caused by an upregulated glycolysis (Di et al. 2013; Zhang et al. 2002; Zhang et al. 2006). Therefore, CtBP activity is inhibited in fructose-adapted MCF7.Control cells. However, the expression of *EGLN3*, *FAM162A*, *TMEM45A*, *INSIG2* and *PDK1* is not regulated in a CtBP-dependent manner, excluding MTOB from the analysis. Therefore, CtBP inhibition is not the reason for impaired gene induction in fructose-adapted MCF7. Control cells. Interestingly, the treatment with DMOG sensitises *FAM162A*, *TMEM54A* and *EGLN3* to the inhibition with 2-DG. DMOG inhibits PHDs in a competitive manner and is widely used in preclinical studies to determine the role of HIFs in biological processes. However, DMOG also exerts pharmacological effects which are independent from HIF and PHDs. Importantly, DMOG inhibits mitochondrial respiration and ATP production within minutes after addition to the cell. The DMOG-mediated inhibition of mitochondrial function precedes the inhibitory effect on PHDs and also results in compensatory upregulation of glycolysis (Zhdanov et al. 2015). Consequently, cells become more sensitive to the inhibition of glycolysis, *e.g*. by 2-DG. Potentially, DMOG does not impact HIF-target genes in fructose-adapted MCF7.Control cells due to their adjusted metabolism. However, why DMOG sensitises MCF7 to the inhibition of *TMEM45A*, *FAM162A* and *EGLN3* by 2-DG but not to the other HIF-target genes analysed in this study remains elusive.

Potentially, hypoxia-induced CA9 is uniquely regulated via the functional interaction between CtBPs and HIF-1. These data further strengthen the role of CtBPs as plastic co-regulators of transcription. More and more studies evaluate the role of CtBPs as co-activators of gene transcription. The corresponding literature is reviewed in the introduction. The idea of CtBPs acting as dual regulators of gene transcription is not contradictory as CtBPs are able to act activating or inhibitory depending on the context. In *Drosophila,* CtBPs activate Wingless targets in the monomeric state but act as a repressor upon dimerization (Bhambhani et al. 2011). Also in *Drosophila*, it was found that CtBP has an established role as repressor of Wnt target genes. However, (Fang *et al*. 2006) also described an activating role for CtBPs as CtBPs are recruited to Wnt responsive elements in promoters of target genes upon Wnt stimulation.

This is the first time a functional interaction between CtBPs and a HIF-target gene as well as a potential role for CtBPs in HIF-mediated pH regulation has been determined. However, it was recently demonstrated that the transcription factor ZEB1 activates CA9 expression which leads to increased intracellular pH and reduced caspase-3-mediated and cisplatin- and pingyangmycin-induced apoptosis. Furthermore, high ZEB1 expression correlates with high CA9 expression and poor prognosis in tongue tumours, showing a novel role of CA9 expression in the resistance to

chemotherapy (Zheng et al. 2015). Additionally, it was described that HIF is able to modulate the expression and activity of other transcription factors involved in epithelial to mesenchymal transition. In this context, the transcription factor SNAIL is up-regulated by hypoxia in breast cancer cell lines which reduces the expression of E-cadherin and enhances vimentin expression (Lundgren et al. 2009). Further, (Zhu et al. 2013) described that targeting of HIF-1α reverses the mesenchymal phenotype in pancreatic cancer cells, and that this process is correlated to levels of SNAIL expression. HIF-1α is also known to interact with the epithelial transcription factor TWIST. It was found that in zebrafish embryos during the formation of the neural crest by highly motile embryonic cells, their mesenchymal phenotype is maintained by repression of *E-cadherin* in an HIF-TWIST-dependent manner (Achouri et al. 2007; Barriga *et al*. 2013). The same effect was also described for hepatocellular carcinoma where the TWIST-HIF-mediated repression of genes which encode the expression of adhesion proteins resolves into a mesenchymal phenotype with enhanced migration and neoplastic capacity (Liu et al. 2014).

Based on co-immunoprecipitation studies performed by (Glasspool *et al*. 2005), CtBPs also interact with the transcription factor SP1 in order to repress induction of gene expression at the promoters of the telomerase-encoding genes *hTERC* and *hTERT* by modifying chromatin structure. This is interesting as *CA9* expression in hypoxia as well as at high cell numbers is regulated via the interaction of HIF-1 with SP1 (Kaluz et al. 2009; Kopacek et al. 2005). This may provide a possible mechanism of CtBP-HIF-1 mediated regulation of *CA9*. All in all, this solidifies the role of CtBPs as transcriptional activators and indicates a novel role for CtBP in pH regulation in hypoxia.

The direct stabilisation of HIF by glycolytic metabolites has been demonstrated to activate HIF target genes (Lu et al. 2002). However, this may not be the case for CA9 as CA9 is not co-expressed with LDH-A in non-small cellular lung cancer (Koukourakis et al. 2003). CA9 is strictly regulated by HIF-1 and SP1, and is activated by MAPK and PI3K signalling in a cell type-specific manner (Grabmaier et al. 2004; Kaluz et al. 2009). Consequently, CA9 expression is regulated by glycolysis in an indirect manner. CtBPs are activated by increased NADH levels generated by augmented glycolysis in hypoxia (Zhang et al. 2006).

Excluding the results generated with MTOB, it was determined that inhibition of CtBP expression by siRNA impairs CA9 expression induced by hypoxia and DMOG, whereas the overexpression of wildtype CtBP upregulated CA9 expression. Therefore, CtBP potentially provide a functional link between enhanced glycolysis in hypoxia and regulation of the HIF-target gene CA9. However, the formation of an activating complex at the *CA9* promoter consisting of CtBPs and HIF-1 could not been demonstrated due to technical difficulties with the chromatin immunoprecipitation assay. This is discussed in greater detail in Appendix B. In this context, it has been demonstrated that

HIF-1α protein responds to glycolysis-dependent NAD^+ concentrations. In normoxia, when NAD^+:NADH ratio is elevated the NAD^+-dependent deacetylase Sirtuin 1 (SIRT1) (Lim et al. 2010) and SIRT2 (Seo et al. 2015) deacetylate the HIF-1α protein, thus enabling hydroxylation by PHD2. In hypoxia, when NAD^+ is decreased SIRTS are inhibited and HIF-1α protein is stabilised. SIRT and HIF-1 have been demonstrated to interact in tissue but *in vivo* implications are less clear. (Fleuriel et al. 2015) first pointed towards a role for CtBPs to co-inhibit *SIRT1* transcription, thereby supporting the stabilisation of HIF-1α protein in hypoxia. However, the paper was retracted and the potential role for CtBPs in the regulation of HIF-1 remains elusive. Therefore, this thesis is the first demonstration of a novel, functional interaction between CtBPs and HIF-1 to regulate CA9 expression in hypoxia.

Gene expression and protein data may suggest a novel and specific role for CtBPs in the regulation of intracellular pH by activating CA9 expression. Upregulated glycolysis in hypoxia protects malignant cells from acid-induced cell death by preserving ATP levels via an undetermined mechanism (Parks et al. 2013). In this context, it is suggested that the activation of CA9 in a glycolysis- and CtBP-dependent manner prevents intracellular acidification and thereby enables cell survival in acidosis. Consequently, it was the next step to investigate the role of CtBP-dependent CA9 expression in the survival of hypoxia-induced acidosis. The outcome and its implications as well as the role of other acid extruding mechanisms are discussed below.

6.3 CtBPs improves CA9-mediated survival of hypoxia-induced acidosis in MCF7 breast cancer cells with transient p53 inhibition

6.3.1 Optimisation process

In order to determine the role of CtBPs and CA9 in the survival of acidosis, MCF7 were first incubated at 1% O_2 for 24 h to induce CA9 expression which was followed by the incubation at pH 6.3 in bicarbonate-free medium at 20% O_2. Cell viability was determined by colony forming assay. These experimental conditions were the outcome of an optimisation process. CA9 protein stability 24 h post-re-oxygenation was confirmed. Therefore, the incubation period in normoxia does not impact CA9 expression. Additionally, the stability of the CA9 protein in MCF7 corresponds with literature findings that demonstrated that CA9 protein expression is stably expressed after re-oxygenation (Vordermark et al. 2005). Further characterisation of CA9 expression in MCF7 determined that CA9 is not induced by acidosis in normoxia. This contradicts (Ihnatko et al. 2006) but agrees with the majority of the literature, and demonstrates the strict reliance of *CA9* induction on hypoxia in MCF7 (Grabmaier et al. 2004; Wykoff et al. 2000).

However, the optimisation experiments also showed that bicarbonate-free medium potentially reduces cell viability (Fig. 5.4 and Fig. 5.6), and thereby masks the impact of experimental parameters such as pH, CtBP expression, and O_2 concentration on cell viability. This may be because, unlike commercially available DMEM, this bicarbonate-free medium was prepared in house following the protocol described in (Parks et al. 2013), and therefore did not undergo the same degree of optimisation. However, the bicarbonate in conventional DMEM overrides CA9 activity (Parks et al. 2013). Therefore, the impact of CA9 on cell survival had to be investigated in an environment low in bicarbonate. Additionally, in section 5.2.2, it was determined that incubation for 24 h in 1% O_2 followed by another 24 h in 1% O_2 at pH 6.3 completely abolishes long-term viability. CA9 protein is destabilised at pH 6.3 compared to pH 7.4 (Fig. 5.7) when MCF7 were transfected with siRNA. This may be due to general poor viability after a total incubation time in hypoxia of 48 h, including 24 h of acidosis. Additionally, the transfection with siRNA may have further aggravated cellular stress.

6.3.2 CtBP and p53 expression promotes CA9-mediated survival of acidosis

The inhibition of CA9 and p53 alone is not sufficient to impair survival, whereas the transfection with CtBP 1/2 siRNA alone or in combination with p53, or with CA9 and p53, reduces long-term survival. Additionally, as elaborated during the optimisation process, MCF7 cells sustain cell viability and proliferation in acidic conditions via p53 expression.

The role of p53 in cancer cell survival is discussed controversially and is highly context-dependent. In colon cancer cells, the survival of acidic conditions is mediated by the selection of p53-negative cells as cells expressing wildtype p53 undergo p53-dependent apoptosis (Williams et al. 1999). There is evidence, that in some tumours the decision between survival and apoptosis in hypoxia is regulated by the competition between HIF-1α and p53 for binding the transcriptional co-activator p300 (Schmid et al. 2004; Vleugel et al. 2005). Therefore, low levels of p53 do not inhibit HIF-1-mediated gene transcription. Also, it was reported that p53-negative cancer cells express higher levels of HIF-1α due to the MDM2-dependent ubiquitination of HIF-1 which is promoted by p53 (Chen et al. 2003). On the same note, (Cosse et al. 2007) reported increased p53 protein expression following 16 h incubation at 1% O_2. However, there is no difference in p53 expression levels at 20% or 1% O_2 in MCF7 cells (Fig. 5.16). Also, the downregulation of p53 expression by siRNA does not alter *CA9* mRNA expression levels (Fig. 5.24). Therefore, this model of hypoxia-mediated p53 regulation does not apply for MCF7.

There is a growing body of evidence suggesting that the expression of wildtype p53 promotes survival in some epithelial-derived tumours, including breast cancer. This results in negative consequences for prognosis and therapy as ER^+ tumours were demonstrated to be more resistant against chemotherapy than their ER^- counterparts (Bertheau et al. 2013). In pre-clinical mice models, (Jackson et al. 2012) demonstrated that mice harbouring wildtype p53-expressing tumours relapsed faster than p53-negative controls. Additionally, mice with wildtype p53-expressing tumours grow tumours of larger volumes than mice harbouring tumours with loss of heterozygosity mutations or which are p53-negative. p53-negative tumours exhibited greater regression, smaller tumour volumes, and relapsed later. This occurs as p53-negative cells are not able to arrest their cell cycle upon cell stress, which leads to aberrant mitosis, and consequently to apoptosis.

Another pro-survival mechanism of p53 relates to its function as metabolic regulator. p53 lowers the rate of glycolysis by reducing the flow of glucose into glycolysis by inhibiting the expression of GLUT1, GLUT4, and by activating TIGAR (Bensaad et al. 2006; Schwartzenberg-bar-yoseph et al. 2004). Additionally, p53 reduces the flow of glucose into lactate by inhibiting mitochondrial PDH kinase 2. This causes an increase in PDH activity and acetyl CoA, which is fed into the TCA cycle

and ultimately into mitochondrial respiration (Contractor & Harris 2012). Further, p53 promotes the survival in an environment of fluctuating nutrient availability by inducing p21-medaited cell cycle arrest (Maddocks et al. 2012; Reid et al. 2013) or autophagy (Broz & Attardi 2013; Lee et al. 2012). Therefore, p53 balances anabolic metabolism, energy generation, and cell survival in an environment of fluctuating nutrients and metabolic stress (Fig. 6.1).

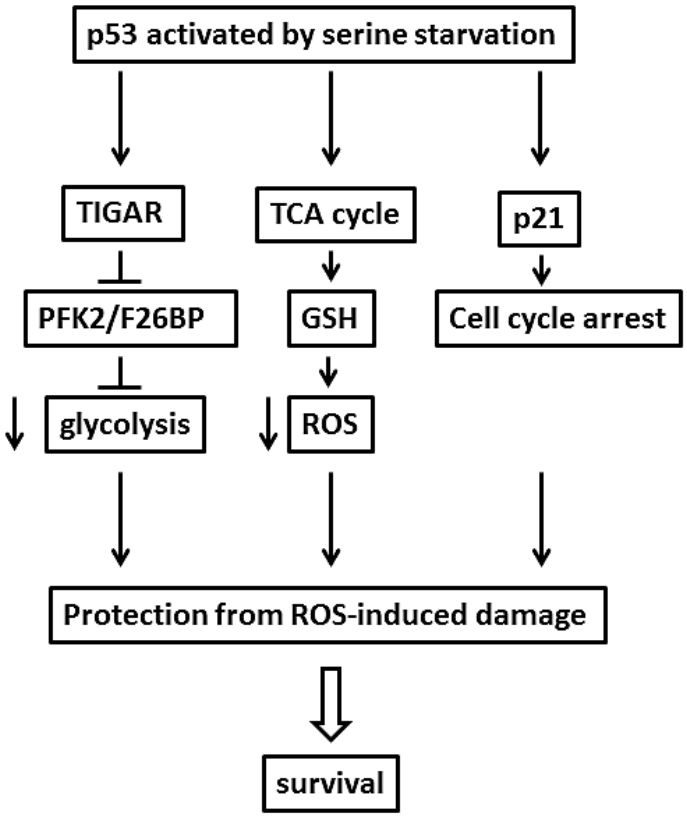

Fig. 6.1: Model of p53-mediated survival of amino acid starvation. P53 may promote survival of fluctuating nutrients by metabolic reprogramming. Serine starvation activates p53 which in turn activates TIGAR and p21. TIGAR reduces glycolysis by inhibiting PFK2/F26BP. Remaining serine is utilised to produce GSH via the TCA cycle. Additionally, p21 induces cell cycle arrest at G_1. Consequently, cells are protected from ROS-induced damage which promotes survival. This model is based on the research of (Maddocks et al. 2012).

These balancing capacities described above are lost in p53-negative cancer cells, such as MDA-MB-231. This loss of p53 expression enables aggressive growth but also impairs the ability to respond to nutrient starvation or hypoxia. In this context, it is suggested that in MCF7 with silenced CtBP and p53 expression, the downregulation of p53 causes an increase in glycolysis and impairs the ability to induce cell cycle arrest. This may lead to upregulated glycolysis, further increasing extracellular acidosis, and to aberrant mitosis. Additionally, reduced CtBP expression may cause a decrease in CA9 expression, and therefore cells are incapable of adjusting to acidosis. MCF7 potentially depend on both mechanisms which have been suggested above, as the combined silencing of p53 and CtBPs, or of p53 and CA9, is required to impair survival (Fig. 6.2).

The outcome that reduction of CA9 expression alone is not sufficient to impair long-term survival points towards the important role of protective wildtype p53 expression in MCF7 breast cancer cells. However, the fact that reduced CA9 and CtBP expression does not reduce survival in the p53-mutant breast cancer line MDA-MB-231 raises the question of the role of p53 in the survival of hypoxia-mediated acid stress.

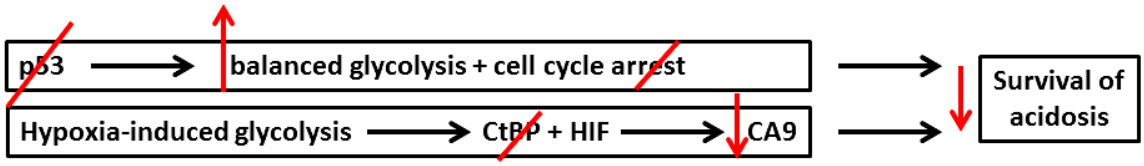

Fig. 6.2: In MCF7 breast cancer cells, the survival of hypoxia-induced acidosis is potentially mediated by the expression of p53 and CtBPs. Experimental evidence suggests that inhibiting p53 upregulates glycolysis, thereby engraving extracellular acidosis, and promotes aberrant mitosis through continuation of the cell cycle. Additionally, the lack of CtBPs impairs CA9 induction in hypoxia. Both processes contribute to reduced long-term viability as inhibition p53 and CA9 alone is not sufficient to impair viability in acidosis.

The dependence on p53 may be cell and tumour type specific as there is no evidence that mutated p53 is causal for tumorigenesis in luminal tumours whereas in basal-like and Claudin-low tumours the expression of mutated p53 leads to epithelial to mesenchymal transition and to a stem cell-like phenotype (Coradini et al. 2012).

The comparatively small impact of siRNA on long-term survival may be due to cell growth in two-dimensional tissue culture. Three-dimensional spheroids substantially differ from monolayers in their biological properties as large spheroids exhibit pH gradients, spatially varying mechanisms of acid extrusion and diffusion distances, and hypoxic cores. Therefore, spheroids are a closer reflection of tumour biology *in situ* (Gatenby et al. 2007). (Swietach et al. 2008) demonstrated that CA9 does not impact pH_i regulation, including H^+ efflux by transporter proteins or the intrinsic buffering capacity in two-dimensional growth, whereas in spheroids CA9 expression reduces the heterogeneity of pH_i by facilitating the venting of intracellular CO_2. Thus, CA9 enables an alkaline pH_i and tumour survival. Consequently, the inhibition of CA9 alone may have not been sufficient to affect survival of cells in two-dimensional cell culture. Therefore, it may be of interest to determine the impact of CtBP-co-activated CA9 on the survival of acidosis in MCF7 with transient p53-silencing in three-dimensional growth. However, this is accompanied by technical challenges as transient silencing of gene expression is only temporary and may not be sustained until spheroids are fully formed. Additionally, considering the potential off-target effects of MTOB, inhibiting CtBP function by MTOB may not be a suitable alternative to the transfection with siRNA. Additionally, the lack of CA9 expression may have been compensated by the CA isoforms CA12 and CA2 (Parks et al. 2016).

Another limitation was that cells did not survive the incubation in 1% O_2 in a hypoxic chamber or in 1 mM DMOG for 48 h. Therefore, it was first demonstrated that CA9 protein expression, and therefore also protein activity, is stable after re-oxygenation. Consequently, the experiment was performed in normoxia once CA9 was activated. However, the growth of large breast cancer spheroids as described in (Gatenby et al. 2007) may also provide the advantage of producing a hypoxic core without relying on a hypoxic chamber.

All in all, the hypothesis is accepted that CtBPs activated by hypoxia-induced glycolysis co-induce CA9 expression in a HIF-dependent manner, and that this co-regulation promotes survival of acidosis. However, further research has to be performed to dissect the role of CtBPs, p53 and CA9 in the survival of acidosis, and to determine a mechanistic interaction between HIF and CtBPs at the *CA9* promoter.

6.4 Future work

It is suggested that future work focuses on the core question of this project which is concerned with the interaction of CtBPs and HIF at the *CA9* promoter, the characterisation of this interaction, and its impact on survival of acidosis. Therefore, it is proposed to optimise the chromatin immunoprecipitation assay described in Appendix B and to determine the mechanistic interaction of HIF and CtBPs at the *CA9* promoter in MCF7.

Additionally, it is suggested to determine whether the interaction of HIF and CtBPs at the *CA9* promoter results in an activated chromatin structure, and therefore to additionally probe for tri-methylation of the lysine residue at histone H3K9 which is a prominent marker of heterochromatin; the "closed" form of chromatin (Ledaki et al. 2015). It may also be of interest to investigate the impact of glucose concentrations or glycolysis on the regulation of hypoxia-induced *CA9* expression by applying ChIP. Alternatively, the pharmacological inhibition of the H3K9 methyltransferase G9a/GLP may rescue the induction of *CA9* expression in MCF7 with silenced CtBP expression or downregulated glycolysis (Ledaki et al. 2015).

(Ledaki et al. 2015) also identified heterogeneous *CA9* expression in MCF7 where hypoxia-induced *CA9* expression is restricted to cell populations with cancer stem cell-like phenotypes. It may be of interest to determine whether this is also true for the CtBP-HIF-mediated regulation of CA9 evaluated in this thesis.

It is proposed that the silencing of p53 potentially upregulates glycolysis, and thereby engraves extracellular acidosis, and may promote aberrant mitosis by progression through the cell cycle while the lack of CtBP expression impairs *CA9* induction in hypoxia. Therefore, it may be interesting to determine the impact of combined p53 and CtBP, or p53 and CA9 silencing on cell cycle progression by staining with bromodeoxyuridine/fluorodeoxyuridine (BrdU) and propidium iodide (PI) and subsequent analysis by flow cytometry. BrdU incorporates into newly synthesised DNA whereas PI labels total DNA and thus enables distinguishing between the transition G_1/S phase or G_2/M (Cecchini et al. 2012; Jones et al. 2005). Consequently, it is expected to find more cells arrested in the G_1 phase if p53 and CtBPs mediate cell viability by preventing aberrant mitosis. Additionally it is expected that in MCF7 with silenced p53 and CtBP p53 and CA9 expression potentially exhibit intracellular acidification due to increased glycolysis and the abolition of CA9 function. Therefore, it is of interest to measure pH_i in these cells.

However, as discussed above, pH regulation is complex and may be more relevant in three-dimensional structures. Consequently, it may be interesting to repeat this experiment in large spheroids with hypoxic cores as described in (Gatenby et al. 2007) and as discussed above. In this

context it may also be of interest to include acid extruding mechanisms, such as bicarbonate uptake by SLC4 transporter proteins (McIntyre et al. 2016; Parks & Pouyssegur 2015).

Chapter 7: Summary and conclusion

Glycolytic metabolism and hypoxia are driving forces of tumour progression and correlate with poor outcome and prognosis. C-terminal binding proteins link glycolysis with the regulation of genes relevant for cancer progression via their NADH-dependent activation. It is unknown, whether CtBPs also regulate the expression of HIF-target genes. Therefore, based on preliminary gene expression data generated prior to the start of this project, it was hypothesised that HIF-mediated responses to hypoxia depend on the redox and glycolytic state of a cell, and that this response is mediated in an HIF-CtBP dependent manner. Consequently, the aims of the project were to determine the impact of glycolysis and hypoxia on the CtBP-HIF-1-dependent regulation of HIF-target gene expression. Further, it was aimed to investigate the mechanistic and functional interactions between CtBPs and HIF to regulate HIF target gene expression. The third aim was to experimentally determine the role of CtBPs and HIF-1 interaction in breast cancer cell survival of hypoxia-induced acidosis.

To address these aims, the preliminary gene expression data were validated for *ADM* and *CA9*. In MCF7, the silencing of CtBP1 and CtBP2 expression with CtBP 1/2 siRNA or partly inhibiting glycolysis with 2-DG demonstrated that hypoxia-induced *ADM* expression is increased by the treatment with 2-DG whereas *ADM* expression is inhibited when CtBPs were silenced, as determined by TaqMan™ reverse-transcription PCR. In MDA-MB-231, glycolysis and CtBP expression have no impact on *ADM*. Based on these results *ADM* was excluded from further experiments as they contradicted preliminary findings. However, it was demonstrated for CA9 protein and gene expression that the transfection with CtBP siRNA and the partial inhibition of glycolysis with 2-DG reduces the hypoxia-induced expression of CA9 in MCF7 breast cancer cells, whereas the treatment with 2-DG has no effect in MDA-MB-231. Therefore, preliminary findings were confirmed for CA9. The functional interaction between HIF-1 and CtBPs to activate CA9 expression was further characterised in the renal carcinoma cell lines with constitutive HIF activation, A498 and 786-O. By transient transfection with CtBP siRNA and incubation in 2-DG, it was determined that CA9 protein expression is not affected by glycolysis and the role of CtBP expression in these cell lines remains unclear. However, cell density majorly effects CA9 expression in both renal carcinoma cell lines. Consequently, A498 and 786-O were omitted from further studies. Cell density also increases CA9 protein expression in normoxia in MDA-MB-231 breast cancer cells but not in MCF7.

In addition to CtBP siRNA and 2-DG, the functional interaction between CtBPs and HIF to regulate CA9 mRNA and protein expression was investigated in fructose-adapted MCF7. The role of CtBPs

was determined in MCF7.CtBP2 and MCF7.CtBP-Mutant. Additionally, CtBP expression was inhibited by MTOB. In order to confirm the induction of the HIF-target genes analysed in this study by HIF, hypoxia was replaced by the PHD inhibitor DMOG.

It was also investigated whether the functional regulation of CA9 is unique or whether other HIF-target genes are also regulated in a CtBP-HIF-dependent manner. Therefore, the HIF-target genes *PDK1*, *INSIG2*, *EGLN3*, *FAM162A* and *TMEM45A* were included in the study. *CA9* is the only HIF-target gene in this study that is activated in a CtBP-HIF-dependent manner as its expression, induced by hypoxia or DMOG, is inhibited when MCF7 were treated with 2-DG or cultivated in fructose. Moreover, silencing of CtBP expression by siRNA and inhibiting CtBP activity by MTOB reduces CA9 expression, whereas CA9 is increased in CtBP2-overexpressing MCF7.CtBP2 cells.

The role of CA9, jointly activated by CtBPs and HIF, in the survival of acidosis was determined in MCF7. As demonstrated by colony forming assay, MCF7 maintain cell viability via the joint activation of p53 and CtBP-HIF-induced CA9 expression. Consequently, it is concluded that:

- *ADM* expression in hypoxia depends on glycolysis and the availability of glucose, independent from CtBPs.
- The regulation of CA9 expression in the renal carcinoma cell lines A498 and 786-O is mediated by multiple factors, and is therefore complex.
- CA9 mRNA and protein expression in hypoxia is uniquely regulated by a functional interaction between CtBPs and HIF-1, whereas the HIF-target genes *PDK1*, *INSIG2*, *EGLN3*, *FAM162A* and *TMEM45A* are not regulated in a CtBP-dependent manner.
- The CtBP-HIF-mediated regulation of CA9 may be limited to epithelial-like (breast) cancer cells such as the ER^+ cell line MCF7.
- The role of p53 and CtBPs in the survival of hypoxia-induced acidosis may be subtype-dependent and unique to epithelial-like, ER^+, luminal breast cancers.

Therefore, this thesis provides experimental evidence for a novel, activating role for CtBPs in the HIF-mediated regulation of CA9 expression. In conjunction with p53, there may be a protective role for CtBP-induced CA9 expression in acidosis. Consequently, the hypothesis stated above is accepted and the aims formed at the beginning of this project have been largely fulfilled. However, this study failed to demonstrate a mechanistic interaction between CtBPs and HIF-1 at the *CA9* promoter due to technical difficulties. Therefore, optimisation of the chromatin immunoprecipitation protocol is required, as well as further research.

The experimental evidence provided in this thesis further strengthens the role of CtBPs as co-activators, and context-dependent and versatile co-regulators of transcription. Additionally, this study provides a novel functional link between upregulated glycolysis in hypoxia and HIF-

mediated responses to acidosis. The experiments performed to determine the impact of CtBP-mediated survival of acidosis further underline the protective role of p53 in luminal, epithelial-derived breast cancer and point towards a subtype-specific regulation of the survival of hypoxia-induced acidosis by p53 and CtBP-HIF. However, further research is required.

Appendices

Appendix A Quality control for TaqMan™ reverse-transcription PCR

In the comparative C_T method which was applied to analyse reverse-transcription PCR data, it is standard praxis to normalise the expression of a gene of interest to the expression of a housekeeping gene (Livak & Schmittgen 2001). Therefore, it is crucial that expression of the selected housekeeping gene is not affected by the experimental procedure. Hypoxia alters the expression of a wide range of genes, highlighting the importance to carefully select a suitable housekeeping gene (Elvidge et al. 2006). The glycolytic enzyme *glyceraldehyde 3-phosphate dehydrogenase* (*GAPDH)* is a commonly used house-keeping gene which is however not suitable in this case as *GAPDH* is upregulated in hypoxia (Graven et al. 1994). Therefore, the cytoskeletal protein β-*actin* (*ACTB*) was selected as housekeeping gene. The following section demonstrates that *ACTB* expression is not affected by hypoxia or the treatment with DMOG, and that the sole application of *ACTB* is sufficient to accurately evaluate HIF-target gene expression. This is demonstrated by applying *CA9* expression in MCF7 as an example.

A.1 The treatment with 1% O_2 or 1 mM DMOG did not biologically alter *ACTB* expression

To determine whether *ACTB* expression is affected by O_2 concentrations or the treatment with 1 mM DMOG, the C_T values of samples treated with either 1% O_2 or 1 mM DMOG of selected experiments were compared to their respective controls. The difference in expression in three independent experiments was evaluated by student's unpaired *t*-test (Fig. A.1). Means in MCF7 treated with siRNA and 2-DG (Fig. A.1A) and in MCF7 treated with MTOB (Fig. A.1B) are significantly different in normoxic and hypoxic samples. However, this is due to the C_T values narrow deviation from the mean, and therefore minor changes in C_T values appear as significantly different while there is no biological relevance. The same accounts for MCF7 treated with siRNA and DMOG (Fig. A.1C). The treatment with DMOG significantly altered *ACTB* expression but within a range that is biologically irrelevant. Therefore, *ACTB* expression is not affected (biologically) by hypoxia or by the treatment with DMOG.

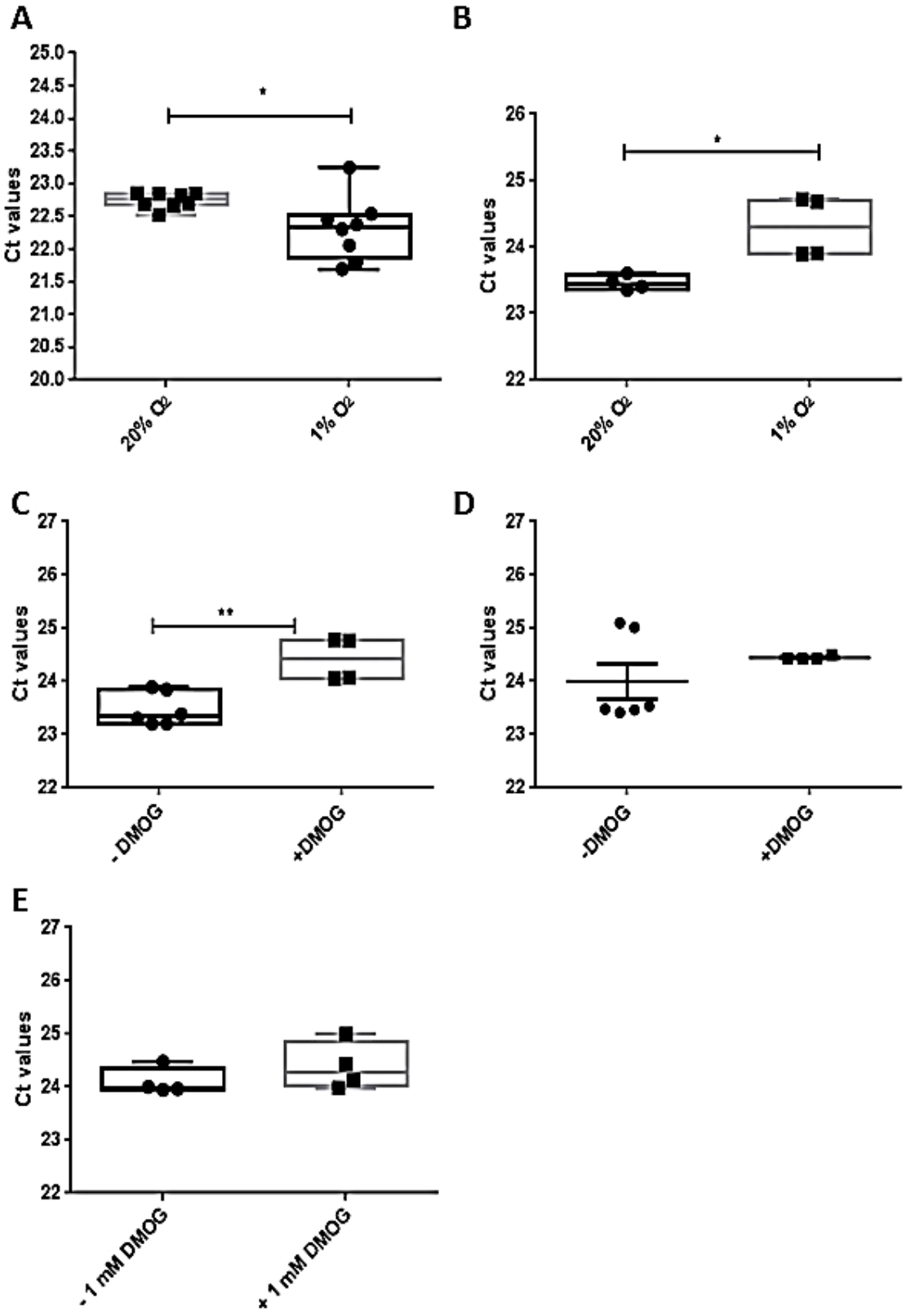

Fig. A.1: The incubation in 1% O_2 or the treatment with 1 mM DMOG has no biological impact on *ACTB* expression in MCF7 breast cancer cells in selected experiments. Displayed is the mean of three independent experiments (n=3) and the range from minimum to maximum. **A:** The impact of hypoxia on MCF7 treated with 50 nM siRNA or 10 mM 2-DG. **B:** The impact of hypoxia on MCF7 treated with 4 mM MTOB. **C:** The impact of DMOG on MCF7 treated with 50 nM siRNA. **D:** The impact of DMOG on MCF7 treated with 10 mM 2-DG. **E:** The impact of DMOG on MCF7 treated with 4 mM MTOB.

A.2 Normalisation to *ubiquitin* as second housekeeping gene does neither alter *CA9* expression nor the level of significance

Normalisation of target gene expression to the expression of a reference gene (housekeeping gene) is standard practise in data analysis of quantitative reverse-transcription PCRs, and is performed to compensate for experimental variations. However, there may be a natural variability in the expression of a reference gene such as variability between different cell lines, tissues or individuals. Therefore, it is common to normalise against a set of reference genes to minimise this natural variability. However, the utilisation of several housekeeping genes is time consuming and expansive. Consequently, it was determined whether the normalisation of *CA9* expression to *ACTB* is sufficient as internal control or whether the application of a second housekeeping gene was required. For evaluating the impact of normalising to two housekeeping genes, *CA9* expression was normalised to the mean C_t values of *ACTB* and *ubiquitin (UBC)* in selected experiments. In MCF7 incubated in 1% O_2 and treated with either siRNA or 2-DG, the additional normalisation to *UBC* does not reduce intra-experimental variability as the level of significance remains unchanged (Fig. A.2).

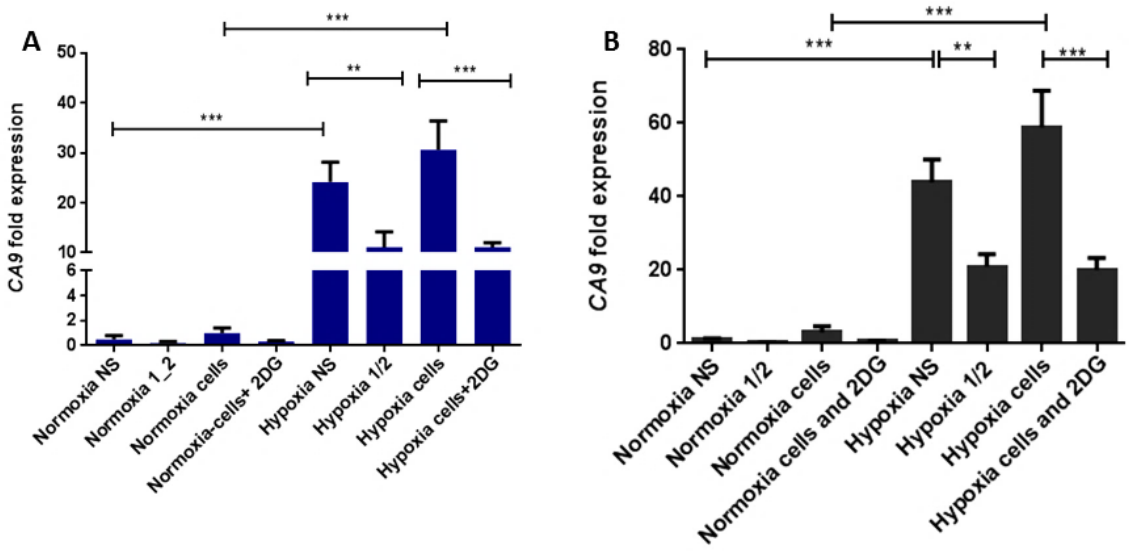

Fig. A.2: The application of *UBC* as second housekeeping gene does not alter the level of significance and the difference in CA9 fold-induction in hypoxia following the treatment of MCF7 with either 50 nM siRNA or 10 mM 2-DG. Displayed is the mean of three independent experiments and the SEM. **A**: *CA9* expression was normalised to *ACTB*. **B:** *CA9* expression was normalised to the mean C_t values of *ACTB* and *UBC*.

Similarly, normalisation to two housekeeping genes also does not reduce variability within MTOB-treated MCF7 (Fig. A.3).

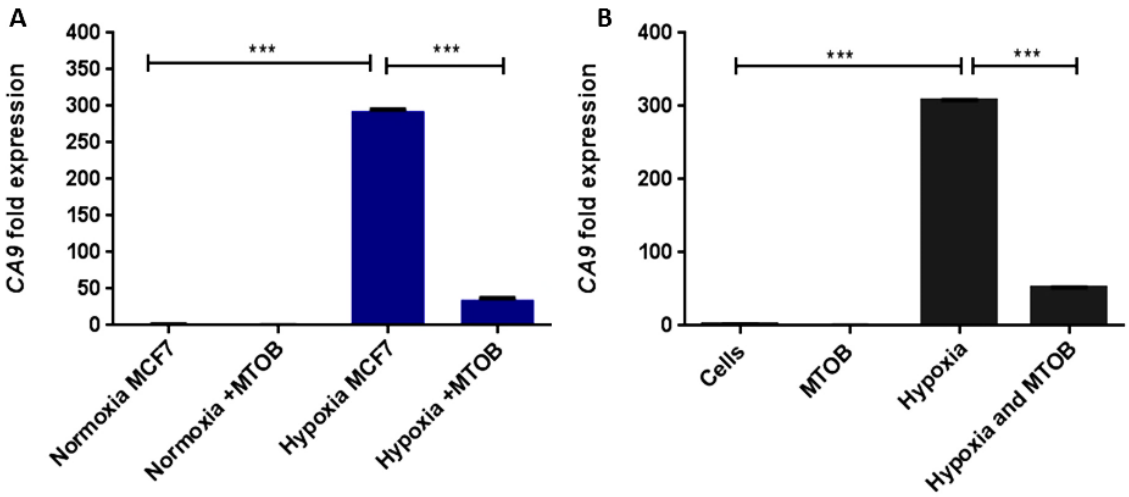

Fig. A.3: The hypoxia-induced fold- expression of *CA9* is not altered in MTOB-treated MCF7 when CA9 expression was normalised to *ACTB* and *UBC*. Displayed is the mean of three independent experiments and the SEM. **A**: *CA9* expression was normalised to *ACTB*. **B**: *CA9* expression was normalised to the mean C_t values of *ACTB* and *UBC*.

In MCF7 treated with DMOG, normalisation to both, *ACTB* and *UBC* slightly reduces intra-sample variation in cells treated with DMOG and CtBP siRNA, thereby slightly increasing the level of significance (Fig. A4). However, the impact is minor, and therefore does not alter overall *CA9* expression in this experiment. Therefore, the conclusions drawn from this experiment remain unchanged.

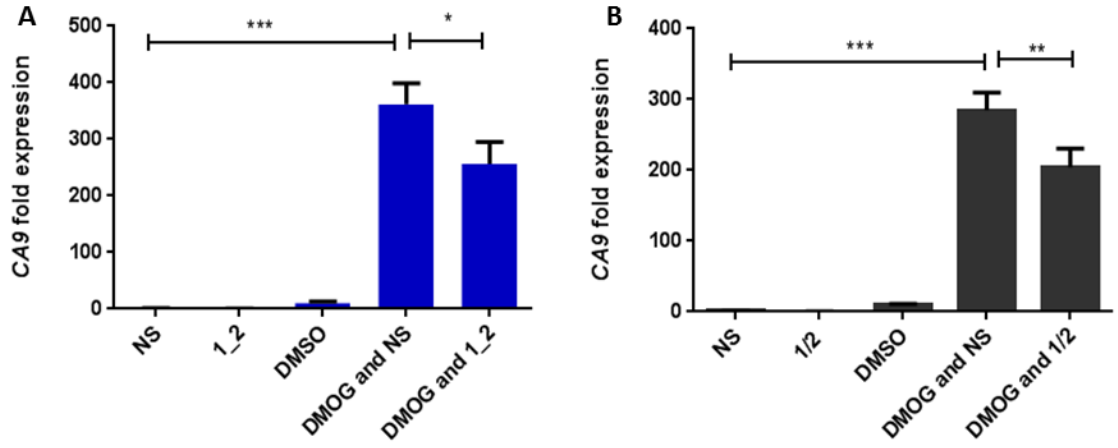

Fig. A.4: The level of significance is increased when DMOG-induced *CA9* expression was normalised to *ACTB* and *UBC* in MCF7 breast cancer cells. Displayed is the mean of three independent experiments and the SEM. **A:** *CA9* expression was normalised to *ACTB*. **B:** *CA9* expression was normalised to the mean C_T values of *ACTB* and *UBC*.

Consequently, the utilisation of *ACTB* as sole housekeeping gene is justified, as normalising to a second housekeeping gene does impact on intra-experimental variability in this case. Also, samples are derived from and compared within the same cell line. Additionally, the fold changes in hypoxia- or DMOG-induced *CA9* expression which are caused by the treatment with CtBP siRNA, MTOB or 2-DG are large enough not to be masked by intra-experimental variation. However, small fold-changes may require normalisation to several housekeeping genes in order to be able to distinguish fold changes from intra-experimental variations.

Appendix B Determination of HIF-1-, CtBP- and RNA polymerase II-binding at the *CA9* promoter

B.1 The principle and workflow of Chromatin Immunoprecipitation

B.1.1 The principle of Chromatin Immunoprecipitation

Chromatin immunoprecipitation (ChIP) is a commonly performed assay to map protein interactions with a gene of interest or the genome as a whole. It is applied to either determine the enrichment of a protein of interest on a locus of interest (Wang et al. 2015; Zheng et al. 2015) or mapping a protein of interest or its modification on a specific locus (Shi et al., 2003), or the whole genome (Schödel et al. 2011; Wei et al. 2006).

Crosslinking chromatin immunoprecipitation comprises of several steps (Fig. B1). First, DNA-interacting proteins are crosslinked to chromatin by formaldehyde. Then, chromatin is fragmented by ultrasound and chromatin fragments in which the antigens of interest are present are enriched by immunoprecipitation. Consequently, unbound chromatin is removed by washing and purified DNA is analysed by either PCR to determine the abundance of the target of interest on a specific locus, or by microarray and next generation sequencing to allow for mapping of the protein of interest over the whole genome. Data interpretation is supported by three controls. In order to distinguish signal from background, isotype matched control antibodies are used as negative controls. To determine the specifity of the enrichment of the target of interest, a positive control locus which is known to be bound to the protein of interest is chosen and is used as positive control locus. In this case the housekeeping gene *GAPDH* was chosen as positive control locus for the immunoprecipitation with RNA polymerase II. Further, sheared chromatin that was not immunopreticipated is used as input control to demonstrate that the designed primers recognise the target regions of interest, in this case the *CA9* promoter.

In order to determine the binding of HIF-1α, CtBPs and RNA polymerase II at the activated *CA9* promoter, the MAGnify™ Chromatin Immunoprecipitation System (Invitrogen™ by *life* technologies™) was used. All reagents excluding primer pairs, PCR reagents, antibodies, PBS and formaldehyde were provided by the manufacturer.

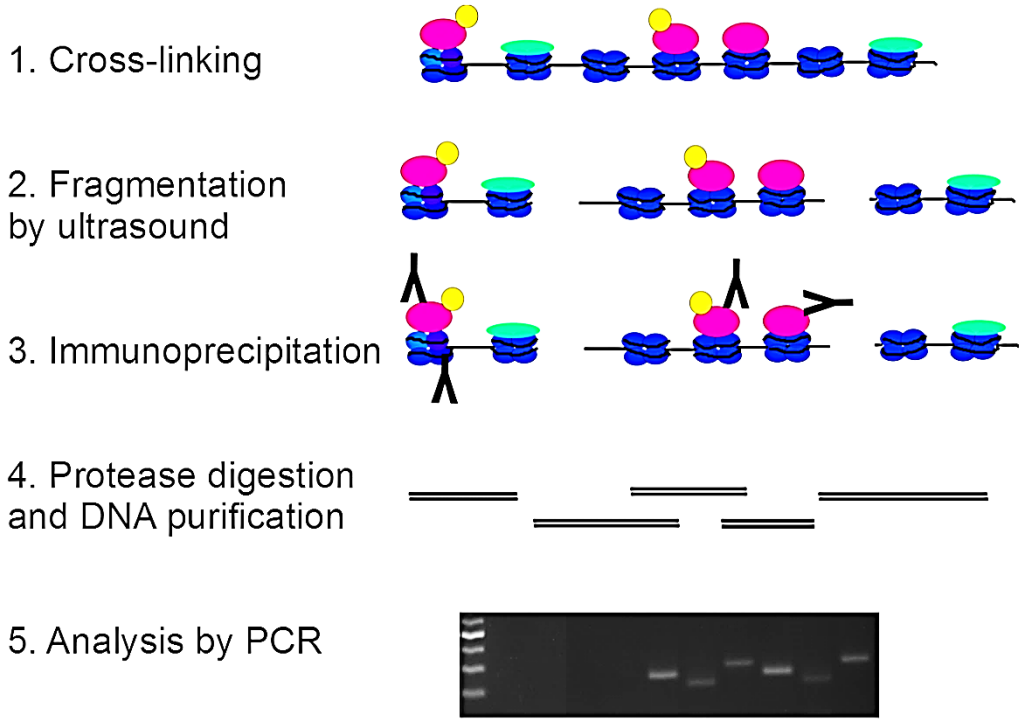

Fig. B.1: The principle of chromatin immunoprecipitation. First, DNA-interacting proteins (pink, yellow, green) and chromatin (blue) are reversibly crosslinked by formaldehyde. In the following, chromatin is sheared into fragments of 200- 500 bp length by sonication and chromatin fragments in which the target antigens are present are enriched by immunoprecipitation. Finally, DNA is purified and analysed by PCR to determine the abundance of target DNA compared to chromatin input control.

B.1.2 Cell culture

MCF7 breast cancer cells were seeded at a density of $2x10^6$ in 10 ml DMEM in a 10 cm dish in order to reach around $4x10^6$ cells for crosslinking DNA bound proteins to the *CA9* promoter. This corresponded to the desired 80% confluency on the day of crosslinking. 24 h after seeding, DMEM was replaced by fresh medium. For *CA9* activation, cells were incubated at either 1% O_2 or 20% O_2 in a hypoxic chamber for 18 h or at 20% O_2 and DMEM supplemented with 1 mM DMOG for 18 h as described before.

B.1.3 Crosslinking DNA-bound proteins to chromatin

The following procedure was performed as fast as possible in order to avoid the oxygen-dependent degradation of HIF-1α. First, the hypoxic medium or the DMOG-containing DMEM was replaced by 5 ml of fresh DMEM. Immediately, 135 µl of 37% formaldehyde (Fisher Scientific, UK) was added to the cells to obtain a final concentration of 1% and incubated at room temperature for 10 min. After the incubation time, crosslinking was stopped by adding 500 µl of room-temperature 1.25 M glycine. After 8 minutes of incubation at room temperature, the medium was aspirated and the crosslinked cells were carefully washed with sterile cold PBS. From this step onwards all samples were handled on ice. Using a cell scraper, the crosslinked cells were transferred into 1.5 ml sterile Eppendorf tubes and centrifuged at 200x *g* for 10 min at 4 °C to form a pellet. The supernatant was carefully aspirated and the remaining cell pellet was lysed immediately.

B.1.4 Lysing the crosslinked cells

In order to lyse the crosslinked cells, lysis buffer containing protease inhibitors was added to the cell pellet (Tab. B.1) and re-suspended by mild pulses on the vortex mixer. Subsequently, the cells were incubated for 10 min on ice, snap frozen with liquid nitrogen, and stored at -70 °C until further use.

Tab. B.1: Lysis buffer preparation

Cell number	*Total volume lysis buffer and protease inhibitors 200x [µl]*	*Volume lysis buffer [µl]*	*Volume protease inhibitors 200x [µl]*
$1x10^6$	50	49.75	0.25
$4x10^6$	200	199	1

B.1.5 Fragmentation of chromatin

For analysis by semi-quantitative endpoint PCR, chromatin fragments between 200-500 bp were recommended by the manufacturer. Sonication was the preferred method for shearing as formaldehyde restricts the access of the enzyme micrococcal nuclease which is used for enzymatic chromatin shearing. During the sonication process all samples were stored on ice to prevent overheating which could lead to a reversion of the crosslinking. The lysed cells were sonicated for five cycles at an intensity of 3.0 consisting of 15 s on and 20 s off. First, sonicated samples were directly sap frozen with liquid nitrogen and stored at -70 °C until further use. However, due to high noise the literature was consulted and based on most protocols a centrifugation step was included where the sonicated samples were centrifuged at 20,000x *g* at 4 °C for 5 min to remove debris. Also, standard PCR and Eppendorf tubes were replaced by low-retention tubes (alpha laboratories) in order to avoid contamination of downstream reactions. Consequently, following centrifugation, the supernatant which contained the chromatin was transferred into 500 µl sterile low-retention tubes and snap frozen with liquid nitrogen. 10 µl from each sample were reserved for evaluation of fragment size by agarose gel electrophoresis.

In order to evaluate the fragment size of the sheared chromatin, agarose gel electrophoresis was performed. To prepare a 2% agarose gel, 1.5 g agarose (Fisher Scientific, genetic analysis grade) was dissolved in 75 ml of 1xTAE buffer (see buffer list in Appendix D) by heating the solution in the microwave at medium to high heat for 2 min. Once the agarose was dissolved 1.8 µl RedSafe™ nucleic acid staining solution 20 000x (iNtRON Biotechnology) was added to the agarose solution and the liquid gel was poured into a cassette to set. Samples were prepared by adding 2 µl of 6x blue/orange loading dye (Promega, UK) to 10 µl of the sheared chromatin and the 100 bp ladder (Promega, UK) was prepared by adding 1 µl of 6x loading dye to 5 µl of ladder. The gel was run in 1xTAE buffer at 60 mA and DNA was visualized by using the GelDoc-It™ Imaging system (UVP).

B.1.6 Coupling the antibodies to Dynabeads®

In order to determine whether HIF-1α and CtBPs bind at the *CA9* promoter to activate gene transcription, chromatin was immunoprecipitated by applying anti- HIF1α-, anti-CtBPs- and anti-RNA polymerase II antibodies and their respective isotype-matched negative controls (Tab. B.2).

Tab. B.2: Antibodies applied in ChIP

Target	*Antibody*	*supplier*	*Stock concentration*	*Final amount*	*Volume added to reaction*
HIF-1α	Polyclonal mouse anti-HIF1α	Novus Biologicals	1 µg/µl	5 µg	5 µl
RNA polymerase II	Monoclonal mouse anti-RNA polymerase II sc47701X (free sample)	Santa Cruz Biotechnology	1 µg/µl	5 µg	5 µl
RNA polymerase II	Polyclonal rabbit anti-RNA polymerase II (N-20X)	Santa Cruz Biotechnology	1 µg/µl	5 µg	5 µl
CtBPs	Polyclonal rabbit anti-CtBPs (H440)	Santa Cruz Biotechnology	0.2 µg/µl	5 µg	25 µl
Mouse	Negative control anti-mouse IgG	Provided by the kit (Invitrogen)	1 µg/µl	1 µg	1 µl
Rabbit	Negative control anti-rabbit IgG	Provided by the kit (Invitrogen)	1 µg/µl	1 µg	1 µl

To conjugate the antibodies to the Dynabeads®, a magnet holding 0.2 ml PCR tubes (DynaMag™-PCR magnet, Invitrogen), tubes, and buffers were placed on ice. All reactions were performed in sterile 200 µl PCR tubes. First, the Dynabeads® were re-suspended by pipetting up and down. Subsequently, 100 µl of cold dilution buffer was added to each sample followed by 10 µl of the re-suspended Protein A/G Dynabeads®. The sample was mixed by pipetting up and down five times. Immediately, the samples were placed into the cold magnet and it was waited until the beads formed a pallet against the wall of the tube. With the tubes still in the magnet, the buffer was carefully removed and replaced by 100 µl of cold dilution buffer. The samples were removed from the magnet and the appropriate amount of antibody was added to its corresponding reaction (Tab. B2). The suspension was gently mixed by flicking the tube. To couple the antibody to the Protein A/G Dynabeads®, the samples were incubated rotating end-over–end at 4 °C for 1 h. After the incubation time, samples were stored at 4 °C to be used at the same day.

B.1.7 Dilution of chromatin

In this step the sheared chromatin with a starting concentration of $1x10^6$/ 50 µl was diluted 1:10 with cold dilution buffer for each ChIP to obtain a cell concentration of $2x10^5$/100 µl (Tab. B.3). For each sample, 100 µl were prepared in excess to provide a margin of safety for clearing unspecific binding chromatin. From this excess chromatin 10 µl of each sample were kept aside to be used as input controls.

Tab. B.3: Pipetting scheme for the dilution of sheared chromatin

Cells per ChIP	*Number of reaction*	*Volume of chromatin*	*Amount of dilution buffer*	*Amount of 200x protease inhibitor*	*Total volume*
$2x10^5$	1	10 µl	89.5 µl	0.5 µl	100 µl

B.1.8 Removing non-specific binding chromatin

The following step was performed on ice. In order to remove nonspecifically binding chromatin, 10 µl protein A/G sapharose beads (GE Healthcare) for every 100 µl diluted chromatin was centrifuged at 3000 rpm for 5 min at 4 °C. The ethanol was removed carefully and the same amount as the beads of cold and sterile PBS was layered onto the pellet and samples were centrifuged at the same conditions as described above. This washing step was repeated one more time. To prevent the beads from drying out they were re-suspended in the same amount of PBS than the ethanol that was removed in the beginning. Subsequently, the A/G sapharose beads were mixed with the diluted chromatin by pipetting up and down with a pipette tip where the end was cut off. The samples were incubated at 4 °C for 60 min rotating end-over-end. After the incubation time, samples were centrifuged at 3000 rpm at 4 °C for 5 min and the supernatant containing the cleared chromatin was transferred to sterile low-retention 1.5 ml Eppendorf tubes (alpha laboratories) and immediately used for ChIP.

B.1.9 Binding chromatin to the beads

During this step, the magnet, buffers, and tubes were kept on ice. To bind the chromatin to the antibody-Dynabeads® complexes, the tubes containing the antibody-beads complexes were centrifuged quickly and placed inside the magnet. After a pellet had formed, the supernatant was removed and immediately replaced by 100 µl diluted and cleared chromatin, spearing 10 µl of each sample to be used as input control. The samples were mixed by gently flicking the tube and incubated for 2 h at 4 °C, rotating end-over-end.

B.1.10 Washing the bound chromatin

Before the washing step, the reverse crosslinking buffer, proteinase K, as well as DNA purification buffer and beads were warmed up to room temperature. All washing steps were performed at 4 °C to keep the buffers, magnets, and samples cold. First, the samples were washed three times with IP buffer 1. For this, tubes were briefly centrifuged to remove liquid trapped in the lids and placed in the magnet for the Dynabeads® to form a pellet. The supernatant was removed carefully without disturbing the pellet and replaced immediately by 100 µl IP buffer 1. The beads were re-suspended by flicking the tube and the samples were rotated end-over-end for 5 min. After the washing step with IP buffer 1, the antibody-Dynabeads®-chromatin complexes were washed with IP buffer 2 in the same way as described for IP buffer 1, but only twice in total.

B.1.11 Reversing the crosslinking

After the unbound chromatin was removed, the crosslinking of DNA-binding proteins to chromatin was reversed. To reverse crosslinking, reverse crosslinking buffer containing proteinase K was prepared (Tab. B.4).

Tab. B.4: Pipetting scheme to prepare reverse crosslinking buffer for one reaction

Component	*Volume [µl]*
Stock reverse crosslinking buffer	53
Proteinase K	1
Total volume	54

The input controls were not bound to Dynabeads® and were therefore prepared separately (Tab. B.5). The reaction was mixed by gently vortexing the tube.

Tab. B.5: Pipetting scheme to prepare reverse crosslinking buffer for input controls

Component	*Volume [µl]*
Cleared chromatin	10
Stock reverse crosslinking buffer	43
Proteinase K	1
Total volume	54

The following steps were performed at room temperature. After washing with IP buffer 2, the tubes were placed in the magnet. Once a pellet had formed the supernatant was carefully removed not to disturb the pellet. The tubes were removed from the magnet and 54 µl of reverse crosslinking buffer containing proteinase K was added to each reaction. The input controls were prepared separately, as described above. In the following, ChIP samples and input controls were incubated at 55 °C for 15 min in a PCR machine (PTC-200, Peltier thermal cycler). After the incubation step, the tubes were quickly centrifuged and placed in the magnet. After the Dynabeads® formed a pellet; the supernatants which contained the samples were transferred into new, sterile 200 µl PCR tubes. Immediately, ChIP samples and input controls were quickly

centrifuged and incubated for 15 min at 65 °C in a PCR machine. Subsequently, the tubes were cooled on ice for at least 5 min. The Dynabeads® were discarded as they were not re-usable.

B.1.12 Purifying the DNA

In order to purify the pulled-down DNA, DNA purification beads were briefly vortexed to re-suspend them. For each sample including the input controls, 50 µl DNA purification buffer was mixed with 20 µl DNA purification beads. After the samples cooled down, 70 µl prepared DNA purification beads was added to the ChIP samples and input controls, and all reactions were re-suspended by gently pipetting up and down. All samples were incubated at room temperature for 5 min. After the incubation time, all samples were placed in the magnet for the magnetic beads to form a pellet. The liquid was removed carefully and replaced by 150 µl DNA wash buffer. The tubes were removed from the magnet and the suspension was re-suspended by gently pipetting up and down. This step was repeated one more time. With the tubes still in the magnet the DNA washing buffer was removed and replaced by 150 µl DNA elution buffer. The samples were removed from the magnet and mixed by pipetting up and down and incubated for 20 min at 55 °C in a PCR machine. Following incubation, the tubes were briefly centrifuged and placed in the magnet. Once the pellet had formed, the supernatant which contained the purified DNA was transferred into sterile 500 µl low-retention tubes. The DNA magnetic purification beads were discarded as they were not re-usable. The purified DNA was stored in aliquots at -20 °C to avoid repeated cycles of freeze-thawing.

B.1.13 Designing CA9 promoter-spanning primers for ChIP

To design primer pairs which span the *CA9* promoter region, the sequence of the *CA9* Promoter region was obtained in the Fasta format from the NCBI homepage (NCBI 2016). The start of transcription was identified as the last 38 base pairs of the sequence by aligning the promoter sequence to the reference *CA9* mRNA ref|NM_001216.2| in the bioinformatic online tool Blast (Tab. B.6).

Tab. B.6: The sequence of the *CA9* promoter region in Fasta format. Alignment with the reference CA9 mRNA ref|NM_001216.2 in Blast is highlighted in red.

>gi|289187424|gb|GU570447.1| Homo sapiens carbonic anhydrase (CA9) gene, promoter region

GCAGAATTCATCTCTCTTCCCTCAATATGATGATATTGACAGGGTTTGCCCTCACTCACTAGATTGTGAG

CTGCTCAGGGCAGGTAGCGTTTTTTGTTTTTGTTTTTGTTTTTCTTTTTTGAGACAGGGTCTTGCTCTGT

CACCCAGGCCAGAGTGCAATGGTACAGTCTCAGCTCACTGCAGCCTCAACCGCCTCGGCTCAAACCATCA

TCCCATTTCAGCCTCCTGAGTAGCTGGGACTACAGGCACATGCCATTACACCTGGCTAATTTTTTTGTAT

TTCTAGTAGAGACAGGGTTTGGCCATGTTGCCCGGGCTGGTCTCGAACTCCTGGACTCAAGCAATCCACC

CACCTCAGCCTCCCAAAATGAGGGACCGTGTCTTATTCATTTCCATGTCCCTAGTCCATAGCCCAGTGCT

GGACCTATGGTAGTACTAAATAAATATTTGTTGAATGCAATAGTAAATAGCATTTCAGGGAGCAAGAACT

AGATTAACAAAGGTGGTAAAAGGTTTGGAGAAAAAAATAATAGTTTAATTTGGCTAGAGTATGAGGGAGA

GTAGTAGGAGACAAGATGGAAAGGTCTCTTGGGCAAGGTTTTGAAGGAAGTTGGAAGTCAGAAGTACACA

ATGTGCATATCGTGGCAGGCAGTGGGGAGCCAATGAAGGCTTTTGAGCAGGAGAGTAATGTGTTGAAAAA

TAAATATAGGTTAAACCTATCAGAGCCCCTCTGACACATACACTTGCTTTTCATTCAAGCTCAAGTTTGT

CTCCCACATACCCATTACTTAACTCACCCTCGGGCTCCCCTAGCAGCCTGCCCTACCTCTTTACCTGCTT

CCTGGTGGAGTCAGGGATGTATACATGAGCTGCTTTCCCTCTCAGCCAGAGGACATGGGGGGCCCCAGCT

CCCCTGCCTTTCCCCTTCTGTGCCTGGAGCTGGGAAGCAGGCCAGGGTTAGCTGAGGCTGGCTGGCAAGC

AGCTGGGTGGTGCCAGGGAGAGCCTGCATAGTGCCAGGTGGTGCCTTGGGTTCCAAGCTAGTCCATGGCC

CCGATAACCTTCTGCCTGTGCACACACCTGCCCCTCACTCCACCCCCATCCTAGCTTTGGTATGGGGGAG

AGGGCACAGGGCCAGACAAACCTGTGAGACTTTGGCTCCATCTCTGCAAAAGGGCGCTCTGTGAGTCAGC

CTGCTCCCCTCCAGGCTTGCTCCTCCCCCACCCAGCTCTCGTTTCCAATGCACGTACAGCCCGTACACAC

CGTGTGCTGGGACACCCCACAGTCAG

To map putative HIF-1α-, CtBPs- and RNA pol II binding sites at the *CA9* promoter, six primers which produce overlapping amplicons were designed by using the online tool http://primer3.ut.ee. After the *CA9* promoter sequence was copied in, the settings were set as "human" in the mispriming library, and both options for left and right primer were selected. Target position was set at 1200. The product size range was chosen to lie between 150-200 bp. Primer size was defined between 20 bp as minimum, 22 bp as medium, and 26 bp as maximum length and the melting temperature was set between 55 °C minimum, 57 °C desired, and 60 °C maximum temperature. The primer GC content was set between 20% minimum, 50% desired, and 80% maximum GC content. The following five primers were designed by adding + 20 bp on the left primer position in order to create overlapping amplicons (Fig. B.2 and Tab. B.7).

Tab. B.7: *CA9* primer sequences and properties

#	*Left primer Sequence*	T_M *[°C]*	*GC [%]*	*Length [bp]*	*Right primer Sequence*	T_M *[°C]*	*GC [%]*	*Length [bp]*	*Amplicon [bp]*
1	TGGGTTCCAA GCTAGTCCAT	59.55	50	20	GTACGTGCATTG GAAACGAG	59.2	50	20	221
2	TGGTGGAGTC AGGGATGTAT	57.78	50	20	GTGCACAGGCA GAAGGTTAT	57.8	50	20	231
3	CTCTGACACAT ACACTTGCTTT	56.65	40.91	22	TGAGAGGGAAA GCAGCTCAT	58.7	50	20	156
4	TAGGAGACAA GATGGAAAGG TC	56.91	45.45	22	AAGTAATGGGT ATGTGGGAGAC	57.2	45.45	22	226
5	AAATAGCATT TCAGGGAGCA AG	57.00	40.91	22	ACTTCTGACTTC CAACTTCCTT	57.2	40.91	22	161
6	AACTCCTGGA CTCAAGCAAT C	57.94	47.62	21	TCCAAACCTTTT ACCACCTTTG	57.0	40.91	22	194

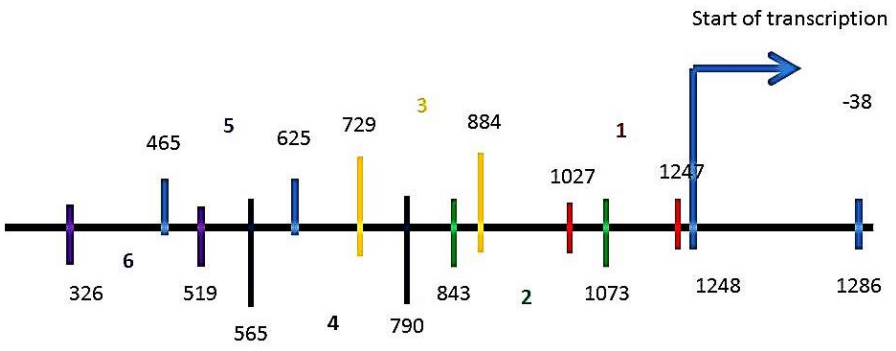

Fig. B.2: **Position of PCR primers along the *CA9* promoter**. 6-1: numbers of primers. Base pairs 326-1286: position of the *CA9* promoter in the *CA9* gene.

B.1.14 Validation of CA9 primers by amplifying genomic MCF7 DNA

First, the designed primers were validated by amplifying MCF7 genomic DNA. For this, primers were reconstituted in nuclease free water, resulting in a stock concentration of 100 pmol/µl. For semi-quantitative PCR, the primers were diluted to result in a working stock concentration of 20 pmol/µl. Genomic DNA was used at a concentration of 100 ng/µl, resulting in 100 ng/reaction. To perform the PCR, 48 µl of mastermix (Tab. B.8) was added to 2 µl of the individual primer sets, resulting in a total reaction volume of 50 µl for each primer set. The reaction was gently mixed by pipetting up and down and semi-quantitative PCR was performed in 35 cycles applying the settings summarized in Tab. B.9. Amplification of the *CA9* promoter region was verified by agarose gel electrophoresis performed with a 2% agarose gel as described earlier.

Tab. B.8: Mastermix for semi-quantitative PCR to validate *CA9* primers

Component	*Supplier*	*Volume per reaction [µl]*
5x Green GoTaq® Flexi buffer	Promega	8
dATP 10 mM	Promega	1
dTTP 10 mM	Promega	1
dCTP 10 mM	Promega	1
dGTP 10 mM	Promega	1
GoTaq® G2 Flexi DNA polymerase 5 U/µl	Promega	0.1
$MgCl_2$ 25 mM	Promega	3
DNA 100 ng/µl		1
Nuclease-free water	Promega	31.9
Total volume		48

Tab. B.9: PCR settings for *CA9* primer validation

	Time [s]	*Temperature [°C]*
Initiation	180	94
Denaturation	30	94
Annealing	30	57
Elongation	30	72
Final extension	120	72

B.1.15 Analysis of ChIP by semi-quantitative PCR and agarose gel electrophoresis

To determine whether the proteins of interest bound to the *CA9* promoter region, ChIP samples and corresponding controls as well as input controls were analysed by semi-quantitative endpoint PCR and agarose gel electrophoresis as described above. However, the protocol required optimisation due to high amounts of unused primers and the formation of primer dimers. Therefore, samples containing primers, DNA, and the goTaq® G2 Flexi DNA polymerase in 5x green goTaq® Flexi buffer were heated to 94 °C separately, immediately added to the reaction and mixed by brief vortexing. Also, the DNA concentration was increased to 2 µl/50 µl (Tab. B.10).

Consequently, 2 µl DNA, 2 µl of the corresponding primer pair and 4.1 µl goTaq® 2G Flexi DNA polymerase mix were added to 41.1 µl mastermix resulting in a total reaction volume of 50 µl (Tab. B.10). PCR was performed under the same cycling conditions as described above.

Tab. B.10: Optimised pipetting scheme for one endpoint PCR reaction

Mastermix			**Enzyme mix**		
Reagent	**Supplier**	**Volume [µl]**	**Reagent**	**Supplier**	**Volume [µl]**
5x Green GoTaq® Flexi buffer	Promega	4	5x Green GoTaq® Flexi buffer	Promega	4
dATP 10 mM	Promega	1	GoTaq® G2 Flexi DNA polymerase 5 U/µl	Promega	0.1
dTTP 10 mM	Promega	1	**Total volume**		**4.1**
dCTP 10 mM	Promega	1			
dGTP 10 mM	Promega	1			
$MagCl_2$ 25 mM	Promega	3			
Nuclease-free H_2O	Promega	30.9			
Total volume		**41.9**			
Components added to tube		**Volume [µl]**			
Mastermix		41.9			
GoTaq® G2 Flexi DNA polymerase mix		4.1			
DNA		2			
Primer pair		2			
Total volume		**50**			

As positive control locus for the ChIP of RNA polymerase II, endpoint PCR of the housekeeping gene *GAPDH* was performed. For this, the validated control primer set GAPDH-2 (active motive®) was applied. It amplified an 82 base pair fragment of the human *GAPDH* promoter. According to the manufacturer's instruction, PCR was performed with 5 µl DNA in a total reaction volume of 20 µl (tab. B10). To prevent evaporation, 15 µl mineral oil were layered on top. Furthermore, the melting temperature was changed to 58 °C (Tab. B.11 and B.12).

Tab. B.11: PCR set up for positive control locus amplification (one reaction)

Reagent	*Supplier*	*Volume [µl]*
Validated primer set GAPDH-2	Active motif	5= 5 µM
dATP 10 mM	Promega	1
dTTP 10 mM	Promega	1
dCTP 10 mM	Promega	1
dGTP 10 mM	Promega	1
$MagCl_2$ 25 mM	Promega	1.2
5x Green GoTaq® Flexi buffer	Promega	8
GoTaq® G2 Flexi DNA polymerase 5 U/µl	Promega	0.1
Nuclease-free H_2O	Promega	0.7
DNA		5
Total volume		20

Tab. B.12: PCR settings for amplification of GAPDH as confirmation of positive pulldown by RNA polymerase II

	Time [s]	*Temperature [°C]*
First Initiation	180	94
Denaturation	30	94
Annealing	30	58
Elongation	30	72
Final extension	120	72

B.2 Determination of HIF-1, RNA polymerase II, and CtBP binding at the *CA9* promoter

B.2.1 Confirmation of fragment size of sheared chromatin

In order to confirm that the sheared chromatin fragments were between 200 and 500 bp of length, agarose gel electrophoresis was performed with the sonicated chromatin of DMOG- and hypoxia- treated MCF7 breast cancer cells and their respective controls (Fig. B.3). In both cases, the fragments were at the correct length and could be applied in ChIP.

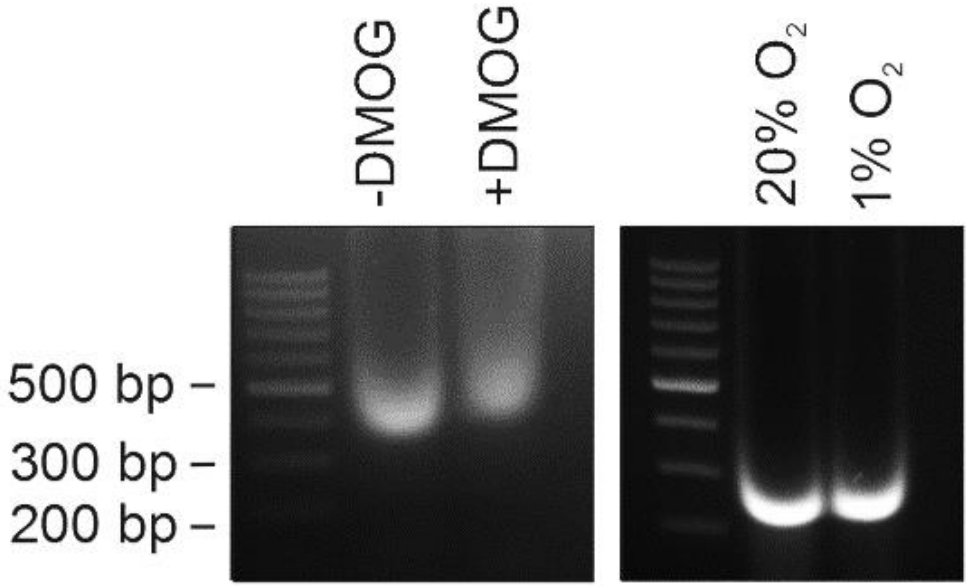

Fig. B.3. **Fragment sizes of chromatin from MCF7 breast cancer cell either treated with 1 mM DMOG (left) or 1% O_2 (right).** For 18 h, MCF7 breast cancer cells were either treated with 1 mM DMOG or 1% O_2. DNA-binding proteins were crosslinked to chromatin by formaldehyde. Subsequently, MCF7 cells were lysed and the chromatin was sheared by ultrasound. To determine fragment size, agarose gel electrophoresis was performed. The 2% agarose gel was loaded with 10 µl chromatin and 5 µl 100 bp DNA ladder.

B.2.2 Validation of *CA9* primers on MCF7 genomic DNA

The primers that were designed to amplify overlapping fragments of the *CA9* promoter region and to map potential HIF-1α, CtBP, and RNA polymerase II binding sides were first validated with genomic MCF7 DNA. Agarose gel electrophoresis involving a 2% agarose gel showed that all amplicons had the expected size and were specifically amplified by the primers. Therefore, the *CA9* primer pairs were used for ChIP analysis (Fig. B.4).

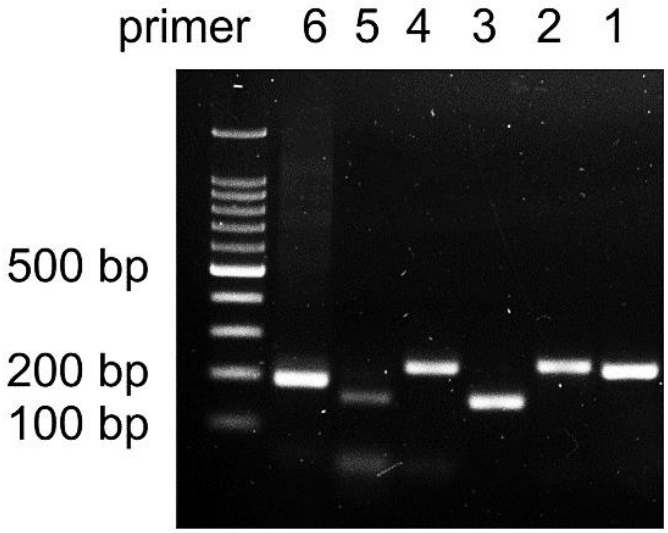

Fig. B.4: **Validation of *CA9* primers on genomic MCF7 DNA**. Primers were designed to amplify overlapping fragments of the *CA9* promoter region to map HIF1α, CtBPs and RNA polymerase II binding sites and were designed with the online platform primer3 and validated on genomic MCF7 DNA by semi-quantitative PCR. Amplification was determined by agarose gel electrophoresis. Starting concentration of the DNA was 100 ng/ 50 µl whereas the concentration for each primer was 20 pmol/ 50 µl. The 2 % agarose gel was loaded with 25 µl amplicons and 5 µl of 100 bp DNA ladder.

B.2.3 Determination of HIF-1, RNA polymerase II, and CtBP enrichment at the *CA9* promoter

In the first immunoprecipitations which were performed, there was background signal in immunoprecipitations performed with HIF-1, RNA polymerase II, and also in the matched isotype controls in non-treated MCF7 cells (Fig. B.5). Similarly, non-specific bands were found in MCF7 cells treated with 1 mM DMOG. However, the signal was stronger. The input controls for both samples were positive, indicating specific primer amplification and correct fragment length.

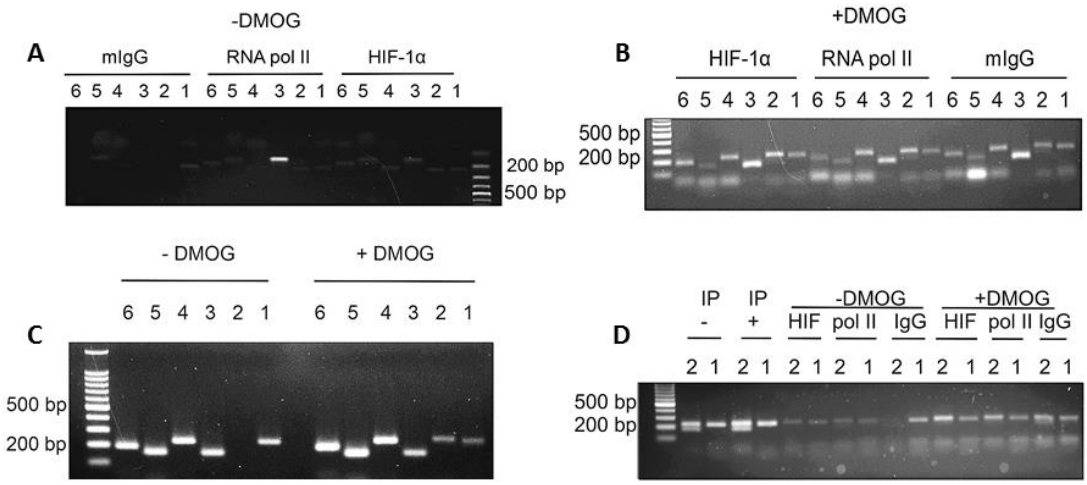

Fig. B.5: **Chromatin immunoprecipitation of HIF-1 and RNA polymerase II at the *CA9* promoter**. *CA9* was induced by 1mM DMOG and ChIP was performed according to the manufacturer's instruction applying an anti-RNA polymerase II antibody and corresponding control antibodies. DNA purified from sheared chromatin was used as input control. Chromatin immunoprecipitation was determined by semi-quantitative endpoint PCR and agarose gel electrophoresis. The 2% agarose gel was loaded with 20 µl PCR reaction and 5 µl 100 bp ladder. **A**: Chromatin immunoprecipitation of untreated MCF7 breast cancer cells being used as negative control. **B**: Chromatin Immunoprecipitation in MCF7 breast cancer cells in which CA9 gene expression was induced with 1 mM DMOG. **C**: Input controls to determine specific binding of the CA9 primers. **D**: Summary of the experiment. As different gels could not be compared, samples amplified with the primer pairs 1 and 2 were re-analysed by agarose gel electrophoresis on a 2% agarose gel. Key: 6-1, number of primer pairs spanning overlapping regions on the CA9 promoter; IP, Input Control; HIF, HIF-1; Pol II, RNA polymerase II; mIgG, mouse isotype control IgG.

In order to determine whether the signal was real, chromatin immunoprecipitation was optimised as described above. Neither HIF-1α nor RNA polymerase II bound at the *CA9* promoter when *CA9* was activated by 1 mM DMOG (Fig. B.6 and B.7). However, optimisation was successful as the non-specific signal disappeared and the matched isotype controls were negative. The input controls were positive for all samples indicating that the designed primers were specific for the region they target and that the fragment sizes were of sufficient length.

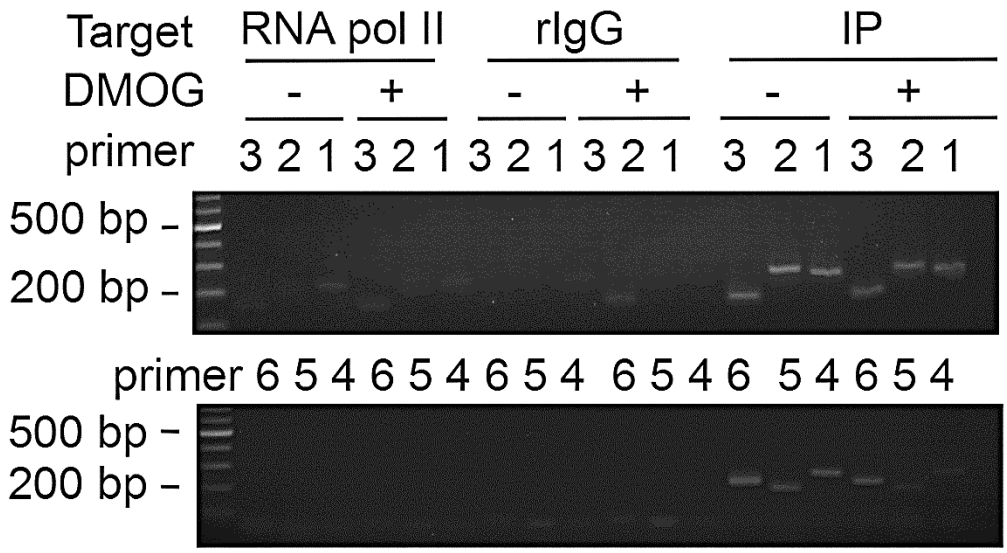

Fig. B.6: Determination of RNA polymerase II binding at the *CA9* promoter by ChIP. *CA9* was induced by 1mM DMOG and ChIP was performed according to the manufacturer's instruction applying an anti-RNA polymerase II antibody and corresponding control antibodies. DNA purified from sheared chromatin was used as input control. Chromatin immunoprecipitation was determined by semi-quantitative endpoint PCR and agarose gel electrophoresis. The 2% agarose gel was loaded with 20 µl PCR reaction and 5 µl 100 bp ladder. rIgG, rabbit isotype control; IP, input control.

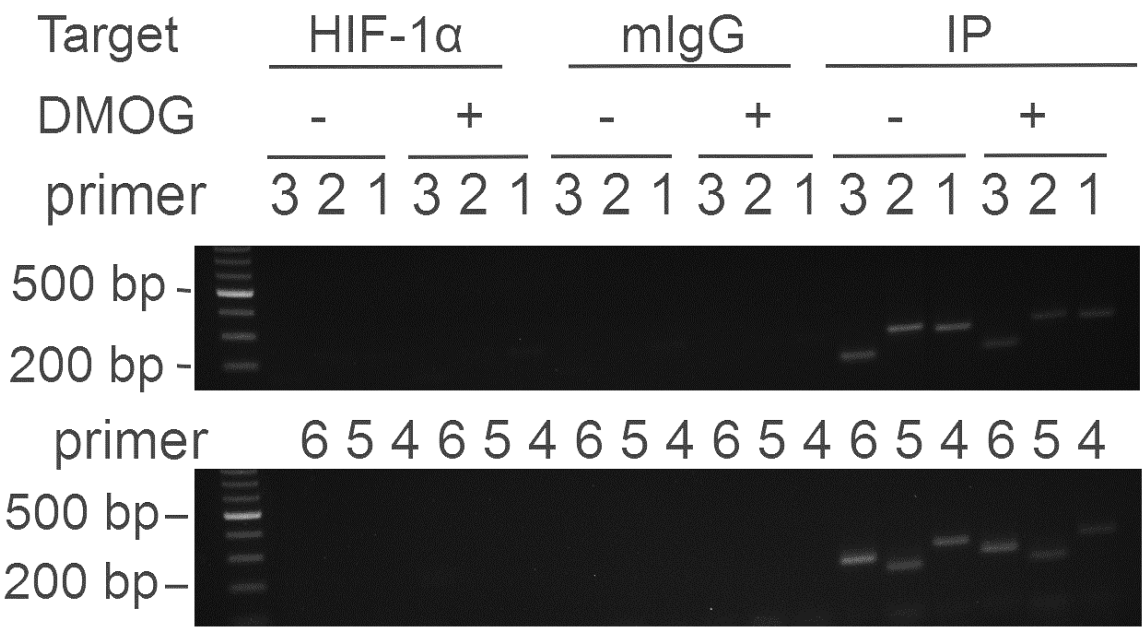

Fig. B.7: Determination of HIF-1α binding at the *CA9* promoter by ChIP. *CA9* was induced by 1mM DMOG and ChIP was performed according to the manufacturer's instruction applying an anti-HIF-1α antibody and corresponding control antibodies. DNA purified from sheared chromatin was used as input control. Chromatin immunoprecipitation was determined by semi-quantitative endpoint PCR and agarose gel electrophoresis. The 2% agarose gel was loaded with 20 µl PCR reaction and 5 µl 100 bp ladder. mIgG, mouse isotype control; IP, input control.

In order to exclude the possibility that DMOG could have negatively interfered with *CA9* gene transcription, ChIP was repeated with hypoxia-treated MCF7 and their respective normoxic control. Further, the immunoprecipitation of CtBPs was included in the assay. However, there was also no binding of HIF-1α (fig. B.9), RNA polymerase II (Fig. B.8) and CtBPs (Fig. B.10) when *CA9* was activated by 1% O_2. The housekeeping gene *GAPDH* was chosen as positive control locus for the immunoprecipitation of RNA polymerase II. However, there was also no amplification. Consequently, no conclusion could be drawn whether HIF-1 and CtBPs interact at the *CA9* promoter in order activate *CA9* gene transcription.

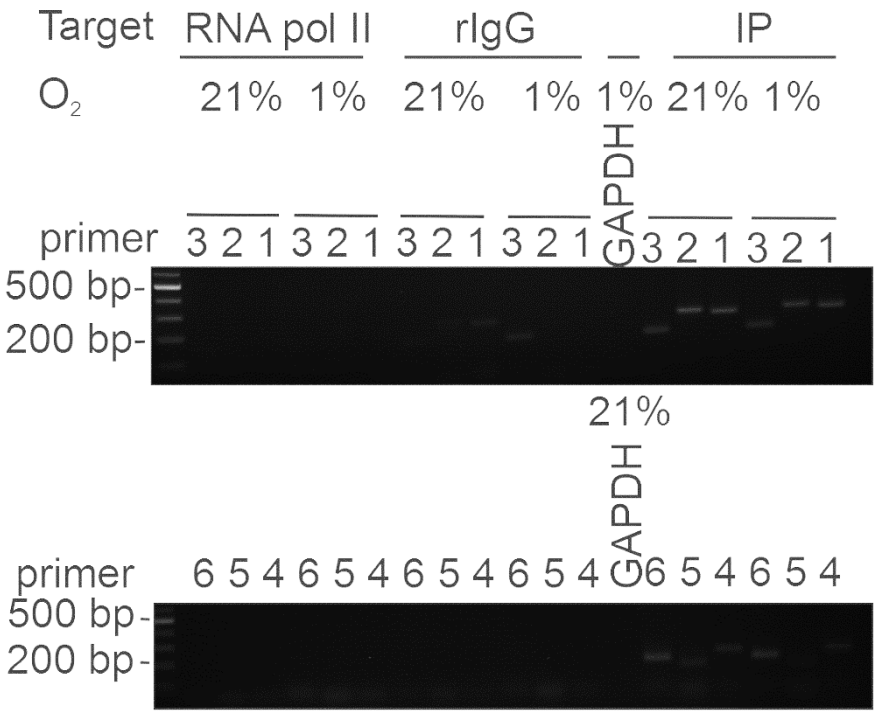

Fig. B.8: Determination of RNA polymerase II-binding at the *CA9* promoter by ChIP. *CA9* was induced by 1% O_2 and ChIP was performed according to the manufacturer's instruction applying an anti-RNA polymerase II and corresponding control antibodies. DNA purified from sheared chromatin was used as input control. Chromatin immunoprecipitation was determined by semi-quantitative endpoint PCR and agarose gel electrophoresis. The 2% agarose gel was loaded with 20 µl PCR reaction and 5 µl 100 bp ladder. PCR for the housekeeping gene GAPDH was performed as a positive control for ChIP of RNA polymerase II at the CA9 promoter. rIgG, rabbit isotype control; IP, input control.

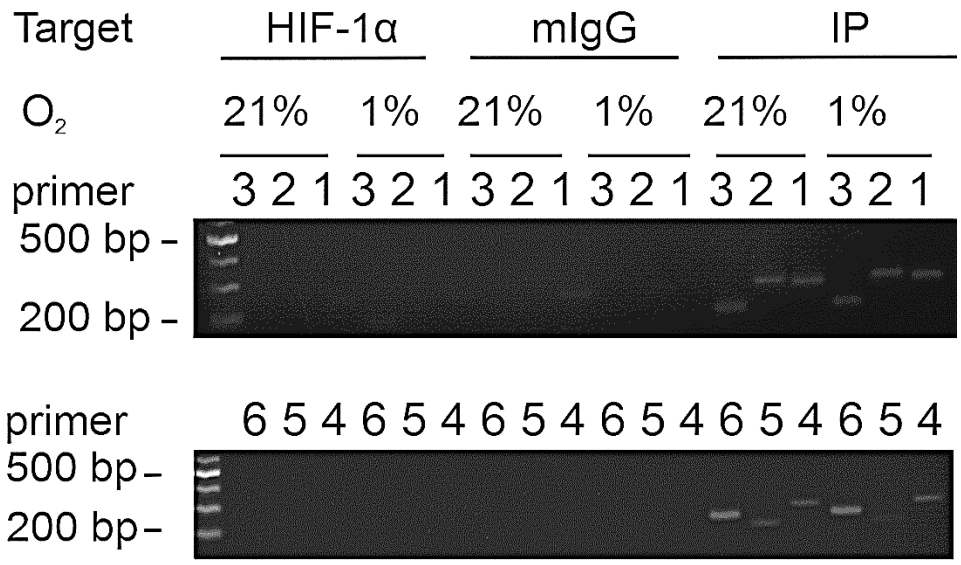

Fig. B.9: Determination of HIF-1 binding at the *CA9* promoter by ChIP. *CA9* was induced by 1% O_2 and ChIP was performed according to the manufacturer's instruction applying an anti-HIF-1α and corresponding control antibodies. DNA purified from sheared chromatin was used as input control. Chromatin immunoprecipitation was determined by semi-quantitative endpoint PCR and agarose gel electrophoresis. The 2% agarose gel was loaded with 20 µl PCR reaction mix and 5 µl 100 bp ladder. mIgG, mouse isotype control IgG; IP, Input control.

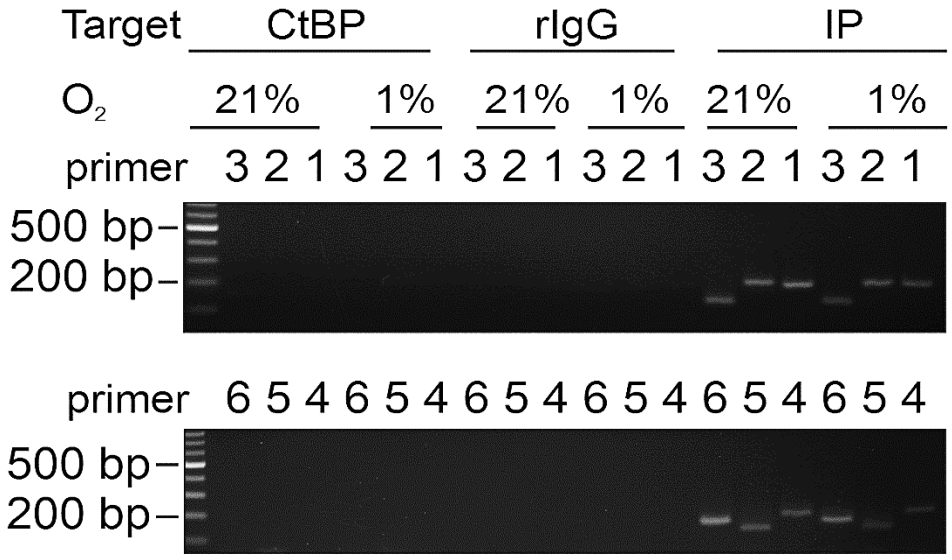

Fig. B.10: Determination of the binding of CtBPs at the *CA9* promoter by ChIP. *CA9* was induced by 1% O_2 and ChIP was performed according to the manufacturer's instruction applying an anti-CtBPs and corresponding control antibodies. DNA purified from sheared chromatin was used as input control. Chromatin immunoprecipitation was determined by semi-quantitative endpoint PCR and agarose gel electrophoresis. The 2% agarose gel was loaded with 20 µl PCR reaction and 5 µl 100 bp ladder. rIgG, rabbit isotype control; IP, Input Control.

Immunoprecipitation is affected by the accessibility of the antigen, the affinity of the antibodies involved in the assay, and the specific environmental conditions occurring during the reaction. Consequently, even though the selected antibodies were widely used in the literature (Liu et al. 2004; Natsuizaka et al. 2012; Sandoval et al. 2004; Yatabe et al. 2004), validated for their application in ChIP by their manufacturers, the affinity could have been too low at the concentration applied in the assay. However, the antibody concentration was 5 µg/ reaction and therefore was within the range suggested by the manufacturer of 1-10 µg. One possibility to confirm immunoprecipitation is Western blot. It was suggested to perform ChIP up to the final washing step, boil the beads in 4xSDS loading buffer for 10 min and perform a Western blot to confirm the presence of the protein of interest (Abcam 2011). If the protein cannot be detected, antibody concentration could be increased further. Also, the salt concentration of the final washing buffer could be decreased to 250 mM as it might have been too stringent for low affinity binding antibodies and therefore eliminate specific binding (Abcam 2011). However, as a commercially available kit was used this should not have been the case. Moreover, excessive crosslinking potentially decreases the amount of the protein of interest causing reduction and changes in epitope availability. Consequently, to optimise crosslinking with formaldehyde a time course could be performed including incubation times from 3 to 30 min (Abcam 2011; Invitrogen™ 2013). Albeit formaldehyde being an effective cross-linker of proteins directly binding to DNA, due to its small molecular size of 2 Å it is less effective in stabilizing proteins that do not directly bind to DNA such as CtBPs (Abcam 2011). Based on this suggestion, immunoprecipitation for RNA polymerase II was performed as it should only be present at the active *CA9* promoter. However, there was no amplification of *GAPDH* in DMOG- or hypoxia-treated samples, indicating that there was no immunoprecipitation of RNA polymerase II. Nevertheless, there could have been no target enrichment in the analysed region. If that was the case, *CA9* primers amplifying different regions of the *CA9* promoter have to be designed.

Bibliography

Abcam, 2011. A Beginner's Guide to ChIP. *Abcam*, pp.1–32.

Achouri, Y., Noel, G. & Van Schaftingen, E., 2007. 2-Keto-4-methylthiobutyrate, an intermediate in the methionine salvage pathway, is a good substrate for CtBP1. *Biochem Biophys Res Commun*, 352(4), pp.903–906.

Ades, F., Zardavas, D., Bozovic-spasojevic, I., Pugliano, L. & Fumagalli, D., 2014. Luminal B Breast Cancer : Molecular Characterization, Clinical Management, and Future Perspectives. *Journal of Clinical Oncology*, 32(25), pp.2794–2803.

Aggarwal M., Boone Ch. D., Kondeti B., M.R., 2013. Structural annotation of human carbonic anhydrase. *Journal of enzyme inhibition and medicinal chemistry*, 28(2), pp.267–277.

Ahmed, S., Thomas, G., Ghoussaini, M., Healey, C.S., Humphreys, M.K., Platte, R. & et al., 2009. Newly discovered breast cancer susceptibility loci on 3p24 and 17q23.2. *Nat Genet*, 41(5), pp.585–590.

Ai, Z., Lu, Y., Qiu, S. & Fan, Z., 2016. Overcoming cisplatin resistance of ovarian cancer cells by targeting HIF-1-regulated cancer metabolism. *Cancer Letters*, 373(1), pp.36–44.

Alterio, V., Hilvo, M., Di Fiore, A., Supuran, C.T., Pan, P., Parkkila, S., Scaloni, A., Pastorek, J., Pastorekova, S., Pedone, C., Scozzafava, A., Monti, S.M. & De Simone, G., 2009. Crystal structure of the catalytic domain of the tumor-associated human carbonic anhydrase IX. *Proceedings of the National Academy of Sciences of the United States of America*, 106(38), pp.16233–16238.

Amann, T., Maegdefrau, U., Hartmann, A., Agaimy, A., Marienhagen, J., Weiss, T.S., Stoeltzing, O., Warnecke, C., Schölmerich, J., Oefner, P.J., Kreutz, M., Bosserhoff, A.K. & Hellerbrand, C., 2009. GLUT1 expression is increased in hepatocellular carcinoma and promotes tumorigenesis. *The American journal of pathology*, 174(4), pp.1544–52.

Amith, S.R., Wilkinson, J.M., Baksh, S. & Fliegel, L., 2015. The Na^+/H^+ exchanger (NHE1) as a novel co-adjuvant target in paclitaxel therapy of triple-negative breast cancer cells. *Oncotarget*, 6(2), pp.1262–75.

Arany, Z., Huang, L.E., Eckner, R., Bhattacharya, S., Jiang, C., Goldberg, M.A., Bunn, H.F. & Livingston, D.M., 1996. An essential role for p300/CBP in the cellular response to hypoxia. *Proc Natl Acad Sci U S A*, 93(23), pp.12969–12973.

Baader, E., Tschank, G., Baringhaus, K.H., Burghard, H. & Günzler, V., 1994. Inhibition of prolyl 4-hydroxylase by oxalyl amino acid derivatives in vitro, in isolated microsomes and in embryonic chicken tissues. *The Biochemical journal*, 300 (Pt 2, pp.525–30.

Baenke, F., Dubuis, S., Brault, C., Weigelt, B., Dankworth, B., Griffiths, B., Jiang, M., Mackay, A., Saunders, B., Spencer-Dene, B., Ros, S., Stamp, G., Reis-Filho, J.S., Howell, M., Zamboni, N. & Schulze, A., 2015. Functional screening identifies MCT4 as a key regulator of breast cancer cell metabolism and survival. *The Journal of Pathology*, 237(June), pp.152–165.

Bannister, A.J. & Kouzarides, T., 2011. Regulation of chromatin by histone modifications. *Cell Research*, 21(3), pp.381–395.

Bannister, A.J., Zegerman, P., Partridge, J.F., Miska, E.A., Thomas, J.O., Allshire, R.C. & Kouzarides, T., 2001. Selective recognition of methylated lysine 9 on histone H3 by the HP1 chromo domain. *Nature*, 410, pp.2–6.

Barriga, E.H., Maxwell, P.H., Reyes, A.E. & Mayor, R., 2013. The hypoxia factor Hif-1alpha controls neural crest chemotaxis and epithelial to mesenchymal transition. *J Cell Biol*, 201(5), pp.759–776.

Basu, S., Chen, W., Tchou, J., Mavi, A., Cermik, T., Czerniecki, B., Schnall, M. & Alavi, A., 2008. Comparison of triple-negative and estrogen receptor-positive/progesterone receptor-positive/HER2-negative breast carcinoma using quantitative fluorine-18 fluorodeoxyglucose/positron emission tomography imaging parameters: A potentially useful method for d. *Cancer*, 112(5), pp.995–1000.

Batlle, E., Sancho, E., Francí, C., Domínguez, D., Monfar, M., Baulida, J. & Herreros, A.G. De, 2000. The transcription factor Snail is a repressor of E-cadherin gene expression in epithelial tumour cells. *Nature Cell Biology*, 2, pp.84–89.

Bauer, K., Brown, M., Cress, R.D., Parise, C.A. & Caggiano, V., 2007. Descriptive Analysis of Estrogen Receptor (ER) - and HER2-Negative Invasive Breast Cancer, the So-called Triple-Negative Phenotype. *Cancer*, 109(9), pp.1721–1728.

Beasley, N.J.P., Wykoff, C.C., Watson, P.H., Leek, R., Turley, H., Gatter, K., Pastorek, J., Cox, G.J., Ratcliffe, P. & Harris, A.L., 2001. Carbonic Anhydrase IX, an Endogenous Hypoxia Marker, Expression in Head and Neck, Squamous Cell Carcinoma and its Relationship to Hypoxia, Necrosis and Microvessel Density. *Cancer Res*, 61, pp.5262–5267.

Bensaad, K., Tsuruta, A., Selak, M.A., Vidal, M.N.C., Nakano, K., Bartrons, R., Gottlieb, E. & Vousden, K.H., 2006. TIGAR, a p53-Inducible Regulator of Glycolysis and Apoptosis. *Cell*, 126(1), pp.107–120.

Bergh, J., Norberg, T., Sjogren, S., Lindgren, A. & Holmberg, L., 1995. Complete sequencing of the p53 gene provides prognostic information in breast cancer patients, particularly in relation to adjuvant systemic therapy and radiotherapy. *Nat.Med.*, 1(10), pp.1029–1034.

Bergman, L.M. & Blaydes, J.P., 2006. C-terminal binding proteins: emerging roles in cell survival and tumorigenesis. *Apoptosis*, 11(6), pp.879–888.

Bergman, L.M., Morris, L., Darley, M., Mirnezami, A.H., Gunatilake, S.C. & Blaydes, J.P., 2006. Role of the unique N-terminal domain of CtBP2 in determining the subcellular localisation of CtBP family proteins. *BMC Cell Biol*, 7, p.35.

Bertheau, P., Lehmann-Che, J., Varna, M., Dumay, A., Poirot, B., Porcher, R., Turpin, E., Plassa, L.-F., de Roquancourt, A., Bourstyn, E., de Cremoux, P., Janin, A., Giacchetti, S., Espié, M. & de Thé, H., 2013. P53 in Breast Cancer Subtypes and New Insights Into Response To Chemotherapy. *Breast (Edinburgh, Scotland)*, 22 Suppl 2, pp.S27-9.

Bhambhani, C., Chang, J.L., Akey, D.L. & Cadigan, K.M., 2011. The oligomeric state of CtBP determines its role as a transcriptional co-activator and co-repressor of Wingless targets. *EMBO J*, 30(10), pp.2031–2043.

Bindra, R.S., Gibson, S.L., Meng, A., Westermark, U., Jasin, M., Pierce, A.J., Bristow, R.G., Classon, M.K. & Glazer, P.M., 2005. Hypoxia-induced down-regulation of BRCA1 expression by E2Fs. *Cancer Research*, 65(24), pp.11597–11604.

Bindra, R.S. & Glazer, P.M., 2007. Co-repression of mismatch repair gene expression by hypoxia in cancer cells: Role of the Myc/Max network. *Cancer Letters*, 252(1), pp.93–103.

Birts, C.N., Bergman, L.M. & Blaydes, J.P., 2011. CtBPs promote mitotic fidelity through their activities in the cell nucleus. *Oncogene*, 30(11), pp.1272–1280.

Birts, C.N., Harding, R., Soosaipillai, G., Halder, T., Azim-Araghi, A., Darley, M., Cutress, R.I., Bateman, A.C. & Blaydes, J.P., 2010. Expression of CtBP family protein isoforms in breast cancer and their role in chemoresistance. *Biol Cell*, 103(1), pp.1–19.

Birts, C.N., Nijjar, S.K., Mardle, C.A., Hoakwie, F., Duriez, P.J., Blaydes, J.P. & Tavassoli, A., 2013. A cyclic peptide inhibitor of C-terminal binding protein dimerization links metabolism with mitotic fidelity in breast cancer cells. *Chemical Science*, 4(8), pp.3046–3057.

Blancher, C., Moore, J.W., Robertson, N. & Harris, a L., 2001. Effects of ras and von Hippel-Lindau (VHL) gene mutations on hypoxia-inducible factor (HIF)-1alpha, HIF-2alpha, and vascular endothelial growth factor expression and their regulation by the phosphatidylinositol 3'-kinase/Akt signaling pathway. *Cancer research*, 61(19), pp.7349–7355.

Blancher, C., Moore, J.W., Talks, K.L., Houlbrook, S. & Harris, A.L., 2000. Relationship of hypoxia-inducible factor (HIF)-1alpha and HIF-2alpha expression to vascular endothelial growth factor induction and hypoxia survival in human breast cancer cell lines. *Cancer Research*, 60(24), pp.7106–7113.

Blum, R., Jacob-hirsch, J., Amariglio, N., Blum, R., Jacob-hirsch, J., Amariglio, N., Rechavi, G. & Kloog, Y., 2005. Ras Inhibition in Glioblastoma Down-regulates Hypoxia-Inducible Factor-1 α , Causing Glycolysis Shutdown and Cell Death. *Cancer Research*, 65(3), pp.999–1006.

Boedtkjer, E., Moreira, J.M.A., Mele, M., Vahl, P., Wielenga, V.T., Christiansen, P.M., Jensen, V.E.D., Pedersen, S.F. & Aalkjaer, C., 2013. Contribution of Na+,HCO3--cotransport to cellular pH control in human breast cancer: A role for the breast cancer susceptibility locus NBCn1 (SLC4A7). *International Journal of Cancer*, 132(6), pp.1288–1299.

Bonnefoi, H., Grellety, T., Tredan, O., Koch, L., Bertram, H., Saghatchian, M., Dalenc, F., Mailliez, A., L'Haridon, T., Cottu, P., Abadie-Lacourtoisue, S., You, B., Mousseau, M., Dauba, J., Del Piano, F., Desmoulins, I., Coussy, F., Madranges, N., Grenier, J., Bidard, F.C., Proudhon, C., MacGrogan, G., Orsini, C., Pulido, M. & Goncalves, A., 2016. A phase II trial of abiraterone acetate plus prednisone in patients with triple-negative androgen receptor positive locally advanced or metastatic breast cancer (UCBG 12-1). *Annals of Oncology*, 27(5), pp.812–818.

Bookstein, C., Xie, Y., Rabenau, K., Musch, M.W., McSwine, R.L., Rao, M.C. & Chang, E.B., 1997. Tissue distribution of Na+/H+ exchanger isoforms NHE2 and NHE4 in rat intestine and kidney. *The American journal of physiology*, 273(5 Pt 1), pp.C1496–C1505.

Boros, L.G., Torday, J.S., Lim, S., Bassilian, S., Cascante, M. & Lee, W.N.P., 2000. Transforming growth factor β2 promotes glucose carbon incorporation into nucleic acid ribose through the nonoxidative pentose cycle in lung epithelial carcinoma cells. *Cancer Research*, 60(5), pp.1183–1185.

Bos, R., Zhong, H., Hanrahan, C.F., Mommers, E.C.M., Semenza, G.L., Pinedo, H.M., Abeloff, M.D., Simons, J.W., van Diest, P.J. & van der Wall, E., 2001. Levels of Hypoxia-Inducible Factor-1a During Breast Carcinogenesis. *Journal of National Cancer Institute*, 93(4), pp.309–314.

Bradner, J.E., Hnisz, D. & Young, R.A., 2017. Transcriptional Addiction in Cancer. *Cell*, 168(4), pp.629–643.

Brodaczewska, K.K., Szczylik, C., Fiedorowicz, M., Porta, C. & Czarnecka, A.M., 2016. Choosing the right cell line for renal cell cancer research. *Molecular Cancer*, 15(83), pp.1–15.

Brown, D.A., Melvin, J.E. & Yule, D.I., 2003. Critical role for NHE1 in intracellular pH regulation in pancreatic acinar cells. *American Journal of Physiology - Gastrointestinal and Liver Physiology*, 285(5 48-5), pp.804–812.

Brown, R.S. & Wahl, R.L., 1993. Overexpression of Glut-1 glucose transporter in human breast cancer: An immunohistochemical study. *Cancer*, 72(10), pp.2979–2985.

Broz, D.K. & Attardi, L.D., 2013. TRP53 activates a global autophagy program to promote tumor suppression. *Autophagy*, 9(9), pp.1440–1442.

Brunet, A., Roux, D., Lenormand, P., Dowd, S., Keyse, S. & Pouysségur, J., 1999. Nuclear translocation of p42/p44 mitogen-activated protein kinase is required for growth factor-induced gene expression and cell cycle entry. *The EMBO journal*, 18(3), pp.664–74.

Buchakjian, M.R. & Kornbluth, S., 2010. The engine driving the ship: metabolic steering of cell proliferation and death. *Nat Rev Mol Cell Biol*, 11(10), pp.715–727.

Bullen, J.W., Tchernyshyov, I., Holewinski, R.J., Devine, L., Wu, F., Venkatraman, V., Kass, D.L., Cole, R.N., Eyk, J. Van & Semenza, G.L., 2016. Protein kinase A–dependent phosphorylation stimulates the transcriptional activity of hypoxia-inducible factor 1. *Cell Biology*, 9(430), p.ra56.

Burstein, M.D., Tsimelzon, A., Poage, G.M., Covington, K.R., Contreras, A., Fuqua, S.A.W., Savage, M.I., Osborne, C.K., Hilsenbeck, G., Chang, J.C., Mills, G.B., Lau, C.C. & Brown, P.H., 2014. Comprehensive Genomic Analysis Identifies Novel Subtypes and Targets of Triple-Negative Breast Cancer. *Clin Cancer Res*, 21(7), pp.1–12.

Bustamante, E., Morris, H.P. & Pedersen, P.L., 1981. Energy metabolism of tumor cells. Requirement for a form of hexokinase with a propensity for mitochondrial binding. *Journal of Biological Chemistry*, 256(16), pp.8699–8704.

Cairns, R.A., Harris, I.S. & Mak, T.W., 2011. Regulation of cancer cell metabolism. *Nat Rev Cancer*, 11(2), pp.85–95.

Cao, D., Hou, M., Guan, Y., Jiang, M., Yang, Y. & Gou, H., 2009. Expression of HIF-1alpha and VEGF in colorectal cancer: association with clinical outcomes and prognostic implications. *BMC cancer*, 9, p.432.

Carey, L.A., Dees, E.C., Sawyer, L., Gatti, L., Moore, D.T., Collichio, F., Ollila, D.W., Sartor, C.I., Graham, M.L. & Perou, C.M., 2007. The Triple Negative Paradox : Primary T umor Chemosensitivity of Breast Cancer Subtypes. *Clin Cancer Res*, 13(8), pp.2329–2335.

Carmeliet, P. & Jain, R.K., 2000. Angiogenesis in cancer and other diseases. *Nature*, 407, pp.249–257.

Cecchini, M.J., Amiri, M. & Dick, F.A., 2012. Analysis of Cell Cycle Position in Mammalian Cells. *Journal of Visualized Experiments*, (59), pp.1–7.

Chafe, S.C., Lou, Y., Sceneay, J., Vallejo, M., Hamilton, M.J., McDonald, P.C., Bennewith, K.L., Möller, A. & Dedhar, S., 2015. Carbonic anhydrase IX promotes myeloid-derived suppressor cell mobilization and establishment of a metastatic niche by stimulating G-CSF production. *Cancer Research*, 75(6), pp.996–1008.

Chandel, N.S., McClintock, D.S., Feliciano, C.E., Wood, T.M., Melendez, J.A., Rodriguez, A.M. & Schumacker, P.T., 2000. Reactive oxygen species generated at mitochondrial Complex III stabilize hypoxia-inducible factor-1?? during hypoxia: A mechanism of O2 sensing. *Journal of Biological Chemistry*, 275(33), pp.25130–25138.

Charafe-Jauffret, E., Ginestier, C., Iovino, F., Tarpin, C., Diebel, M., Esterni, B., Houvenaeghel, G., Extra, J.M., Bertucci, F., Jacquemier, J., Xerri, L., Dontu, G., Stassi, G., Xiao, Y., Barsky, S.H., Birnbaum, D., Viens, P. & Wicha, M.S., 2010. Aldehyde dehydrogenase 1-positive cancer stem cells mediate metastasis and poor clinical outcome in inflammatory breast cancer. *Clinical Cancer Research*, 16(1), pp.45–55.

Cheang, M.C.U., Voduc, D., Bajdik, C., Leung, S., Mckinney, S., Chia, S.K., Perou, C.M. & Nielsen, T.O., 2008. Basal-Like Breast Cancer Defined by Five Biomarkers Has Superior Prognostic Value thanT riple-Negative Phenotype. *Clin Cancer Res*, 14(5), pp.1368–1377.

Chen, D., Li, M., Luo, J. & Wei, G., 2003. Direct Interactions between HIF-1α and Mdm2 Modulate p53 Function. *The Journal of Biological Chemsirty*, 278(16), pp.13595–13598.

Chen, C., Pore, N., Behrooz, A., Ismail-Beigi, F. & Maity, A., 2001. Regulation of glut1 mRNA by hypoxia-inducible factor-1. Interaction between H-ras and hypoxia. *J Biol Chem*, 276(12), pp.9519–9525.

Chesney, J., Mitchell, R., Benigni, F., Bacher, M., Spiegel, L., Al-Abed, Y., Han, J.H., Metz, C. & Bucala, R., 1999. An inducible gene product for 6-phosphofructo-2-kinase with an AU-rich instability element: role in tumor cell glycolysis and the Warburg effect. *Proceedings of the National Academy of Sciences of the United States of America*, 96(6), pp.3047–3052.

Chia, S. K., Wykoff, Ch. C., Watson, P. H., Han, C., Leek, R. D., Pastorek, J., Gatter, K. C., Ratcliffe, P., Harris, A.L., 2001. Prognostic Significance of a Novel Hypoxia-Regulated Marker, Carbonic Anhydrase IX, in Invasive Breast Carcinoma. *J Clin Oncol*, 19(16), pp.3660–3668.

Chiche, J., Ilc, K., Laferriere, J., Trottier, E., Dayan, F., Mazure, N.M., Brahimi-Horn, M.C. & Pouyssegur, J., 2009. Hypoxia-inducible carbonic anhydrase IX and XII promote tumor cell growth by counteracting acidosis through the regulation of the intracellular pH. *Cancer Research*, 69(1), pp.358–368.

Cho, M., Uemura, H., Kim, S.C., Kawada, Y., Yoshida, K., Hirao, Y., Konishi, N., Saga, S. & Yoshikawa, K., 2001. Hypomethylation of the MN/CA9 promoter and upregulated MN/CA9 expression in human renal cell carcinoma. *British journal of cancer*, 85(4), pp.563–7.

Cho, Y.E., Kim, J.Y., Kim, Y.J., Kim, Y.W., Lee, S. & Park, J.H., 2010. Expression and clinicopathological significance of human growth and transformation-dependent protein (HGTD-P) in uterine cervical cancer. *Histopathology*, 57(3), pp.479–482.

Cho, Y.E., Kim, J.Y., Kim, Y.W., Park, J.H. & Lee, S., 2009. Expression and prognostic significance of human growth and transformation-dependent protein in gastric carcinoma and gastric adenoma. *Human Pathology*, 40(7), pp.975–981.

Christofk, H. R., Vander Heiden, M. G., Harris, M. H., Ramanathan, A., Gerszten, R. E., Wei, R., Fleming, M. D., Schreiber, S. L.& Cantley, L.C., 2008. The M2 splice isoform of pyruvate kinase is important for cancer metabolism and tumour growth. *Nature*, 452, pp.230–233.

Colegio, O.R., Chu, N.-Q., Szabo, A.L., Chu, T., Rhebergen, A.M., Jairam, V., Cyrus, N., Brokowski, C.E., Eisenbarth, S.C., Phillips, G.M., Cline, G.W., Phillips, A.J. & Medzhitov, R., 2014. Functional polarization of tumour-associated macrophages by tumour-derived lactic acid. *Nature*, 513(7519), pp.559–63.

Conley, S.J., Gheordunescu, E., Kakarala, P., Newman, B., Korkaya, H., Heath, A.N., Clouthier, S.G. & Wicha, M.S., 2012. Antiangiogenic agents increase breast cancer stem cells via the generation of tumor hypoxia. *Proceedings of the National Academy of Sciences of the United States of America*, 109(8), pp.2784–9.

Contractor, T. & Harris, C.R., 2012. p53 negatively regulates transcription of the pyruvate dehydrogenase kinase Pdk2. *Cancer Research*, 72(2), pp.560–567.

Coradini, D., Fornili, M., Ambrogi, F., Boracchi, P. & Biganzoli, E., 2012. TP53 mutation, epithelial-mesenchymal transition, and stemlike features in breast cancer subtypes. *Journal of Biomedicine and Biotechnology*, 2012.

Corzo, C.A., Condamine, T., Lu, L., Cotter, M.J., Youn, J., Cheng, P., Cho, H., Celis, E., Quiceno, D.G., Padhya, T., Mccaffrey, T. V, Mccaffrey, J.C. & Gabrilovich, D.I., 2010. HIF-1 □ regulates function and differentiation of myeloid-derived suppressor cells in the tumor microenvironment.

Cosse, J.-P., Sermeus, A., Vannuvel, K., Ninane, N., Raes, M. & Michiels, C., 2007. Differential effects of hypoxia on etoposide-induced apoptosis according to the cancer cell lines. *Molecular cancer*, 6, p.61.

Crosby, M.E., Kulshreshtha, R., Ivan, M. & Glazer, P.M., 2009. MicroRNA Regulation of DNA Repair Gene Expression in Hypoxic Stress. *Cancer Research*, 69(3), pp.1221–1229.

Dai, X., Li, T., Bai, Z., Yang, Y., Liu, X., Zhan, J. & Shi, B., 2015. Breast cancer intrinsic subtype classification , clinical use and future trends. *Am J Cancer Res*, 5(10), pp.2929–2943.

Dales, J., Garcai, S., Meunier-Carpentier, S., Andrac-Meyer, L., Haddad, O., Lavaut, M., Allasia, C., Bonnier, P. & Charpin, C., 2005. Overexpression of hypoxia-inducible factor HIF-1 a predicts early relapse in breast cancer : Retrospective study in a series of 745 patients. *Int. J. Cancer*, 116, pp.734–739.

Dayan, F., Bilton, R.L., Laferriére, J., Trottier, E., Roux, D., Pouyssegur, J. & Mazure, N.M., 2009. Activation of HIF-1α in exponentially growing cells via hypoxic stimulation is independent of the Akt/mTOR pathway. *Journal of Cellular Physiology*, 218(1), pp.167–174.

Deng, H., Liu, J., Deng, Y., Han, G., Shellman, Y.G., Robinson, S.E., Tentler, J.J., Robinson, W.A., Norris, D.A., Wang, X.J. & Zhang, Q., 2013. CtBP1 is expressed in melanoma and represses the transcription of p16INK4a and Brca1. *J Invest Dermatol*, 133(5), pp.1294–1301.

Deng, Y., Liu, J., Han, G., Lu, S.L., Wang, S.Y., Malkoski, S., Tan, A., Deng, C., Wang, X.J. & Zhang, Q., 2010. Redox-dependent Brca1 transcriptional regulation by an NADH-sensor CtBP1. *Oncogene*, 29(50), pp.6603–6608.

Deng Yu, Deng Hui, Liu Jing, Han Gangwen, Malkoski Stephen, Liu Bolin, Zhao Rui, Wang Xiao-Jing, Z.Q., 2012. Transcriptional Down-Regulation of Brca1 and E-cadherin by CtBP1 in Breast Cancer. *Mol Carcinog*, 51(6), pp.500–5007.

Denker, S.P., Huang, D.C., Orlowski, J., Furthmayr, H. & Barber, D.L., 2000. Direct binding of the Na-H exchanger NHE1 to ERM proteins regulates the cortical cytoskeleton and cell shape independently of H+ translocation. *Molecular Cell*, 6(6), pp.1425–1436.

Denkert, C., Liedtke, C., Tutt, A. & Minckwitz, G. Von, 2017. Molecular alterations in triple-negative breast cancer — the road to new treatment strategies. *The Lancet*, 389, pp.2430–2442.

Di, L.J., Byun, J.S., Wong, M.M., Wakano, C., Taylor, T., Bilke, S., Baek, S., Hunter, K., Yang, H., Lee, M., Zvosec, C., Khramtsova, G., Cheng, F., Perou, C.M., Miller, C.R., Raab, R., Olopade, O.I. & Gardner, K., 2013. Genome-wide profiles of CtBP link metabolism with genome stability and epithelial reprogramming in breast cancer. *Nat Commun*, 4, p.1449.

Dimmer, K.S., Friedrich, B., Lang, F., Deitmer, J.W. & Bröer, S., 2000. The low-affinity monocarboxylate transporter MCT4 is adapted to the export of lactate in highly glycolytic cells. *The Biochemical journal*, 350 Pt 1(1), pp.219–27.

Ditte, P., Dequiedt, F., Svastova, E., Hulikova, A., Ohradanova-Repic, A., Zatovicova, M., Csaderova, L., Kopacek, J., Supuran, C.T., Pastorekova, S. & Pastorek, J., 2011. Phosphorylation of carbonic anhydrase IX controls its ability to mediate extracellular acidification in hypoxic tumors. *Cancer Research*, 71(24), pp.7558–7567.

Dodd, K.M., Yang, J., Shen, M.H., Sampson, J.R. & Tee, A.R., 2015. mTORC1 drives HIF-1α and VEGF-A signalling via multiple mechanisms involving 4E-BP1, S6K1 and STAT3. *Oncogene*, 34(17), pp.2239–50.

Doherty, J.R., Yang, C., Scott, K.E.N., Cameron, M.D., Fallahi, M., Li, W., Hall, M.A., Amelio, A.L., Mishra, J.K., Li, F., Tortosa, M., Genau, H.M., Rounbehler, R.J., Lu, Y., Dang, C. V., Kumar, K.G., Butler, A.A., Bannister, T.D., Hooper, A.T., Unsal-Kacmaz, K., Roush, W.R. & Cleveland, J.L., 2014. Blocking lactate export by inhibiting the myc target MCT1 disables glycolysis and glutathione synthesis. *Cancer Research*, 74(3), pp.908–920.

Dorai, T., Sawczuk, I.S., Pastorek, J., Wiernik, P.H. & Dutcher, J.P., 2005. The role of carbonic anhydrase IX overexpression in kidney cancer. *Eur J Cancer*, 41(18), pp.2935–2947.

Doyen, J., Trastour, C., Ettore, F., Peyrottes, I., Toussant, N., Gal, J., Ilc, K., Roux, D., Parks, S.K., Ferrero, J.M. & Pouysségur, J., 2014. Expression of the hypoxia-inducible monocarboxylate transporter MCT4 is increased in triple negative breast cancer and correlates independently with clinical outcome. *Biochemical and Biophysical Research Communications*, 451(1), pp.54–61.

Du, R., Lu, K. V., Petritsch, C., Liu, P., Ganss, R., Passegué, E., Song, H., VandenBerg, S., Johnson, R.S., Werb, Z. & Bergers, G., 2008. HIF1?? Induces the Recruitment of Bone Marrow-Derived Vascular Modulatory Cells to Regulate Tumor Angiogenesis and Invasion. *Cancer Cell*, 13(3), pp.206–220.

Dupuy, F., Tabariès, S., Andrzejewski, S., Dong, Z., Blagih, J., Annis, M.G., Omeroglu, A., Gao, D., Leung, S., Amir, E., Clemons, M., Aguilar-Mahecha, A., Basik, M., Vincent, E.E., St.-Pierre, J., Jones, R.G. & Siegel, P.M., 2015. PDK1-dependent metabolic reprogramming dictates metastatic potential in breast cancer. *Cell Metabolism*, 22(4), pp.577–589.

Ebert, B.L., 1995. Hypoxic Regulation of Lactate Dehydrogenase A. *Journal of Biological Chemistry*, 270(36), pp.21021–21027.

Ebert, B.L. & Bunn, H.F., 1998. Regulation of transcription by hypoxia requires a multiprotein complex that includes hypoxia-inducible factor 1, an adjacent transcription factor, and p300/CREB binding protein. *Molecular and cellular biology*, 18(7), pp.4089–4096.

Ebert, B.L., Firth, J.D. & Ratcliffe, P.J., 1995. Hypoxia and mitochondrial inhibitors regulate expression of glucose transporter-1 via distinct cis-acting sequences. *Journal of Biological Chemistry*, 270(49), pp.29083–29089.

Elstrom, R.L., Bauer, D.E., Buzzai, M., Karnauskas, R., Harris, M.H., Plas, D.R., Zhuang, H., Cinalli, R.M., Alavi, A., Rudin, C.M. & Thompson, C.B., 2004. Akt stimulates aerobic glycolysis in cancer cells. *Cancer Research*, 64(11), pp.3892–3899.

Elvidge, G.P., Glenny, L., Appelhoff, R.J., Ratcliffe, P.J., Ragoussis, J. & Gleadle, J.M., 2006. Concordant regulation of gene expression by hypoxia and 2-oxoglutarate-dependent dioxygenase inhibition: The role of HIF-1??, HIF-2??, and other pathways. *Journal of Biological Chemistry*, 281(22), pp.15215–15226.

Endo, K., Oriuchi, N., Higuchi, T., Iida, Y., Hanaoka, H., Miyakubo, M., Ishikita, T. & Koyama, K., 2006. PET and PET/CT using 18F-FDG in the diagnosis and management of cancer patients. *International Journal of Clinical Oncology*, 11(4), pp.286–296.

Epstein, A.C.R., Gleadle, J.M., McNeill, L.A., Hewitson, K.S., O'Rourke, J., Mole, D.R., Mukherji, M., Metzen, E., Wilson, M.I., Dhanda, A., Tian, Y.M., Masson, N., Hamilton, D.L., Jaakkola, P., Barstead, R., Hodgkin, J., Maxwell, P.H., Pugh, C.W., Schofield, C.J. & Ratcliffe, P.J., 2001. C. elegans EGL-9 and mammalian homologs define a family of dioxygenases that regulate HIF by prolyl hydroxylation. *Cell*, 107(1), pp.43–54.

Estrella, V., Chen, T., Lloyd, M., Wojtkowiak, J., Cornnell, H.H., Ibrahim-Hashim, A., Bailey, K., Balagurunathan, Y., Rothberg, J.M., Sloane, B.F., Johnson, J., Gatenby, R.A. & Gillies, R.J., 2013. Acidity generated by the tumor microenvironment drives local invasion. *Cancer Research*, 73(5), pp.1524–1535.

Facciabene, A., Peng, X., Hagemann, I.S., Balint, K., Barchetti, A., Wang, L.-P., Gimotty, P.A., Gilks, C.B., Lal, P., Zhang, L. & Coukos, G., 2011. Tumour hypoxia promotes tolerance and angiogenesis via CCL28 and Treg cells. *Nature*, 475(7355), pp.226–230.

Fang, H. M., Li, J., Blauwkamp, T., Bhambhani, Ch., Campbell, N., Cadigan, K.M., 2006. C-terminal-binding protein directly activates and represses Wnt transcriptional targets in Drosophila. *EMBO J*, 25(12), pp.2735–2745.

Fantin, V.R., St-Pierre, J. & Leder, P., 2006. Attenuation of LDH-A expression uncovers a link between glycolysis, mitochondrial physiology, and tumor maintenance. *Cancer Cell*, 9(6), pp.425–434.

Favaro, E., Ramachandran, A., Mccormick, R., Gee, H., Blancher, C., Crosby, M., Devlin, C., Blick, C., Buffa, F., Li, J., Vojnovic, B., Pires, R., Glazer, P., Iborra, F., Ivan, M., Ragoussis, J. & Harris, A.L., 2010. MicroRNA-210 Regulates Mitochondrial Free Radical Response to Hypoxia and Krebs Cycle in Cancer Cells by Targeting Iron Sulfur Cluster Protein ISCU. *PLoS ONE*, 5(4), p.e10345.

Feinman, R., Deitch, E.A., Watkins, A.C., Abungu, B., Colorado, I., Kannan, K.B., Sheth, S.U., Caputo, F.J., Lu, Q., Ramanathan, M., Attan, S., Badami, C.D., Doucet, D., Barlos, D., Bosch-Marce, M., Semenza, G.L. & Xu, D.Z., 2010. HIF-1 mediates pathogenic inflammatory responses to intestinal ischemia-reperfusion injury. *Am J Physiol Gastrointest Liver Physiol*, 299(4), pp.G833–G843.

Ferlay J, Soerjomataram I, Ervik M, Dikshit R, Eser S, Mathers C, Rebelo M, Parkin DM, Forman D, Bray, F., 2013. GLOBOCAN 2012 v1.0, Cancer Incidence and Mortality Worldwide: IARC CancerBase No. 11. *Lyon, France: International Agency for Research on Cancer*. Available at: http://globocan.iarc.fr.

Flamant, L., Roegiers, E., Pierre, M., Hayez, A., Sterpin, C., De Backer, O., Arnould, T., Poumay, Y. & Michiels, C., 2012. TMEM45A is essential for hypoxia-induced chemoresistance in breast and liver cancer cells. *BMC Cancer*, 12(1), p.391.

Fleuriel, C., Leprince, D., Jonathan, V., Piston, D.W., Goodman, R.H., Wang, S., Rocheleau, J. V, Zhang, Q., Wang, S., Fleuriel, C., Leprince, D., Rocheleau, J. V & Piston, D.W., 2015. Retraction for Zhang et al., Metabolic regulation of SIRT1 transcription via a HIC1:CtBP corepressor complex. *Proceedings of the National Academy of Sciences*, 112(7), pp.E819–E819.

Forsythe, J.O.A., Jiang, B., Iyer, N. V, Agani, F. & Leung, S.W., 1996. Activation of vascular endothelial growth factor gene transcription by hypoxia-inducible factor Activation of Vascular Endothelial Growth Factor Gene Transcription by Hypoxia-Inducible Factor 1. *Molecular and Cellular Biology*, 16(9), pp.4604–4612.

Foster, R., Griffin, S., Grooby, S., Feltell, R., Christopherson, C., Chang, M., Sninsky, J., Kwok, S., Torrance, C., 2012. Multiple Metabolic Alterations Exist in Mutant PI3K Cancers, but Only Glucose Is Essential as a Nutrient Source. *PloS one*, 7(9), p.e45061.

Foulkes, W.D., Smith, I.E. & Reis-Filho, J.S., 2010. Triple-Negative Breast Cancer. *The New England Journal of Medicine*, 363(20), pp.1938–48.

Furusawa, T., Moribe, H., Kondoh, H., Higashi, Y., 1999. Identifiaction of CtBP1 and CtBP2 as Corepressor of Zinc Finger-Homeodomain Factor EF1. *Mol Cell Biol*, 19(12), pp.8581–8590.

Gaglio, D., Metallo, C.M., Gameiro, P.A., Hiller, K., Danna, L.S., Balestrieri, C., Alberghina, L., Stephanopoulos, G. & Chiaradonna, F., 2011. Oncogenic K-Ras decouples glucose and glutamine metabolism to support cancer cell growth. *Molecular systems biology*, 7(523), p.523.

Garayoa, M., Martínez, A., Lee, S., Pío, R., An, W.G., Neckers, L., Trepel, J., Montuenga, L.M., Ryan, H., Johnson, R., Gassmann, M. & Cuttitta, F., 2000. Hypoxia-Inducible Factor-1 (HIF-1) Up-Regulates Adrenomedullin Expression in Human Tumor Cell LInes during Oxygen Deprivation: A possible Promotion Mechanism of Carcinogenesis. *Mol Endocrinol*, 14(6), pp.848–862.

Gatenby, R.A., Smallbone, K., Maini, P.K., Rose, F., Averill, J., Nagle, R.B., Worrall, L. & Gillies, R.J., 2007. Cellular adaptations to hypoxia and acidosis during somatic evolution of breast cancer. *British journal of cancer*, 97(5), pp.646–53.

Generali, D., Berruti, A., Brizzi, M.P., Campo, L., Bonardi, S., Wigfield, S., Bersiga, A., Allevi, G., Milani, M., Aguggini, S., Gandolfi, V., Dogliotti, L., Bottini, A., Harris, A.L. & Fox, S.B., 2006. Hypoxia-inducible factor-1?? expression predicts a poor response to primary chemoendocrine therapy and disease-free survival in primary human breast cancer. *Clinical Cancer Research*, 12(15), pp.4562–4568.

Geng, H., Harvey, C.T., Pittsenbarger, J., Liu, Q., Beer, T.M., Xue, C. & Qian, D.Z., 2011. HDAC4 Protein Regulates HIF1a Protein Lysine Acetylation and Cancer Cell Response to Hypoxia. *The Journal of Biological Chemsirty*, 286(44), pp.38095–38102.

German, M.S., 1993. Glucose sensing in pancreatic islet beta cells: the key role of glucokinase and the glycolytic intermediates. *Proceedings of the National Academy of Sciences of the United States of America*, 90(5), pp.1781–1785.

Giatromanolaki, A., Koukourakis, M.I., Simopoulos, C., Polychronidis, A., Gatter, K.C., Harris, A.L. & Sivridis, E., 2004. c- erb B-2 Related Aggressiveness in Breast Cancer Is Hypoxia Inducible Factor-1 ⌴ Dependent. *Clinical Cancer Research*, 10(23), pp.7972–7977.

Glasspool, R. M., Burns, S., Hoare, S. F., Svensson, C., Keith, W.N., 2005. The hTERT and hTERC Telomerase Gene Promoters Are Activated by the Second Exon of the Adenoviral Protein, E1A, Identifying the Transcriptional Corepressor CtBP as a Potential Repressor of Both Genes. *Neoplasia*, 7(6), pp.614–622.

Gnarra, J.R., Tory, K., Weng, Y., Schmidt, L., Wei, M.H., Li, H., Latif, F., Liu, S., Chen, F., Duh, F.M. & et al., 1994. Mutations of the VHL tumour suppressor gene in renal carcinoma. *Nat Genet*, 7(1), pp.85–90.

Goldstein, J.L., DeBose-Boyd, R.A. & Brown, M.S., 2006. Protein sensors for membrane sterols. *Cell*, 124(1), pp.35–36.

Golias, T., Papandreou, I., Sun, R., Kumar, B., Brown, N. V, Swanson, B.J., Pai, R., Jaitin, D., Le, Q.-T., Teknos, T.N. & Denko, N.C., 2016. Hypoxic repression of pyruvate dehydrogenase activity is necessary for metabolic reprogramming and growth of model tumours. *Scientific reports*, 6(July), p.31146.

Grabmaier, K., MC, A. de W., Verhaegh, G.W., Schalken, J.A. & Oosterwijk, E., 2004. Strict regulation of CAIX(G250/MN) by HIF-1alpha in clear cell renal cell carcinoma. *Oncogene*, 23(33), pp.5624–5631.

Grampp, S., Platt, J.L., Lauer, V., Salama, R., Kranz, F., Neumann, V.K., Hartmann, A., Eckardt, K., Ratcliffe, P.J., Mole, D.R., Sto, C. & Scho, J., 2016. Genetic variation at the 8q24.21 renal cancer susceptibility locus affects HIF binding to a MYC enhancer. *Nature Communications*, 7, pp.1–11.

Graven, K.K., Troxler, R.F., Kornfeld, H., Panchenko, M. V. & Farber, H.W., 1994. Regulation of endothelial cell glyceraldehyde-3-phosphate dehydrogenase expression by hypoxia. *Journal of Biological Chemistry*, 269(39), pp.24446–24453.

Grivas, P.D. & Papavassiliou, A.G., 2013. Transcriptional corepressors in cancer: emerging targets for therapeutic intervention. *Cancer*, 119(6), pp.1120–1128.

Groeger, N., Vitzthum, H., Fřhlich, H., Kŕger, M., Ehmke, H., Braun, T. & Boettger, T., 2012. Targeted mutation of SLC4A5 induces arterial hypertension and renal metabolic acidosis. *Human Molecular Genetics*, 21(5), pp.1025–1036.

Groheux, D., Hindié, E., Giacchetti, S., Delord, M., Hamy, A.-S., de Roquancourt, A., Vercellino, L., Berenger, N., Marty, M. & Espié, M., 2012. Triple-negative breast cancer: early assessment with 18F-FDG PET/CT during neoadjuvant chemotherapy identifies patients who are unlikely to achieve a pathologic complete response and are at a high risk of early relapse. *Journal of nuclear medicine : official publication, Society of Nuclear Medicine*, 53(2), pp.249–54.

Grooteclaes, M., Deveraux, Q., Hildebrand, J., Zhang, Q., Goodman, R.H. & Frisch, S.M., 2003. C-terminal-binding protein corepresses epithelial and proapoptotic gene expression programs. *Proc Natl Acad Sci U S A*, 100(8), pp.4568–4573.

Guenther, M.G., Levine, S.S., Boyer, L.A., Jaenisch, R. & Young, R.A., 2007. A Chromatin Landmark and Transcription Initiation at Most Promoters in Human Cells. *Cell*, 130, pp.77–88.

Guo, J., Chen, L., Luo, N., Yang, W., Qu, X. & Cheng, Z., 2015. Inhibition of TMEM45A suppresses proliferation, induces cell cycle arrest and reduces cell invasion in human ovarian cancer cells. *Oncology Reports*, 33(6), pp.3124–3130.

Gut, M.O., Parkkila, S., Vernerová, Z., Rohde, E., Závada, J., Höcker, M., Pastorek, J., Karttunen, T., Gibadulinová, A., Závadová, Z., Knobeloch, K.P., Wiedenmann, B., Svoboda, J., Horak, I. & Pastoreková, S., 2002. Gastric hyperplasia in mice with targeted disruption of the carbonic anhydrase gene Car9. *Gastroenterology*, 123(6), pp.1889–1903.

Ha, M. & Kim, V.N., 2014. Regulation of microRNA biogenesis. *Nature Reviews Molecular Cell Biology*, 15(8), pp.509–524.

Halestrap, A.P. & Price, N.T., 1999. The proton-linked monocarboxylate transporter (MCT) family: structure, function and regulation. *Biochem J*, 343 Pt 2, pp.281–299.

Han, H., Silverman, J.F., Santucci, T.S., Macherey, R.S., d'Amato, T. a, Tung, M.Y., Weyant, R.J. & Landreneau, R.J., 2001. Vascular endothelial growth factor expression in stage I non-small cell lung cancer correlates with neoangiogenesis and a poor prognosis. *Annals of surgical oncology*, 8(1), pp.72–79.

Hanahan, D. & Weinberg, R.A., 2011. Hallmarks of cancer: the next generation. *Cell*, 144(5), pp.646–674.

Handy, D., Castro, R. & Loscalozo, J., 2011. Epigenetic Modifications: basic Mechanisms and Role in Cardiovascular Disease. *Circulation*, 123(19), pp.2145–2156.

Harada, H., Inoue, M., Itasaka, S., Hirota, K., Morinibu, A., Shinomiya, K., Zeng, L., Ou, G., Zhu, Y., Yoshimura, M., McKenna, W.G., Muschel, R.J. & Hiraoka, M., 2012. Cancer cells that survive radiation therapy acquire HIF-1 activity and translocate towards tumour blood vessels. *Nat Commun*, 3, p.783.

Hashizume, H., Baluk, P., Morikawa, S., McLean, J.W., Thurston, G., Roberge, S., Jain, R.K. & McDonald, D.M., 2000. Openings between Defective Endothelial Cells Explain Tumor Vessel Leakiness. *The American Journal of Pathology*, 156(4), pp.1363–1380.

Haupt, Y., Maya, R., Kazaz, A. & Oren, M., 1997. Mdm2 promotes the rapid degradation of p53. *Nature*, 387, pp.296–299.

He, T.L., Zhang, Y.J., Jiang, H., Li, X. hui, Zhu, H. & Zheng, K.L., 2015. The c-Myc–LDHA axis positively regulates aerobic glycolysis and promotes tumor progression in pancreatic cancer. *Medical Oncology*, 32(7), pp.1–8.

Vander Heiden, M.G., Cantley, L.C. & Thompson, C.B., 2009. Understanding the Warburg Effect : The Metabolic Requirements of Cell Proliferation. *Science*, 324(May), pp.1029–1034.

Helmlinger, G., Sckell, A., Dellian, M., Forbers, N. S., Jain, R.K., 2002. Acid Production in Glycolysis-impaired Tumors Provides New Insighrs into Tumor Metabolism. *Clin Cancer Res*, 8, pp.1284–1291.

Henze, A.T., Riedel, J., Diem, T., Wenner, J., Flamme, I., Pouyseggur, J., Plate, K.H. & Acker, T., 2010. Prolyl hydroxylases 2 and 3 act in gliomas as protective negative feedback regulators of hypoxia-inducible factors. *Cancer Research*, 70(1), pp.357–366.

Hermann, P.C., Huber, S.L., Herrler, T., Aicher, A., Ellwart, J.W., Guba, M., Bruns, C.J. & Heeschen, C., 2007. Distinct Populations of Cancer Stem Cells Determine Tumor Growth and Metastatic Activity in Human Pancreatic Cancer. *Cell Stem Cell*, 1(3), pp.313–323.

Herzog, J., Ehrlich, S.M., Pfitzer, L., Liebl, J., Fröhlich, T., Arnold, G.J., Mikulits, W., Haider, C., Vollmar, A.M. & Zahler, S., 2016. Cyclin-dependent kinase 5 stabilizes hypoxia-inducible factor-1α : a novel approach for inhibiting angiogenesis in hepatocellular carcinoma. *Oncotarget*, 7(19), pp.27108–27121.

Hilbert, B.J., Grossman, S.R., Schiffer, C.A. & Royer Jr., W.E., 2014. Crystal structures of human CtBP in complex with substrate MTOB reveal active site features useful for inhibitor design. *FEBS Lett*, 588(9), pp.1743–1748.

Hildebrand, J.D. & Soriano, P., 2002. Overlapping and Unique Roles for C-Terminal Binding Protein 1 (CtBP1) and CtBP2 during Mouse Development. *Mol Cell Biol*, 22(15), pp.5296–5307.

Höckel, M. & Vaupel, P., 2001. Tumor hypoxia: definitions and current clinical, biologic, and molecular aspects. *Journal of the National Cancer Institute*, 93(4), pp.266–276.

Huang, C.-H., Yang, W.-H., Chang, S.-Y., Tai, S.-K., Tzeng, C.-H., Kao, J.-Y., Wu, K.-J. & Yang, M.-H., 2009. Regulation of membrane-type 4 matrix metalloproteinase by SLUG contributes to hypoxia-mediated metastasis. *Neoplasia (New York, N.Y.)*, 11(12), pp.1371–82.

Huang, L.E., Gu, J., Schau, M. & Bunn, H.F., 1998. Regulation of hypoxia-inducible factor 1alpha is mediated by an O2-dependent degradation domain via the ubiquitin-proteasome pathway. *Proceedings of the National Academy of Sciences of the United States of America*, 95(14), pp.7987–92.

Hulikova, A., Harris, A.L., Vaughan-Jones, R.D. & Swietach, P., 2013. Regulation of intracellular pH in cancer cell lines under normoxia and hypoxia. *J Cell Physiol*, 228(4), pp.743–752.

Hulikova, A., Vaughan-Jones, R.D. & Swietach, P., 2011. Dual role of CO2/HCO3- buffer in the regulation of intracellular pH of three-dimensional tumor growths. *Journal of Biological Chemistry*, 286(16), pp.13815–13826.

Hulikova, A., Zatovicova, M., Svastova, E., Ditte, P., Brasseur, R., Kettmann, R., Supuran, C.T., Kopacek, J., Pastorek, J. & Pastorekova, S., 2009. Intact intracellular tail is critical for proper functioning of the tumor-associated, hypoxia-regulated carbonic anhydrase IX. *FEBS Lett*, 583(22), pp.3563–3568.

Ibrahim-Hashim, A., Robertson-Tessi, M., Enriquez-Navas, P.M., Damaghi, M., Balagurunathan, Y., Wojtkowiak, J.W., Russell, S., Yoonseok, K., Lloyd, M.C., Bui, M.M., Brown, J.S., Anderson, A.R.A., Gillies, R.J. & Gatenby, R.A., 2017. Defining Cancer Subpopulations by Adaptive Strategies Rather Than Molecular Properties Provides Novel Insights into Intratumoral Evolution. *Cancer Research*, 77(9), pp.2242–2254.

Ihnatko, R., Kubes, M., Takacova, M., Sedlakova, O., Sedlak, J., Pastorek, J., Kopacek, J. & Pastorekova, S., 2006. Extracellular acidosis elevates carbonic anhydrase IX in human glioblastoma cells via transcriptional modulation that does not depend on hypoxia. *Int J Oncol*, 29(4), pp.1025–1033.

Iida, H., Suzuki, M., Goitsuka, R. & Ueno, H., 2012. Hypoxia induces CD133 expression in human lung cancer cells by up-regulation of OCT3/4 and SOX2. *International Journal of Oncology*, 40(1), pp.71–79.

Imai, T., Horiuchi, A., Wang, C., Oka, K., Ohira, S., Nikaido, T. & Konishi, I., 2003. Hypoxia attenuates the expression of E-cadherin via up-regulation of SNAIL in ovarian carcinoma cells. *The American journal of pathology*, 163(4), pp.1437–1447.

Innocenti, A., Pastorekova, S., Pastorek, J., Scozzafava, A., Simone, G. De & Supuran, C.T., 2009. The proteoglycan region of the tumor-associated carbonic anhydrase isoform IX acts as anintrinsic buffer optimizing CO2 hydration at acidic pH values characteristic of solid tumors. *Bioorganic and Medicinal Chemistry Letters*, 19(20), pp.5825–5828.

Invitrogen™, life technologies™, 2013. MAGnify ™ Chromatin Invitrogen MAGnify Chromatin Immunoprecipitation System. *Life Technologies Corporation*, p.49.

Ivan, M., Kondo, K., Yang, H., Kim, W., Valiando, J., Ohh, M., Salic, A., Asara, J.M., Lane, W.S. & Kaelin, W.G., 2001. HIFalpha targeted for VHL-mediated destruction by proline hydroxylation: implications for O2 sensing. *Science (New York, N.Y.)*, 292(5516), pp.464–468.

Ivanov, S., Liao, S. Y., Ivanova, A., Danilkovitch-Miagkova, A., Tarasova, N., Weirich, g., Merrill, M. J., Proescholdt, M. A., Oldfield, E. H., Lee, J., Zavada, J., Waheed, A., Sly, W., Lerman, M. I., Stanbridge, E.J., 2001. Expression of Hypoxia-Inducible Cell-Surface Transmembrane Carbonic Anhydrases in Human Cancer. *Am J Pathol*, 158(3), pp.905–919.

Jaakkola, P., Mole, D.R., Tian, Y.M., Wilson, M.I., Gielbert, J., Gaskell, S.J., von Kriegsheim, A., Hebestreit, H.F., Mukherji, M., Schofield, C.J., Maxwell, P.H., Pugh, C.W. & Ratcliffe, P.J., 2001. Targeting of HIF-alpha to the von Hippel-Lindau ubiquitylation complex by O2-regulated prolyl hydroxylation. *Science*, 292(5516), pp.468–472.

Jackson, J.G., Pant, V., Li, Q., Chang, L.L., Quintás-Cardama, A., Garza, D., Tavana, O., Yang, P., Manshouri, T., Li, Y., El-Naggar, A.K. & Lozano, G., 2012. P53-Mediated Senescence Impairs the Apoptotic Response to Chemotherapy and Clinical Outcome in Breast Cancer. *Cancer Cell*, 21(6), pp.793–806.

Jenuwein, T., Laible, G., Dorn, R. & Reuter, G., 1998. SET domain proteins modulate chromatin domains in eu- and heterochromatin. *Cellular and Molecular Life Sciences*, 54, pp.80–93.

Jin, L., Li, D., Alesi, G.N., Fan, J., Kang, H.B., Lu, Z., Boggon, T.J., Jin, P., Yi, H., Wright, E.R., Duong, D., Seyfried, N.T., Egnatchik, R., DeBerardinis, R.J., Magliocca, K.R., He, C., Arellano, M.L., Khoury, J.H.J., Shin, D.M., Khuri, F.R. & Kang, S., 2015. Glutamate Dehydrogenase 1 Signals through Antioxidant Glutathione Peroxidase 1 to Regulate Redox Homeostasis and Tumor Growth. *Cancer Cell*, 27(2), pp.257–270.

Jin, W., Scotto, K.W., Hait, W.N. & Yang, J.M., 2007. Involvement of CtBP1 in the transcriptional activation of the MDR1 gene in human multidrug resistant cancer cells. *Biochem Pharmacol*, 74(6), pp.851–859.

Jing L, Clifford Yen*, Danny Liaw*, Katrina Podsypanina*, Shikha Bose, Steven I. Wang, Janusz Puc, Christa Miliaresis, Linda Rodgers, Richard McCombie, Sandra H. Bigner, Beppino C. Giovanella, Michael Ittmann, Ben Tycko, Hanina Hibshoosh, Michael H. Wig, R.P., 1997. PTEN, a putative protein tyrosine phosphatase gene mutated in human brain, breast, and prostate cancer. *Science*, 275(March), pp.1943–1948.

Jones, R.G., Plas, D.R., Kubek, S., Buzzai, M., Mu, J., Xu, Y., Birnbaum, M.J. & Thompson, C.B., 2005. AMP-activated protein kinase induces a p53-dependent metabolic checkpoint. *Molecular Cell*, 18(3), pp.283–293.

Juel, 2000. Expression of the Na+/H+ exchanger isoform NHE1 in rat skeletal muscle and effect of training. *Acta Physiologica Scandinavica*, 170(1), pp.59–63.

Kaluz, S., Kaluzova, M., Chrastina, A., Olive, P.L., Pastorekova, S., Pastorek, J., Lerman, M.I. & Stanbridge, E.J., 2002. Lowered oxygen tension induces expression of the hypoxia marker MN/carbonic anhydrase IX in the absence of hypoxia-inducible factor 1 alpha stabilization: a role for phosphatidylinositol 3'-kinase. *Cancer Research*, 62(15), pp.4469–4477.

Kaluz, S., Kaluzova, M., Liao, S.Y., Lerman, M. & Stanbridge, E.J., 2009. Transcriptional control of the tumor- and hypoxia-marker carbonic anhydrase 9: A one transcription factor (HIF-1) show? *Biochim Biophys Acta*, 1795(2), pp.162–172.

Kaluz, S., Kaluzová, M. & Stanbridge, E.J., 2003. Expression of the hypoxia marker carbonic anhydrase IX is critically dependent on SP1 activity. Identification of a novel type of hypoxia-responsive enhancer. *Cancer Research*, 63(5), pp.917–922.

Kang, S.S., Chun, Y.K., Hur, M.H., Lee, H.K., Kim, Y.J., Hong, R., Lee, J.H., Lee, S.G. & Park, Y.K., 2002. Clinical Significance of Glucose Transporter 1 (GLUT1) Expression in Human Breast Carcinoma. *Jpn. J. Cancer Res.*, 93, pp.1123–1128.

Kasper, L.H., Boussouar, F., Boyd, K., Xu, W., Biesen, M., Rehg, J., Baudino, T.A., Cleveland, J.L. & Brindle, P.K., 2005. Two transactivation mechanisms cooperate for the bulk of HIF-1-responsive gene expression. *The EMBO journal*, 24(22), pp.3846–58.

Kawauchi, K., Araki, K., Tobiume, K. & Tanaka, N., 2008. p53 regulates glucose metabolism through an IKK-NF-kappaB pathway and inhibits cell transformation. *Nature cell biology*, 10(5), pp.611–618.

Kayashima, T., Nakata, K., Ohuchida, K., Ueda, J., Shirahane, K., Fujita, H., Cui, L., Mizumoto, K. & Tanaka, M., 2011. Insig2 is overexpressed in pancreatic cancer and its expression is induced by hypoxia. *Cancer Science*, 102(6), pp.1137–1143.

Kenneth, N.S., Mudie, S., Uden, P. Van & Rocha, S., 2009. SWI / SNF Regulates the Cellular Response to Hypoxia. *The Journal of Biological Chemsirty*, 284(7), pp.4123–4131.

Kim, J.H., Cho, E.J., Kim, S.T. & Youn, H.D., 2005. CtBP represses p300-mediated transcriptional activation by direct association with its bromodomain. *Nature Structural & Molecular Biology*, 12(5), pp.423–428.

Kim, J.W., Gao, P., Liu, Y.-C., Semenza, G.L. & Dang, C. V., 2007. Hypoxia-Inducible Factor 1 and Dysregulated c-Myc Cooperatively Induce Vascular Endothelial Growth Factor and Metabolic Switches Hexokinase 2 and Pyruvate Dehydrogenase Kinase 1. *Molecular and Cellular Biology*, 27(21), pp.7381–7393.

Kim, J.W., Tchernyshyov, I., Semenza, G.L. & Dang, C. V, 2006. HIF-1-mediated expression of pyruvate dehydrogenase kinase: a metabolic switch required for cellular adaptation to hypoxia. *Cell Metab*, 3(3), pp.177–185.

Kim, J.Y., Kim, S.M., Ko, J.H., Yim, J.H., Park, J.H. & Park, J.H., 2006. Interaction of pro-apoptotic protein HGTD-P with heat shock protein 90 is required for induction of mitochondrial apoptotic cascades. *FEBS Letters*, 580(13), pp.3270–3275.

Kim, Y., Nam, H.J., Lee, J., Park, D.Y., Kim, C., Yu, Y.S., Kim, D., Park, S.W., Bhin, J., Hwang, D., Lee, H., Koh, G.Y. & Baek, S.H., 2016. Methylation-dependent regulation of HIF-1a stability restricts retinal and tumour angiogenesis. *Nature Communications*, 7, p.doi:10.1038/ncomms10347.

Kocemba, K.A., van Andel, H., de Haan-Kramer, A., Mahtouk, K., Versteeg, R., Kersten, M.J., Spaargaren, M. & Pals, S.T., 2013. The hypoxia target adrenomedullin is aberrantly expressed in multiple myeloma and promotes angiogenesis. *Leukemia*, 27(8), pp.1729–1737.

Koipally, J. & Georgopoulos, K., 2000. Ikaros interactions with CtBP reveal a repression mechanism that is independent of histone deacetylase activity. *Journal of Biological Chemistry*, 275(26), pp.19594–19602.

Kondo, A., Safaei, R. & Mishima, M., 2001. Hypoxia-induced Enrichment and Mutagenesis of Cells That Have Lost DNA Mismatch Repair Hypoxia-induced Enrichment and Mutagenesis of Cells That Have Lost DNA Mismatch Repair 1. , pp.7603–7607.

Kopacek, J., Barathova, M., Dequiedt, F., Sepelakova, J., Kettmann, R., Pastorek, J. & Pastorekova, S., 2005. MAPK pathway contributes to density- and hypoxia-induced expression of the tumor-associated carbonic anhydrase IX. *Biochim Biophys Acta*, 1729(1), pp.41–49.

Kornberg, R.D. & Thomas, J.O., 1974. Chromatin Structure : Oligomers of the Histones. *Science*, 184(4139), pp.865–868.

Korneeva, N.L., Song, A., Gram, H., Edens, M.A. & Rhoads, R.E., 2016. Inhibition of Mitogen-activated Protein Kinase (MAPK)-interacting Kinase (MNK) Preferentially Affects Translation of mRNAs Containing Both a 5’ -Terminal Cap and Hairpin. *The Journal of Biological Chemsirty*, 291(7), pp.3455–3467.

Korwar, S., Morris, B.L., Parikh, H.I., Coover, R.A., Doughty, T.W., Love, I.M., Hilbert, B.J., Royer, W.E., Kellogg, G.E., Grossman, S.R. & Ellis, K.C., 2016. Design, synthesis, and biological evaluation of substrate-competitive inhibitors of C-terminal Binding Protein (CtBP). *Bioorganic and Medicinal Chemistry*, 24(12), pp.2707–2715.

Koukourakis, M.I., Giatromanolaki, A., Sivridis, E., Bougioukas, G., Didilis, V., Gatter, K.C. & Harris, A.L., 2003. Lactate dehydrogenase-5 (LDH-5) overexpression in non-small-cell lung cancer tissues is linked to tumour hypoxia, angiogenic factor production and poor prognosis. *British Journal of Cancer*, 89(5), pp.877–885.

Kovi, R.C., Paliwal, S., Pande, S. & Grossman, S.R., 2010. An ARF/CtBP2 complex regulates BH3-only gene expression and p53-independent apoptosis. *Cell death and differentiation*, 17(3), pp.513–521.

Krapivner, S., Opov, S.P., Chernogubova, E., Hellénius, M.L., Fisher, R.M., Hamsten, A. & Van't Hooft, F.M., 2008. Insulin-induced gene 2 involvement in human adipocyte metabolism and body weight regulation. *Journal of Clinical Endocrinology and Metabolism*, 93(February), pp.1995–2001.

Krieg, M., Haas, R., Brauch, H., Acker, T., Flamme, I. & Plate, K.H., 2000. Up-regulation of hypoxia-inducible factors HIF-1α and HIF-2α under normoxic conditions in renal carcinoma cells by von Hippel-Lindau tumor suppressor gene loss of function. *Oncogene*, 19(48), pp.5435–5443.

Kubbutat, M.H.G., Jones, S.N. & Vousden, K.H., 1997. Regulation of p53 stability by Mdm2. *Nature*, 387, pp.299–303.

Kulshreshtha, R., Ferracin, M., Wojcik, S.E., Garzon, R., Alder, H., Agosto-perez, F.J., Davuluri, R., Liu, C., Croce, C.M., Negrini, M., Calin, G.A. & Ivan, M., 2007. A MicroRNA Signature of Hypoxia. *Molecular and Cellular biology*, 27(5), pp.1859–1867.

Kuo, C.Y., Cheng, C.T., Hou, P., Lin, Y.P., Ma, H., Chung, Y., Chi, K., Chen, Y., Li, W., Kung, H.J., Ann, D.K., Kuo, C.Y., Cheng, C.T., Hou, P., Lin, Y.P., Ma, H., Chung, Y., Chi, K., Chen, Y., Li, W., Kung, H.J. & Ann, D.K., 2016. HIF-1-alpha links mitochondrial perturbation to the dynamic acquisition of breast cancer tumorigenicity. *Oncotarget*, 7(23), pp.34052–34069.

Kyo, S., Takakura, M., Taira, T., Kanaya, T., Itoh, H., Yutsudo, M., Ariga, H. & Inoue, M., 2000. Sp1 cooperates with c-Myc to activate transcription of the human telomerase reverse transcriptase gene (hTERT). *Nucleic Acids Research*, 28(3), pp.669–677.

Lando, D., Peet, D.J., Gorman, J.J., Whelan, D.A., Whitelaw, M.L. & Bruick, R.K., 2002. FIH-1 is an asparaginyl hydroxylase enzyme that regulates the transcriptional activity of hypoxia-inducible factor. *Genes and Development*, 16(12), pp.1466–1471.

Lando, D., Peet, D.J., Whelan, D, A., Gorman, J., J. & Whitelaw, M.L., 2002. Asparagine Hydroxylation of the HIF Transactivation Domain: A Hypoxic Switch. *Science*, 295(5556), pp.858–861.

Lange-Carter, C.A. & Johnson, G.L., 1994. Ras-dependent growth factor regulation of MEK kinase in PC12 cells. *Science*, 265(September), pp.1458–1461.

Lau, K.W., Tian, Y.M., Raval, R.R., Ratcliffe, P.J. & Pugh, C.W., 2007. Target gene selectivity of hypoxia-inducible factor-alpha in renal cancer cells is conveyed by post-DNA-binding mechanisms. *Br J Cancer*, 96(8), pp.1284–1292.

Laughner, E., Taghavi, P., Chiles, K., Patrick, C., Semenza, G.L. & Mahon, P.C., 2001. HER2 (neu) Signaling Increases the Rate of Hypoxia-Inducible Factor 1α (HIF-1α) Synthesis : Novel Mechanism for HIF-1-Mediated Vascular Endothelial Growth Factor Expression. *American Society for Microbiology*, 21(12), pp.3995–4004.

Le, A., Cooper, C.R., Gouw, A.M., Dinavahi, R., Maitra, A., Deck, L.M., Royer, R.E., Vander Jagt, D.L., Semenza, G.L. & Dang, C. V, 2010. Inhibition of lactate dehydrogenase A induces oxidative stress and inhibits tumor progression. *Proceedings of the National Academy of Sciences*, 107(5), pp.2037–2042.

Ledaki, I., McIntyre, A., Wigfield, S., Buffa, F., McGowan, S., Baban, D., Li, J. & Harris, A.L., 2015. Carbonic anhydrase IX induction defines a heterogeneous cancer cell response to hypoxia and mediates stem cell-like properties and sensitivity to HDAC inhibition. *Oncotarget*, 6(23), pp.19413–19427.

Lee, G., Won, H.-S., Lee, Y.-M., Choi, J.-W., Oh, T.-I., Jang, J.-H., Choi, D.-K., Lim, B.-O., Kim, Y.J., Park, J.-W., Puigserver, P. & Lim, J.-H., 2016. Oxidative Dimerization of PHD2 is Responsible for its Inactivation and Contributes to Metabolic Reprogramming via HIF-1α Activation. *Scientific reports*, 6(November 2015), p.18928.

Lee, I.H., Kawai, Y., Fergusson, M.M., Rovira, I.I., Bishop, A.J.R., Motoyama, N., Cao, L. & Finkel, T., 2012. Atg7 Modulates p53 Activity to Regulate Cell Cycle and Survival During Metabolic Stress. *Science*, 336(6078), pp.225–228.

Lee, M.-J., Kim, J.-Y., Suk, K. & Park, J.-H., 2004. Identification of the hypoxia-inducible factor 1 alpha-responsive HGTD-P gene as a mediator in the mitochondrial apoptotic pathway. *Molecular and cellular biology*, 24(9), pp.3918–3927.

Lee, S., Axelsen, T. V, Andersen, A.P., Vahl, P., Pedersen, S.F. & Boedtkjer, E., 2016. Disrupting Na(+),HCO3(-)-cotransporter NBCn1 (Slc4a7) delays murine breast cancer development. *Oncogene*, 35(16), pp.2112–2122.

Lee, S., Mele, M., Vahl, P., Christiansen, P.M., Jensen, V.E.D. & Boedtkjer, E., 2014. Na+,HCO3--- cotransport is functionally upregulated during human breast carcinogenesis and required for the inverted pH gradient across the plasma membrane. *Pflugers Archiv European Journal of Physiology*, 467(2), pp.367–377.

Lee Hamm, L., Nakhoul, N. & Hering-Smith, K.S., 2015. Acid-base homeostasis. *Clinical Journal of the American Society of Nephrology*, 10(12), pp.2232–2242.

Lehmann, B.D., Bauer, J.A., Chen, X., Sanders, M.E., Chakravarthy, A.B., Shyr, Y. & Pietenpol, J.A., 2011. Identification of human triple-negative breast cancer subtypes and preclinical models for selection of targeted therapies. *The Journal of Clinical Investigation*, 121(7), pp.2750–2767.

Lenormand, P., Brondello, J., Brunet, A. & Pouysségur, J., 1998. Growth Factor–induced p42/p44 MAPK Nuclear Translocation and Retention Requires Both MAPK Activation and Neosynthesis of Nuclear Anchoring Proteins. *The Journal of Cell Biology*, 142(3), pp.625–633.

Li, C.G., Gruidl, M., Eschrich, S., Mccarthy, S., Wang, H., Mark, G. & Yeatman, T.J., 2008. Insig2 is associated with colon tumorigenesis and inhibits Bax-mediated apoptosis. , 123(2), pp.273–282.

Li, Y., Tu, C., Wang, H., Silverman, D.N. & Frost, S.C., 2011. Catalysis and pH control by membrane-associated carbonic anhydrase IX in MDA-MB-231 breast cancer cells. *Journal of Biological Chemistry*, 286(18), pp.15789–15796.

Li, Y., Wang, H., Oosterwijk, E., Tu, C., Shiverick, K.T., Silverman, D.N. & Frost, S.C., 2009. Expression and activity of carbonic anhydrase IX is associated with metabolic dysfunction in MDA-MB-231 breast cancer cells. *Cancer investigation*, 27(6), pp.613–623.

Lim, J.-H., Lee, Y.-M., Chun, Y.-S., Chen, J., Kim, J.-E. & Park, J.-W., 2010. Sirtuin 1 Modulates Cellular Responses to Hypoxia by Deacetylating Hypoxia-Inducible Factor 1α. *Molecular Cell*, 38(6), pp.864–878.

Linderholm, B.K., Hellborg, H., Johansson, U., Elmberger, G., Skoog, L., Lehtio, J. & Lewensohn, R., 2009. Significantly higher levels of vascular endothelial growth factor (VEGF) and shorter survival times for patients with primary operable triple-negative breast cancer. *Annals of Oncology Oncol*, 20(10), pp.1639–1646.

Liu, H., Wang, J. & Epner, E.M., 2004. Cyclin D1 activation in B-cell malignancy: Association with changes in histone acetylation, DNA methylation, and RNA polymerase II binding to both promoter and distal sequences. *Blood*, 104(8), pp.2505–2513.

Liu, Y., Liu, Y., Yan, X., Xu, Y., Luo, F., Ye, J., Yan, H., Yang, X., Huang, X., Zhang, J. & Ji, G., 2014. HIFs enhance the migratory and neoplastic capacities of hepatocellular carcinoma cells by promoting EMT. *Tumor Biology*, pp.8103–8114.

Liu, Y., Murray-Stewart, T., Casero, R., Kagiampakis, I., Jin, L., Zhang, J., Wang, H., Che, Q., Tong, H., Ke, J., Jiang, F., Wang, F. & Wan, X., 2017. Targeting hexokinase 2 inhibition promotes radiosensitization in HPV16ï¿½E7-induced cervical cancer and suppresses tumor growth. *International Journal of Oncology*, pp.2011–2023.

Livak, K.J. & Schmittgen, T.D., 2001. Analysis of relative gene expression data using real-time quantitative PCR and. *Methods*, 25, pp.402–408.

Lock F E, McDonald P C, Lou Y, Serrano I, Chafe S C, Ostlund C, Aparicio S, Winum J-Y, Supuran C-T, Dedhar, S., 2013. Targeting carbonic anhydrase IX depletes breast cancer stem cells within the hypoxic niche. *Oncogene*, 32(44), pp.5210–9.

Long, H.K., Prescott, S.L. & Wysocka, J., 2016. Ever-Changing Landscapes: Transcriptional Enhancers in Development and Evolution. *Cell*, 167(5), pp.1170–1187.

Lou, Y., McDonald, P.C., Oloumi, A., Chia, S., Ostlund, C., Ahmadi, A., Kyle, A., Auf dem Keller, U., Leung, S., Huntsman, D., Clarke, B., Sutherland, B.W., Waterhouse, D., Bally, M., Roskelley, C., Overall, C.M., Minchinton, A., Pacchiano, F., Carta, F., Scozzafava, A., Touisni, N., Winum, J.Y., Supuran, C.T. & Dedhar, S., 2011. Targeting tumor hypoxia: suppression of breast tumor growth and metastasis by novel carbonic anhydrase IX inhibitors. *Cancer Research*, 71(9), pp.3364–3376.

Louie, E., Nik, S., Chen, J.-S., Schmidt, M., Song, B., Pacson, C., Chen, X.F., Park, S., Ju, J. & Chen, E.I., 2010. Identification of a stem-like cell population by exposing metastatic breast cancer cell lines to repetitive cycles of hypoxia and reoxygenation. *Breast cancer research : BCR*, 12(6), p.R94.

Lu, H., Dalgard, C.L., Mohyeldin, A., McFate, T., Tait, A.S. & Verma, A., 2005. Reversible inactivation of HIF-1 prolyl hydroxylases allows cell metabolism to control basal HIF-1. *J Biol Chem*, 280(51), pp.41928–41939.

Lu, H., Forbes, R.A. & Verma, A., 2002. Hypoxia-inducible factor 1 activation by aerobic glycolysis implicates the Warburg effect in carcinogenesis. *J Biol Chem*, 277(26), pp.23111–23115.

Lundgren, K., Nordenskjold, B. & Landberg, G., 2009. Hypoxia, Snail and incomplete epithelial-mesenchymal transition in breast cancer. *Br J Cancer*, 101(10), pp.1769–1781.

Luo, W., Chang, R., Zhong, J., Pandey, A. & Semenza, G.L., 2012. Histone demethylase JMJD2C is a coactivator for hypoxia-inducible factor 1 that is required for breast cancer progression. *Proceedings of the National Academy of Sciences of the United States of America*, 109(49), pp.E3367-76.

Luo, W., Hu, H., Chang, R., Zhong, J., Knabel, M., O'Meally, R., Cole, R.N., Pandey, A. & Semenza, G.L., 2011. Pyruvate kinase M2 is a PHD3-stimulated coactivator for hypoxia-inducible factor 1. *Cell*, 145(5), pp.732–744.

Maddocks, O.D.K., Berkers, C.R., Mason, S.M., Zheng, L., Blyth, K., Gottlieb, E. & Vousden, K.H., 2012. Serine starvation induces stress and p53-dependent metabolic remodelling in cancer cells. *Nature*, 493(7433), pp.542–546.

Makino, Y., Cao, R., Svensson, K., Bertilsson, G., Asman, M., Tanaka, H., Cao, Y., Berkenstam, A. & Poellinger, L., 2001. Inhibitory PAS domain protein is a negative regulator of hypoxia-inducible gene expression. *Nature*, 414(6863), pp.550–554.

Mandriota, S.J., Turner, K.J., Davies, D.R., Murray, P.G., Morgan, N. V., Sowter, H.M., Wykoff, C.C., Maher, E.R., Harris, A.L., Ratcliffe, P.J. & Maxwell, P.H., 2002. HIF activation identifies early lesions in VHL kidneys: Evidence for site-specific tumor suppressor function in the nephron. *Cancer Cell*, 1(5), pp.459–468.

Marmorstein, R. & Trievel, R.C., 2009. Histone modifying enzymes: structures, mechanisms, and specificities. *Biochim Biophys Acta*, 1789(1), pp.58–68.

Marxsen, J.H., Stengel, P., Doege, K., Heikkinen, P., Jokilehto, T., Wagner, T., Jelkmann, W., Jaakkola, P. & Metzen, E., 2004. Hypoxia-inducible factor-1 (HIF-1) promotes its degradation by induction of HIF-alpha-prolyl-4-hydroxylases. *The Biochemical journal*, 381(Pt 3), pp.761–767.

Mathieu, J., Zhang, Z., Zhou, W., Wang, A.J., Heddleston, J.M., Pinna, C.M., Hubaud, A., Stadler, B., Choi, M., Bar, M., Tewari, M., Liu, A., Vessella, R., Rostomily, R., Born, D., Horwitz, M., Ware, C., Blau, C.A., Cleary, M.A., Rich, J.N. & Ruohola-Baker, H., 2011. HIF induces human embryonic stem cell markers in cancer cells. *Cancer Research*, 71(13), pp.4640–4652.

Mathupala, S.P., Rempel, A. & Pedersen, P.L., 2001. Glucose catabolism in cancer cells: Identification and characterization of a marked activation response of the type II hexokinase gene to hypoxic conditions. *Journal of Biological Chemistry*, 276(46), pp.43407–43412.

May, T., Yang, J., Shoni, M., Liu, S., He, H., Gali, R., Ng, S.K., Crum, C., Berkowitz, R.S. & Ng, S.W., 2013. BRCA1 Expression is Epigenetically repressed in Sporadic Ovarian Cancer Cells by Overexpression of C-Terminal Binding Protein. *Neop*, 15(6), pp.600–608.

McFate, T., Mohyeldin, A., Lu, H., Thakar, J., Henriques, J., Halim, N.D., Wu, H., Schell, M.J., Tsz, M.T., Teahan, O., Zhou, S., Califano, J.A., Nam, H.J., Harris, R.A. & Verma, A., 2008. Pyruvate dehydrogenase complex activity controls metabolic and malignant phenotype in cancer cells. *Journal of Biological Chemistry*, 283(33), pp.22700–22708.

McIntyre, A., Hulikova, A., Ledaki, I., Snell, C., Singleton, D., Steers, G., Seden, P., Jones, D., Bridges, E., Wigfield, S., Li, J.L., Russell, A., Swietach, P. & Harris, A.L., 2016. Disrupting hypoxia-induced bicarbonate transport acidifies tumor cells and suppresses tumor growth. *Cancer Research*, 76(13), pp.3744–3755.

Meierhofer, D., Mayr, J.A., Foetschl, U., Berger, A., Fink, K., Schmeller, N., Hacker, G.W., Hauser-Kronberger, C., Kofler, B. & Sperl, W., 2004. Decrease of mitochondrial DNA content and energy metabolism in renal cell carcinoma. *Carcinogenesis*, 25(6), pp.1005–1010.

Meima, M.E., Webb, B.A., Witkowska, H.E. & Barber, D.L., 2009. The sodium-hydrogen exchanger NHE1 is an akt substrate necessary for actin filament reorganization by growth factors. *Journal of Biological Chemistry*, 284(39), pp.26666–26675.

Melvin, A., Mudie, S. & Rocha, S., 2011. The chromatin remodeler ISWI regulates the cellular response to hypoxia: role of FIH. *Molecular biology of the cell*, 22(21), pp.4171–81.

Mendez, L.E., Manci, N., Cantuaria, G., Gomez-Marin, O., Penalver, M., Braunschweiger, P. & Nadji, M., 2002. Expression of Glucose Transporter-1 in Cervical Cancer and Its Precursors. *Gynecologic Oncology*, 86(2), pp.138–143.

Merlos-Suárez, A., Barriga, F.M., Jung, P., Iglesias, M., Céspedes, M.V., Rossell, D., Sevillano, M., Hernando-Momblona, X., Da Silva-Diz, V., Muñoz, P., Clevers, H., Sancho, E., Mangues, R. & Batlle, E., 2011. The intestinal stem cell signature identifies colorectal cancer stem cells and predicts disease relapse. *Cell Stem Cell*, 8(5), pp.511–524.

Metellus, P., Voutsinos-Porche, B., Nanni-Metellus, I., Colin, C., Fina, F., Berenguer, C., Dussault, N., Boudouresque, F., Loundou, A., Intagliata, D., Chinot, O., Martin, P.M., Figarella-Branger, D. & Ouafik, L., 2011. Adrenomedullin expression and regulation in human glioblastoma, cultured human glioblastoma cell lines and pilocytic astrocytoma. *Eur J Cancer*, 47(11), pp.1727–1735.

Minchenko, A., Leshchinsky, I., Opentanova, I., Sang, N., Srinivas, V., Armstead, V. & Caro, J., 2002. Hypoxia-inducible factor-1-mediated expression of the 6-phosphofructo-2-kinase/fructose-2,6-bisphosphatase-3 (PFKFB3) gene: Its possible role in the warburg effect. *Journal of Biological Chemistry*, 277(8), pp.6183–6187.

Moeller, B.J., Cao, Y., Li, C.Y. & Dewhirst, M.W., 2004. Radiation activates HIF-1 to regulate vascular radiosensitivity in tumors: Role of reoxygenation, free radicals, and stress granules. *Cancer Cell*, 5(5), pp.429–441.

Morgan, P.E., Pastoreková, S., Stuart-Tilley, A.K., Alper, S.L. & Casey, J.R., 2007. Interactions of transmembrane carbonic anhydrase, CAIX, with bicarbonate transporters. *American journal of physiology. Cell physiology*, 293(2), pp.C738-48.

Morikawa, S., Baluk, P., Kaidoh, T., Haskell, A., Jain, R.K. & McDonald, D.M., 2002. Abnormalities in Pericytes on Blood Vessels and Endothelial Sprouts in Tumors. *The American Journal of Pathology*, 160(3), pp.985–1000.

Moscatello, D.K., Holgado-Madruga, M., Emlet, D.R., Montgomery, R.B. & Wong, A.J., 1998. Constitutive Activation of Phosphatidylinositol 3-Kinase by a Naturally Occurring Mutant Epidermal Growth Factor Receptor. *Journal of Biological Chemistry*, 273(1), pp.200–206.

da Motta, L.L., Ledaki, I., Purshouse, K., Haider, S., Bastiani, M.A. De, Baban, D., Morotti, M., Steers, G., Wig, S., Bridges, E., Li, J.-L., Knapp, S., Ebner, D., Klamt, F., Harris, A.L. & McIntyre, A., 2017. The BET inhibitor JQ1 selectively impairs tumour response to hypoxia and downregulates CA9 and angiogenesis in triple negative breast cancer. *Oncogene*, 36, pp.122–132.

Mroz, E.A., Baird, A.H., Michaud, W.A. & Rocco, J.W., 2008. COOH-terminal binding protein regulates expression of the p16INK4A tumor suppressor and senescence in primary human cells. *Cancer Res*, 68(15), pp.6049–6053.

Musa-Aziz, R., Occhipinti, R. & Boron, W.F., 2014. Evidence from simultaneous intracellular- and surface-pH transients that carbonic anhydrase IV enhances CO2 fluxes across Xenopus oocyte plasma membranes. *AJP: Cell Physiology*, 307(9), pp.C814–C840.

Mylonis, I., Chachami, G., Samiotaki, M., Panayotou, G., Paraskeva, E., Kalousi, A., Georgatsou, E., Bonanou, S. & Simos, G., 2006. Identification of MAPK phosphorylation sites and their role in the localization and activity of hypoxia-inducible factor-1α. *Journal of Biological Chemistry*, 281(44), pp.33095–33106.

Nakamura, N., Tanaka, S., Teko, Y., Mitsui, K. & Kanazawa, H., 2005. Four Na+/H+ exchanger isoforms are distributed to Golgi and post-Golgi compartments and are involved in organelle pH regulation. *Journal of Biological Chemistry*, 280(2), pp.1561–1572.

Nanda, R., Chow, L.Q.M., Dees, E.C., Berger, R., Gupta, S., Geva, R., Pusztai, L., Pathiraja, K., Aktan, G., Cheng, J.D., Karantza, V. & Buisseret, L., 2016. Pembrolizumab in Patients With Advanced Triple-Negative Breast Cancer : Phase Ib KEYNOTE-012 Study. *Journal of Clinical Endocrinology and Metabolism*, 34(21), pp.2460–2467.

Natsuizaka, M., Naganuma, S., Kagawa, S., Ohashi, S., Ahmadi, A., Subramanian, H., Chang, S., Nakagawa, K.J., Ji, X., Liebhaber, S., Klein-Szanto, A.J. & Nakagawa, H., 2012. Hypoxia induces IGFBP3 in esophageal squamous cancer cells through HIF-1α-mediated mRNA transcription and continuous protein synthesis. *FASEB journal : official publication of the Federation of American Societies for Experimental Biology*, 26(6), pp.2620–30.

Natsuizaka, M., Ozasa, M., Darmanin, S., Miyamoto, M., Kondo, S., Kamada, S., Shindoh, M., Higashino, F., Suhara, W., Koide, H., Aita, K., Nakagawa, K., Kondo, T., Asaka, M., Okada, F. & Kobayashi, M., 2007. Synergistic up-regulation of Hexokinase-2, glucose transporters and angiogenic factors in pancreatic cancer cells by glucose deprivation and hypoxia. *Exp Cell Res*, 313(15), pp.3337–3348.

NCBI, 2016. Homo Sapiens carbonic anhydrase (CA9) gene, promoter region. Available at: https://www.ncbi.nlm.nih.gov/nuccore/289187424?report=fasta.

Neve, R.M., Chin, K., Fridlyand, J., Yeh, J., Baehner, F.L., Fevr, T., Clark, L., Bayani, N., Coppe, J.P., Tong, F., Speed, T., Spellman, P.T., DeVries, S., Lapuk, A., Wang, N.J., Kuo, W.L., Stilwell, J.L., Pinkel, D., Albertson, D.G., Waldman, F.M., McCormick, F., Dickson, R.B., Johnson, M.D., Lippman, M., Ethier, S., Gazdar, A. & Gray, J.W., 2006. A collection of breast cancer cell lines for the study of functionally distinct cancer subtypes. *Cancer Cell*, 10, pp.515–527.

Newell K, Franchi A, Pouyssegur J, T.I., 1993. Studies with glycolysis-defficient cells suggest that production of lactic acid is not the only cause of tumor acidity. *Proc Natl Acad Sci U S A*, 90, pp.1127–1131.

Noel, J., Roux, D. & Pouysségur, J., 1996. Differential localization of Na+/H+ exchanger isoforms (NHE1 and NHE3) in polarized epithelial cell lines. *Journal of cell science*, 109(5), pp.929–939.

Noman, M.Z., Buart, S., Van Pelt, J., Richon, C., Hasmim, M., Leleu, N., Suchorska, W.M., Jalil, A., Lecluse, Y., El Hage, F., Giuliani, M., Pichon, C., Azzarone, B., Mazure, N., Romero, P., Mami-Chouaib, F. & Chouaib, S., 2009. The cooperative induction of hypoxia-inducible factor-1 alpha and STAT3 during hypoxia induced an impairment of tumor susceptibility to CTL-mediated cell lysis. *Journal of immunology (Baltimore, Md. : 1950)*, 182(6), pp.3510–21.

Noman, M.Z., Desantis, G., Janji, B., Hasmim, M., Karray, S., Dessen, P., Bronte, V. & Chouaib, S., 2014. PD-L1 is a novel direct target of HIF-1 , and its blockade under hypoxia enhanced MDSC-mediated T cell activation. *Journal of Experimental Medicine*, 211(5), pp.781–790.

Nouguerede, E., Berenguer, C., Garcia, S., Bennani, B., Delfino, C., Nanni, I., Dahan, L., Gasmi, M., Seitz, J.F., Martin, P.M. & Ouafik, L., 2013. Expression of adrenomedullin in human colorectal tumors and its role in cell growth and invasion in vitro and in xenograft growth in vivo. *Cancer Med*, 2(2), pp.196–207.

Obach, M., Navarro-Sabaté, À., Caro, J., Kong, X., Duran, J., Gómez, M., Perales, J.C., Ventura, F., Rosa, J.L. & Bartrons, R., 2004. 6-Phosphofructo-2-kinase (pfkfb3) gene promoter contains hypoxia-inducible factor-1 binding sites necessary for transactivation in response to hypoxia. *Journal of Biological Chemistry*, 279(51), pp.53562–53570.

Ogryzko, V. V., Schiltz, R.L., Russanova, V., Howard, B.H. & Nakatani, Y., 1996. The transcriptional coactivators p300 and CBP are histone acetyltransferases. *Cell*, 87(5), pp.953–959.

Ohh, M., Park, C.W., Ivan, M., Hoffman, M.A., Kim, T.-Y., Huang, L.E., Pavletich, N., Chau, V. & Kaelin, W.G., 2000. Ubiquitination of hypoxia-inducible factor requires direct binding to the &bgr;-domain of the von Hippel–Lindau protein. *Nature cell biology*, 2(7), pp.423–427.

Orlowski, A., De Giusti, V.C., Morgan, P.E., Aiello, E. a. & Alvarez, B. V., 2012. Binding of carbonic anhydrase IX to extracellular loop 4 of the NBCe1 Na+/HCO3- cotransporter enhances NBCe1-mediated HCO3- influx in the rat heart. *AJP: Cell Physiology*, 303(1), pp.C69–C80.

Orlowski, J. & Grinstein, S., 2004. Diversity of the mammalian sodium/proton exchanger SLC9 gene family. *Pflugers Archiv European Journal of Physiology*, 447(5), pp.549–565.

Osthus, R.C., Shim, H., Kim, S., Li, Q., Reddy, R., Mukherjee, M., Xu, Y., Wonsey, D., Lee, L.A. & Dang, C. V., 2000. Deregulation of glucose transporter 1 and glycolytic gene expression by c-Myc. *Journal of Biological Chemistry*, 275(29), pp.21797–21800.

Oudet, P., Gross-Bellard, M. & Chambon, P., 1975. Electron Microscopic and Biochemical Evidence that Chromatin Structure Is a Repeating Unit. *Cell*, 4, pp.281–300.

Paliwal, S., Ho, N., Parker, D. & Grossman, S.R., 2012. CtBP2 Promotes Human Cancer Cell Migration by Transcriptional Activation of Tiam1. *Genes Cancer*, 3(7–8), pp.481–490.

Paliwal, S., Kovi, R.C., Nath, B., Chen, Y.W., Lewis, B.C. & Grossman, S.R., 2007. The alternative reading frame tumor suppressor antagonizes hypoxia-induced cancer cell migration via interaction with the COOH-terminal binding protein corepressor. *Cancer Research*, 67(19), pp.9322–9329.

Papandreou, I., Cairns, R.A., Fontana, L., Lim, A.L. & Denko, N.C., 2006. HIF-1 mediates adaptation to hypoxia by actively downregulating mitochondrial oxygen consumption. *Cell Metab*, 3(3), pp.187–197.

Parks, S.K., Cormerais, Y., Durivault, J. & Pouyssegur, J., 2016. “Genetic disruption of the pH i -regulating proteins Na + /H + exchanger 1 (SLC9A1) and carbonic anhydrase 9 severely reduces growth of colon cancer cells.” *Oncotarget*, 8(6), pp.10225–10237.

Parks, S.K., Mazure, N.M., Counillon, L. & Pouysségur, J., 2013. Hypoxia promotes tumor cell survival in acidic conditions by preserving ATP levels. *Journal of Cellular Physiology*, 228(9), pp.1854–1862.

Parks, S.K. & Pouyssegur, J., 2015. The Na^+/HCO_3^- Co-Transporter SLC4A4 Plays a Role in Growth and Migration of Colon and Breast Cancer Cells. *Journal of Cellular Physiology*, 230(8), pp.1954–1963.

Pastorekova, S, Ratcliffe, P. J., Pastorek, J., 2008. Molecular mechanisms of carbonic anhydrase IX-medaited pH regualtion under hypoxia. *BJU International*, 101(4), pp.8–15.

Patel, J., Baranwal, S., Love, I.M., Patel, N.J., Grossman, S.R. & Patel, B.B., 2014. Inhibition of C-terminal binding protein attenuates transcription factor 4 signaling to selectively target colon cancer stem cells. *Cell Cycle*, 13(22), pp.3506–3518.

Pavlova, N.N. & Thompson, C.B., 2016. The Emerging Hallmarks of Cancer Metabolism. *Cell Metabolism*, 23(1), pp.27–47.

Pelletier, J., Graff, J., Ruggero, D. & Sonenberg, N., 2015. Targeting the eIF4F Translation Initiation Complex : A Critical Nexus for Cancer Development. *Cancer Research*, 75(2), pp.250–264.

Pescador, N., Cuevas, Y., Naranjo, S., Alcaide, M., Villar, D., Landázuri, M.O. & Del Peso, L., 2005. Identification of a functional hypoxia-responsive element that regulates the expression of the egl nine homologue 3 (egln3/phd3) gene. *The Biochemical journal*, 390(Pt 1), pp.189–197.

Pinheiro, C., Albergaria, A., Paredes, J., Sousa, J., Dufloth, R., Vieira, D., Schmitt, F. & Baltazar, F., 2010. Monocarboxylate transporter 1 is up-regulated in basal-like breast carcinoma. *Histopathology*, 56, pp.860–867.

Pires, I.M., Bencokova, Z., Milani, M., Folkes, L.K., Li, J.A., Stratford, M.R., Harris, A.L. & Hammond, E.M., 2010. Effects of acute versus chronic hypoxia on DNA damage responses and genomic instability. *Cancer Research*, 70(3), pp.925–935.

Postigo, A.A. & Dean, D.C., 1999. ZEB represses transcription through interaction with the corepressor CtBP. *Proceedings of the National Academy of Sciences of the United States of America*, 96(12), pp.6683–8.

Postigo, A.A., Depp, J.L., Taylor, J.J. & Kroll, K.L., 2003. Regulation of Smad signaling through a differential recruitment of coactivators and corepressors by ZEB proteins. *EMBO Journal*, 22(10), pp.2453–2462.

Pouyssegur, J., Sardet, C., Franchi, A. & Allemain, G.L., 1984. A specific mutation abolishing Na+/H+ antiport activity in hamster fibroblasts precludes growth at neutral and acidic pH. *Proc Natl Acad Sci U S A*, 81(August), pp.4833–4837.

Prat, A., Karginova, O., Parker, J.S., Fan, C., He, X., Bixby, L., Harrell, J.C., Roman, E., Adamo, B., Troester, M. & Perou, C.M., 2013. Characterization of cell lines derived from breast cancers and normal mammary tissues for the study of the intrinsic molecular subtypes. *Breast Cancer Res Treat*, 142(2), pp.237–255.

Quinlan, K.G., Verger, A., Kwok, A., Lee, S.H., Perdomo, J., Nardini, M., Bolognesi, M. & Crossley, M., 2006. Role of the C-terminal binding protein PXDLS motif binding cleft in protein interactions and transcriptional repression. *Mol Cell Biol*, 26(21), pp.8202–8213.

Radhakrishnan, P., Ruh, N., Harnoss, J.M., Kiss, J., Mollenhauer, M., Scherr, A.L., Platzer, L.K., Schmidt, T., Podar, K., Opferman, J.T., Juergen, W., Schulze-Bergkamen, H., Koehler, B.C., Ulrich, A. & Schneider, M., 2016. Prolyl hydroxylase 3 attenuates MCL-1-mediated ATP production to suppress the metastatic potential of colorectal cancer cells. *Cancer Research*, 76(8), pp.2219–2230.

Radvak, P., Repic, M., Svastova, E., Takacova, M., Csaderova, L., Strnad, H., Pastorek, J., Pastorekova, S. & Kopacek, J., 2013. Suppression of carbonic anhydrase IX leads to aberrant focal adhesion and decreased invasion of tumor cells. *Oncol Rep*, 29(3), pp.1147–1153.

Rankin, E.B. & Giaccia, A.J., 2008. The role of hypoxia-inducible factors in tumorigenesis. *Cell Death Differ*, 15(4), pp.678–685.

Rao, B., Lain, S. & Thompson, A.M., 2013. p53-Based cyclotherapy: exploiting the “guardian of the genome” to protect normal cells from cytotoxic therapy. *British journal of cancer*, 109(12), pp.2954–8.

Rathmell, J.C., Fox, C.J., Plas, D.R., Hammerman, P.S., Cinalli, R.M. & Thompson, C.B., 2003. Akt-directed glucose metabolism can prevent Bax conformation change and promote growth factor-independent survival. *Molecular and cellular biology*, 23(20), pp.7315–28.

Ray, S.K., Li, H.J., Metzger, E., Schule, R. & Leiter, A.B., 2014. CtBP and associated LSD1 are required for transcriptional activation by NeuroD1 in gastrointestinal endocrine cells. *Mol Cell Biol*, 34(12), pp.2308–2317.

Rea, S., Eisenhaber, F., O'Carroll, D., Strahl, B., Sun, Z.-W., Schmid, M., Opravil, S., Mechtler, K., Ponting, C.P., Allis, C.D. & Jenuwein, T., 2000. Regulation of chromatin structure by site-specific histone H3 methyltransferases. *Nature*, 406, pp.593–599.

Reid, M.A., Wang, W.I., Rosales, K.R., Welliver, M.X., Pan, M. & Kong, M., 2013. The B55α Subunit of PP2A Drives a p53-Dependent Metabolic Adaptation to Glutamine Deprivation. *Molecular Cell*, 50(2), pp.200–211.

Reitzer, J., Wice, M. & Kennell, D., 1979. Evidence That Glutamine, Not Sugar, Is the Major Energy Source for Cultred HeLa Cells. *The Journal of biological chemistry*, 254(8), pp.2669–2676.

Ren, J.M., Marshall, B.A., Gulve, E.A., Gao, J., Johnson, D.W., Holloszy, J.O. & Mueckler, M., 1993. Evidence from transgenic mice that glucose transport is rate-limiting for glycogen deposition and glycolysis in skeletal muscle. *Journal of Biological Chemistry*, 268(22), pp.16113–16115.

Reshkin, S.J., Bellizzi, A., Albarani, V., Guerra, L., Paradiso, A., Chem, J.B., Tommasino, M. & Casavola, V., 2000. MEMBRANE TRANSPORT STRUCTURE FUNCTION AND BIOGENESIS : Phosphoinositide 3-Kinase Is Involved in the Tumor-specific Activation of Human Breast Cancer Cell Na + / H + Exchange , Motility , and Invasion Induced by Serum Deprivation Phosphoinositide 3-Kinase. *The Journal of Biological Chemsirty*, 275(8), pp.5361–5369.

Reshkin, S.J., Bellizzi, A., Caldeira, S., Albarani, V., Malanchi, I., Poignee, M., Alunni-Fabbroni, M., Casavola, V. & Tommasino, M., 2000. Na+/H+ exchanger-dependent intracellular alkalinization is an early event in malignant transformation and plays an essential role in the development of subsequent transformation-associated phenotypes. *FASEB journal : official publication of the Federation of American Societies for Experimental Biology*, 14(14), pp.2185–97.

Richard, D.E., Berra, E., Gothié, E., Roux, D. & Pouysségur, J., 1999. p42/p44 mitogen-activated protein kinases phosphorylate hypoxia-inducible factor 1alpha (HIF-1alpha) and enhance the transcriptional activity of HIF-1. *The Journal of biological chemistry*, 274(46), pp.32631–32637.

Robertson, N., Potter, C. & Harris, A.L., 2004. Role of Carbonic Anhydrase IX in Human Tumor Cell Groth, Survival and Invasion. *Cancer Res*, 64, pp.6160–6165.

Robey, I.F., Baggett, B.K., Kirkpatrick, N.D., Roe, D.J., Dosescu, J., Sloane, B.F., Hashini, A.I., Morse, D.L., Raghunand, N., Gatenby, R.A. & Gillies, R.J., 2009. Bicarbonate increases tumor pH and inhibits spontaneous metastases. *Cancer Research*, 69(6), pp.2260–2268.

Robey, I.F., Lien, A.D., Welsh, S.J., Baggett, B.K. & Gillies, R.J., 2005. Hypoxia-inducible factor-1alpha and the glycolytic phenotype in tumors. *Neoplasia (New York, N.Y.)*, 7(4), pp.324–30.

Robey, R.B. & Hay, N., 2006. Mitochondrial hexokinases, novel mediators of the antiapoptotic effects of growth factors and Akt. *Oncogene*, 25(34), pp.4683–4696.

Robson, M., Im, S., Senkus, E., Xu, B., Domcheck, S., Masuda, N., Delaloge, S., Tung, N., Armstrong, A., Wu, W., Goessl, C., Runswick, S. & Conte, P., 2017. Olaparib for Metastatic Breast Cancer in Patients with a Germline BRCA Mutation. *The New England Journal of Medicine*, 377(6), pp.523–533.

Rodrigues, N.R., Rowan, A., Smith, M.E., Kerr, I.B., Bodmer, W.F., Gannon, J. V & Lane, D.P., 1990. P53 Mutations in Colorectal Cancer. *Proc.Natl.Acad.Sci.U.S.A*, 87, pp.7555–7559.

Romero, M.F., Chen, A.P., Parker, M.D. & Boron, W.F., 2013. The SLC4 family of bicarbonate (HCO3-) transporters. *Molecular Aspects of Medicine*, 34(2–3), pp.159–182.

Ros, S., Santos, C.R., Moco, S., Baenke, F., Kelly, G., Howell, M., Zamboni, N. & Schulze, A., 2012. Functional metabolic screen identifies 6-phosphofructo-2-kinase/fructose-2, 6-biphosphatase 4 as an important regulator of prostate cancer cell survival. *Cancer Discovery*, 2(4), pp.328–343.

Rouzier, R., Perou, C.M., Symmans, W.F., Ibrahim, N., Cristofanilli, M., Anderson, K., Hess, K.R., Stec, J., Ayers, M., Wagner, P., Morandi, P., Fan, C., Rabiul, I., Ross, J.S., Hortobagyi, G.N. & Pusztai, L., 2005. Human Cancer Biology Breast Cancer Molecular Subtypes Respond Differently to Preoperative Chemotherapy. *Clin Cancer Res*, 11(16), pp.5678–5686.

de Saedeleer, C.J., Copetti, T., Porporato, P.E., Verrax, J., Feron, O. & Sonveaux, P., 2012. Lactate Activates HIF-1 in Oxidative but Not in Warburg-Phenotype Human Tumor Cells. *PLoS ONE*, 7(10), p.e46571.

Said, M.S., Hagemann, C., Carta, F., Katzer, A., Polat, B., Staab, A., Scozzafava, A., Anacker, J., Vince, G., Flentje, M. & Supuran, C.T., 2013. Hypoxia induced CA9 inhibitory targeting by two different sulfonamide derivatives including Acetazolamide in human Glioblastoma. *Bioorg Med Chem*, 21, pp.3949–3957.

Samanta, D., Gilkes, D.M., Chaturvedi, P., Xiang, L. & Semenza, G.L., 2014. Hypoxia-inducible factors are required for chemotherapy resistance of breast cancer stem cells. *Proceedings of the National Academy of Sciences of the United States of America*, 111(50), pp.E5429-38.

Samuels, Y., Wang, Z., Bardelli, A., Silliman, N., Ptak, J., Szabo, S., Yan, H., Gazdar, A., Powell, S.M., Riggins, G.J., Willson, J.K. V., Markowitz, S., Kinzler, K.W., Vogelstein, B. & Velculescu, V.E., 2004. High Frequency of Mutations of the PIK3CA Gene in Human Cancers. *Science*, 304(5670), pp.554–554.

Sandoval, J., Rodríguez, J.L., Tur, G., Serviddio, G., Pereda, J., Boukaba, A., Sastre, J., Torres, L., Franco, L. & López-Rodas, G., 2004. RNAPol-ChIP: a novel application of chromatin immunoprecipitation to the analysis of real-time gene transcription. *Nucleic acids research*, 32(11), p.e88.

Sang, N., Stiehl, D.P., Bohensky, J., Leshchinsky, I., Srinivas, V. & Caro, J., 2003. MAPK signaling up-regulates the activity of hypoxia-inducible factors by its effects on p300. *Journal of Biological Chemistry*, 278(16), pp.14013–14019.

Santos-Rosa, H., Schneider, R., Bannister, A.J., Sherriff, J., Bernstein, B.E., Emre, N.C.T., Schreiber, S.L., Mellor, J. & Kouzarides, T., 2002. Active genes are tri-methylated at K4 of histone H3. *Nature*, 419, pp.407–411.

Schmid, T., Zhou, J., Köhl, R. & Brüne, B., 2004. p300 relieves p53-evoked transcriptional repression of hypoxia-inducible factor-1 (HIF-1). *The Biochemical journal*, 380, pp.289–95.

Schödel, J., Oikonomopoulos, S., Ragoussis, J., Pugh, C.W., Ratcliffe, P.J. & Mole, D.R., 2011. High-resolution genome-wide mapping of HIF-binding sites by ChIP-seq. *Blood*, 117(23), pp.207–217.

Schoedel, J., Grampp, S., Maher, E.R., Moch, H., Ratcliffe, P.J., Russo, P., Mole, D.R. & Catto, J., 2016. Hypoxia , Hypoxia-inducible Transcription Factors , and Renal Cancer. *European Urology*, 69, pp.646–657.

Schulze, A. & Harris, A.L., 2012. How cancer metabolism is tuned for proliferation and vulnerable to disruption. *Nature*, 491(7424), pp.364–73.

Schwartzenberg-bar-yoseph, F., Armoni, M. & Karnieli, E., 2004. The Tumor Suppressor p53 Down-Regulates Glucose Transporters GLUT1 and GLUT4 Gene Expression The Tumor Suppressor p53 Down-Regulates Glucose Transporters GLUT1 and GLUT4 Gene Expression. *Cancer Res*, 2(1), pp.2627–2633.

Semenza, G.L., 2012. Molecular mechanisms mediating metastasis of hypoxic breast cancer cells. *Trends Mol Med*, 18(9), pp.534–543.

Semenza, G.L., Roth, P.H., Fang, H.M. & Wang, G.L., 1994. Transcriptional regulation of genes encoding glycolytic enzymes by hypoxia-inducible factor 1. *J Biol Chem*, 269(38), pp.23757–23763.

Semenza, G.L. & Wang, G.L., 1992. A nuclear factor induced by hypoxia via de novo protein synthesis binds to the human erythropoietin gene enhancer at a site required for transcriptional activation. *Molecular and cellular biology*, 12(12), pp.5447–5454.

Senkus, E., Kyriakides, S., Ohno, F., Penault-Llorca, F., Poortmans, P., Rutgers, E., Zackrisson, S., Cardoso, F. & Committee, on behalf of the E.G., 2015. Primary breast cancer : ESMO Clinical Practice Guidelines for diagnosis , treatment and follow-up. *Annals of Oncology*, 26(Supplement 5), pp.v8–v30.

Seo, K.-S., Park, J.-H., Heo, J.-Y., Jing, K., Han, J., Min, K.-N., Kim, C., Koh, G.Y., Lim, K., Kang, G.-Y., Uee Lee, J., Yim, Y.-H., Shong, M., Kwak, T.-H. & Kweon, G.R., 2015. SIRT2 regulates tumour hypoxia response by promoting HIF-1α hydroxylation. *Oncogene*, 34(11), pp.1354–1362.

Sewalt, R.G., Gunster, M.J., van der Vlag, J., Satijn, D.P. & Otte, a P., 1999. C-Terminal binding protein is a transcriptional repressor that interacts with a specific class of vertebrate Polycomb proteins. *Molecular and cellular biology*, 19(1), pp.777–87.

Shi, Y., Lan, F., Matson, C., Mulligan, P., Whetstine, J.R., Cole, P.A., Casero, R.A. & Shi, Y., 2004. Histone Demethylation Mediated by the Nuclear Amine Oxidase Homolog LSD1. *Cell*, 119(7), pp.941–953.

Shi, Y., Sawada, J., Sui, G., Affar, E.B., Whetstine, J.R., Lan, F., Ogawa, H., Luke, M.P.S., Nakatani, Y. & Shi, Y., 2003. Coorinated histone modifications mediated by CtBP co-repressor complex. *letters to nature*, 422, pp.735–738.

Shin, H.J., Rho, S.B., Jung, D.C., Han, I.O. & Kim, J.Y., 2010. Carbonic anhydrase IX (CA9) modulates tumor- associated cell migration and invasion. *Journal of Cell Science*, 124(7), pp.1077–1087.

Shinojima, T., Oya, M., Takayanagi, A., Mizuno, R., Shimizu, N. & Murai, M., 2007. Renal cancer cells lacking hypoxia inducible factor (HIF)-1a expression maintain vascular endothelial growth factor expression through HIF-2a. *Carcinogenesis*, 28(3), pp.529–536.

Shmakova, A., Batie, M., Druker, J. & Rocha, S., 2014. Chromatin and oxygen sensing in the context of JmjC histone demethylases. *Biochemical Journal*, 462(3), pp.385–395.

Siclari, V.A., Mohammad, K.S., Tompkins, D.R., Davis, H., McKenna, C.R., Peng, X., Wessner, L.L., Niewolna, M., Guise, T.A., Suvannasankha, A. & Chirgwin, J.M., 2014. Tumor-expressed adrenomedullin accelerates breast cancer bone metastasis. *Breast cancer research*, 16(6), p.458.

Slamon, D.J., Clark, G.M., Wong, S.G., Levin, W.J., Ullrich, A. & Mcguire, W.L., 1987. Human Breast Cancer: Correlation of Relapse and Surival with Amplification of the HER-2/neu Oncogene. *Science*, 235(4785), pp.177–182.

Smith, A.J.P., Cooper, J.A., Li, L.K. & Humphries, S.E., 2007. INSIG2 gene polymorphism is not associated with obesity in Caucasian, Afro-Caribbean and Indian subjects. *International Journal of Obesity*, 31, pp.1753–1755.

Smith, H., Board, M., Pellagatti, A., Turley, H., Boultwood, J. & Callaghan, R., 2016. The Effects of Severe Hypoxia on Glycolytic Flux and Enzyme Activity in a Model of Solid Tumours. *Journal of Cellular Biochemistry*, 117, pp.1890–1901.

Smith, I., Procter, M., Gelber, R.D., Guillaume, S., Feyereislova, A., Dowsett, M., Goldhirsch, A., Untch, M., Mariani, G., Baselga, J., Kaufmann, M., Cameron, D., Bell, R., Bergh, J., Coleman, R., Wardley, A., Harbeck, N., Lopez, R.I., Mallmann, P., Gelmon, K., Wilcken, N., Wist, E., Sánchez Rovira, P., Piccart-Gebhart, M.J. & Team, for the H. study, 2007. 2-year follow-up of trastuzumab after adjuvant chemotherapy in HER2-positive breast cancer : a randomised controlled trial. *The Lancet*, 369, pp.29–36.

Soilleux, E.J., Turley, H., Tian, Y.M., Pugh, C.W., Gatter, K.C. & Harris, A.L., 2005. Use of novel monoclonal antibodies to determine the expression and distribution of the hypoxia regulatory factors PHD-1, PHD-2, PHD-3 and FIH in normal and neoplastic human tissues. *Histopathology*, 47(6), pp.602–610.

Spitz, F. & Furlong, E.E.M., 2012. Transcription factors : from enhancer binding to developmental control. *Nature Reviews Genetics*, 13(9), pp.613–626.

Spitzer, K.W., Skolnick, R.L., Peercy, B.E., Keener, J.P. & Vaughan-Jones, R.D., 2002. Facilitation of intracellular H(+) ion mobility by CO(2)/HCO(3)(-) in rabbit ventricular myocytes is regulated by carbonic anhydrase. *The Journal of physiology*, 541(Pt 1), pp.159–67.

Spring, L.M., Gupta, A., Reynolds, K.L., Gadd, M.A., Ellisen, L.W., Isakoff, S.J., Moy, B. & Bardia, A., 2016. Neoadjuvant Endocrine Therapy for Estrogen Receptor–Positive Breast Cancer: A Systematic Review and Meta-analysis. *JAMA Oncology*, 2114(11), pp.1477–1486.

Srinivasan, L. & Atchison, M.L., 2004. YY1 DNA binding and PcG recruitment requires CtBP. *Genes and Development*, 18(21), pp.2596–2601.

Straza, M.W., Paliwal, S., Kovi, R.C., Rajeshkumar, B., Trenh, P., Parker, D., Whalen, G.F., Lyle, S., Schiffer, C.A. & Grossman, S.R., 2010. Therapeutic targeting of C-terminal binding protein in human cancer. *Cell Cycle*, 9(18), pp.3740–3750.

Su, W., Tjian, R. & Echols, H., 1991. DNA looping between sites for transcriptional activation : self-association of DNA-bound Sp1. *Genes and Development*, 5, pp.820–826.

Sun, S., Zhang, G., Sun, Q., Wu, Z., Shi, W., Yang, B. & Li, Y., 2016. Insulin-induced gene 2 expression correlates with colorectal cancer metastasis and disease outcome. *IUBMB Life*, 68(1), pp.65–71.

Sun, W., Qiu, G., Zou, Y., Cai, Z., Wang, P., Lin, X. & Huang, J., 2015. Knockdown of TMEM45A inhibits the proliferation , migration and invasion of glioma cells. *Int J Clin Exp Pathol*, 8(10), pp.12657–12667.

Švastová, E., Hulíková, A., Rafajová, M., Zaťovičová, M., Gibadulinová, A., Casini, A., Cecchi, A., Scozzafava, A., Supuran, C.T., Pastorek, J. & Pastoreková, S., 2004. Hypoxia activates the capacity of tumor-associated carbonic anhydrase IX to acidify extracellular pH. *FEBS Letters*, 577(3), pp.439–445.

Svastova, E., Witarski, W., Csaderova, L., Kosik, I., Skvarkova, L., Hulikova, A., Zatovicova, M., Barathova, M., Kopacek, J., Pastorek, J. & Pastorekova, S., 2012. Carbonic anhydrase IX interacts with bicarbonate transporters in lamellipodia and increases cell migration via its catalytic domain. *J Biol Chem*, 287(5), pp.3392–3402.

Swietach, P., Vaughan-Jones, R.D. & Harris, A.L., 2007. Regulation of tumor pH and the role of carbonic anhydrase 9. *Cancer Metastasis Rev*, 26(2), pp.299–310.

Swietach, P., Vaughan-Jones, R.D., Harris, A.L. & Hulikova, A., 2014. The chemistry, physiology and pathology of pH in cancer. *Philosophical transactions of the Royal Society of London. Series B, Biological sciences*, 369(1638), p.20130099.

Swietach, P., Wigfield, S., Cobden, P., Supuran, C.T., Harris, A.L. & Vaughan-Jones, R.D., 2008. Tumor-associated carbonic anhydrase 9 spatially coordinates intracellular pH in three-dimensional multicellular growths. *Journal of Biological Chemistry*, 283(29), pp.20473–20483.

Taha, C., Liu, Z., Jin, J., Al-hasani, H., Sonenberg, N. & Klip, A., 1999. Opposite Translational Control of GLUT1 and GLUT4 Glucose Transporter mRNAs in Response to Insulin. *Journal of Biological Chemistry*, 274(46), pp.33085–33091.

Talks, K.L., Turley, H., Gatter, K.C., Maxwell, P.H., Pugh, C.W., Ratcliffe, P.J. & Harris, A.L., 2000. The expression and distribution of the hypoxia-inducible factors HIF-1alpha and HIF-2alpha in normal human tissues, cancers, and tumor-associated macrophages. *Am J Pathol*, 157(2), pp.411–421.

Tan, E.Y., Yan, M., Campo, L., Han, C., Takano, E., Turley, H., Candiloro, I., Pezzella, F., Gatter, K.C., Millar, E.K.A., O'Toole, S.A., McNeil, C.M., Crea, P., Segara, D., Sutherland, R.L., Harris, A.L. & Fo, S.B., 2009. The key hypoxia regulated gene CAIX is upregulated in basal-like breast tumours and is associated with resistance to chemotherapy. *Br J Cancer*, 100(2), pp.405–411.

Tang, B., Kadariya, Y., Murphy, M.E. & Kruger, W.D., 2006. The methionine salvage pathway compound 4-methylthio-2-oxobutanate causes apoptosis independent of down-regulation of ornithine decarboxylase. *Biochemical Pharmacology*, 72(7), pp.806–815.

Tennant, D.A., Frezza, C., MacKenzie, E.D., Nguyen, Q.D., Zheng, L., Selak, M. a, Roberts, D.L., Dive, C., Watson, D.G., Aboagye, E.O. & Gottlieb, E., 2009. Reactivating HIF prolyl hydroxylases under hypoxia results in metabolic catastrophe and cell death. *Oncogene*, 28(45), pp.4009–4021.

Tennant, D.A. & Gottlieb, E., 2010. HIF prolyl hydroxylase-3 mediates alpha-ketoglutarate-induced apoptosis and tumor suppression. *Journal of Molecular Medicine*, 88(8), pp.839–849.

The Cancer Genome Atlas Network, 2012. Comprehensive molecular portraits of human breast tumours. *Nature*, 490, pp.61–70.

Thiery, J.P., Acloque, H., Huang, R.Y.J. & Nieto, M.A., 2009. Epithelial-Mesenchymal Transitions in Development and Disease. *Cell*, 139, pp.871–890.

Thiry, A., Dogné, J.M., Masereel, B. & Supuran, C.T., 2006. Targeting tumor-associated carbonic anhydrase IX in cancer therapy. *Trends in Pharmacological Sciences*, 27(11), pp.566–573.

Thompson, C.B., 2011. Rethinking the Regulation of Cellular Metabolism. *Cold Spring Harbor Symposia on Quantitative Biology*, 76, pp.23–29.

Tian, S., Hayes, A.J., Metheny-Barlow, L.J. & Li, L.-Y., 2002. Stabilization of breast cancer xenograft tumour neovasculature by angiopoietin-1. *British journal of cancer*, 86(4), pp.645–51.

Tripathi, M.K., Misra, S., Khedkar, S. V, Hamilton, N., Irvin-Wilson, C., Sharan, C., Sealy, L. & Chaudhuri, G., 2005. Regulation of BRCA2 gene expression by the SLUG repressor protein in human breast cells. *J Biol Chem*, 280(17), pp.17163–17171.

Turner, K.J., Moore, J.W., Jones, A., Taylor, C.F., Cuthbert-heavens, D., Han, C., Leek, R.D., Gatter, K.C., Maxwell, P.H., Ratcliffe, P.J., Cranston, D. & Harris, A.L., 2002. Expression of Hypoxia-inducible Factors in Human Renal Cancer : Relationship to Angiogenesis and to the von Hippel-Lindau Gene Mutation. *Cancer Research*, 62, pp.2957–2961.

Tuttle, 2014. Placental Lactogen Is Expressed but Is Not Translated into Protein in Breast Cancer. *PloS one*, 9(1).

Ullah, M.S., Davies, A.J. & Halestrap, A.P., 2006. The plasma membrane lactate transporter MCT4, but not MCT1, is up-regulated by hypoxia through a HIF-1a-dependent mechanism. *Journal of Biological Chemistry*, 281(14), pp.9030–9037.

Vaughan-Jones, R.D. & Wu, M.L., 1990. Extracellular H+ inactivation of Na(+)-H+ exchange in the sheep cardiac Purkinje fibre. *The Journal of physiology*, 428, pp.441–66.

Vaupel, P., Schlenger, K., Knoop, C. & Hockel, M., 1991. Oxygenation of human tumors: evaluation of tissue oxygen distribution in breast cancers by computerized O2 tension measurements. *Cancer Research*, 51(12), pp.3316–3322.

Verger, A., Quinlan, K.G., Crofts, L.A., Spano, S., Corda, D., Kable, E.P., Braet, F. & Crossley, M., 2006. Mechanisms directing the nuclear localization of the CtBP family proteins. *Mol Cell Biol*, 26(13), pp.4882–4894.

Vignali, M., Hassan, A.H., Neely, K.E. & Workman, J.L., 2000. ATP-Dependent Chromatin-Remodeling Complexes. *Molecular and Cellular biology*, 20(6), pp.1899–1910.

Vleugel, M.M., Greijer, A.E., Shvarts, A., van der Groep, P., van Berkel, M., Aarbodem, Y., van Tinteren, H., Harris, A.L., van Diest, P.J., van der Wall, E. & J van Diest, P.P., 2005. Differential prognostic impact of hypoxia induced and diffuse HIF-1a expression in invasive breast cancer. *J Clin Pathol*, 58, pp.172–177.

Vollan, M., Quigley, D.A. & Kristensen, V.N., 2015. TP53 Mutation Spectrum in Breast Cancer Is Subtype Specific and Has Distinct Prognostic Relevance. *Clinical Cancer Research*, 21(6), pp.1502–1502.

Vordermark, D., Kaffer, A., Riedl, S., Katzer, A. & Flentje, M., 2005. Characterization of carbonic anhydrase IX (CA IX) as an endogenous marker of chronic hypoxia in live human tumor cells. *Int J Radiat Oncol Biol Phys*, 61(4), pp.1197–1207.

Wang, G., Cheng, Z., Liu, F., Zhang, H., Li, J. & Li, F., 2015. CREB is a key negative regulator of carbonic anhydrase IX (CA9) in gastric cancer. *Cellular Signalling*, 27, pp.1369–1379.

Wang, G.L., Jiang, B.H., Rue, E.A. & Semenza, G.L., 1995. Hypoxia-inducible factor 1 is a basic-helix-loop-helix-PAS heterodimer regulated by cellular 02 tension. *Proceedings of the National Academy of Sciences of the United States of America*, 92(12), pp.5510–5514.

Wang, G.L. & Semenza, G.L., 1993a. Characterization of hypoxia-inducible factor 1 and regulation of DNA binding activity by hypoxia. *J Biol Chem*, 268(29), pp.21513–21518.

Wang, G.L. & Semenza, G.L., 1993b. General involvement of hypoxia-inducible factor 1 in transcriptional response to hypoxia. *Proceedings of the National Academy of Sciences of the United States of America*, 90(9), pp.4304–8.

Wang, G.L. & Semenza, G.L., 1995. Purification and Characterization of Hypoxia-inducible Factor 1. *The Journal of biological chemistry*, 270(3), pp.1230–1237.

Warburg, 1956. Origin of cancer cells. *Oncologia*, 9(2), pp.75–83.

Warburg, O., 1924. Ueber den Stoffwechsel der Carcinomzelle. *Naturwissenschaften*, 50(12), pp.1131–1137.

Warburg, O., Wind, F. & Negelein, E., 1927. Killing-Off of Tumor Cells in Vitro. *The Journal of General Physiology*, pp.519–530.

Ward, C., Langdon, S.P., Mullen, P., Harris, A.L., Harrison, D.J., Supuran, C.T. & Kunkler, I.H., 2013. New strategies for targeting the hypoxic tumour microenvironment in breast cancer. *Cancer Treat Rev*, 39(2), pp.171–179.

Warfel, N.A., Dolloff, N.G., Dicker, D.T., Malysz, J. & El-Deiry, W.S., 2013. CDK1 stabilizes HIF-1α via direct phosphorylation of Ser668 to promote tumor growth. *Cell Cycle*, 12(23), pp.3689–3701.

Wei, C.L., Wu, Q., Vega, V.B., Chiu, K.P., Ng, P., Zhang, T., Shahab, A., Yong, H.C., Fu, Y., Weng, Z., Liu, J., Zhao, X.D., Chew, J.L., Lee, Y.L., Kuznetsov, V.A., Sung, W.K., Miller, L.D., Lim, B., Liu, E.T., Yu, Q., Ng, H.H. & Ruan, Y., 2006. A global map of p53 transcription-factor binding sites in the human genome. *Cell*, 124(1), pp.207–219.

Wiesener, M.S., Jurgensen, J.S., Rosenberger, C., Scholze, C.K., Horstrup, J.H., Warnecke, C., Mandriota, S., Bechmann, I., Frei, U.A., Pugh, C.W., Ratcliffe, P.J., Bachmann, S., Maxwell, P.H. & Eckardt, K.U., 2003. Widespread hypoxia-inducible expression of HIF-2alpha in distinct cell populations of different organs. *FASEB J*, 17(2), pp.271–273.

Wiesener, M.S., Munchenhagen, P.M., Berger, I., Morgan, N. V, Roigas, J., Schwiertz, A., Jurgensen, J.S., Gruber, G., Maxwell, P.H., Loning, S.A., Frei, U., Maher, E.R., Grone, H.J. & Eckardt, K.U., 2001. Constitutive activation of hypoxia-inducible genes related to overexpression of hypoxia-inducible factor-1alpha in clear cell renal carcinomas. *Cancer Res*, 61(13), pp.5215–5222.

Williams, A.C., Collard, T.J. & Paraskeva, C., 1999. An acidic environment leads to p53 dependent induction of apoptosis in human adenoma and carcinoma cell lines: implications for clonal selection during colorectal carcinogenesis. *Oncogene*, 18(21), pp.3199–204.

Wise, D.R., DeBerardinis, R.J., Mancuso, A., Sayed, N., Zhang, X.-Y., Pfeiffer, H.K., Nissim, I., Daikhin, E., Yudkoff, M., McMahon, S.B. & Thompson, C.B., 2008. Myc regulates a transcriptional program that stimulates mitochondrial glutaminolysis and leads to glutamine addiction. *Proceedings of the National Academy of Sciences*, 105(48), pp.18782–18787.

Wong, C.C.L., Zhang, H., Gilkes, D.M., Chen, J., Wei, H., Chaturvedi, P., Hubbi, M.E. & Semenza, G.L., 2012. Inhibitors of hypoxia-inducible factor 1 block breast cancer metastatic niche formation and lung metastasis. *Journal of Molecular Medicine*, 90(7), pp.803–815.

Wykoff, C., Beasley, N.J.P., Watson, P.H., Turner, K.J., Pastorek, J., Sibtain, A., Wilson, G.D., Turley, H., Talks, K.L., Maxwell, P.H., Pugh, C.W., Ratcliffe, P.J. & Harris, A.L., 2000. Hypoxia-inducible Expression of Tumor-associated Carbonic Anhydrases. *Cancer Research*, 60, pp.7075–7083.

Yabe, D., Brown, M.S. & Goldstein, J.L., 2002. Insig-2, a second endoplasmic reticulum protein that binds SCAP and blocks export of sterol regulatory element-binding proteins. *Proceedings of the National Academy of Sciences of the United States of America*, 99(20), pp.12753–8.

Yamagata, M., Hasuda, K., Stamato, T. & Tannock, I.F., 1998. The contribution of lactic acid to acidification of tumours: studies of variant cells lacking lactate dehydrogenase. *British journal of cancer*, 77(11), pp.1726–31.

Yang, M., Wu, M., Chiou, S., Chen, P., Chang, S. & Liu, C., 2008. Direct regulation of TWIST by HIF-1 α promotes metastasis. *Nature cell biology*, 10(3), pp.295–305.

Yatabe, N., Kyo, S., Maida, Y., Nishi, H., Nakamura, M., Kanaya, T., Tanaka, M., Isaka, K., Ogawa, S. & Inoue, M., 2004. HIF-1-mediated activation of telomerase in cervical cancer cells. *Oncogene*, 23(December 2003), pp.3708–3715.

Ying, H., Kimmelman, A.C., Lyssiotis, C.A., Hua, S., Chu, G.C., Fletcher-Sananikone, E., Locasale, J.W., Son, J., Zhang, H., Coloff, J.L., Yan, H., Wang, W., Chen, S., Viale, A., Zheng, H., Paik, J.H., Lim, C., Guimaraes, A.R., Martin, E.S., Chang, J., Hezel, A.F., Perry, S.R., Hu, J., Gan, B., Xiao, Y., Asara, J.M., Weissleder, R., Wang, Y.A., Chin, L., Cantley, L.C. & Depinho, R.A., 2012. Oncogenic kras maintains pancreatic tumors through regulation of anabolic glucose metabolism. *Cell*, 149(3), pp.656–670.

Yokoyama, H., Gunasegaram, S., Harding, S.E. & Avkiran, M., 2000. Sarcolemmal Na+/H+ exchanger activity and expression in human ventricular myocardium. *J Am Coll Cardiol*, 36(2), pp.534–540.

Yu-Rice, Y., Jin, Y., Han, B., Qu, Y., Johnson, J., Watanabe, T., Cheng, L., Deng, N., Tanaka, H., Gao, B., Liu, Z., Sun, Z. & Bose, S., 2016. FOXC1 is involved in ER α silencing by counteracting GATA3 binding and is implicated in endocrine resistance. *Onco*, 35, pp.5400–5411.

Yu, F., White, S.B., Zhao, Q. & Lee, F.S., 2001. HIF-1a binding to VHL is regulated by stimulus-sensitive proline hydroxylation. *PNAS*, 98(25), pp.9630–9635.

Yuan, F., Chen, Y., Dellian, M., Safabakhsh, N., Ferrara, N. & Jain, R.K., 1996. Time-dependent vascular regression and permeability changes in established human tumor xenografts induced by an anti-vascular endothelial growth factor/vascular permeability factor antibody. *Proceedings of the National Academy of Sciences of the United States of America*, 93(25), pp.14765–70.

Zammit, V.A., Beis, I. & Newsholme, E.A., 1978. Maximum activities and effects of fructose bisphosphate on pyruvate kinase from muscles of vertebrates and invertebrates in relation to the control of glycolysis. *Biochem J*, 174(3), pp.989–998.

Zancan, P., Sola-Penna, M., Furtado, C.M. & Da Silva, D., 2010. Differential expression of phosphofructokinase-1 isoforms correlates with the glycolytic efficiency of breast cancer cells. *Molecular Genetics and Metabolism*, 100(4), pp.372–378.

Zhang, H., Wong, C.C., Wei, H., Gilkes, D.M., Korangath, P., Chaturvedi, P., Schito, L., Chen, J., Krishnamachary, B., Winnard Jr., P.T., Raman, V., Zhen, L., Mitzner, W.A., Sukumar, S. & Semenza, G.L., 2012. HIF-1-dependent expression of angiopoietin-like 4 and L1CAM mediates vascular metastasis of hypoxic breast cancer cells to the lungs. *Oncogene*, 31(14), pp.1757–1770.

Zhang, P., Yao, Q., Lu, L., Li, Y., Chen, P. & Duan, C., 2014. Hypoxia-Inducible Factor 3 Is an Oxygen-Dependent Transcription Activator and Regulates a Distinct Transcriptional Response to Hypoxia. *Cell Reports*, 6, pp.1110–1121.

Zhang, Q., Piston, D.W. & Goodman, R.H., 2002. Regulation of corepressor function by nuclear {NADH}. *Science*, 295(5561), pp.1895–1897.

Zhang, Q., Wang, S.Y., Nottke, A.C., Rocheleau, J. V, Piston, D.W. & Goodman, R.H., 2006. Redox sensor CtBP mediates hypoxia-induced tumor cell migration. *Proc Natl Acad Sci U S A*, 103(24), pp.9029–9033.

Zhang, W., Shi, X., Peng, Y., Wu, M., Zhang, P., Xie, R., Wu, Y., Yan, Q., Liu, S. & Wang, J., 2015. HIF-1α Promotes Epithelial-Mesenchymal Transition and Metastasis through Direct Regulation of ZEB1 in Colorectal Cancer. *PloS one*, 10(6), p.e0129603.

Zhang, X.L., Huang, C.X., Zhang, J., Inoue, A., Zeng, S.E. & Xiao, S.J., 2013. CtBP1 is involved in epithelial-mesenchymal transition and is a potential therapeutic target for hepatocellular carcinoma. *Oncol Rep*, 30(2), pp.809–814.

Zhao, L.Z. & Chinnadurai, G., 2010. Incapacitating CtBP to kill cancer. *Cell Cycle*, 9(18), pp.3660–3665.

Zhdanov, A. V, Okkelman, I.A., Collins, F.W.J., Melgar, S. & Papkovsky, D.B., 2015. A novel effect of DMOG on cell metabolism: direct inhibition of mitochondrial function precedes HIF target gene expression. *Biochimica Et Biophysica Acta-Bioenergetics*, 1847(10), pp.1254–1266.

Zheng, G., Peng, C., Jia, X., Gu, Y., Zhang, Z., Deng, Y., Wang, C., Li, N., Yin, J., Liu, X., Lu, M., Tang, H. & He, Z., 2015. ZEB1 transcriptionally regulated carbonic anhydrase 9 mediates the chemoresistance of tongue cancer via maintaining intracellular pH. *Molecular cancer*, 14(1), pp.84–95.

Zhong, H., Chiles, K., Feldser, D., Laughner, E., Hanrahan, C., Georgescu, M.-M., Simons, J.W. & Semenza, G.L., 2000. Modulation of Hypoxia-inducible Factor 1 α Expression by the Epidermal Growth Factor / Phosphatidylinositol 3-Kinase / PTEN / AKT / FRAP Pathway in Human Prostate Cancer Cells : Implications for Tumor Angiogenesis and Therapeutics. *Cancer Research*, 60, pp.1541–1545.

Zhu, G.H., Huang, C., Feng, Z.Z., Lv, X.H. & Qiu, Z.J., 2013. Hypoxia-induced snail expression through transcriptional regulation by HIF-1?? in pancreatic cancer cells. *Digestive Diseases and Sciences*, 58(12), pp.3503–3515.

Zundel, W., Schindler, C., Haas-Kogan, D., Koong, A., Kaper, F., Chen, E., Gottschalk, A.R., Ryan, H.E., Johnson, R.S., Jefferson, A.B., Stokoe, D. & Giaccia, A.J., 2000. Loss of PTEN facilitates HIF-1-mediated gene expression. *Genes and Development*, 14(4), pp.391–396.